

EXPRESSION OF GROWTH FACTOR RECEPTORS BY HAEMATOPOIETIC STEM AND PROGENITOR CELLS

Ciarán James Mooney

A thesis submitted to
The University of Birmingham
for the degree of
DOCTOR OF PHILOSOPHY

School of Immunity and Infection
College of Medical and Dental Sciences
The University of Birmingham
August 2016

UNIVERSITY OF
BIRMINGHAM

University of Birmingham Research Archive

e-theses repository

This unpublished thesis/dissertation is copyright of the author and/or third parties. The intellectual property rights of the author or third parties in respect of this work are as defined by The Copyright Designs and Patents Act 1988 or as modified by any successor legislation.

Any use made of information contained in this thesis/dissertation must be in accordance with that legislation and must be properly acknowledged. Further distribution or reproduction in any format is prohibited without the permission of the copyright holder.


ABSTRACT

The mechanisms that govern the lineage commitment of haematopoietic stem and progenitor cells (HSPCs) have been a topic of debate since the 1960s. Two models of lineage commitment have been described; a permissive model, in which haematopoietic growth factors (HGFs) stimulate proliferation and survival of distinct HSPC subpopulations to permit stochastic lineage-specification, and a deterministic model which proposes that HGFs instruct HSPCs to differentiate towards a specific cell lineage. To provide further insight into whether HGFs provide instructive cues or act in a selective manner, this study has investigated the expression of fms-like tyrosine kinase 3 (Flt3), and the receptors for erythropoietin (EpoR) and macrophage-colony stimulating factor (M-CSFR) by single HSPCs within the bone marrow. Using single-cell qRT-PCR and flow cytometry, a large number of novel HSPC subpopulations have been identified based on receptor expression. Importantly, multiplex analysis of protein and mRNA expression revealed that the above receptors are rarely co-expressed during the early stages of haematopoiesis. Furthermore, Flt3 expression was identified within the haematopoietic stem cell compartment and *in vitro* analysis demonstrated that Flt3 ligand primarily acts on a subpopulation of downstream progenitors. These findings suggest that Flt3, EpoR and M-CSFR differentially regulate distinct early HSPC subpopulations.

ACKNOWLEDGEMENTS

Firstly, I would like to thank both of my supervisors. Dr. Geoffrey Brown, thank you for providing me with the opportunity to carry out this project, and thank you for all of your help and support from beginning to end. Thank you to Dr. Kai Toellner for all of your help with the qRT-PCR data, and for all of the time spent de-stressing at the rock climbing gym. A thank you also needs to go out to everyone involved in the DECIDE Marie Curie consortium. It has been a pleasure working alongside such dedicated scientists.

A huge thank you to everyone in the Toellner group for welcoming me with open arms and for letting me crash lab meetings and journal club, despite my lack of B-lymphocyte knowledge. Similarly, everyone in Prof. Adam Cunningham's lab has been ridiculously helpful throughout my time at the university. Sarah, Charlie and Jenny, you were absolutely amazing when I first arrived. You showed me the ropes, and were always happy to help, regardless of how many questions I asked. Although it took a while for her to spell my name correctly, a big thank you goes out to Spyda for helping me with my flow experiments, providing the office with an endless supply of snacks, and for just being an awesome person in general! Thank you to Yang and Adrianna for being a constant fountain of knowledge when I needed help troubleshooting problems or analysing data.

Thanks to Tom for showing me how to keep fit in the lab, for questioning whether I lift or not on a very regular basis, and for assuring me that it does, indeed, fit my macros. A big shout out to Matt for always staying late on the sorter with me, and for introducing me the beautiful world of craft beers! Laura, Coral, Claire, Anna and Lloyd, thank you so much for all of the banter you provided in the lab, and at Staff House. All of you made my time at the university enjoyable. For everyone else on the 4th floor of the IBR, thank you for your continuous support, and for supplying me with mouse legs during my project. With that, I'd like to thank everyone in  for all of their help with my animal work.

For all in Prof. Jon Frampton's lab, thank you so much for consistently being there to answer my questions, teach me techniques and lend me reagents. Specifically, thanks to Giacomo for always finding time to talk with me about the wonders of Flt3, for helping me with my

colony forming assays and for proofreading my thesis - You're an absolute legend! And to Mary, thank you for being so patient and putting up with my continuous pestering while helping me with my phosphoflow experiments.

A special thanks must go out to my family. Thank you for always providing me with an endless supply of love, support and happiness, no matter what I choose to do. Specifically, to my parents, thank you for always pushing me to be a better person and for encouraging me to go after what I love. I could not have done any of this without you. And thank you for supporting me through yet another degree... I promise I'll get a job eventually.

To Erin, you have been a source of strength for me. Thank you for sharing my passion for research, and for always being understanding of my late nights in the lab, insane writing schedule and general grumpiness when things were not going as planned.

Finally, thank you to all of my friends outside of the university for their support during my studies. To Aisling, Ken, Chris and Emma, who are always up for pints when I'm in Ireland, sláinte! And a big thanks to James, who grossly underestimates the amount of work that has gone into writing this thesis. Without his distractions, this thesis would probably have been finished a couple of months ago.

To everyone mentioned above, and for anyone that I may have missed; you helped me to complete this thesis, and I will never be able to thank you enough.

ABBREVIATIONS

AgPC	Antigen presenting cell
APC	Allophycocyanin
AU	Arbitrary unit
BFU-E	Erythroid burst forming unit
BLAST	Basic local alignment search tool
BM	Bone marrow
C/EBP α	CCAAT enhancer-binding protein α
cDNA	Complementary DNA
CFU-blast	Blast colony forming unit
CFU-E	Erythroid colony forming unit
CFU-G	Granulocyte colony forming unit
CFU-GEMM	Granulocyte-erythroid-megakaryocyte-macrophage colony forming unit
CFU-GM	Granulocyte-macrophage colony forming unit
CFU-M	Macrophage colony forming unit
CFU-Meg	Megakaryocyte colony forming unit
CFU-MegMix	Mixed megakaryocyte colony forming unit
CFU-S	Spleen colony forming unit
CLP	Common lymphoid progenitor
CMLP	Common granulocyte-myelomonocyte-lymphoid progenitor
CMP	Common myeloid progenitor
CMRP	Long-term repopulating common myeloid progenitor
CSF	Colony stimulating factor
Ct	Threshold cycle
DC	Dendritic cell
DPBS	Dulbecco's Phosphate buffered saline
E(#)	Embryonic day #
EGFC	Erythroid growth factor combination
eGFP	Enhanced green fluorescent protein
EM-grade	Electron microscopy-grade
EML	Erythroid-Myeloid-Lymphoid
EP	Erythroid progenitor
Epo	Erythropoietin
EpoR	Erythropoietin receptor
ERK	Extracellular-signal-regulated kinase
ESC	Embryonic stem cell
ETP	Early thymic progenitor
eYFP	Enhanced yellow fluorescent protein
FACS	Fluorescent activated cell sorting
FCS	Fetal calf serum
FDCP	Factor-dependent cell Paterson
Flt3	Fms-like tyrosine kinase 3
Flt3-ITD	Fms-like tyrosine kinase 3 containing internal tandem duplications
Flt3L	Fms-like tyrosine kinase 3 ligand
FSC	Forward scatter

G-CSF	Granulocyte colony stimulating factor
G-CSFR	Granulocyte colony stimulating factor receptor
gDNA	Genomic DNA
GFP	Green fluorescent protein
GM	Granulocytic-myelomonocytic
GM-CSF	Granulocyte-macrophage colony stimulating factor
GM-CSFR	Granulocyte-macrophage colony stimulating factor receptor
GMP	Granulocyte-macrophage progenitor
GPI-1	Glucose phosphate isomerase 1
hG-CSF	Human granulocyte colony stimulating factor
HGF	Haematopoietic growth factor
hGM-CSFR	Human granulocyte-macrophage colony stimulating factor receptor
hHSC	Human haematopoietic stem cell
HIM	Haematopoietic inductive microenvironment
hM-CSFR	Human macrophage colony stimulating factor receptor
HPC	Haematopoietic progenitor cell
HSC	Haematopoietic stem cell
HSPCs	Haematopoietic stem and progenitor cells
IL-1	Interleukin-1
IL-3	Interleukin-3
IL-6	Interleukin-6
IL-7	Interleukin-7
IMDM	Iscoe's modified dulbecco's medium
Lin	Lineage associated cell surface markers
LMPP	Lymphoid-primed multipotent progenitor
LS ⁻ K	Lin ⁻ Sca1 ⁻ c-Kit ⁺
LSK	Lin ⁻ Sca1 ⁺ c-Kit ⁺
LT-HSC	Long-term repopulating haematopoietic stem cell
LTC-IC	Long-term culture-initiating cell
LyHSC	Lymphoid-biased haematopoietic stem cell
M-CSF	Macrophage colony stimulating factor
M-CSFR	Macrophage colony stimulating factor receptor
MAPK	Mitogen-activated protein kinase
MegE	Megakaryocyte-erythroid
MEP	Megakaryocyte-erythroid progenitor
MERP	Long-term repopulating megakaryocyte-erythroid progenitor
MFI	Mean fluorescence intensity
MGFC	Myeloid growth factor combination
MHC	Major histocompatibility complex
MkRP	Long-term repopulating megakaryocyte-restricted progenitor
Mpl	myeloproliferative leukaemia
MPP	Multipotent progenitor
mTOR	Mammalian target of rapamycin
MyHSC	Myeloid-biased haematopoietic stem cell
MyRP	Long-term repopulating myeloid-restricted progenitor
NK	Natural killer
NTC	No template control

PFA	Paraformaldehyde
PI3K	Phosphoinositide 3 kinase
pS6	Phospho-ribosomal protein S6
qRT-PCR	Quantitative reverse transcriptase polymerase chain reaction
rcf	Relative centrifugal force
Rh	Rhodamine 123
rm	Recombinant mouse
RT	Reverse transcriptase
RT-PCR	Reverse transcriptase polymerase chain reaction
SCF	Stem cell factor
sh	Small-hairpin
SLAM	Signaling lymphocytic activation molecule
SP	Side population
SSC	Side scatter
ST-HSC	Short-term repopulating haematopoietic stem cell
STAT	Signal transducer and activator of transcription
TF	Transcription factor
TGF	Transforming growth factor
Tpo	Thrombopoietin
vWF	Von Willebrand Factor
WT	Wild type
YFP	Yellow fluorescent protein

TABLE OF CONTENTS

ACKNOWLEDGEMENTS.....	i
ABBREVIATIONS	iii
LIST OF FIGURES	ix
LIST OF TABLES	xii
Chapter 1: INTRODUCTION	1
1.1 The nature of early haematopoietic stem and progenitor cells in the adult	3
1.2 Models of haematopoiesis: The progeny of haematopoietic stem cells.....	8
1.3 Decision-making during haematopoiesis	16
1.3.1 A stochastic model of haematopoiesis	16
1.3.2 Haematopoietic growth factors	32
1.3.3 Lineage-bias in the haematopoietic system.....	66
1.4 Aims of project	70
Chapter 2: MATERIALS AND METHODS.....	72
2.1 Mice.....	72
2.2 Analysis of HemaExplorer and BloodSpot databases	72
2.3 Bone marrow cell preparation	73
2.4 Preparation of bone marrow for flow cytometric analysis	74
2.5 Preparation of bone marrow for fluorescent activated cell sorting.....	75
2.6 Antibody titration for fluorescent activated cell sorting and flow cytometric analysis	77
2.7 Preparation of bone marrow cell lysates for testing and optimisation of qRT-PCR assays	78
2.8 qRT-PCR assay design and optimisation for gene expression analysis.....	79
2.8.1 Identification of candidate sequences for the design of qRT-PCR assays	79
2.8.2 Optimisation of qRT-PCR primer concentrations.....	82
2.8.3 Optimisation of hydrolysis probe concentrations.....	86
2.9 qRT-PCR analysis	88
2.9.1 Preparation of cells previously sorted into LightCycler 480 384-well plates for qRT-PCR analysis	88
2.9.2 Amplification program used on the Roche LC480 II PCR instrument for analysis of gene expression	90
2.10 Conjugation of purified antibodies to APC using Lightning Link.....	91
2.11 Haematopoietic stem cell and multipotent progenitor <i>in vitro</i> culture	92

2.12 Phosphoflow: Analysis of phosphorylated proteins using flow cytometry	92
2.13 Methylcellulose colony forming assays	93
2.13.1 Plating of haematopoietic stem cells on MethoCult M3434	93
2.13.2 Cytospin preparations	94
2.13.3 Identification of colonies	95
2.14 Graphing of data and statistical analysis	96
2.15 Figure illustration	97
Chapter 3: EXPRESSION OF RECEPTORS FOR GROWTH FACTORS DURING	
HAEMATOPOIESIS	98
3.1 Introduction.....	98
3.1.1 Aims of chapter	101
3.2 Investigation of <i>FLT3</i> , <i>EPOR</i> , <i>CSF1R</i> and <i>CSF3R</i> expression during haematopoiesis using the HemaExplorer and BloodSpot databases	102
3.3 Gating strategy for the isolation and analysis of haematopoietic stem and progenitor cells.....	108
3.4 Optimisation of qRT-PCR assays for the detection of growth factor receptor gene expression	111
3.4.1 <i>ACTB</i> as an endogenous control gene for qRT-PCR analysis	111
3.4.2 <i>ACTB</i> , <i>FLT3</i> , <i>EPOR</i> , <i>CSF1R</i> and <i>CSF3R</i> qRT-PCR assay design	113
3.4.3 Optimisation of <i>ACTB</i> , <i>FLT3</i> , <i>EPOR</i> , <i>CSF1R</i> and <i>CSF3R</i> qRT-PCR assays	117
3.5 Expression of growth factor receptor transcripts during haematopoiesis.....	133
3.5.1 Expression of <i>Flt3</i> , <i>Epor</i> and <i>Csf1r</i> transcripts by haematopoietic stem and progenitor cells	133
3.5.2 Analysis of <i>FLT3</i> and <i>EPOR</i> co-expression within the haematopoietic stem cell and multipotent progenitor compartments	143
3.6 Expression of growth factor receptor protein during haematopoiesis	153
3.6.1 Flt3 and M-CSFR protein expression on the surface of single haematopoietic stem and progenitor cells	153
3.6.2 Investigation of Flt3 and M-CSFR co-expression by haematopoietic stem cells and multipotent progenitors	160
3.6.3 Correlation between the presence of Flt3 and the levels of CD150 expressed on the surface of haematopoietic stem cells	164
3.7 Discussion.....	167
3.7.1 Flt3, EpoR and M-CSFR mark distinct subpopulations of haematopoietic stem cells and multipotent progenitors and these receptors are rarely co-expressed	167

3.7.2 Expression of Flt3 within the haematopoietic stem cell compartment is associated with decreased self-renewal capacity.....	176
3.7.3 Heterogenic patterns of Flt3, EpoR and M-CSFR expression identify distinct subpopulations within maturing progenitor compartments.	178
3.7.4 The HemaExplorer and BloodSpot databases provide accurate information regarding the expression of <i>FLT3</i> , <i>EPOR</i> and <i>CSF1R</i> during haematopoiesis.	181
Chapter 4: INVESTIGATION OF FUNCTIONAL FLT3 RECEPTOR EXPRESSION WITHIN THE HAEMATOPOIETIC STEM CELL COMPARTMENT	184
4.1 Introduction.....	184
4.1.1 Role of Flt3 during early haematopoiesis.....	185
4.1.2 Flt3 signalling in haematopoietic stem and progenitor cells	188
4.1.3 Aims of chapter	190
4.2 Phospho-protein analysis of downstream signalling proteins within the haematopoietic stem cell compartment following stimulation with Flt3L	191
4.3 Expression of <i>SPI1</i> within the haematopoietic stem cell compartment following stimulation with Flt3L.....	203
4.4 Effects of Flt3L on haematopoietic stem cells during colony formation <i>in vitro</i>	213
4.5 Discussion.....	219
4.5.1 Multipotent progenitors but not haematopoietic stem cells respond to Flt3L stimulation <i>in vitro</i>	219
4.5.2 A role for Flt3L in the regulation of multipotent progenitors during steady-state haematopoiesis.....	224
Chapter 5: CONCLUSIONS	228
5.1 Final Discussion	228
5.2 Future Directions.....	240
APPENDIX A: Materials.....	243
APPENDIX B: Antibodies	244
REFERENCES	245

LIST OF FIGURES

Figure 1.1. Models used to identify haematopoietic stem and progenitor cells in the adult mouse bone marrow	5
Figure 1.2. Models of haematopoiesis	9
Figure 1.3. The pairwise relationship model of haematopoiesis	12
Figure 1.4. HSPC hierarchy applied to the pairwise relationship model	14
Figure 1.5. Alternative developmental routes of HSCs towards neutrophils.....	15
Figure 1.6. A timeline for the discovery and early characterisation of haematopoietic growth factors	35
Figure 1.7. Permissive actions of HGFs	45
Figure 1.8. Instructive actions of HGFs	55
Figure 2.1. Isolation of single LT-HSCs.....	76
Figure 2.2. Example of an antibody titration used for flow cytometry	78
Figure 2.3. Workflow of multiplex qRT-PCR assay design and optimisation for detection of gene expression in single cells.	79
Figure 2.4. 384-well plate format used to determine limiting primer concentrations for qRT-PCR assays.....	84
Figure 2.5. Selection of limiting primer concentrations for a qRT-PCR assay	85
Figure 2.6. Optimisation of hydrolysis probe concentrations for a qRT-PCR assay.	87
Figure 3.1. Expression of growth factor receptors by haematopoietic stem and progenitors according to the HemaExplorer and BloodSpot databases	104
Figure 3.2. Isolation of haematopoietic stem and progenitor cells from mouse BM	109
Figure 3.3. Investigation of <i>ACTB</i> expression by HSPC populations.....	112
Figure 3.4. Sequence alignment of <i>ACTB</i> , <i>FLT3</i> , <i>EPOR</i> , <i>CSF1R</i> and <i>CSF3R</i> qRT-PCR assays within regions of their target genes	115
Figure 3.5. Amplification of qRT-PCR assay targets in whole BM with and without reverse transcriptase	119
Figure 3.6. Ct values obtained during primer optimisation of qRT-PCR assays	120
Figure 3.7. Peak fluorescence obtained during primer optimisation of qRT-PCR assays....	121
Figure 3.8. Optimisation of hydrolysis probe concentration for <i>ACTB</i> , <i>FLT3</i> , <i>EPOR</i> , <i>CSF1R</i> and <i>CSF3R</i> qRT-PCRs	123
Figure 3.9. Isolation of CD115+ leukocytes, Ly6G ⁺ granulocytes and EPs from mouse BM to test the single cell sensitivity of the <i>CSF1R</i> , <i>CSF3R</i> and <i>EPOR</i> qRT-PCR assays.....	124
Figure 3.10. Detection of <i>ACTB</i> , <i>FLT3</i> , <i>EPOR</i> and <i>CSF1R</i> gene expression in single cells	125
Figure 3.11. Amplification of <i>Csf1r</i> and <i>Csf3r</i> from single cells.....	127
Figure 3.12. Validation of <i>FLT3</i> , <i>EPOR</i> and <i>CSF1R</i> qRT-PCR assays in duplex with <i>ACTB</i> using single cells.....	128
Figure 3.13. Validation of triplex qRT-PCR assays using single cells	130

Figure 3.14. Amplification of <i>Actb</i> , <i>Flt3</i> and <i>Epor</i> in single cells using triplex qRT-PCR reactions	131
Figure 3.15. Amplification of <i>Actb</i> , <i>Epor</i> and <i>Csf1r</i> in single cells using triplex qRT-PCR reactions	132
Figure 3.16. Analysis of <i>FLT3</i> expression by single LT-HSCs	134
Figure 3.17. Expression of <i>Flt3</i> , <i>Epor</i> and <i>Csf1r</i> transcripts by HSPCs	138
Figure 3.18. Levels of <i>FLT3</i> , <i>EPOR</i> and <i>CSF1R</i> expression within HSPC populations	142
Figure 3.19. Sequence alignment of <i>EPOR-2</i> qRT-PCR assay within a region of the <i>EPOR</i> gene	144
Figure 3.20. Optimisation of <i>EPOR-2</i> qRT-PCR assay for detection of single cell gene expression.....	146
Figure 3.21. Amplification of target transcripts using the <i>ACTB</i> , <i>FLT3</i> and <i>EPOR-2</i> qRT-PCR assays in singleplex and triplex	147
Figure 3.22. Single-cell sensitivity of <i>ACTB</i> , <i>FLT3</i> and <i>EPOR-2</i> qRT-PCR assays in triplex....	149
Figure 3.23. Amplification of <i>Actb</i> , <i>Flt3</i> and <i>Epor</i> transcripts in single ST-HSCs using a triplex qRT-PCR assay.....	150
Figure 3.24. Co-expression analysis of <i>Flt3</i> and <i>Epor</i> transcripts by haematopoietic stem and progenitor cells	150
Figure 3.25. Levels of <i>FLT3</i> and <i>EPOR</i> co-expression by ST-HSCs.....	152
Figure 3.26. Specificity of anti-G-CSFR antibody after APC conjugation	154
Figure 3.27. Flt3 and M-CSFR expression profiles of haematopoietic stem and progenitor cells	155
Figure 3.28. Cell surface expression of Flt3 and M-CSFR by haematopoietic stem and progenitor cells	157
Figure 3.29. Cell surface expression of IL-7R α by BM haematopoietic stem and progenitor cells	158
Figure 3.30. Gating strategy used to investigate the co-expression of Flt3 and M-CSFR on the surface of HSCs	161
Figure 3.31. Co-expression of Flt3 and M-CSFR on the surface of HSCs and MPPs	162
Figure 3.32. Expression of Flt3 and M-CSFR within the LT-HSC, ST-HSC and MPP compartments	164
Figure 3.33. Analysis of CD150 expression levels on the surface of HSCs. CD150 ^{hi} and CD150 ^{int} cells were gated when analysing Flt3 and M-CSFR expression on the surface of HSCs	165
Figure 3.34. Levels of CD150 expressed by Flt3 ⁺ and M-CSFR ⁺ HSCs	166
Figure 3.35. Mapping of <i>FLT3</i> , <i>CSF1R</i> and <i>EPOR</i> gene expression to the pairwise model ..	170
Figure 3.36. Mapping of Flt3 and M-CSFR protein expression to the pairwise model.....	174
Figure 4.1. Verification of cell surface marker antigenicity following fixation and permeabilisation of cells.....	193
Figure 4.2. Breakdown of APC-Cy7 following fixation and permeabilisation treatment	195

Figure 4.3. Verification of HSPC staining protocol following fixation with PFA and permeabilisation with acetone	197
Figure 4.4. Staining of pS6 in BM cells using flow cytometry.....	198
Figure 4.5. Staining of pS6 in MPPs using flow cytometry	199
Figure 4.6. Comparison of lab prepared PFA to commercial EM-grade PFA for the use in the phosphoflow pS6 staining protocol for LSK cells	201
Figure 4.7. Response of HSCs and MPPs to Flt3L	202
Figure 4.8. Sequence alignment of <i>SPI1</i> qRT-PCR assays within the <i>SPI1</i> gene	205
Figure 4.9. Optimisation of the <i>SPI1</i> qRT-PCR assay for detection of single cell gene expression.....	206
Figure 4.10. Detection of single cell gene expression using the <i>SPI1</i> qRT-PCR assay.	208
Figure 4.11. Sorting of single cells to determine the effects Flt3L stimulation on <i>SPI1</i> expression.....	209
Figure 4.12. Expression of <i>SPI1</i> by HSCs after culture with or without Flt3L	211
Figure 4.13. Sorting of single cells to determine the effects Flt3L stimulation after a serum-free starvation period on <i>SPI1</i> expression	212
Figure 4.14. Brightfield images of colonies formed after seeding HSCs into methylcellulose medium.....	214
Figure 4.15. Cytospin preparations of colonies formed after seeding HSCs into methylcellulose medium	216
Figure 4.16. Effects of Flt3L on colony formation after seeding HSCs into methylcellulose medium.....	217
Figure 5.1. Selective expression of haematopoietic growth factors within the MPP compartment	234

LIST OF TABLES

Table 1: Example of a master mix preparation for the optimisation of qRT-PCR primer concentrations	83
Table 2: Example of a master mix preparation for the optimisation of qRT-PCR hydrolysis probe concentrations	86
Table 3: Example of a master mix preparation for the analysis of gene expression in single cells.....	89
Table 4: Amplification program used for the one-step gene expression analysis using the Qiagen Quntitect qRT-PCR kit	90
Table 5: Surface marker expression profile of the HSPC populations included in the HemaExplorer and BloodSpot databases	106
Table 6: Proportion and phenotype of haematopoietic stem and progenitor cells within the mouse BM	110
Table 7: Intron size for the interrogated exon-exon junctions in the <i>ACTB</i> , <i>FLT3</i> , <i>EPOR</i> , <i>CSF1R</i> and <i>CSF3R</i> genes.....	114
Table 8: Primer and hydrolysis probe sequence for the <i>ACTB</i> , <i>FLT3</i> , <i>EPOR</i> , <i>CSF1R</i> and <i>CSF3R</i> qRT-PCR assays.....	116
Table 9: Optimum primer and hydrolysis probe concentrations of qRT-PCR assays for the detection of gene expression by single cells	126
Table 10: Percentage of wells assayed that produced successful amplification of <i>Actb</i> for each HSPC population	136
Table 11: Details of the <i>EPOR</i> -2 qRT-PCR assay	148
Table 12: Details of the <i>SPI1</i> qRT-PCR assay	204
Table 13: Types and number of colonies identified when scoring the growth and development of HSCs in M3434 with and without Flt3L.....	218
Table 14: Materials used during study.....	243
Table 15: Monoclonal antibodies used for flow cytometric analysis.....	244

CHAPTER 1: INTRODUCTION

The formation of blood and immune cells in adult mammals is a complex and tightly regulated system controlled by the self-renewal and differentiation of rare quiescent haematopoietic stem cells (HSCs) that reside within the bone marrow (BM). HSCs are at the apex of the haematopoietic hierarchy, and have the ability to self-renew and differentiate to maintain the haematopoietic system. As HSCs mature, they give rise to multipotent progenitors (MPPs), which are more proliferative than HSCs and lack long-term self-renewal capacity. MPPs then differentiate to give rise to functional cell types *via* progenitor cell intermediates. These terminally differentiated cells are typically divided into the lymphoid and myeloid families and will be discussed briefly below. For a detailed description of immune cell function, see [1].

The lymphoid family contains cells of both the innate and adaptive immune systems, and is comprised of T-lymphocytes, B-lymphocytes and natural killer (NK) lymphocytes [1]. T-lymphocytes, which mature in the thymus, are mainly involved in cell-mediated immunity, and can be divided into a number of subfamilies that are responsible for immunological memory, cell-mediated cytotoxicity and regulating the immune response. B-lymphocytes mature in the BM and are classically involved in regulating immune function *via* humoral immunity. NK lymphocytes, which classically form the innate component of the lymphoid family, are cytotoxic cells that rapidly respond to tumor cells and viral infection, and are key players in transplant rejection.

The myeloid family includes monocytes/macrophages, granulocytes, megakaryocytes and erythrocytes [1]. Monocytes, which are precursors to macrophages, circulate in the blood and play an important role in both homeostasis and inflammation. Following inflammation, monocytes migrate to target tissues and differentiate into macrophages which act as phagocytes and professional antigen presenting cells (AgPCs) [1]. Under normal physiological conditions, tissue-resident macrophages perform general and tissue-specific functions, such as removal of cellular debris and immune surveillance [2]. Granulocytes make up the polymorphonuclear family of cells and can be divided into neutrophils, eosinophils, basophils and mast cells. Neutrophils are the most abundant immune cells within the blood and are key players in the early innate immune response to infection. In response to inflammation, neutrophils act as phagocytes, AgPCs and undergo degranulation, releasing molecules with antimicrobial properties into the surrounding extracellular matrix [1]. Eosinophils are the main component of the immune system that defend against multicellular parasites, such as helminths, and also contribute towards allergic responses [1]. Similarly, basophils and mast cells are integral in the development of allergy, and protect against parasitic infections [1]. While mast cells are classically thought to arise from basophils, this has been contested [3].

Megakaryocytes are large BM-resident cells that undergo fragmentation of their plasma membrane and cytoplasm to generate thrombocytes (platelets), which contribute to haemostasis: a process that prevents bleeding following vessel injury [4]. Erythrocytes, are responsible for oxygen homeostasis, and mature cells are enucleated in adults [5]. As megakaryocytes and erythrocytes are not classically considered to be involved in immune responses [6, 7], the myeloid family is commonly divided into granulo-myelomonocytic (GM)

and megakaryocyte-erythroid (MegE) subfamilies, which segregate the immune and non-immune cells respectively.

The final cellular component of the immune system is the dendritic cell (DC), which does not align with conventional myeloid and lymphoid dichotomy (Further discussed in **Section 1.2**). DCs are AgPCs that are important in linking the innate and adaptive immune responses, and can be derived from both myeloid and lymphoid progenitor cells. Myeloid- and lymphoid-derived DCs have been shown to be phenotypically and transcriptomically homogeneous [8], and it has been suggested that DCs should be considered as a separate lineage given their ancestry [9].

This introduction aims to give a comprehensive review of the haematopoietic system with emphasis on how haematopoietic stem and progenitor cells (HSPCs) make decisions during differentiation to give rise to the mature cell-fates highlighted above. First, characterisation of the adult HSC and the haematopoietic hierarchy will be addressed. Then the mechanisms underlying decision making in haematopoiesis will be explored with particular focus on two models of haematopoietic lineage commitment.

1.1 The nature of early haematopoietic stem and progenitor cells in the adult

Advancements in cell isolation techniques have facilitated the purification of highly homogeneous murine HSPC populations based on the expression of a range of cell surface markers. These techniques have permitted the functional classification of rare

subpopulations of HSCs and MPPs within the mouse BM. In the adult mouse, HSCs and their early progeny express the surface markers c-Kit and Sca1 [10, 11]. These markers are lost as they begin to differentiate and acquire lineage associated cell surface markers (Lin), including; B220, which is present on B-lymphocytes [12]; CD3, a marker for mature T-lymphocytes [13]; CD11b and Gr-1, mature DC and myeloid cell markers [14, 15]; and TER-119, which is expressed by erythroid cells [16]. As such, virtually all of the multilineage potential of the BM resides within the Lin⁻ Sca1⁺ c-Kit⁺ (LSK) compartment.

Traditionally, early HSPCs are functionally classified based on their ability to provide multilineage reconstitution for a defined period of time when transplanted into an irradiated host. These functionalities are assessed by performing competitive repopulating unit assays whereby varying numbers of genetically distinct test cells (such as HSCs) and helper cells (usually whole BM cell suspensions) are transplanted into irradiated mice. The contribution of the donor test cells to haematopoietic cells in the peripheral blood is then measured over time. Usually, donor contribution of >1% to each lineage is required to confirm multilineage reconstitution [17]. Long-term repopulating HSCs (LT-HSCs) are defined as cells that are capable of multilineage reconstitution in primary irradiated recipients for at least six months, and can subsequently repopulate a secondary irradiated recipient [18]. Short-term repopulating HSCs (ST-HSCs) are considered to possess multilineage potential, and reconstitute the haematopoietic system in an irradiated host for 8-12 weeks [19, 20]. Finally, MPPs have very little self-renewal ability, and are only capable of transient multilineage engraftment when transferred into primary irradiated hosts [21, 22]. Interestingly, recent studies have shown that not all long-term repopulating cells in the mouse and human are capable of multilineage reconstitution [23, 24], and some are biased towards particular

lineages [9, 25-32]. These findings suggest that the current functional criteria used to define early HSPCs is outdated (discussed in **Section 1.3.3**).

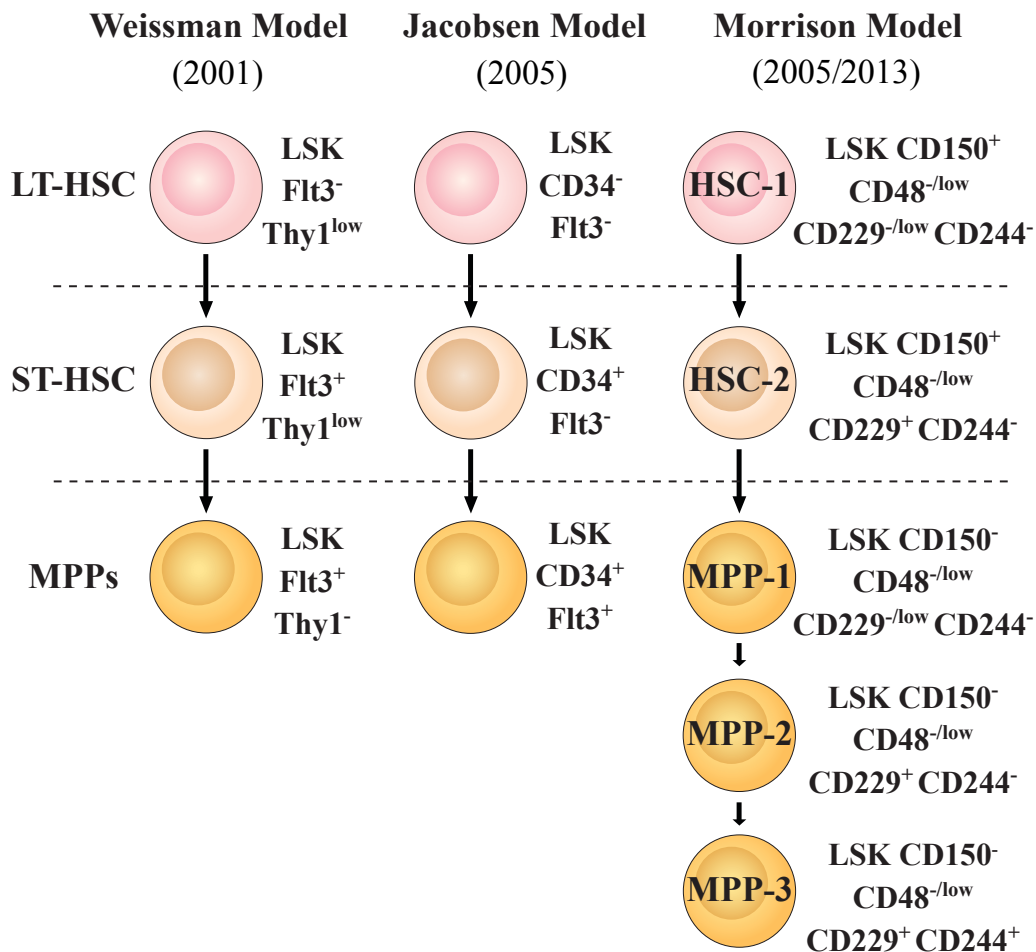


Figure 1.1. Progression of the models used to identify HSPCs in the adult mouse bone marrow. Cell surface antigens are used to distinguish LT-HSCs, ST-HSCs, and MPPs. Early reports from the Weissman group made use of the LSK and Thy1.1 to identify HSCs and MPPs, and the group later used Flt3 expression to distinguish between LT-HSCs and ST-HSCs in 2001 [20, 33]. In 2005, the Jacobsen further refined the Weissman model by showing that Flt3 is absent from ST-HSCs, and that CD34 can be used to distinguish between LT-HSCs and ST-HSCs [21]. That same year, the Morrison group proposed a staining strategy to identify early HSPCs using the signalling lymphocytic activation molecule family markers; CD150, CD48, and CD244 [22]. In 2013, the Morrison group added CD229 to their staining strategy to distinguish myeloid-biased HSC-1 and lymphoid-biased HSC-2 subpopulations, which share characteristics with LT-HSCs and ST-HSCs, respectively. They also identified three MPP subpopulations [34]. HSPCs, haematopoietic stem and progenitor cells; LT-HSC, long-term haematopoietic stem cell; ST-HSC, short-term haematopoietic stem cell; MPP, multipotent progenitor; LSK, lineage associated surface markers⁻, Sca1⁺, c-Kit⁺; Flt3, fms-like tyrosine kinase 3.

The LSK compartment was originally subdivided based on the expression of Thy1.1 and fms-like tyrosine kinase 3 (Flt3), as described by the Weissman group (**Figure 1.1; Weissman model**) [20, 33, 35, 36]. At the time, the group proposed that these markers could be used to distinguish between Thy1.1^{lo}Flt3⁻ LT-HSCs, Thy1.1^{lo}Flt3⁺ ST-HSCs, and Thy1.1⁻Flt3⁺ MPPs. In 2005, Jacobsen's group showed that Flt3 was, in fact, absent on ST-HSCs [21]. This finding led the Jacobsen group to propose the use of Flt3 and CD34, a marker previously shown to be absent from the surface of LT-HSCs [37, 38], in combination with the LSK immunophenotype to identify LT-HSCs (LSK CD34⁻ Flt3⁻), ST-HSCs (LSK CD34⁺ Flt3⁻), and MPPs (LSK CD34⁺ Flt3⁺) (**Figure 1.1; Jacobsen model**) [21].

The Morrison group has used the signalling lymphocytic activation molecule (SLAM) family markers (CD150, CD48, CD229 and CD244) to resolve HSC and MPP subpopulations (**Figure 1.1; Morrison model**) [22, 34]. In 2005, Kiel *et al.* defined HSCs and MPPs based on their expression of CD150, CD48 and CD244 [22]. They reported that CD48 expression in the BM marks lineage restricted progenitors, and that HSCs and MPPs are CD150⁺ CD48⁻ CD244⁻ and CD150⁻ CD48⁻ CD244⁺, respectively. In this study, they also investigated the expression of these markers by cells within the LSK compartment to show that 47% of CD150⁺ CD48⁻ LSK cells provide long-term reconstitution in transplantation assays, while only 20% of Thy1^{lo} LSK cells were capable of the same [22]. The addition of CD229 to this panel led Oguro and co-workers to characterise the HSC-1 and HSC-2 populations [34]. The CD229⁻ HSC-1 are myeloid-biased (MyHSCs) and rarely divide, while the CD229⁺ HSC-2 are lymphoid-biased (LyHSCs) and are more proliferative, and share similarities with LT-HSCs and ST-HSCs, respectively [34]. The Morrison group has proposed that the loss of CD150 expression marks

the loss of self-renewal ability, while others have reported that this marker can be used to identify CD150^{high/med} MyHSCs (discussed in **Section 1.3.3**) [25-27].

While HSC isolation strategies have primarily relied on the use of cell surface markers, Wiessman's group has recently identified the transcription factor (TF) Hoxb5 as a highly specific marker of LT-HSCs [39]. Chen *et al.* used a *Hoxb5:tri-mCherry* reporter system to show that high levels of Hoxb5 strongly correlated with long-term repopulating potential [39]. Notably, the authors demonstrated that 63.9% ± 3% of LSK CD48⁻ CD150⁺ CD229⁻ CD244⁻ HSCs and 82.5% ± 0.4% LSK CD34^{-/lo} CD150⁺ CD41⁻ HSCs were Hoxb5⁺, indicating that HSC isolation strategies that only utilise cell surface markers have limited specificity for true LT-HSCs.

Human HSCs (hHSCs) are not as well characterised as their mouse counterparts, and a number of immunophenotypes have been described for their isolation. hHSCs are commonly identified *in vitro* using long-term culture-initiating cell (LTC-IC) assays, which use BM stromal co-culture systems to provide quantitative assessment of haematopoietic cell production over time [40]. Another, more recent, method for characterising hHSCs is the use of xenograft assays. These assays involve the xenotransplantation of human haematopoietic cells into nonobese diabetic–severe combined immunodeficient mice, which support engraftment of human HSPCs [41, 42]. In contrast to mouse HSCs, hHSCs are traditionally considered to be CD34⁺ CD38⁻, and express low levels of c-Kit [43-51].

Controversy exists regarding whether CD34 is a reliable marker for hHSCs. A number of research groups have identified long-term repopulating cells as Lin⁻ CD34⁺ CD38⁻, suggesting that hHSCs are present within this compartment of the adult BM and umbilical cord blood

[47-51]. On the other hand, other workers have demonstrated that Lin⁻ CD34⁻ cells possess hHSC characteristics, and that Lin⁻ CD34⁻ cells are able to provide multilineage engraftment in primary and secondary recipients [52-54]. Furthermore, there is evidence to suggest that CD34 expression on human HSPCs is reversible, as CD34⁺ cells capable of long-term multilineage engraftment can give rise to CD34⁻ cells and vice versa [53, 55-57]. In 2011, Notta and co-workers identified CD49f as a highly specific marker for hHSCs, and demonstrated that single CD49f⁺ adult BM cells were capable of long-term multilineage engraftment [58]. Other markers that have been proposed to enrich for hHSCs include AC133, HLA-DR, Thy1 and CD45R [58-65].

1.2 Models of haematopoiesis: The progeny of haematopoietic stem cells

Classically, the development of HSCs has been modelled in regards to a dichotomy of the lymphoid and myeloid lineages (**Figure 1.2A**). The model proposes that as HSCs mature, there is a point in their development whereby they irreversibly commit towards either a lymphoid or myeloid fate. In this model, there are only single 'routes' of differentiation towards cells of a particular fate, suggesting a rigid haematopoietic architecture. The myeloid-lymphoid dichotomy model was proposed by the Weissman group following the isolation of two progenitors in the adult mouse BM. In 1997, Kondo *et al.* described a Lin⁻ Sca1^{lo} c-Kit^{lo} Thy1⁻ IL-7R⁺ BM cell which could rapidly generate T-lymphocytes and B-lymphocytes when transplanted into an irradiated host [66]. As the authors did not detect significant myeloid potential during these experiments, the cell was termed the common

lymphoid progenitor (CLP) [66]. Shortly after this, Akashi and co-workers identified a common myeloid progenitor (CMP) as $\text{Lin}^- \text{Sca1}^- \text{c-Kit}^+$ ($\text{LS}^- \text{K}^+$) $\text{IL-7R}^- \text{CD16/32}^{\text{lo}} \text{CD34}^{\text{hi}}$ [67]. This cell gives rise to all myeloid cells *in vivo* through megakaryocyte-erythroid progenitor (MEP) and granulocyte-macrophage progenitor (GMP) intermediates [67].

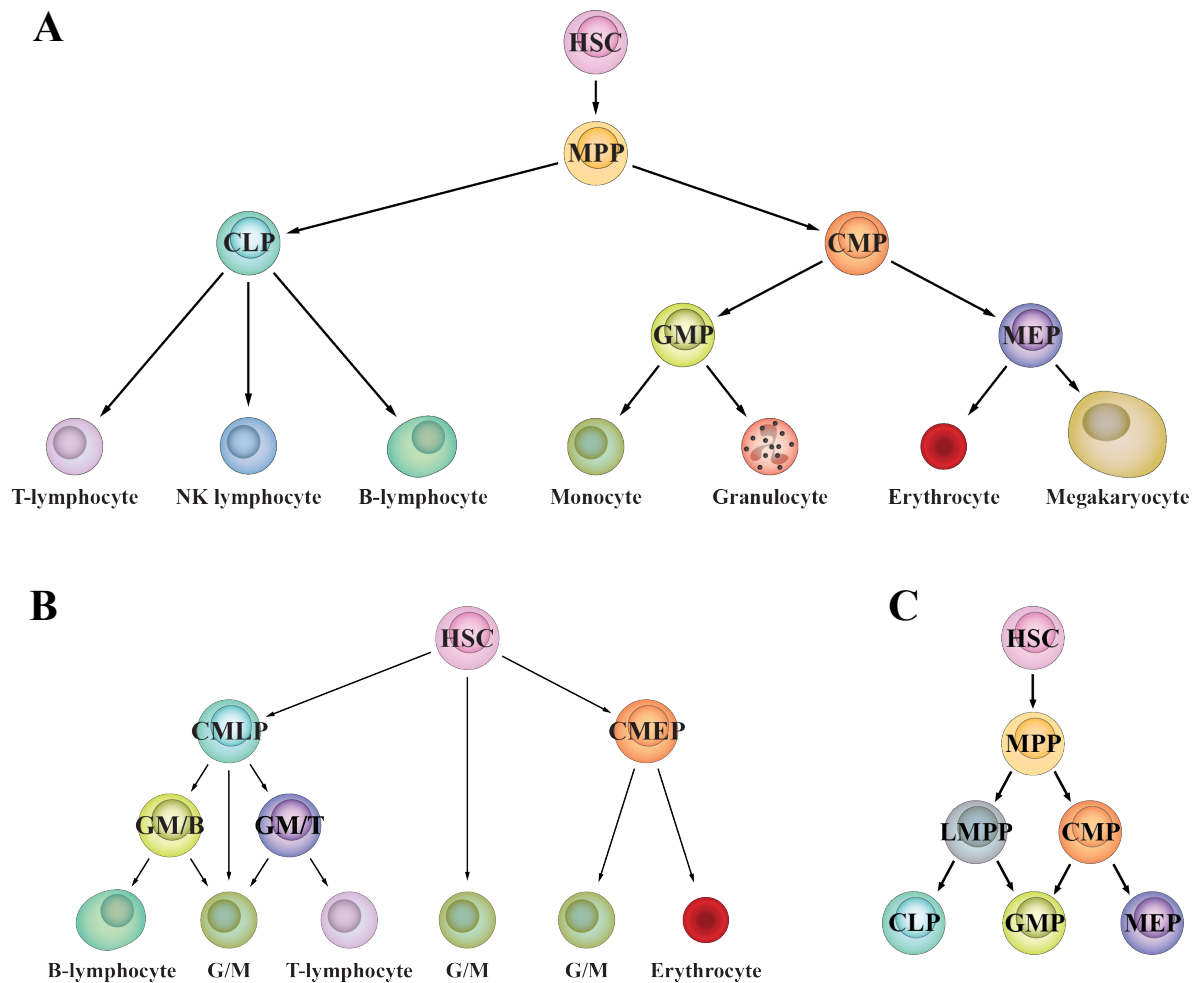


Figure 1.2. Models of haematopoiesis. (A) Following the identification of CLPs [66] and CMPs [67], the Weissman group proposed a myeloid-lymphoid dichotomy model of haematopoiesis whereby HSCs irreversibly commit towards either the lymphoid or myeloid lineage during the early stages of maturation. (B) The Katsura group has used fetal thymic cultures to describe a myeloid-based model of haematopoiesis in which GM potential is maintained as a default during HSPC differentiation towards erythroid, B-lymphocyte and T-lymphocyte cell fates [68-72]. (C) depicts a model proposed by the Jacobsen group following the characterisation of the LMPP [73]. HSC, haematopoietic stem cell; CMP, common myeloid progenitor; CLP, common lymphoid progenitor; GMP, granulocyte-macrophage progenitor; MEP, megakaryocyte-erythroid progenitor; LMPP, lymphoid-primed multipotent progenitor; CMLP, common myelo-lymphoid progenitor; CMEP, common myelo-erythroid progenitor; GM/B, granulocyte-macrophage/B-lymphocyte progenitor; GM/T, granulocyte-macrophage/T-lymphocyte progenitor; G/M, granulocyte/monocyte.

Although the myeloid-lymphoid dichotomy model of haematopoiesis became a very popular model following the studies published by the Weissman group [66, 67], a number of other groups have reported findings that disagree with a myeloid-lymphoid dichotomy. In 1997, Kawamoto *et al.* isolated single Sca1⁺ progenitor cells from mouse fetal livers and used an *in vitro* fetal thymic organ culture system to monitor their differentiation potential [68]. After 10 days in culture, the colonies generated by single Sca1⁺ progenitors were analysed for the presence of T-lymphocytes, B-lymphocytes and GM cells. Some of these cells gave rise to colonies containing all three lineages, while others contained only one or two lineages. Of the colonies containing two lineages, T-lymphocytes and GM cells or B-lymphocytes and GM cells were commonly observed together. However, the authors never observed colonies containing T-lymphocytes and B-lymphocytes without GM cells. Using a similar *in vitro* approach, the group later identified two distinct progenitor cells; i) a cell with GM and lymphoid potential (common myelolymphoid progenitor [CMLP]) and, ii) a cell with GM and erythroid potential (common myeloerythroid progenitor [CMEP]) [71]. This led the Katsura group to propose a myeloid-based model of haematopoiesis (**Figure 1.2B**) [69, 70]. In this model, GM potential is retained as HSPCs differentiate towards the T-lymphocyte, B-lymphocyte and erythroid lineages. GM potential is only lost during the final stages of the T-lymphocyte, B-lymphocyte and erythroid maturation. The myeloid-based model is controversial, especially considering that it is based solely on findings from *in vitro* culture experiments. The identification of restricted lymphoid progenitors *in vivo*, such as the CLP and T-lymphocyte/NK lymphocyte progenitor, argues against such a model [66, 74].

Other, more recent studies have also challenged the myeloid-lymphoid dichotomy. In 2005, Adolfsson *et al.* described the lymphoid-primed multipotent progenitor (LMPP), a Flt3^{hi} LSK

progenitor cell which preferentially generates lymphoid cells but also possesses significant GM potential [73]. The authors noted that these cells generated few erythrocytes and megakaryocytes both *in vitro* and *in vivo*, and proposed a new model in which the first commitment decision made during haematopoiesis results in either loss of lymphoid or MegE potential (**Figure 1.2C**). Subsequently, the Rolink group described another progenitor cell with similar potential to the LMPP [75, 76]. This cell, termed the early progenitor with lymphoid and myeloid potential, has the ability to differentiate into lymphocytes and macrophage/monocytes *in vitro*, and gives rise to B-lymphocytes and T-lymphocytes *in vivo* [75, 76]. Furthermore, Chi and co-workers have shown that CD150⁺ CMPs (preGMs) can generate T-lymphocytes, but not B-lymphocytes, *in vivo* [77].

The myeloid-lymphoid dichotomy, myeloid-based and Jacobsen models of haematopoiesis all rely on strict branching patterns during HSC differentiation, and depict lineage commitment as a rigid process. A more recent model described by Ceredig *et al.* forgoes a lineage branching architecture and proposes that HSCs can progressively differentiate *via* intermediate progenitors towards a continuum of mature cell fates (**Figure 1.3**). This model, termed the pairwise relationship model, proposes that as HSCs differentiate towards a specific cell fate, fates that are the least related to this dominant cell type become latent first, while more closely related fates persist as possible, but less preferred, potentials. The arcs within each layer of the model depict the lineage potential of a particular HSPC. As HSPCs mature, they progress from the centre towards the outer mature cell fates and they become more restricted in regard to their lineage potential (represented by the shortening of the arcs). HSPCs can only lose lineage potentials as they progress along a maturation path, they cannot gain lineage potential. Therefore, the only maturation paths permitted by the

representative illustration (**Figure 1.3**) are ones where each subsequent arc is fully encompassed by the previous arc. For example, the LMPP can give rise to an EPLM because this step results in the loss of granulocyte potential. However, an EPLM cannot then progress a neutrophil-monocyte progenitor stage as this would require the restoration of neutrophil potential.

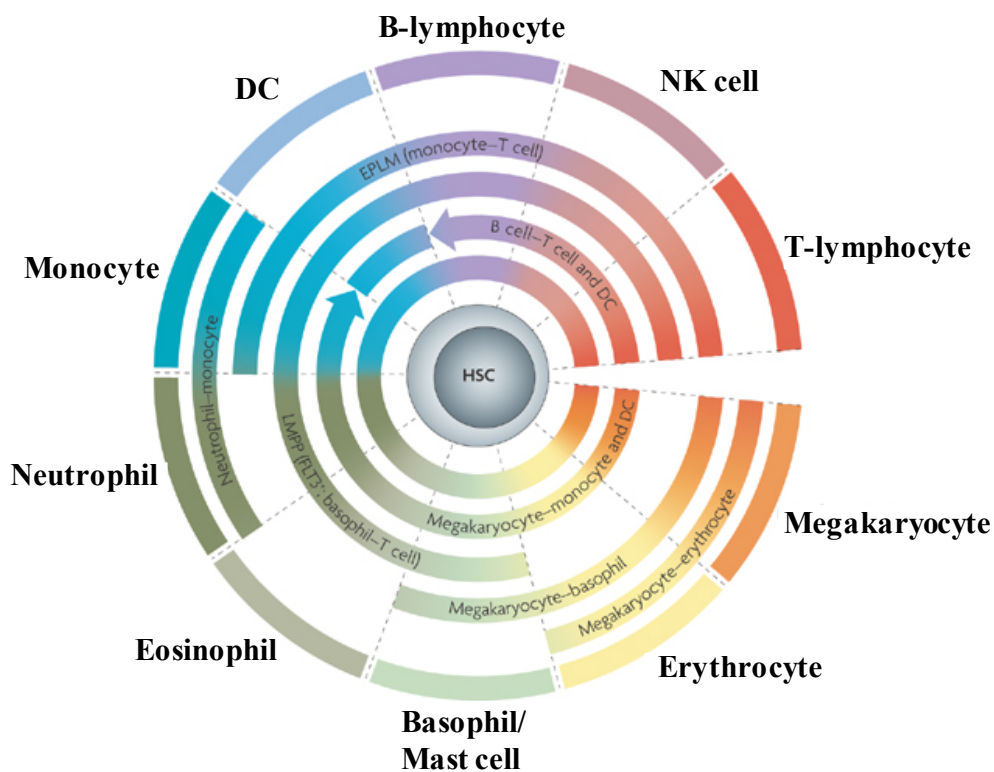


Figure 1.3. The pairwise relationship model of haematopoiesis. The pairwise relationship model describes HSC maturation towards a continuum of mature cell fates, forgoing traditional lineage-branching. The inner arcs depict the maturation potential of haematopoietic progenitors. Both CMPs and CLPs can give rise to DCs [8], as depicted by the arrowheads. Modified from [78] © Macmillan Magazines Ltd. HSC, haematopoietic stem cell; DC, dendritic cell; CMP, common myeloid progenitor; CLP, common lymphoid progenitor; LMPP, lymphoid-primed multipotent progenitor; EPLM, early progenitor with lymphoid and myeloid potential.

The arrangement of mature cell fates is supported by mapping of TF expression; cell fates that are placed adjacent to each other have been shown to share similar TF expression patterns [78, 79]. Additionally, this arrangement of cell lineages is also supported by the possibility of bipotent progenitor cells and infers the existence of only certain bipotent

progenitors. For example, monocyte-DC progenitors and MEPs exist, while a megakaryocyte-T-lymphocyte bipotent progenitor has not yet been described. However, it should be noted that this model is not consistent with some progenitors that have been previously identified. In particular, ETP progenitors do not differentiate into B-lymphocytes but possess GM, DC, NK lymphocyte and T-lymphocyte potential [80-82]. Additionally, T-lymphocyte, but not B-lymphocyte, potential has been detected in the preGM compartment of the mouse BM [77]. Lastly, a monocyte-B-lymphocyte bipotent progenitor has been described, but the DC potential of this cell has not yet been investigated [83, 84]. As the authors state, certain environments and factors may alter the availability and loss of potential cell fates, explaining such progenitors.

Although the pairwise relationship model outlines a less restrictive and more flexible model of haematopoiesis, it does not describe a detailed haematopoietic hierarchy. As such, **Figure 1.4** shows the mapping of a number of previously described progenitor cells to the pairwise relationship model. The CLP and EPLM have been combined in **Figure 1.4** given their similar maturation potentials [66, 75, 76]. As described for **Figure 1.3**, each arc represents the lineage potential of a given cell. Again, cells can only mature along a path that does not result in a gain of lineage potential. The CMP cannot give rise to a CLP or EPLM, as this would require the resoration of lymphoid potential. However, it can give rise to GMPs and MEPs. The figure depicts multiple paths of differentiation to end cell types and forgoes the restrictive nature of past models. For example, neutrophils can be generated from both CMPs and LMPPs (**Figure 1.5**) [67, 73]. Similarly, Ishikawa *et al.* have shown that CLP- and CMP-derived DCs are indistinguishable from each other, indicating two routes of DC differentiation [8].

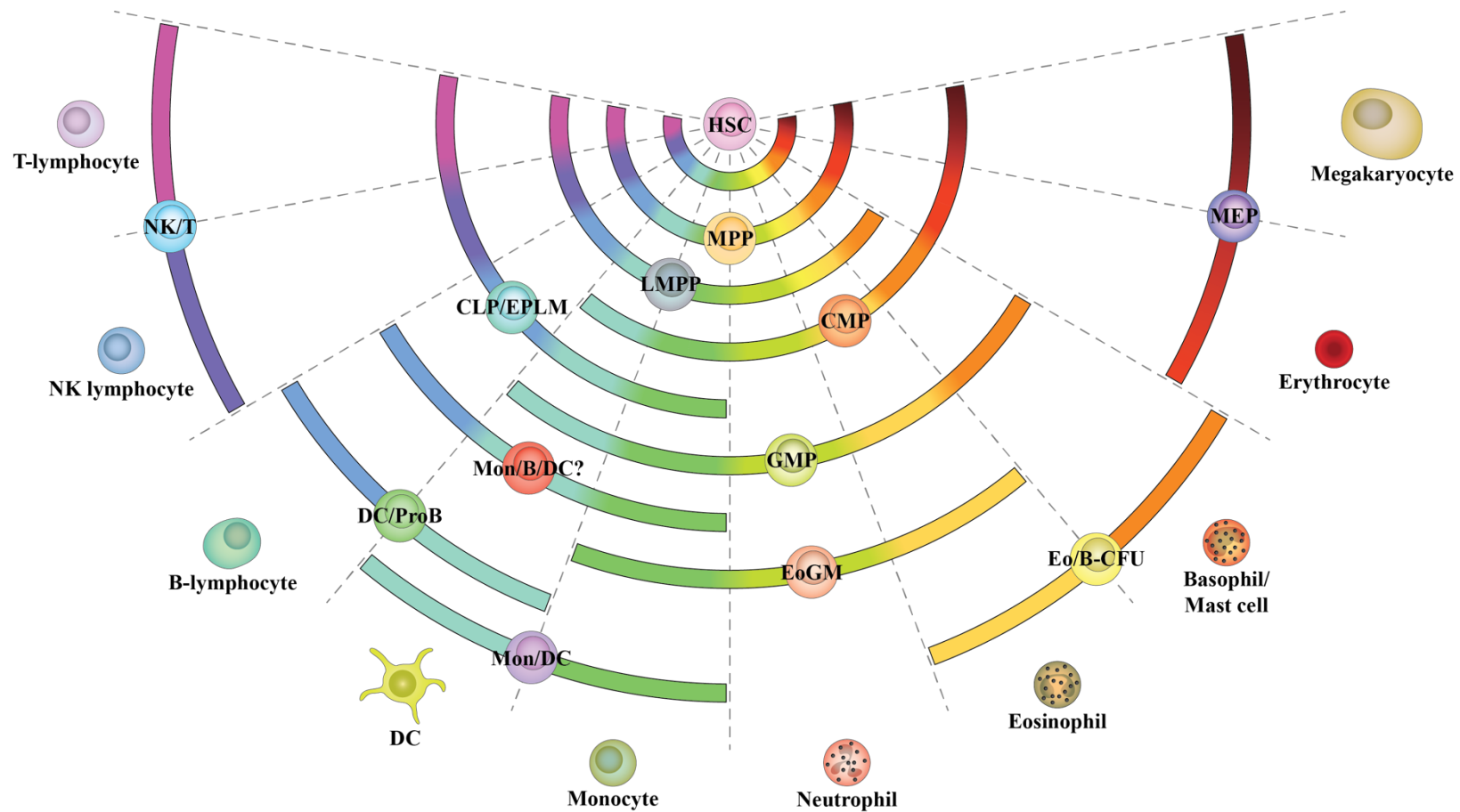


Figure 1.4. HSPC hierarchy applied to the pairwise relationship model. The maturation potential of HSPCs is depicted by the inner arcs. HSPC, haematopoietic stem and progenitor cell; HSC, haematopoietic stem cell; MPP, multipotent progenitor; LMPP, lymphoid-primed multipotent progenitor [73]; CMP, common myeloid progenitor [67]; CLP, common lymphoid progenitor [66]; EPLM, early progenitor with lymphoid and myeloid potential [75]; MEP, megakaryocyte-erythroid progenitor [67]; GMP, granulocyte-macrophage progenitor [67]; DC/Pro-B, dendritic cell/B-lymphocyte progenitor [85]; Mon/B/DC?, monocyte/B-lymphocyte progenitor (dendritic cell potential has not been assessed) [83, 84, 86]; EoGM, eosinophil-neutrophil-monocyte progenitor; Eo/B-CFU, eosinophil/basophil progenitor [87]; NK/T, natural killer lymphocyte/T-lymphocyte progenitor [74]; Mon/DC, monocyte/dendritic cell progenitor [88].

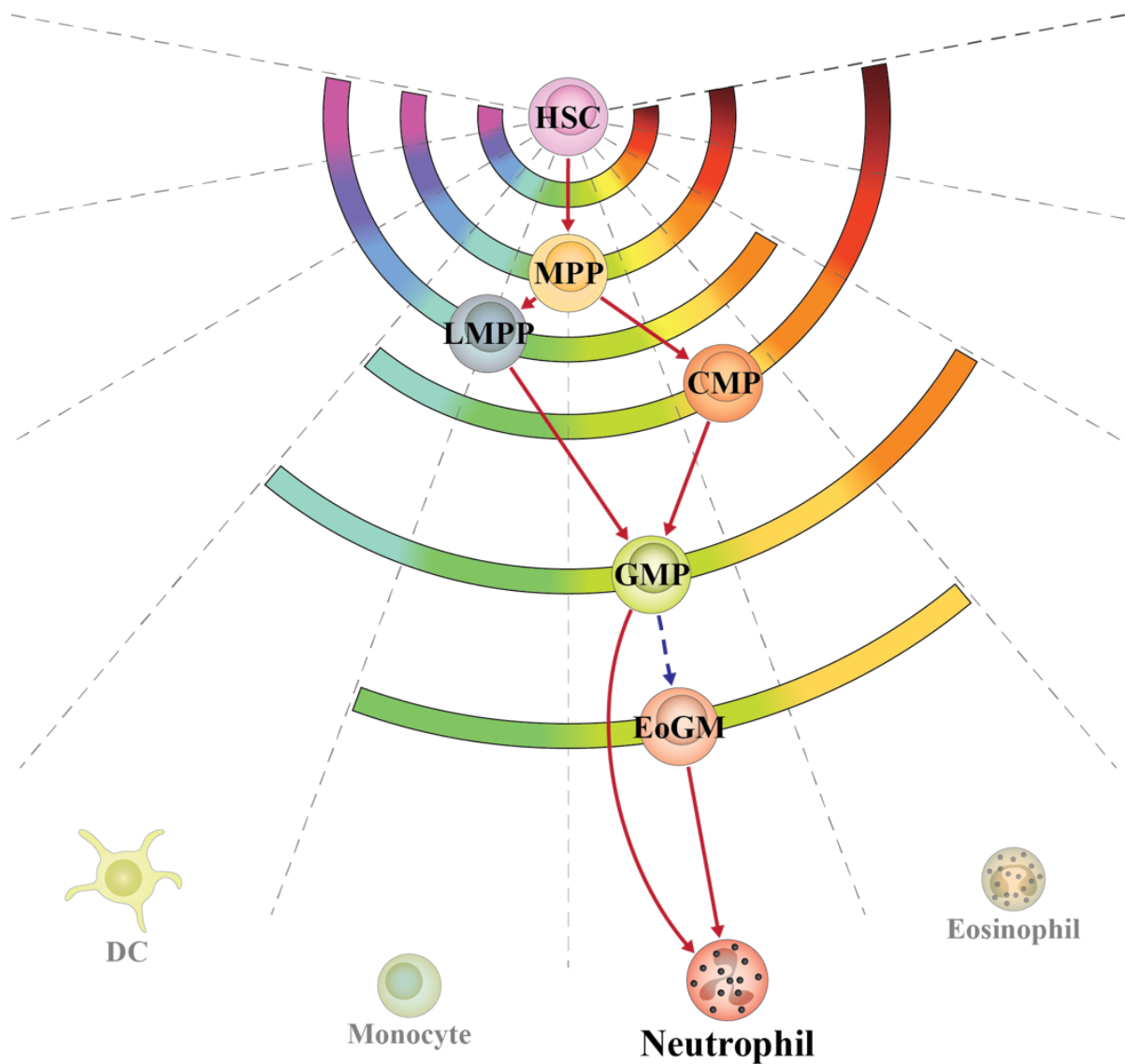


Figure 1.5. Alternative developmental routes of HSCs towards neutrophils. The red solid arrows depict routes that have been confirmed by previous studies, while the blue dashed arrow depicts putative routes. HSC, haematopoietic stem cell; MPP, multipotent progenitor; LMPP, lymphoid-primed multipotent progenitor; CMP, common myeloid progenitor; GMP, granulocyte-macrophage progenitor; EoGM, eosinophil-neutrophil-monocyte progenitor.

1.3 Decision-making during haematopoiesis

1.3.1 A stochastic model of haematopoiesis

Whether the behavior of cells can be described as a stochastic process has been a matter of debate since the 1960s. In the case of haematopoiesis, various aspects of the behavior of haematopoietic cells appear to be governed in a random manner. These include the self-renewal of HSCs, differentiation and lineage commitment of HSPCs, and death of these cells by apoptosis. In the case of lineage commitment, the adult organism is generated from an embryo in seemingly flawless and predictable manner. At first sight, it might seem odd that random cellular events can underlie this process. However, the throw of a dice enough times gives rise to the same and predictable number of 1s, 2s, 3s etc. Such behaviour, together with environmental influences, can give rise to a proper and predictable outcome during normal development. This premise underlies a stochastic model of haematopoiesis.

1.3.1.1 Stochastic self-renewal and differentiation of HSPCs

The notion that stochastic events might occur during haematopoiesis was first proposed by Till and colleagues in 1964 [89]. These workers examined the extent to which HSPCs undergo self-renewal as compared to differentiation or death. Individual HSPCs are capable of forming discrete colonies in the spleen of a mouse when transplanted into an irradiated host [90]. The group performed serial transplantation experiments and examined the number of CFUs within spleen colonies [89]. Ten days post-transplantation, Till *et al.* prepared cell suspensions from individual spleen colonies from the recipient mice, performed a second set of

transplantation experiments, and counted the number of spleen colonies in secondary recipients after 10-14 days. As to the spleen colonies observed in the secondary recipients, the number present in each mouse was not uniform. The data obtained followed a γ -distribution, and Till *et al.* concluded that the distribution of spleen colony forming units (CFU-S) within each of the spleen colonies was variable [89]. The group proposed that the frequency of CFU-S within an individual spleen colony was due to a 'birth and death' process. Using a Monto Carlo method [91], a mathematical equation, the authors concluded the process in which CFU-S undergo self-renewal (birth) and differentiation (or death) was stochastic. In 1973, the Till group provided further evidence to support the notion that the self-renewal and differentiation of CFU-S is a stochastic process. Using the same approach as before [89], they examined the differentiation of CFU-S towards the erythroid and granulocyte lineages [92]. The authors concluded that the fate of CFU-S is determined by random probabilities of the cell undergoing either self-renewal, granulocytic differentiation or erythroid differentiation. They also reported that a granulocytic fate is favoured over an erythroid fate by a factor of 10.

In 1982, Humphries *et al.* performed experiments whereby the non-adherent cells generated from a primary BM-derived cell line were seeded into methylcellulose cultures [93]. The number of CFUs in each of the secondary colonies were found to be heterogeneous in their capacity to generate tertiary colonies. The results could not be explained by Poisson distribution, and Humphries *et al.* concluded the self-renewal versus differentiation of CFUs during colony-formation is governed by a stochastic process. Similar results were obtained when the experiments were repeated using fresh whole BM. The following year, the Ogawa group examined the extent to which spleen colonies are capable of forming granulocyte-

erythroid-megakaryocyte-macrophage colonies (CFUs-GEMM) or colonies of blast cells (CFU-blast) *in vitro* [94]. The group reported that the number of CFU-blast and CFU-GEMM cells generated from each spleen colony was variable, and that the data fit a γ -distribution model. *In vitro* analysis of the generation of T-lymphocyte and erythroid CFUs have led to similar findings, adding support to the viewpoint that self-renewal versus differentiation of HSPCs occurs in a stochastic manner [95, 96].

Later work by Abkowitz *et al.* examined the extent to which clones of individual HSCs contribute to haematopoiesis [97]. Safari cats were used, which possess two distinct X-linked *G6PD* alleles (encoding glucose-6-phosphate dehydrogenase), *d-G6PD* and *G-G6PD*. Inactivation of the X chromosome during embryogenesis is a random process, and therefore, the somatic cells of the Safari cat express either *d-G6PD* or *G-G6PD*. Autologous BM cells were transplanted into irradiated Safari cats and the *G6PD* phenotypes of peripheral erythroid blast forming units (BFU-Es) and granulocyte-macrophage CFUs (CFU-GMs) were monitored over a period of 6 years. This work revealed that the contribution of *d-G6PD* and *G-G6PD* HSCs to peripheral progenitors was highly variable for up to 4.5 years after transplantation. After this time, the contribution of HSCs to peripheral cells stabilised. To determine whether this pattern of HSC behaviour was due to chance, the authors performed computer simulations of the experiments in which the fate of HSCs was designated at random. The findings from the computer simulations accurately mirrored the findings obtained from the *in vivo* analysis. Hence, the results suggest that the manner in which an individual HSC does or does not contribute to steady-state haematopoiesis at any given time is governed by a stochastic process. Although, it should be noted that the simulated model did not predict the stable clonal contribution of HSCs that ultimately occurred in the *in vivo* experiments [97].

In 2000, Abkowitz and colleagues carried out an analysis similar to the above in mice [98]. These workers transplanted a limited number of glucose phosphate isomerase 1 a (GPI-1^a) BM cells alongside competitor GPI-1^b BM cells into irradiated mice. The number of peripheral granulocytes generated from these cells was assessed for 30 weeks. When individual mice were compared, the ratios of GPI-1^a/GPI-1^b contribution to peripheral cells were found to be variable and to change over time. As before, the group accurately reproduced the experimental data using a stochastic computational model, adding support to their experiments performed in Safari cats. The Loeffler group has also examined the contribution of DBA/2 and C57BL/6 fetal liver cells to peripheral leukocytes for up to 20 months following competitive transplantation into primary and secondary hosts [99]. Again, a computational simulation was used to examine the data obtained and the authors reported that the kinetics of the contribution of DBA/2 and C57BL/6 cells to peripheral leukocytes in both primary and secondary recipients fitted a stochastic model.

Evidence to support a stochastic model of haematopoiesis has also been obtained from the analysis of restricted haematopoietic progenitor cells (HPCs). Recently, Hyrien *et al.* employed sub-lethal irradiation to generate a murine model of stress erythropoiesis and investigated the kinetics of murine erythroid colony forming unit (CFU-E) and BFU-E recovery [100]. BM CFU-E and BFU-E were quantified during the recovery phase using *in vitro* colony forming assays, and the findings were compared to a stochastic computer simulation whereby single cells from each cell type either underwent self-renewal, differentiation or death at random. The authors concluded that emergency erythropoiesis can be explained by a stochastic process and that the probability of BFU-E and CFU-E replicating during stress is increased when compared to steady state haematopoiesis.

1.3.1.2 Stochastic lineage commitment of haematopoietic stem and progenitor cells

In 1973, the Till group reported that the probability of CFU-S undergoing commitment towards the granulocyte lineage was greater than the probability of these cells undergoing commitment to the erythroid pathway, and concluded that differentiation of CFU-S towards both granulocyte and erythroid fates occurs in a random manner [92]. Ten years later, Ogawa *et al.* extended this theory, and proposed that commitment of HPCs to all lineages is governed by a stochastic process [101]. To test this theory, Ogawa's group undertook *in vitro* experiments to analyse the commitment of HSPCs towards a specific lineage [102, 103]. In their first study, Suda *et al.* isolated single cells from primary blast cell colonies (prepared from suspensions of mouse spleen cells) and performed methylcellulose colony forming assays to determine their patterns of lineage commitment [102]. The authors noted that the blast colony-derived cells generated colonies that contained variable combinations of cell lineages, and reported that the types of cells generated by each colony displayed no pattern.

To further characterise the lineage specification of single blast colony-derived cells, Suda *et al.* performed a second study whereby the lineage commitment of two cells that were the progeny of a single parent cell was compared [103]. Single cells were isolated from primary blast colonies, and cultured in methylcellulose medium for 18-24 hours until one round of cell proliferation had occurred. The two daughter cells were then harvested, separated and cultured under the same conditions. Colony forming assays were performed using each of the daughter cells, and the lineage composition of secondary and tertiary colonies was examined. Five hundred pairs of daughter cells were cultured, and 387 pairs generated colonies. Of these

pairs, 319 pairs produced colonies that contained the same number and types of cell lineages, while for 68 pairs the daughter cells generated colonies that were dissimilar. These 68 pairs differed as to their lineage combinations, and displayed varying potency, from unipotency to multipotency. As not all of the paired daughter cells displayed homologous lineage potential, Suda and co-workers proposed that both the lineage commitment and lineage potential of HPC progeny are not ordered, and are therefore, governed by a stochastic process [103].

The Ogawa group has performed similar studies using human HPCs and have arrived at the same conclusion. In 1984, Leary and co-workers prepared blast colonies from either fresh human cord blood or BM, and used individual cells from these blast colonies to generate secondary colonies [104]. The investigators then compared the number and types of cells present in each secondary colony. The authors reported that the types of cells found in the secondary colonies were variable. For example, one cell derived from a blast colony formed a secondary colony containing approximately 1,000 eosinophils and basophils, while another cell from the same blast colony generated a secondary colony which contained 180 neutrophils and macrophages. A year later, Leary and co-workers used a similar approach to generate paired daughter cells from My-10⁺ cord blood-derived blast colonies [105]. The group successfully generated colonies from 75 pairs of daughter cells. When the colonies were characterised, forty of these pairs were shown to generate homologous colonies, while the other 35 pairs generated non-homologous colonies. Though the homologous paired colonies displayed similar lineage compositions, the colony size and number of cells from each lineage was variable. Thus, the Ogawa group reported that human haematopoiesis, like murine haematopoiesis, is a stochastic process.

1.3.1.3 Mechanisms underlying stochastic lineage commitment

In a stochastic model of haematopoiesis, lineage specification is regulated by fluctuations in cell-intrinsic factors that occur through stochastic gene expression and competitive interactions between TFs, which eventually result in the manifestations of specific lineage-associated transcriptional programs. These lineage-associated programs are then enforced through positive feedback mechanisms, leading to commitment of the cell towards a particular cell fate. This model is underscored by studies which show that multipotent haematopoietic cells express a number of genes that are associated with several different lineages. This permissive multilineage gene expression activity has been seen as a state of transcriptional priming that precedes lineage commitment. Due to the limitations of isolating and maintaining HSPCs from the mouse BM, early studies investigating the gene expression of multipotent haematopoietic cells made use of haematopoietic cell lines. In particular, factor-dependent cell Paterson (FDCP)-mix cell lines have been indispensable due to their extensive self-renewal capacity when cultured in the presence of IL-3 [106].

In 1992, Herberlein and colleagues performed gene expression analysis of a number of different embryonic stem cell (ESC) and HPC lines, including the FDCP-mix cell line [107]. Using reverse transcriptase polymerase chain reaction (RT-PCR) and northern blot analysis, the authors showed that the genes encoding the erythropoietin (Epo) receptor (EpoR) and the erythroid-associated TF, GATA-1, are expressed in erythroid committed progenitors, multipotent HPCs and ESCs. The authors then performed DNase hypersensitivity analysis of FDCP-mix and commitment progenitor cells, demonstrating that the accessibility of the chromatin within the *EPOR* locus changes as multipotent cells commit to different lineages. The chromatin within the *EPOR* locus is in an open conformation in multipotent cells and

either becomes more accessible as these cells differentiate towards erythroid fates, or becomes less accessible as they differentiate towards non-erythroid fates. In the same year, Jimenez *et al.* demonstrated that the β -globin (*HBB*) locus is DNase I hypersensitive in FDCP-mix cells, but not in granulocytes and monocytes derived from granulocyte-macrophage colony stimulating factor (GM-CSF)/granulocyte colony stimulating factor (G-CSF) treated FDCP-mix cells [108]. Thus, Jimenez and colleagues reported that erythroid genes are expressed in multipotent haematopoietic cells prior to lineage commitment [108].

The Greaves group has observed the expression of lymphoid-associated genes in FDCP-mix cells. Using RT-PCR analysis, Ford *et al.* detected expression of *TCRG* (T-cell receptor γ) transcripts in these cells [109]. DNase I hypersensitivity analysis also revealed that FDCP-mix cell chromatin within the loci encoding the CD3 δ (*CD3D*) and immunoglobulin heavy chain (*IGH*) proteins is in an active conformation [110]. Differentiation of FDCP-mix cells towards non-T-lymphocyte lineages suppresses *TCRG* expression and results in a decrease in DNase I hypersensitivity within the *CD3D* and *IGH* regions [109, 110]. The expression of other lymphoid-associated genes, such as *GZMB*, has also been confirmed in FDCP-mix cells and human CD34⁺ HPCs [111, 112]. Finally, both Ford *et al.* [113] and Zhu *et al.* [114] have shown that FDCP-mix cells express low levels of the gene encoding the myeloperoxidase protein (*MPO*), which is associated with the GM lineage.

The studies highlighted above provided early evidence to support the viewpoint that multilineage gene expression in haematopoietic cells precedes lineage commitment. However, these studies examined gene expression by performing analysis on whole populations of cells, and do not exclude the possibility that a number of transcriptionally distinct subpopulations exist within multipotent haematopoietic cell populations. To

investigate this premise, the Enver group has performed multiplex RT-PCR analysis of individual HPCs to determine if multiple lineage-associated transcriptional programs are expressed simultaneously in single multipotent cells [115].

Hu *et al.* studied the expression of *HPRT*, *KIT*, *EPOR*, *GCSFR*, *GATA1*, *HBB*, and *MPO* by single FDCP-mix cells, and 77 individual cells were successfully analysed using this assay [115]. Sixty-seven percent and 61% of single cells expressed *HBB* and *MPO*, respectively, and 37% of these cells co-expressed these genes, displaying an erythroid-macrophage expression profile. Similarly, 30% of cells co-expressed *HBB* and *GCSFR*, and were considered to express an erythroid-granulocyte profile. Using a second multiplex RT-PCR assay, the group then investigated the co-expression of *HPRT*, and the haematopoietic growth factor (HGF) receptor genes, *KIT*, *EPOR*, *GCSFR*, *IL3R*, *GMCSFR*, and *MCSFR*. The findings demonstrated that FDCP-mix cells are highly heterogeneous in regards to the expression of HGF receptors, and co-expression of these genes was noted in a number of cells. For example, 36% of the 87 individual cells assayed were positive for *Csf3r*, *Kit* and *Csf2r* mRNA, while 6% of single cells co-expressed *Csf2r* and *Epor* transcripts. The expression of multiple lineage-associated transcripts was then confirmed in purified mouse Lin⁻ CD34⁺ BM cells, demonstrating that the observed multilineage expression was not an artifact of the FDCP-mix cell line. As such, Enver and colleagues were the first to provide evidence for the expression of several distinct lineage-associated transcripts by single HPCs, confirming the existence of multilineage transcriptional programmed states in multipotent cells [115].

In 2002, Miyamoto *et al.* provided further evidence to support a model of multilineage gene expression in HSPCs [116]. Using single cell RT-PCR, the authors first demonstrated that a subpopulation of HSCs (LSK CD34⁻ Thy1.1^{lo}) and CMPs (LS⁻K CD16/32^{lo}CD34⁺) co-express

MegE- and GM-associated genes. Within the CMP population, 39% of single cells analysed co-expressed *HBB*, *EPOR*, *MPO* and *GCSFR*, and a further 9% expressed a combination of three of these genes. In comparison, 16% of single HSCs expressed three of the four MegE- and GM-associated genes, indicating a lower level of promiscuous gene expression in this population. Lymphoid-associated gene expression was then determined in HSCs and CLPs ($\text{Lin}^- \text{Sca1}^{\text{lo}} \text{c-Kit}^{\text{lo}} \text{IL-7R}^+$) using a second multiplex RT-PCR primer set. Interestingly, only 9% of single HSCs expressed T-lymphocyte-associated genes, while expression of genes associated with the B-lymphocyte lineage were not detected. On the other hand, 21% of single CLPs displayed a promiscuous lymphoid profile, expressing genes associated with both the B-lymphocyte and T-lymphocyte lineages. Finally, the authors demonstrated that HPCs express lineage-associated genes at much lower levels (approximately 10-fold lower) than mature cells. Miyamoto and colleagues concluded that promiscuous multilineage gene expression occurs in both multipotent and oligopotent HPCs, and that expression of MegE- and GM-associated mRNAs predominates over the expression of lymphoid transcripts in HSCs.

While neither Hu *et al.* [115] nor Miyamoto *et al.* [116] investigated if multilineage expression patterns in single cells resulted in translation of functional proteins, Enver and colleagues have proposed that the increase in expression and accessibility of particular gene loci during differentiation demonstrates a transition between transcriptional priming and protein expression [115]. In this transcriptionally primed state, multilineage gene expression is governed by stochastic fluctuations in cell-intrinsic factors, such as lineage-determining TFs. Stochastic fluctuations in cell-intrinsic factors have been studied in many organisms and are thought to propagate 'gene expression noise' through TF networks to provide cell-to-cell individuality (reviewed in [117]).

In 2008, Chang *et al.* proposed that stochastic fluctuations in gene expression in HPCs reflect transitions through metastable states which confer priming of cells towards particular lineages [118]. The authors isolated cells from a mouse Erythroid-Myeloid-Lymphoid (EML) cell line according to the levels of Sca1 expressed on their surface, dividing the population into Sca1^{lo}, Sca1^{med} and Sca1^{hi} fractions. When maintained *in vitro* for over 9 days, all Sca1 fractions were capable of generating a cell population that displayed a similar Sca1 surface expression profile as the parent population. To determine if this behaviour could be explained by a stochastic model, Chang and colleagues performed computer simulations [118]. They reported that the experimental data could only be described by a stochastic process in which cells are attracted towards particular pseudo-subpopulations. Thus, the authors proposed the existence of transitional stable cellular states that are briefly maintained by the equilibrium of intrinsic factors.

Chang *et al.* then examined the lineage potential of the Sca1^{lo}, Sca1^{med} and Sca1^{hi} EML cells to investigate whether fluctuations in Sca1 expression marked distinct functional subpopulations [118]. When cultured in the presence of Epo immediately after isolation, the Sca1^{lo} fraction generated erythroid cells more efficiently than the other populations. Conversely, the Sca1^{hi} cells were the most efficient at generating myeloid cells (Mac⁺/Gr-1⁺) when stimulated with GM-CSF immediately after sorting. If the Sca1^{lo}, Sca1^{med} and Sca1^{hi} EML cells were stimulated with Epo 7, 14 and 21 days after isolation, the variation in erythroid potential was seen to gradually disappear over time. This loss of distinct erythroid potentials reflected the change in Sca1 expression profiles. The authors then investigated whether the disparities in lineage potential immediately following isolation was due to variation in the expression of lineage-determining TFs. Analysis of protein and transcript expression revealed

that GATA-1 expression was highest in erythroid-primed Sca1^{lo} EML cells, while expression of PU.1, a GM-lymphoid-associated TF, was highest in Sca1^{lo} cells. The differences in gene expression between cells were steadily lost over a period of two weeks. Lastly, Chang *et al.* performed microarray mRNA expression analysis to show that the fluctuations in GATA-1 and PU.1 seen in EML subpopulations reflected variations in global gene expression [118].

These findings indicate that differentiation of a cell towards a particular lineage is governed by the transition of cells through metastable states that display differing affinities for particular cell fates. As highlighted by Chang *et al.*, these transitions appear to occur due to fluctuations in cell-intrinsic factors, such as lineage-determining TFs, which generate transcriptome wide noise and mediate lineage specification [118]. Studies of prokaryotic and eukaryotic cells have shown that stochastic fluctuations in gene expression are affected by many factors, including cell size and location of gene loci [119-122]. However, studies investigating regulation of gene expression during haematopoietic lineage specification have largely focused on interactions between lineage-associated TFs. In particular, the mutually antagonistic interactions between GATA-1 and PU.1 have been extensively characterised.

In 1999, Rekhtman and co-workers provided the initial evidence for a direct interaction between PU.1 and GATA-1 using a erythroleukaemia cell line [123]. Using a combination of glutathione S-transferase pull down and immunoprecipitation assays, PU.1 and GATA-1 were shown to directly interact through their respective DNA binding domains. The binding of PU.1 to GATA-1 was then shown to result in a dose-dependent inhibition of GATA-1 transcriptional activity, suggesting that the aberrant expression of PU.1 by erythroleukaemia cells prevents erythroid specification and maintains the cells in an undifferentiated state. Further analysis provided evidence for such an interaction in normal haematopoiesis, as ectopic expression of

PU.1 was shown to reduce normal erythropoiesis in *Xenopus* embryos. Increasing the levels of GATA-1 expression in these cells restored erythropoiesis to normal levels.

Since the study by Rekhtman and colleagues [123], a number of others have reported similar findings [124-126], and have shown that GATA-1 is capable of inhibiting PU.1 activity [127, 128], indicating that a cross-inhibitory relationship exists between the two TFs. For example, the Graf group has shown that ectopic expression of GATA-1 in chicken myoblasts decreases expression of a myeloid associated marker, major histocompatibility complex (MHC) class II γ chain, and increases expression of EOS47, a marker for eosinophils [127]. By using a PU.1 responsive luciferase reporter construct, the authors reported that GATA-1 was capable of inhibiting PU.1 transcriptional activity. The Graf group demonstrated that the interaction between PU.1 and GATA-1 is mediated *via* their respective DNA binding motifs [127], adding support to the findings of Rekhtman *et al.* [123].

Given the interactions between PU.1 and GATA-1, the two TFs are thought to form a competitive transcriptional network, or developmental switch, that primarily regulates the choice between the GM-lymphoid and MegE lineages. Once this developmental switch is triggered, the selected lineage-associated transcriptional program is thought to be reinforced through autoregulatory feedback mechanisms in which TFs positively self-regulate themselves. These autoregulatory loops have been identified for PU.1 [129], GATA-1 [130] and a number of other lineage-associated TFs [131, 132].

Other lineage-determining TF factors have been shown to directly interact with each other, providing evidence to support the existence of other developmental switches that regulate lineage commitment. For example, the ratio of MafB to PU.1 expression mediates the

differentiation of myeloid progenitor cells towards either a macrophage or DC fate *in vitro* [133], and CCAAT enhancer-binding protein α (C/EBP α), a granulocyte-associated TF, has been shown to antagonise PU.1 to promote a granulocyte rather than a DC/macrophage fate [134, 135]. Similarly, co-operative and inhibitory interactions between GATA-2 and PU.1 have been shown to be important in the differentiation of mast cells [136]. The Akashi group has also shown that the order in which TFs are expressed is important for lineage commitment [137]. Iwasaki *et al.* transduced mouse CLPs with a gene construct that enforced C/EBP α expression and reported that these cells almost exclusively formed GM cells in methylcellulose colony forming assays [137]. When CLPs were transduced to express C/EBP α , and then GATA-2 24 hours later, they only gave rise to eosinophil colonies. Strikingly, if CLPs were forced to express GATA-2 first, followed by C/EBP α , they generated mostly basophils/mast cells. Thus, the authors concluded that a hierarchy exists in which step-wise expression of specific TFs drives particular fates. While the list of TF networks highlighted here is not exhaustive, it provides an overview of the complex interplay that occurs between TFs in haematopoietic cells. The existence of such TF developmental switches has increased support for a stochastic model of haematopoiesis.

Most of the studies investigating the existence of TF-driven developmental switches have relied on the use of cell lines, ectopic expression systems and the analysis of whole populations. However, in 2016, Hoppe *et al.* examined the co-expression of GATA-1 and PU.1 by individual endogenous HSPCs from mouse BM [138]. The authors developed a knock-in reporter mouse model that expresses functional GATA-1:mCherry and PU.1:eYFP (enhanced yellow fluorescent protein), and examined the HSC, CMP and GMP compartments to determine if GATA-1 and PU.1 are co-expressed in a single cell at any time during

haematopoiesis. Within the CMP population there were two discrete subpopulations that could be identified based on GATA-1-mCherry and PU.1-eYFP expression; the first exclusively expressed high levels of PU.1-eYFP, while the second expressed high levels of GATA-1-mCherry with low to no expression of PU.1-eYFP. When these cells were characterised using colony forming assays, the results showed that the PU.1^{hi} GATA-1⁻ population was restricted to the GM population, while the PU.1^{-/lo} GATA-1^{hi} population was composed of distinct GM- and MegE-restricted progenitors. A small number of PU.1⁺ GATA-1⁺ GMPs were also detected, but these were shown to lack MegE potential. When analysing the LSK CD150⁺ CD48⁻ CD34⁻ HSC compartment, the authors only detected low levels of PU.1-eYFP expression. In contradiction with a stochastic model of haematopoiesis, these findings indicate that no multipotent HSPC population is maintained in a PU.1⁺ GATA-1⁺ state prior to lineage commitment.

To determine if HSCs transitioned through a PU.1⁺ GATA-1⁺ phenotype during differentiation, Hoppe and coworkers cultured *GATA-1:mCherry/PU.1:eYFP* HSCs in conditions that promoted GM and MegE differentiation, and tracked the fate of single cells by expression of GATA-1, and CD16/32 which are markers of GM maturation [138]. At the time of isolation, these cells were PU.1^{lo}. During differentiation of HSCs towards a GM fate, eYFP intensity increased over time until onset of CD16/32 expression, while GATA-1 expression was not detected at any time. On the other hand, all HSCs that acquired mCherry expression during tracking eventually committed to a GATA-1⁺ PU.1⁻ MegE fate. Further analysis of these cells showed that the decrease in PU.1-eYFP was independent of GATA-1-mCherry expression, and in some cases PU.1-eYFP expression had already disappeared before the onset of GATA-1-mCherry expression. As such, the authors concluded that GATA-1 is not expressed at any point during

the GM differentiation of HSCs, and that the commitment of HSCs towards a MegE fate does not rely on interactions between GATA-1 and PU.1 [138].

Overall, the findings of Hoppe *et al.* are inconsistent with a developmental PU.1-GATA1 switch [138]. While these findings do not entirely rule out the possibility of PU.1 and GATA-1 competitive interplay occurring, they strongly argue against a stochastic model of commitment whereby differentiation is initiated by a PU.1/GATA-1 network. As this study is the first to investigate the role of these TFs in differentiation at the single cell level, further work will be required to confirm the findings, and determine how PU.1 and GATA-1 expression are regulated in the absence of developmental switches. On a technical note, it is possible that PU.1 and GATA-1 are co-expressed at levels below the limits of detection for the techniques used in this study, and that only low levels of expression are required for competitive interactions.

Ultimately, a stochastic model of haematopoiesis concerns the apparent random behavior of HSPCs. Early studies of HSPCs support this model by demonstrating that the fate of a cell can be predicted using stochastic computational simulations. According to these findings, cell fate is determined by random probabilities of a cell undergoing self-renewal, differentiation, lineage commitment or death. This would imply that haematopoiesis is determined by factors that alter these probabilities. It has been suggested that stochastic fluctuations in cell-intrinsic factors are sufficient to regulate such probabilities. However, this theory has been contested [138], and the exact mechanisms that lead to established transcriptional programs are largely unknown. As such, the current stochastic model of haematopoiesis cannot fully explain how cell fate is determined. As an alternative, a model of haematopoiesis has been described in

which the decisions of HSPCs are regulated by cell-extrinsic factors, such as HGFs. This model, known as the deterministic model of haematopoiesis, will be discussed in **Section 1.3.2.4**.

1.3.2 Haematopoietic growth factors

HGFs shape haematopoiesis by regulating the survival, proliferation and differentiation of haematopoietic cells. These factors may be expressed on the cell surface in a membrane-bound form to provide growth signals through direct cell contact, or they may be secreted by the producing cell to act in an autocrine, paracrine or endocrine fashion [139-141]. There is a wide range of HGFs with differing activities, including some that are associated with particular cell lineages, and others that act on multiple different cell types. Early studies of HGFs characterised them according to their ability to promote cell survival and proliferation, and provided little evidence to suggest they played a role in cell fate. This led some to propose that HGF act permissively, and that lineage-associated factors provide committed progenitor cell populations with a proliferative advantage. However, as techniques allowing the manipulation of haematopoietic cells *in vitro* advanced, evidence supporting a role for HGFs in the regulation of HSPC fate materialised. These studies support a deterministic model of haematopoiesis, in which individual HGFs are capable of instructing the self-renewal of HSCs, and the differentiation and lineage commitment of HSPCs towards particular lineage fates. This section will first introduce a number of HGFs that are relevant to HSPC function, and then discuss how the perceptions of HGF functionality has changed over time. Finally, the current evidence supporting a deterministic model of haematopoiesis will be considered.

1.3.2.1 The discovery and early history of haematopoietic growth factors

The first HGF to be described was Epo. In 1906, Carnot and Deflandre demonstrated that the production of erythrocytes was increased in rabbits that received a transfusion of serum from hypoxic animals [142]. The authors proposed the existence of a humoral factor, which they named haemopoietine, which was produced to stimulate erythropoiesis during hypoxia. However, this factor, now known as Epo, was not purified until 1977 [143], and cloning of the gene encoding Epo was achieved in the mid-1980's [144-146]. EpoR was later cloned in 1991 [147, 148], and is the only known receptor for Epo. Epo is primarily produced by peritubular fibroblasts in the cortex of the kidneys, though perisinusoidal cells and hepatocytes in the liver have also been shown to secrete Epo [149]. Early *in vitro* studies showed that Epo was integral for the proliferation [150] and, subsequently, the survival [151] of erythroid progenitors (EPs). As a result, Epo quickly became a routine therapeutic for the treatment of anaemia in patients with renal disease [152].

The next HGFs to be identified were the colony stimulating factors (CSFs). These molecules were first described as factors that are required for the formation of haematopoietic colonies *in vitro*. In 1965, Pluznik and Sachs reported that cell suspensions prepared from mouse spleens were only capable of forming granulocyte colonies in soft agar medium when co-cultured with a feeder layer derived from mouse embryo cells [153]. The following year, Bradley and Metcalf demonstrated that the generation of mouse BM-derived myeloid colonies required the presence of kidney-derived feeder cells [154]. These findings led the authors of both studies to propose that the feeder cells were capable of producing factors

that stimulate haematopoietic cells to produce colonies. Further characterisation of such molecules eventually led the identification of 4 CSFs.

In 1975, Stanley *et al.* purified the first CSF from human urine [155]. This CSF was capable of stimulating the formation of mouse macrophage colonies *in vitro*, hence why it is now known as macrophage-CSF (M-CSF). Mouse M-CSF was later purified in 1977 from medium that was conditioned from intestinal endocrine cells [156]. The same year, GM-CSF, a CSF capable of stimulating the formation of GM colonies *in vitro*, was purified from murine lung-conditioned medium [157]. Recombinant murine GM-CSF was successfully synthesised in 1984 [158]. A third CSF, multi-CSF, also known as interleukin-3 (IL-3), was purified from leukaemic cell-conditioned medium by Ihle and colleagues in 1982 [159]. Early studies of IL-3 showed that it is required for the maintenance of a number of murine BM-derived cell lines [160], and that it promotes BM-derived CFU to form a number of different colony types *in vitro*, including macrophage, granulocytic and megakaryocytic colonies [161, 162]. The final CSF, G-CSF, was identified by Metcalf and coworkers in 1983. The group purified G-CSF from medium that was conditioned by murine lung cells [163], and demonstrated that it was highly efficient at stimulating the generation of granulocytic colonies *in vitro* [164]. Studies have also revealed that G-CSF stimulates the mobilisation of HSPCs from the BM into the blood, and so it is now commonly used in the isolation of human haematopoietic cells for clinical therapies [165]. A number of different sources have been identified for the production of CSFs, and some tissues produce more than one CSF. These include skeletal and cardiac muscle, lung and haematopoietic cells [166, 167]. CSFs act on target cells by binding their cognate receptors, M-CSFR [168], GM-CSFR [169], IL-3R [170] and G-CSFR [171].

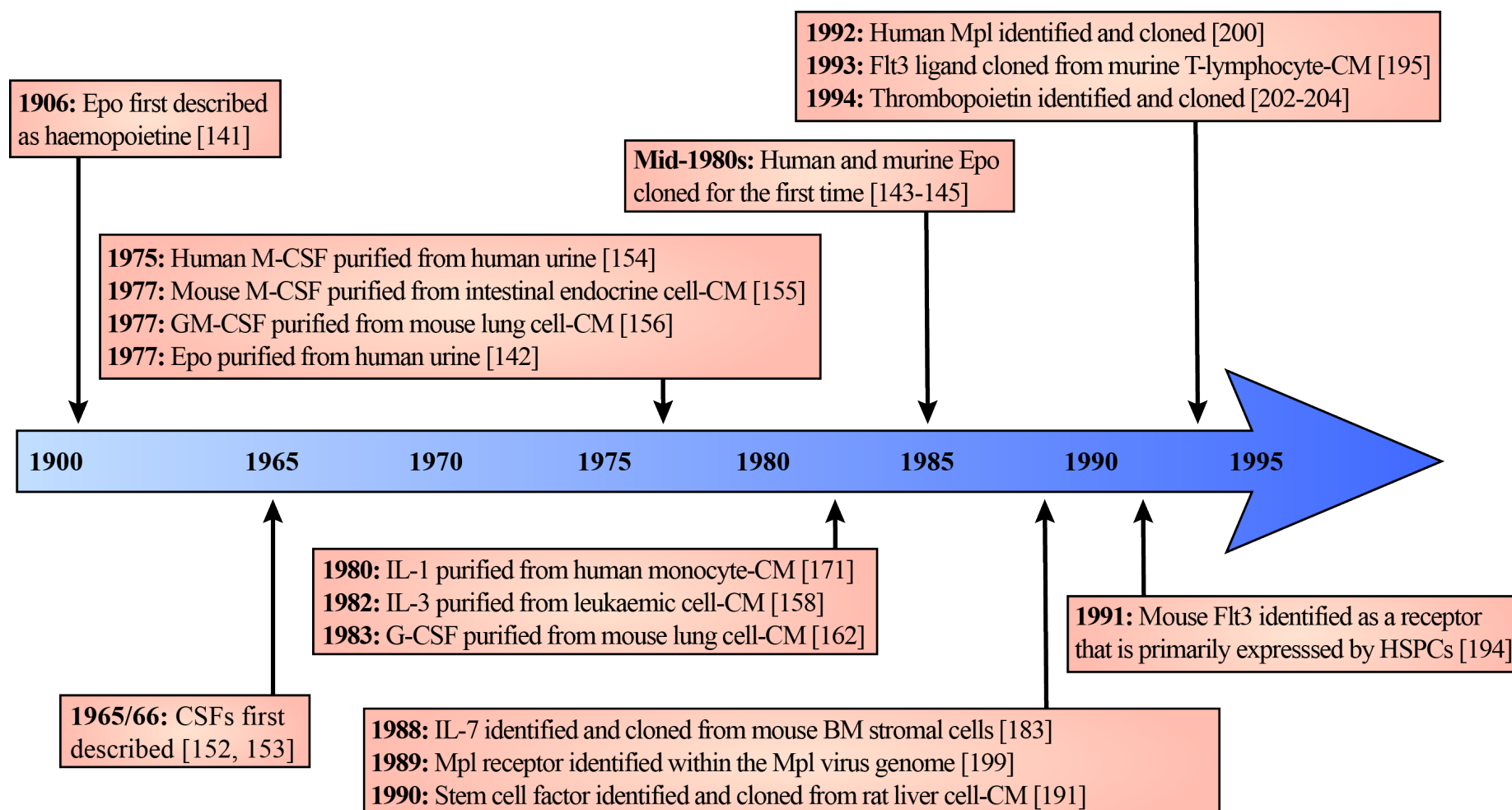


Figure 1.6. A timeline for the discovery and early characterisation of haematopoietic growth factors. Citations are shown in square brackets. Epo, erythropoietin; CSF, colony stimulating factor; M, macrophage; G, granulocyte; GM, granulocyte-macrophage; Mpl, myeloproliferative leukaemia; IL-1, interleukin-1; IL-3, interleukin-3; IL-7, interleukin-7; Flt3, fms-like tyrosine kinase 3; BM, bone marrow; CM, conditioned medium; HSPC, haematopoietic stem and progenitor cell.

IL-3 is a member of the interleukin superfamily of HGFs. This large family of factors contains many members. However, given the purpose of this section, only two other interleukins will be discussed, interleukin-1 (IL-1) and interleukin-7 (IL-7). IL-1 was the first member of the interleukin family to be described, and was purified from human monocyte-conditioned medium in 1980 [172]. IL-1 exists in two forms, IL-1 α and IL-1 β [173], and is extremely diverse in regards to its function. These molecules primarily act as pro-inflammatory agents, but recent evidence has shown that IL-1 also acts on HSPCs [174, 175]. IL-1 is expressed mostly by mature haematopoietic cells, such as myelomonocytic cells [176, 177] and lymphocytes [178], but it is also expressed by epithelial cells [179, 180] and fibroblasts [181]. There are two IL-1 receptors, IL-1 receptor type I mediates IL-1 signalling, while IL-1 receptor type II exists as a cell surface receptor and a soluble receptor to inhibit the action of IL-1 [182, 183].

IL-7 was first identified by Namen *et al.* in 1988 [184]. The authors cloned the *IL7* gene from BM stromal cells, and then demonstrated its ability to promote proliferation of B-lymphocyte progenitors. IL-7 was also shown to be important for T-lymphocyte progenitors, as addition of IL-7 to thymic organ cultures greatly increased the generation of thymocytes [185]. IL-7 is primarily expressed by stroma cells in the thymus, spleen and BM [186-188], but is also expressed by intestinal epithelium [189] and keratinocytes [190]. IL-7 signals through a single receptor, IL-7R [191].

In 1990, Zsebo *et al.* identified a HGF that is capable of maintaining primitive haematopoietic cells *in vitro* [192]. They treated mice with 5-fluorouracil, an agent that induces apoptosis in highly proliferative cells, and harvested BM cells 2 days later. The BM samples, which were enriched for early HSPCs, were shown to require rat liver cell-conditioned medium to form colonies when cultured in soft agar. Zsebo and coworkers identified and isolated a molecule

from the conditioned medium and reported that it acts synergistically with other factors, such as IL-1, to promote expansion of HSPCs. They concluded that this molecule, commonly known as stem cell factor (SCF), acted on pre-CFUs to activate and sensitise them to other HGFs. SCF was cloned later that year [139], and its receptor was identified as c-Kit [193], which is primarily expressed by early HSPCs [194].

Shortly after the isolation of SCF, another stem and progenitor cell factor-ligand pair was identified. In 1991, Matthews *et al.* cloned a receptor that is predominantly expressed by fetal liver HSPCs in mice [195]. The authors identified the receptor as a member of the tyrosine kinase receptor family, and named it fetal liver kinase-2, though it is more commonly known as Flt3. The ligand for Flt3 (Flt3L) was later cloned from a murine T-lymphocyte line in 1993, and was shown to stimulate the proliferation of early murine HSPCs enriched from the fetal liver, and human CD34⁺ BM cells [196]. Since, Flt3L has been shown to be important for the development and function of DCs [197].

In 1989, Wendling and co-workers reported that murine BM HSPCs infected with myeloproliferative leukemia (Mpl) virus were capable of forming colonies in semisolid medium in the absence of supplementary HGFs, such as Epo or IL-3 [198, 199]. When cloning the virus, the group identified a gene encoding a protein that shared sequence and structural similarities with numerous HGF receptors [200]. This led to the identification and cloning of a human homolog [201], named the Mpl receptor, which was shown to be primarily expressed by megakaryocytes [202]. This led to the eventual purification and cloning of its ligand, thrombopoietin (Tpo), in 1994 [203-205]. While Tpo was quickly identified as an important regulator of thrombopoiesis/megakaryocytopoiesis [206], it regulates HSC quiescence [207], and has been shown to protect a number of tissues against ischaemia [208, 209]. Tpo is

predominately expressed by hepatocytes in the liver, but it is also synthesised in the spleen, kidney, BM and brain [210, 211]. See **Figure 1.6** for a timeline of the discovery, purification and cloning of the HGFs discussed above.

1.3.2.2 The mitogenic and pro-survival properties of haematopoietic growth factors

Initial characterisation of HGFs demonstrated that they were essential for the formation of haematopoietic colonies *in vitro*. At the time, it was unclear whether HGFs acted to stimulate cell cycling, cell survival, or both. Early studies investigating the function of HGFs provided evidence that they were capable of recruiting cells into active cell cycling. This was first demonstrated in the 1980s using conditioned medium containing CSFs. Using lung-, spleen- and leukaemic cell-conditioned medium as a source of CSFs, Pluznik and co-workers investigated the effects of CSFs on the cell cycle kinetics of a GM-CSF-dependent mast cell/basophil line, PT-18 [212]. Following culture in the presence of CSF, propidium iodide staining revealed that CSF stimulation increased the proportion of PT-18 cells in the G₂ + M and S phases of the cell cycle. In addition, the incorporation of [³H]-thymidine into PT-18 cells was increased following culture with CSFs.

In 1987, London *et al.* investigated the effects of a number of HGFs, including IL-3 and GM-CSF, on the cell cycle status of an IL-3-dependent myeloid progenitor cell line, FDCP-1, and an IL-3 dependent lymphoid progenitor cell line, FL5.12 [213]. By monitoring the DNA and RNA content of haematopoietic cells using acridine orange, the authors demonstrated that IL-3, but not GM-CSF, is capable of recruiting FDCP-1 and FL5.12 cells from a quiescent state into

active cycling. However, once cells were drawn into active cycling by IL-3, GM-CSF was capable of maintaining proliferation. Although this demonstrates that both HGFs are capable of stimulating cell proliferation, the authors concluded that GM-CSFR is likely to be absent from quiescent HSPCs and that its expression is stimulated by IL-3 signalling. Shortly after this study, Spivak and co-workers used an erythroleukaemic cell line, HCD-17, to demonstrate the mitogenic activity of Epo [214]. When stimulated with Epo, the incorporation of [³H]-thymidine and [³H]-uridine into HCS-17 cells increased significantly when compared to cells cultured without Epo, indicating an increase in DNA and RNA synthesis, respectively. Further investigation demonstrated that Epo recruited the factor-deprived HCS-17 into the S-phase. These reports were shortly followed by a number of studies showing that other HGFs, such as M-CSF [215], IL-7 [216] and SCF [217], possess mitogenic activity, and that certain factors act synergistically to promote cell proliferation [218, 219].

Similar studies of HGF activity have demonstrated that these factors also promote survival by suppressing apoptosis. This was first demonstrated by Williams *et al.* in 1990 [220]. The authors investigated the effects of withdrawing CSFs from a number of factor-dependent FDCP-1 and FDCP-mix cell lines. Withdrawal of IL-3, GM-CSF and G-CSF from factor-dependent cells resulted in DNA fragmentation. As apoptosis is dependent on protein synthesis, the authors treated factor-deprived cells with cycloheximide, a protein synthesis inhibitor, and noted that it significantly reduced the rate of cell death. In the same year, two independent studies reported that Epo [151] and IL-3 [221] are capable of suppressing apoptosis in erythroleukaemia and multipotent progenitor cell lines, respectively. Using a similar approach as Williams *et al.*, Epo and IL-3 were shown to prevent DNA fragmentation in target cells and

increase cell viability. The same has been shown for a number of other factors, indicating that suppression of cell death programs is a common property of HGFs [222-224].

As HGFs display mitogenic and pro-survival properties, it was of interest to determine if these responses were distinct, or the result of a single signalling pathway. This required characterisation of HGF receptors, and studies of G-CSFR [225], M-CSFR [226] and IL-3R [227] eventually revealed that these responses were independent of each other. In the case of G-CSFR, Ward and colleagues have reported that the proliferative and survival responses of human G-CSF (hG-CSF) signalling are mediated by different regions of the G-CSFR cytoplasmic domain and activate two distinct signalling pathways [225]. G-CSFR contains 4 tyrosine residues within its cytoplasmic domain that are phosphorylated upon binding of G-CSF. The authors transduced a myeloid progenitor cell line, 32D, with wild-type (WT) G-CSFR and a series of G-CSFR mutants lacking specific cytoplasmic tyrosine residues. Cells transduced with G-CSFR mutants lacking all four tyrosine residues were capable of surviving in the presence of G-CSFR for 10 days but did not divide. This response was primarily mediated by signal transducer and activator of transcription (STAT) 3 activation. The cytoplasmic tyrosine residues of G-CSFR were required for proliferation of 32D cells, particularly the residues at positions 704 and 764. These residues were shown to bind and activate the accessory proteins SHP-2, Grb2, and Shc.

Given these findings, it quickly became well accepted that HGFs are required to stimulate the proliferation and survival of haematopoietic cells. However, the role of HGFs in HSC self-renewal and HSPC differentiation/lineage-specification was less clear at this time. In an attempt to explain how HGFs influenced cell fate, two models of HGF activity were proposed,

a permissive model (**Section 1.3.2.3, Figure 1.7**) and a deterministic model (**Section 1.3.2.4, Figure 1.8**).

1.3.2.3 A permissive role for haematopoietic growth factors in the maintenance of haematopoietic cells

Studies investigating the biological activity of HGFs indicated that a number of these factors, such as Epo, M-CSF, G-CSF and IL-7, are associated with the survival and proliferation of particular lineages. For example, Metcalf and Johnson assessed the ability of Epo to stimulate mouse fetal liver cells to form colonies in soft agar. When these cells were cultured in the presence of spleen conditioned medium, they generated multilineage colonies. However, when cultured with Epo alone, they did not form any colonies [228]. Epo was only able to stimulate these cells to generate erythroid colonies after they had been pre-cultured with spleen conditioned medium. In the same year, Udupa *et al.* examined its effects on stimulating CFU-S, CFU-E and BFU-E proliferation in mice following administration of chemotherapeutic agents [229]. After treatment with alkylating agents, there was a dramatic decrease in the number of BM CFU-S, CFU-E and CFU-B, and the authors monitored their regeneration over a period of 14 days. Daily injections of Epo following treatment with alkylating agents resulted in a significant increase in the number of BM CFU-E and BFU-E when compared to control animals. However, the number of CFU-S following Epo treatment was unchanged. As such, the authors of both studies concluded that pluripotent cells only become sensitive to Epo once they have become committed towards the erythroid lineage.

Early studies of G-CSF suggest that it primarily acts on committed progenitors. In 1983, Metcalf and Nicola performed colony forming assays with mouse BM and fetal liver to examine if G-CSF could promote colony formation *in vitro* [164]. When BM and fetal liver cells were treated with serum-containing medium supplemented with G-CSF, they exclusively formed colonies containing GM cells. When monitoring BM and fetal liver cultures that were treated with G-CSF alone, the authors noted that cells survived for a short period of time but did not proliferate, suggesting that G-CSF has limited pro-survival activity on multipotent cells. A later study by the Ogawa group also indicates that G-CSF alone is ineffective at stimulating multipotent cells to form colonies [230]. When 1,000 BM cells were cultured in serum-free methylcellulose medium supplemented with G-CSF, only 7 granulocytic colonies were observed. However, when IL-3 was added, 20 granulocytic colonies, 1 GM colony and 2 eosinophil colonies were generated. When the BM cells were cultured in serum-containing medium supplemented with G-CSF, over 80 colonies containing granulocytes and/or macrophages formed. Thus, Sonoda *et al.* proposed that multipotent BM cells require factors such as IL-3 to survive and produce GM-committed progenitors, which are sensitive to G-CSF.

At this time, other HGFs were considered to be lineage-non-specific HGFs that acted on early HSPCs. This included factors such as IL-3, SCF and GM-CSF. GM-CSF was initially thought to be lineage-specific based on its ability to promote the formation of GM colonies, but some studies showed that it was also capable of acting on multipotent and erythroid cells. For instance, when fetal liver cells are cultured in GM-CSF for 2 days and then transferred to mouse spleen cell-conditioned medium, they are capable of forming multilineage and erythroid colonies [231]. Similarly, the addition of GM-CSF to serum-free methylcellulose

cultures containing human Lin⁻ BM cells allows the formation of erythroid, GM and multipotent colonies [232].

The categorisation of HGFs based on their lineage-specific and non-specific activities led advocates of a stochastic model of haematopoiesis to propose that such factors do not influence the self-renewal of HSCs, differentiation of HSPCs or the lineage commitment of these cells [233-235]. Instead, HSPC fate is governed by a cell-intrinsic stochastic process that is facilitated by factor-induced proliferation and survival. In this model, HGFs are thought to act permissively. In the case of committed progenitors, expression of receptors for lineage-specific HGFs allows for the selective expansion of cell populations. For example, in cases where lineage-specific HGFs promote the development of particular lineages from multipotent cells, it is thought that these factors provide a proliferative advantage to a subpopulation of committed cells, rather than providing instructive cues to multipotent cells (**Figure 1.7**).

In 1985, the Ogawa group published the first study supporting a permissive role of HGFs. Suda *et al.* generated blast cell colonies using spleen cells from 5-fluorouracil treated mice and then isolated 254 individual cells from the colonies. Individual cells were cultured in serum-rich medium containing IL-3, and after the first cell division occurred, the progeny were separated within the culture dish allowing the formation of two distinct colonies [235]. One-hundred and five paired daughter cells were successfully separated, and 97 of these formed colonies. Sixty-six pairs formed colonies with the same lineage-composition. However, when comparing these colonies, the total cellularity and composition of each cell type within the colony differed wildly between paired daughter cells. The remaining paired daughter cells formed colonies with differing lineage-composition. Given the variation between colonies,

the authors concluded that IL-3 does not play a role in regulating the differentiation and/or fate of multipotent cells.

In 1993, Fairbairn *et al.* provided more evidence to support the viewpoint that cell-extrinsic factors are not required for differentiation and/or cell fate determination [236]. The authors transduced IL-3-dependent FDCP-Mix cells with the human *BCL2* gene, a gene encoding an anti-apoptotic factor, and reported that they were capable of factor-independent survival for 2-3 weeks *in vitro*. In comparison, almost all control FDCP-Mix cells transduced with an empty vector died after 2 days of culture in the absence of HGFs. The *BCL2*-transduced FDCP-Mix cells did not proliferate in cultures lacking HGFs. However, cytopsin preparations of *BCL2*-transduced FDCP-Mix cells revealed that they matured into granulocytes, monocytes and erythroid cells over an 8-day period. Northern blotting analysis of the *BCL2*-transduced FDCP-Mix cells showed that they did not express the genes encoding GM-CSF (*CSF2*), G-CSF (*CSF3*) and IL-3 (*IL3*), and conditioned medium from these cells was not sufficient to promote differentiation of untransduced FDCP-Mix cells. This ruled out the possibility of differentiation being caused by autocrine signalling, and indicated that the suppression of apoptosis is sufficient for survival and differentiation of multipotent cells in the absence of HGFs. These findings led Fairbairn *et al.* to conclude that while the data do not exclude the possibility of HGFs stimulating differentiation, they do suggest that these factors are not required for this process.

Studies of mice lacking the expression of particular HGFs and their receptors further support a permissive action of these factors. Introduction of null mutations into the gene encoding *CSF2* results in mice that display normal haematopoiesis and they have comparable numbers of mature myeloid and lymphoid cells to WT controls [237, 238]. Only minor haematological

differences were observed during initial characterisation of *CSF2*^{-/-}, as they showed more variability in the weight of their spleens and granulocyte counts when compared to control animals. However, the lung physiology of *CSF2*^{-/-} mice is significantly different from WT mice. *CSF2*^{-/-} have increased numbers of infiltrating lymphocytes and large intra-alveolar macrophages, and are more prone to bacterial and fungal infections than WT mice. This suggests that GM-CSF signalling is required for the function of mature GM cells in the lung but not for their development.

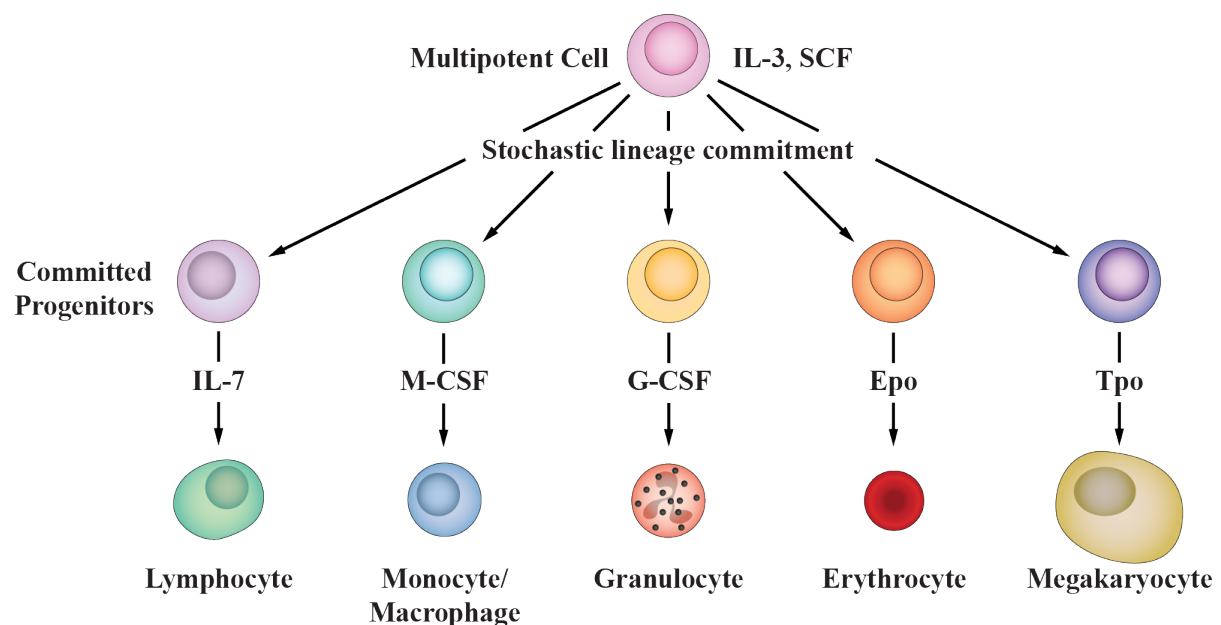


Figure 1.7. Permissive actions of HGFs. In a permissive model of haematopoiesis, HGFs are envisaged to provide survival and proliferative cues that permit HSPC differentiation/lineage commitment and the self-renewal of HSCs. Lineage non-specific factors, such as IL-3 and SCF, stimulate the proliferation and survival of multipotent haematopoietic cells, resulting in the generation of committed progenitors through a stochastic process. Lineage specific factors, such as M-CSF and Epo, then act selectively to provide a survival/proliferative advantage to lineage committed progenitors. HSC, haematopoietic stem cell; IL-3, interleukin-3; IL-7, interleukin-7; SCF, stem cell factor; M-CSF, macrophage-colony stimulating factor; G-CSF, granulocyte-colony stimulating factor; Epo, erythropoietin; Tpo, thrombopoietin; HGF, haematopoietic growth factor.

Targeted disruption of *EPO* and *EPOR* is embryonically lethal, at approximately embryonic day 13 (E13), due to a lack of mature definitive erythrocytes [239, 240]. However, definitive pro-

erythroblasts and yolk-sac derived erythrocytes are present in the fetal liver. As shown using colony forming assays, E13 $EPO^{-/-}$ fetal livers contain higher numbers of BFU-E and CFU-E than fetal livers from WT animals [239]. When transduced with $EPOR$, E13 $EPOR^{-/-}$ fetal liver cells form similar numbers BFU-E and CFU-E in the presence of Epo [239, 240]. Wu *et al.* have demonstrated an increased number of cells with pyknotic nuclei in $EPO^{-/-}$ and $EPOR^{-/-}$ fetal livers compared to WT fetal livers, suggesting an increased rate of apoptosis. These findings indicate that Epo is required for the survival of definitive EPs, but not for the commitment of upstream progenitors towards the erythroid lineage.

Knock-out of IL-7R in mice led to the suggestion that IL-7 is not required for the differentiation of cells towards a lymphoid fate. $IL7R^{-/-}$ mice generate a limited number of mature T- and B-lymphocytes. However, the number of pre-pro-B-lymphocytes in these mice is comparable to controls, indicating that the generation of lymphoid progenitors is unaffected [241]. Furthermore, work from Akashi and co-workers indicates that selective over-expression of Bcl-2 in $IL7R^{-/-}$ lymphoid cells is sufficient to rescue lymphopoiesis in these mice [242]. The introduction of the $E\mu$ - $BCL2$ gene ($BCL2$ under the control of the IGH $E\mu$ enhancer) into the $IL7R^{-/-}$ mouse strain restored T-lymphopoiesis to normal levels. Additionally, T-lymphocytes from these mice functionally respond to activating stimuli *in vitro*. Together, these studies suggest that IL-7R does not influence lineage choice and only serves to stimulate the survival of committed lymphocyte progenitors.

Mice lacking M-CSFR have decreased numbers of macrophages and osteoclasts when compared to littermate controls [243, 244]. However, $CSF1R^{-/-}$ mice have similar numbers of BM macrophage progenitors to WT mice and heterozygous $CSF1R^{+/-}$ controls, when compared using colony forming assays [245]. Lagasse and Weissman have demonstrated that

ectopic expression of human Bcl2 in $CSF1R^{-/-}$ myeloid cells partially restores monocyte/macrophage counts *in vivo* [246]. Using a *BCL-MRP8* transgene, the authors selectively suppressed the apoptosis of myeloid cells in $CSF1R^{-/-}$ mice and reported an increase in peripheral blood monocytes compared to $CSF1R^{-/-}$ control mice. The findings from both studies indicate that, like IL-7R, M-CSF is not required for lineage commitment decisions but does facilitate the survival of committed progenitors *in vivo*.

Although these knock-out studies support a permissive role of HGFs, they should be interpreted with caution. Firstly, they do not exclude the possibility of compensatory/redundant mechanisms between the actions of HGFs. For instance, G-CSF, GM-CSF and M-CSF all stimulate the growth of GM cells. Secondly, in the case of receptor knock-out studies, it is possible that certain HGFs act through currently unidentified receptors. Although, given that these factors have been the center of intense scrutiny over the past 40 years, this is unlikely.

Some studies that have investigated the ectopic expression of HGF receptors in lineage-restricted cells suggest that these do not influence lineage specification. In 1994, Pharr and colleagues transduced blast cell colonies with a constitutively active viral form of EpoR, EPOR(R129C), or human M-CSFR (hM-CSFR) and examined their ability to form colonies *in vitro* [247]. In the presence of SCF, IL-3 and Epo, EPOR(R129C)-transduced cells produced comparable numbers of erythroid and GM colonies when compared to control cells, though the colonies were larger. Similarly, when cultured with IL-3 and M-CSF, hM-CSFR-transduced cells and control cells generated comparable numbers of GM colonies, with similar macrophage compositions. Although, M-CSFR transduced-cells displayed increased secondary plating efficiency when compared to control cultures. As such, the authors

concluded that neither EpoR nor M-CSFR is capable of influencing lineage-choice in multipotent cells, though they do provide a proliferative/survival advantage.

McArthur *et al.* have performed a similar study using mouse M-CSFR [248]. They transduced mouse fetal liver cells and BM cells from 5-fluorouracil treated mice with M-CSFR and assessed their colony forming potential. M-CSF was capable of maintaining EPs, and increased the number of megakaryocyte and GM colonies formed when compared to cells transduced with an empty vector. These findings suggest that M-CSF signalling provides permissive proliferative cues, and does not instruct lineage specification.

Some studies using chimeric fusion HGF receptors have also provided evidence of a permissive model of HGF activity. Stoffel *et al.* generated a chimeric Mpl receptor by replacing its cytoplasmic domain with the cytoplasmic domain of G-CSFR [249]. This receptor, which binds Tpo and stimulates G-CSFR-mediated intracellular signalling, was introduced into an *MPL*^{-/-} mouse strain to prevent Mpl signalling *in vivo*. Characterisation of these mice revealed similar platelet and granulocyte counts, and comparable numbers of BM megakaryocyte and GM progenitors to WT controls. Using a similar approach, Semerad *et al.* have created a transgenic mouse model that expresses a chimeric receptor that binds G-CSF and transmits EpoR signalling [250]. These mice have normal granulopoiesis and erythropoiesis. However, G-CSF-mediated mobilisation of haematopoietic cells from the BM is deficient. Given the findings, both studies suggest that Tpo, G-CSF and Epo signalling do not influence the lineage choice of HSPCs.

Finally, Mayani and co-workers have provided evidence for a permissive role of HGFs in human haematopoiesis by analysing the fate of paired multipotent daughter cells cultured in

the presence of different HGFs. [251]. Individual CD34⁺ CD45RA^{lo} CD71^{lo} haematopoietic progenitors were sorted from human umbilical cord blood, and it was shown that 34% of these cells are capable of forming multilineage colonies *in vitro* [252]. CD34⁺ CD45RA^{lo} CD71^{lo} cells were cultured until their first cell division (2-5 days), and then separated into serum-free medium containing either an erythroid growth factor combination (EGFC: SCF, interleukin-6 [IL-6], IL-3 and Epo) or a myeloid growth factor combination (MGFC: SCF, IL-6, M-CSF, G-CSF and an IL-3/GM-CSF fusion protein). Two-hundred and six pairs were split and 96 of these pairs formed colonies following separation.

When daughter cells were placed in separate erythroid growth factor cultures (EGFC/EGFC), 58% of paired daughter cells gave rise to similar colonies (29% GM, 14% erythroid, 15% mixed). In 31% of EGFC/EGFC cases, the daughter cells generated colonies of different types. This included cases where cells formed small cell clusters that could not be identified due to limited cell numbers. In the remaining cases, both cells generated small unidentifiable clusters. In cases where daughter cells were placed in separate myeloid growth factor cultures (MGFC/MGFC), 67% of colonies formed the same colony type (47% GM, 3% mixed, 17% small unidentifiable cell clusters). In 3% of MGFC/MGFC cases, one daughter cell gave rise to a mixed colony while the other gave rise to a GM colony. In 30% of MGFC/MGFC cases, one daughter cell gave rise to a GM colony while the other formed a small unidentified cluster. No erythroid colonies were detected in MGFC/MGFC cultures. When daughter cells were placed in differing HGF mixtures (EGFC/MGFC), both paired daughter cells gave rise to similar colonies in 49% of cases (26% GM, 18% mixed colonies, 5% of unidentifiable clusters). In the remaining EGFC/MGFC cases, daughter cells gave rise to different colonies. For 8% of cases, one cell gave rise a GM colony, while the other gave rise to an erythroid colony.

Mayani *et al.* proposed that in cases when; *i*) daughter cells formed the same colony types, both daughter cells were already committed to a fate when they were placed in culture; *ii*) daughter cells formed distinct colonies, this was primarily due to an asymmetrical cell division which gave rise to a committed daughter cell and a multipotent daughter cell; *iii*) cells formed unidentified clusters, either this occurred as a result of manipulation or these colonies contained cells that could not thrive in particular HGF mixtures [251]. For example, in the myeloid cytokine mixture, the small unidentified clusters may have represented erythroid cells that could not proliferate in the absence of Epo. The authors also stated that there was no evidence for lineage instructive by HGFs from the data, and that these factors likely act permissively to facilitate a stochastic model of haematopoiesis.

A recent study by Ward *et al.* suggests that Epo is not required for the commitment of CMPs towards the erythroid lineage [253]. The group isolated CMPs from human peripheral blood and monitored their proliferation and maturation into MEPs in cultures with or without Epo. Both the proliferation and maturation rates of CMPs were unchanged when stimulated with Epo. In both culture conditions (\pm Epo), 20% of CMPS differentiated into MEPs over 24 hours. However, after 9 days, Epo cultures contained over 20-fold more MEPs when compared to control cultures. Examination of MEP proliferation revealed that there was a significant increase in the expansion of MEPs in the presence of Epo. These results agreed with a stochastic mathematical model, so the authors concluded that Epo does not influence lineage specification of CMPs.

As evident from the studies highlighted above, a wide range of studies support a model of haematopoiesis whereby cell fate is governed by cell-intrinsic stochastic processes, and

proliferation and survival are mediated by cell-extrinsic factors. However, other studies carried out at the same time disagree with such a model, and provide evidence for an instructive role of HGFs. This model will be discussed below.

1.3.2.4 The role of haematopoietic growth factors in instructing cell fate: A deterministic model of haematopoiesis

At odds with a stochastic model of haematopoiesis, a deterministic model of HGFs proposes that the cell fate of HSPCs is regulated by cell-extrinsic factors (**Figure 1.8**). Such a model was first postulated by Trentin and colleagues in the late 1960s. When transplanting irradiated mice with whole BM, Curry and Trentin noted a pattern in the distribution of different colony types within the spleen. Over a number of experiments, approximately 60% of colonies were erythroid, 20% were granulocytic, 15% were megakaryocytic and 2% were eosinophilic, suggesting that the spleen microenvironment regulated the lineage commitment of CFU-S. In a subsequent study, Wolf and Trentin demonstrated that BM stroma selectively promoted the formation of granulocytic colonies, while erythroid colonies primarily formed in the spleen [254]. The authors transplanted BM stroma containing a small number of CFU-S into the spleens of irradiated hosts, and reported that CFU-S that gave rise to granulocytic colonies remained in the BM stroma, while CFU-S that gave rise to erythroid colonies migrated from the BM stroma to the surrounding spleen stroma before maturation. As such, Trentin *et al.* proposed the existence of distinct stromal haematopoietic inductive microenvironments (HIMs) that regulate the fate of HSPCs, although it was unclear how at the time [255].

A decade after Trentin and colleagues proposed the HIM model [254-256], Metcalf and Burgess provided strong evidence to suggest that HGFs can act directly on HPCs to regulate

their differentiation and lineage commitment. In 1980, Metcalf examined the colony forming potential of paired GM-CFU daughter cells in cultures with varying GM-CSF concentrations [257]. Whole BM cells were cultured in the presence of GM-CSF until the first cell division, and then paired daughter cells separated into different cultures. In the first experiment, one daughter cell was transferred to a culture containing a high concentration of GM-CSF (2,500 units), while the other was transferred to a culture containing a low concentration of GM-CSF (50 units). Of the 41 cases where at least one cell formed a colony (>50 cells), 15 paired daughter cells displayed differing lineage potentials. The progeny cultured in medium containing 2,500 units GM-CSF were more likely to form colonies containing granulocytes, while progeny cultured in the presence of 50 units GM-CSF formed more macrophage-containing colonies. In the remaining cases, paired daughter cells formed colonies of similar lineage composition and size. In a second experiment, both paired daughter cells were transferred into separate cultures containing 2,500 units of GM-CSF. At least one colony (>50 cells) was detected in 48 cases, and in 45 of these cases the daughter cells generated colonies/clusters of similar lineage composition and size. Statistical analysis of these experiments showed that dissimilar colony formation from paired daughter cell formation was significantly more likely when two different concentrations of GM-CSF were used. Furthermore, it was shown that the formation of colonies containing macrophages occurred more often when BM progenitors were cultured in low concentration of GM-CSF. As such, Metcalf concluded that GM-CSF regulates lineage commitment of GM bipotent progenitors in a dose-dependent manner [257].

The following year, Metcalf and Burgess performed a similar study by separating paired daughter cells of BM progenitors into medium containing either M-CSF or high concentrations

of GM-CSF and examined their colony forming potential [258]. BM cells were first dispersed in medium containing either M-CSF or GM-CSF and individual cells were monitored until the first cell division. One daughter cell was then transferred to a culture containing M-CSF, while the other was cultured in GM-CSF. When cells were pre-cultured with M-CSF before cell division, 88% of the progeny separated into M-CSF formed colonies containing macrophages, while 56% of progeny separated into medium containing GM-CSF formed colonies containing granulocytes. In a parallel experiment, cells were pre-cultured with GM-CSF before cell division. Eighty-six percent of daughter cells transferred to media containing GM-CSF formed colonies containing granulocytes, while 76% of daughter cells transferred to M-CSF containing cultures formed colonies containing macrophages. The authors noted that the progeny of cells cultured in GM-CSF prior to cell division were statistically more likely to form granulocyte colonies in cultures containing GM-CSF or M-CSF. On the contrary, the progeny of cells cultured in M-CSF prior to cell division were more likely to differentiation into macrophages in the presence of GM-CSF or M-CSF.

When the initial stimulation of BM cells with GM-CSF or M-CSF was increased from 24 hours to 2-3 days before separating the progeny into cultures containing either GM-CSF or M-CSF, it was even more evident that these factors influence lineage commitment. Over 90% of the clones pre-cultured with M-CSF for 2-3 days generated macrophage colonies when transferred to cultures containing either M-CSF or GM-CSF. Similarly, when compared to cells pre-treated with GM-CSF for 24 hours, the clones initiated with GM-CSF for 2-3 days formed a significantly higher number of granulocyte-containing colonies regardless of whether they were transferred to medium containing GM-CSF or M-CSF. Given these findings, Metcalf and

Burgess concluded that GM-CSF and M-CSF are capable of influencing the differentiation of GM-CFU towards granulocyte and macrophage fates, respectively [258].

Since the studies from Metcalf and Burgess, a large number of studies have been published that argue against the permissive action of HGFs, and provide evidence against individual aspects of a stochastic model of haematopoiesis. Firstly, a role for HGFs in the maturation of HSPCs is supported by studies that have investigated the effects of HGF stimulation on leukaemic cell lines. A number of independent studies have shown that both human and mouse G-CSF suppresses proliferation and stimulates the terminal differentiation of the murine myelomonocytic leukaemic cells [259-261]. In one particular study, Souza *et al.* showed that hG-CSF can also induce the differentiation of primary human promyelocytic and myeloblastic leukaemic cells, as observed by colony forming assays [261]. Bedi *et al.* have also shown that IL-6 and GM-CSF are capable of stimulating the differentiation of mouse *BCR-ABL*-transduced FDCP-1 cells and human chronic myeloid leukaemia cells *in vitro*, respectively [262].

The identification of HGF receptor cytoplasmic domains that are required for differentiation has provided further evidence to support the viewpoint that HGFs influence HSPC maturation. A number of studies have demonstrated that the C-terminal region of G-CSFR is necessary for the transduction of differentiation signals [225, 226, 263, 264]. Specifically, targeted mutation of the four tyrosine residues in the cytoplasmic region of G-CSF have demonstrated that tyrosine residues at positions 704, 729 and 744 are involved in mediating differentiation signals [225, 265]. Furthermore, mutations in human *CSF3R* that result in proteins with truncated C-terminals have been identified in patients with congenital neutropenia, demonstrating the importance of this region in differentiation [266].

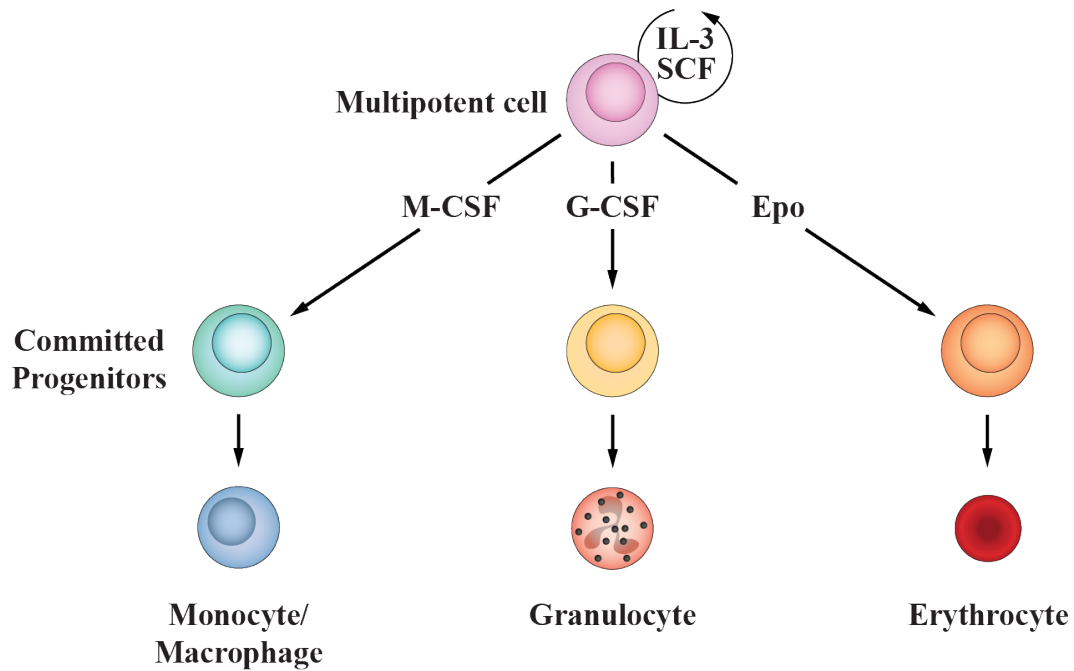


Figure 1.8. Instructive actions of HGFs. In a deterministic model of haematopoiesis, HGFs influence proliferation, survival and cell-fate decisions. Some HGFs, such as IL-3 and SCF, act on HSCs to regulate their self-renewal. Other lineage-associated HGFs instruct HSPCs towards a specific cell lineage. For example, M-CSF has been reported to act on HSCs to upregulate PU.1 and drive them towards a granulocyte/monocyte fate [267]. There is also evidence to suggest that G-CSF [268] and Epo [269] stimulate HPCs to differentiate towards the granulocyte and erythroid lineages, respectively. These HGFs are shown as examples, though there are a number of other HGFs that have been reported to instruct lineage fate. HSC, haematopoietic stem cell; IL-3, interleukin-3; SCF, stem cell factor; M-CSF, macrophage-colony stimulating factor; G-CSF, granulocyte-colony stimulating factor; Epo, erythropoietin; HPC, haematopoietic progenitor cell; HGF, haematopoietic growth factor.

Targeted mutation of the *CSF1R* gene, which encodes M-CSFR, has also been used to identify residues within M-CSFR that are required for progenitor cell differentiation. Like G-CSFR, M-CSFR has 4 tyrosine residues in the cytoplasmic region that are phosphorylated following ligand binding. Rohrschneider *et al.* transduced a series of M-CSFR mutants into FDCP-1 cells and demonstrated that the tyrosine residue at position 807 is essential to mediate differentiation of these cells in the presence of M-CSF [270]. The other three tyrosine residues at positions 697, 706, and 721 promote maturation, but are not required. Regions within both the α and β subunits of human GM-CSFR (hGM-CSFR) have also been shown to be

important in inducing differentiation. Transduction of the myelomonocytic leukaemia cell lines M1 and WEHI-3B with hGM-CSFR containing a WT β subunit promotes their differentiation when cultured with GM-CSF [271]. However, when these cells are transduced with hGM-CSFR containing a truncated β subunit lacking the amino acid residues from position 541 to 897, GM-CSF does not stimulate differentiation. Similarly, mutant GM-CSFR α subunits that lack a proline residue at either position 385 or 360 are unable to transmit differentiation signals when transduced into FCDP-1 cells [272].

Targeted disruption of the Mpl cytoplasmic domain also suggests that Tpo can stimulate maturation. In 1996, Alexander *et al.* transduced two myelomonocytic leukaemia cell lines with WT Mpl, and C-terminal truncated Mpl mutants [273]. In colony forming assays, the myelomonocytic leukaemia cells formed large undifferentiated blast colonies in the presence of Tpo. However, when the myelomonocytic leukaemia cells were transduced with WT Mpl and cultured in the presence of Tpo, they formed myelomonocytic colonies, as confirmed by northern blotting analysis. In contrast, cells transduced with the mutant Mpl receptors displayed an impaired ability to form differentiated colonies when stimulated with Tpo. Targeted disruption of specific tyrosine residues in the cytoplasmic domain of the Mpl C-terminal revealed that the tyrosine-599 residue was required for leukaemia cell differentiation. These data provide evidence to suggest that Mpl can drive the differentiation but not the lineage-specification of cells. However, as leukaemic cells were used in this study, it is possible that aberrant expression of other factors may have pre-determined the lineage commitment of the cells. Performing a similar study using WT haematopoietic progenitors would provide more information regarding the potential instructive properties of Tpo.

In contrast to the above study, ectopic expression of other HGF receptors by lineage-restricted progenitors substantiates a role for these factors in promoting lineage specification. In 1990, Borzillo *et al.* transduced a number of early pre-B lymphocyte lines with WT human *CSF1R* and a viral oncogene, *v-fms*, which encodes a constitutively activated form of M-CSFR [274]. When these cells were cultured in medium supplemented with human M-CSF, they formed small colonies of macrophage-like cells, displayed phagocytic activity, upregulated expression of Mac1 α , and decreased expression of the B-lymphocyte antigen marker, B220. In 2000, Kondo *et al.* demonstrated that transduction of hGM-CSFR into mouse BM CLPs confers GM potential in these cells when assessed using colony forming assays [275]. Similarly, lineage switching has also been observed in human MEPs transduced with human Flt3 *in vitro* [276]. When cultured in the presence of Flt3L, Flt3-transduced MEPs are capable of upregulating cell surface DC markers and forming GM colonies in methycellulose medium.

Carroll and colleagues have demonstrated that transduction of mouse EpoR into pro-B-lymphocytes from the Ba/F3 cell line confers Epo-dependent erythroid maturation [277]. Interestingly, when the authors transduced the cells with chimeric receptors consisting of the extracellular EpoR domain and the IL-3R cytoplasmic domain, these cells also differentiated into erythroid cells in the presence of Epo. However, enforced expression of truncated EpoR mutants lacking the cytoplasmic domain in these cells showed that the cytoplasmic domain alone is not sufficient to stimulate erythroid differentiation. This study suggests that the extracellular regions of HGF receptors are important in transmitting differentiation signals. If this is the case, then it may explain why the studies of Mpl/G-CSFR [249] and EpoR/G-CSFR [250] chimeric fusion receptors described in **Section 1.3.2.3** did not observe any changes in the haematopoiesis of transgenic mouse models.

HGFs have also been shown to regulate the self renewal of both human and mouse HSCs. This is evident by the need for HGFs to expand and maintain long-term HSC cultures. For example, in 1997, Zandstra *et al.* examined the effects of varying HGF concentrations on the expansion of LTC-ICs in cultures derived from human CD34⁺ CD38⁻ BM cells [278]. CD34⁺ CD38⁻ BM cells were cultured in serum-free medium supplemented with different concentrations of Flt3L, IL-3 and SCF for 10 days. Self-renewal of these cells was assessed by the number of LTC-ICs present in the culture after this period. LTC-ICs were quantified by transferring cells to fibroblast feeder layers and monitoring the production of CFUs over a period of 6 weeks. The differentiation of CD34⁺ CD38⁻ BM cells was measured by the number of CFUs present in the cultures following a 10 day period. The authors demonstrated that cultures containing high concentrations of Flt3L produced an increased ratio of LTC-ICs:CFUs when compared to cultures containing low concentrations of Flt3L. Using a similar approach, Audit *et al.* have shown that IL-6 promotes the self-renewal of hHSCs *in vitro* [279].

These studies strongly support a role for HGFs in the self-renewal of HSCs and the differentiation of HSPCs, and this is now generally accepted. However, their role in lineage commitment is still controversial. Although the findings highlighted above provide evidence to suggest that HGFs can influence cell-fate decisions, a large number of conflicting studies exist (see **Section 1.3.2.3**). In this regard, it is difficult to discern which model of haematopoiesis is correct. With the exception of studies examining the fate of paired daughter cells, most investigations have been limited by their ability to thoroughly examine and monitor differentiation at the single cell level. Furthermore, a number of reports have manipulated haematopoietic cells to ectopically express HGF receptors. As a result, these studies do not provide an understanding of how HGFs influence the lineage commitment of individual

haematopoietic cells *in vivo*. Insight into such a mechanism was not provided until the late 2000s, and a number of recent studies have used live imaging techniques to track the fate of single cells following stimulation with HGFs.

In 2009, Rieger *et al.* provided the first real-time analysis of HPC differentiation in the presence of cytokines at the single cell level [268]. The authors purified GMPs from a *LYSM:eGFP* transgenic mouse model, in which the enhanced green fluorescent protein (eGFP) is expressed under the control of the LysozymeM gene locus, and monitored them in culture using real-time bioimaging techniques. Mature granulocytes and monocytes/macrophages express LysM, but GMPs do not. Therefore, the onset of eGFP expression in *LYSM:eGFP* GMPs marks their maturation towards a GM fate. First, Rieger and co-workers performed colony forming assays using freshly isolated *LYSM:eGFP* GMPs and reported that 23 ± 6 % of cells formed macrophage colonies while 53 ± 7 % of cells formed granulocyte colonies [268]. When *LYSM:eGFP* GMPs were pre-treated with either G-CSF or M-CSF before the colony forming assay, they almost exclusively formed granulocyte or macrophage colonies, respectively.

To determine whether this result occurred due to the instruction of bipotent GMPs or the selective expansion of unilineage progenitors, the authors monitored the death and maturation of individual GMPs following G-CSF or M-CSF treatment using live imaging. In cultures containing M-CSF, 88 ± 2 % of individual cells matured to form eGFP⁺ macrophage colonies, while in G-CSF cultures, 87 ± 6 % of individual cells formed eGFP⁺ granulocyte colonies. From comparing these results to the outcome of the colony forming assays prepared with freshly isolated GMPs, the authors concluded that G-CSF and M-CSF instructed at least 34% and 65% of individual cells to differentiate towards granulocyte and macrophage fates, respectively. The number of cell deaths observed when GMPs were cultured with either G-

CSF or M-CSF was very low, and therefore this result strongly argues against a permissive action of HGFs.

Mossadegh-Keller *et al.* have used *PU.1:GFP* (green fluorescent protein) reporter mice and bioimaging techniques to show that M-CSF is also capable of instructing LT-HSCs towards a GM fate [267]. First, they reported that M-CSF induced *PU.1* expression in LSK Flt3⁻ CD34⁺ CD150⁺ HSCs. When *PU.1:GFP* HSCs were cultured in medium lacking M-CSF, *PU.1* expression in single cells was not detected until after 8 hours. After 24 hours, approximately 17% of HSCs were GFP⁺. In cultures containing M-CSF, *PU.1* expression was detected almost immediately, and approximately 35% of HSCs were GFP⁺ after 24 hours. No cell division was detected during the 24-hour culture period, indicating that these findings were not due to the expansion of a *PU.1*⁺ HSC subpopulation. Following 16 hours of culture in the presence of M-CSF, transcriptome analysis revealed an increase in the expression of GM-associated genes by HSCs. When *PU.1*⁺ HSCs were transplanted into irradiated recipients, they generated significantly more GMPs and peripheral myelomonocytic cells at the expense of MegE and lymphoid development when compared to *PU.1*⁻ HSCs. Finally, when injecting mice with M-CSF, the authors noted that there was no change in the number of MyHSCs or expression of M-CSFR, arguing against a selective process [267]. Carras *et al.* have since used a bipotent-GM cell line to determine the mechanism of M-CSF instruction [280]. M-CSF was shown to stimulate extracellular signal-regulated kinase (ERK) signalling [280], which is important for macrophage differentiation [281]. Additionally, the authors reported that M-CSF causes activation of protein kinase C δ [280], which activates *PU.1* [282] and inhibits the expression of *FLI1*, an important TF for granulocytic differentiation [283]. These results strongly suggest that M-CSF is capable of stimulating HSCs to undergo monocyte/macrophage specification.

In 2011, Tsapogas *et al.* provided evidence to suggest that IL-7 signalling promotes commitment of mouse CLPs toward the B-lymphocyte lineage [284]. The authors generated IL-7 knock-out mice and noted that they displayed impaired B-lymphopoiesis, and that the number of CLPs in $IL7^{-/-}$ mice was 5-fold less than the number of CLPs in WT mice. Analyses revealed that this decrease is largely due to the reduced number of $Ly6D^{+}$ CLPs, a subpopulation of CLPs that is restricted to the B-lymphocyte lineage [285]. When $Ly6D^{+}$ CLPs from $IL7^{-/-}$ mice were cultured on an OP9 stromal layer in the presence of IL-7 and other supplementary HGFs, they were capable of generating both NK lymphocytes and B-lymphocytes. This was in contrast to $Ly6D^{+}$ CLPs from WT mice which only formed B-lymphocytes, suggesting that there was a developmental block that prevented $Ly6D^{+}$ CLPs from undergoing commitment to the B-lineage in $IL7^{-/-}$ mice.

Gene expression analysis revealed that the expression of the early B-lymphocyte TF, *EBF1*, was significantly reduced in $Ly6D^{+}$ CLPs from $IL7^{-/-}$ mice when compared to $Ly6D^{+}$ CLPs from WT mice. Previous work has shown that the enforced expression of *EBF1* in $IL7R^{-/-}$ BM progenitors restores B-lymphopoiesis [286], and *EBF1* has been proposed to be a target of IL-7 signalling [287]. Thus, Tsapogas and colleagues investigated whether *EBF1* deficient mice displayed a similar phenotype to $IL7^{-/-}$ mice [284]. Indeed, when single $EBF1^{-/-}$ CLPs were seeded onto OP9 feeder layers, in the presence of the relevant HGFs, they were capable of developing into NK lymphocytes, but not B-lymphocytes. Analysis of $EBF1^{-/-}$ mice demonstrated that they had normal levels of $Ly6D^{-}$ and $Ly6D^{+}$ CLPs, indicating that the decreased number of $Ly6D^{+}$ CLPs in $IL7^{-/-}$ mice is a direct result of impaired IL-7 signalling rather than *EBF1* expression. Thus, the authors concluded that IL-7 likely drives expression of *EBF1* in lymphoid progenitors, which results in the commitment of these cells towards a B-

lymphocyte fate. Interestingly, these findings are in direct contrast with studies of *IL7R*^{-/-} mice that show no change in the number of B-lymphocyte progenitors [241, 242].

Tsapogas *et al.* have also proposed that Flt3 signalling influences HSPC fate [288]. They developed a transgenic mouse model (*FLT3L*-Tg) which expresses the human *FLT3L* gene under the regulation of the *ACTB* promoter. This mouse constitutively expresses a high concentration of Flt3L, resulting in anemia, thrombocytopenia, and a large expansion of DCs in both the BM and spleen. Analysis of other cell populations showed that BM B-lymphocytes are reduced, while GM and T-lymphocytes are increased in the spleen. The BM progenitor compartments are also altered in *FLT3L*-Tg when compared to WT mice. All of the analysed progenitor cell populations were shown to be increased in *FLT3L*-Tg mice, apart from the MEP population. There are two possible explanations for this; *i*) Flt3L selectively expands all haematopoietic progenitor populations except MEP, or; *ii*) Flt3L drives early HSPCs to differentiate towards non-MegE fates. To examine this, Tsapogas and colleagues administered recombinant Flt3L to WT mice and noted that this resulted in a rapid decrease in the percentage of MEPs in the BM after injection. From the kinetics of this result, the authors concluded that low concentrations of Flt3L lead to commitment of multipotent cells towards the MegE fates, while at high concentrations of Flt3L multipotent cells are instructed towards the GM-lymphoid lineages [288].

It should be noted that, while the study by Tsapogas *et al.* suggests Flt3L acts to instruct lineage fate, the data provided does not exclude the possibility of selective expansion of non-MegE progenitors. A figure for the absolute number of MEPs was not provided from the studies in which mice were administered with Flt3L. Therefore, it is difficult to determine whether the percentage of MEPs decreased due to a reduced influx of upstream progenitors

or due to the proliferation of other BM progenitors. In this regard, more work will be required to investigate whether Flt3L can instruct progenitors upstream of MEPs.

In contrast to the findings of Ward *et al.* [253], Grover *et al.* have reported that Epo is capable of stimulating erythroid commitment in early HSPCs [269]. The group analysed the response of haematopoietic progenitors to high systemic Epo levels by injecting mice with a viral vector encoding the *EPO* gene. Analysis of the BM progenitor compartments in these mice showed an expansion of committed erythroid and MegE progenitors, whereas megakaryocyte progenitor (MkPs), preGMP, GMP and LMPP populations were decreased. When examining the LSK Flt3⁻ BM compartment, the authors reported an increase in the expression of erythroid lineage-associated genes, such as *KLF1* and *GATA1*, relative to LSK Flt3⁻ cells from control mice that had received a control vector. Analysis of single LSK Flt3⁻ cells 2 days after injection of the *EPO* vector revealed a 50% increase in the number of cells expressing one or more erythroid associated genes. Additionally, these cells significantly decreased their expression of GM-associated genes when compared to LSK Flt3⁻ from control mice. Further work indicated that these changes were mediated by GATA-1-dependent signalling, as HSPCs lacking *GATA1* did not respond to Epo. Finally, transplantation of LSK Flt3⁻ CD150⁺ cells from mice that had received the *EPO* vector, or control vector, into irradiated hosts revealed that Epo skewed the differentiation of these cells towards an erythroid fate *in vitro*. As such, the authors concluded that Epo stimulates erythroid specification of early HSPCs.

Recently, Pietras *et al.* have shown that IL-1 promotes the differentiation of HSCs towards the GM lineage [175]. When stimulated with IL-1 β , LSK Flt3⁻ CD48⁻ CD150⁺ HSCs were shown to increase the expression of GM-associated genes, such as *CSF2R*, *CSF3R* and *SPI1* (which encodes PU.1), and form more GM colonies in methylcellulose relative to unstimulated cells.

By monitoring *PU.1:GFP* HSCs in culture until the first cell division (>20 hours), the authors demonstrated that IL-1 β stimulated 87% of these cells to upregulate *SP1* expression. In contrast, only 32% of these cells upregulated *SP1* expression in cultures lacking IL-1 β . When IL-1 β treated HSCs were transplanted into irradiated recipients, they generated an increased number of myeloid cells at the expense of lymphoid cells when compared to unstimulated HSCs. As such, the results indicate that IL-1 β can activate and drive GM differentiation of at least 55% of LSK Flt3 $^-$ CD48 $^-$ CD150 $^+$ HSCs.

There is also evidence to suggest that other extrinsic factors, such as hormones and metabolites, influence the lineage specification of HSPCs. In 2014, Oburoglu and colleagues isolated CD34 $^+$ CD38 $^-$ hHSCs and investigated the effects of inhibiting glutaminolysis or glycolysis on Epo-mediated erythroid specification *in vitro* [289]. First, the authors performed small-hairpin (sh)RNA-mediated knock-down of the glutamine transporter gene, *ASCT2*, and examined the differentiation of hHSCs towards the erythroid lineage by monitoring the expression of the erythroid-associated cell surface marker, glycophorin A. Following 6 days of culture, only 10% of sh*ASCT2*-transduced hHSCs had acquired expression of glycophorin A when compared to 40-80% of control cells. In contrast, approximately 50% of sh*ASCT2*-transduced hHSCs differentiated into CD11b $^+$ myeloid cells. Similar results were observed when hHSCs were treated with a glutaminase inhibitor. When the authors inhibited glycolysis in hHSCs using a phosphoglucoisomerase inhibitor, an increased number of these cells differentiated into erythroid cells in the presence of Epo. Finally, these findings were re-created in anaemic mouse models by the administration of glutaminase and phosphoglucoisomerase enzyme inhibitors.

The following year, Xia and colleagues showed that insulin skews the development of LMPPs towards a lymphoid fate [290]. LMPPs that were pre-treated with insulin for 18 hours produced significantly more lymphoid cells, at the expense of myeloid cells in colony forming and *in vivo* transplantation assays when compared to untreated cells. Using gene expression analysis, the authors demonstrated that insulin stimulated the expression of *IKZF1*, a lymphoid-associated TF, in all of the LMPPs assayed, indicating that the insulin-induced lymphoid bias of LMPPs is not a result of selective expansion of a distinct subpopulation. As such, these two studies indicate that the lineage commitment of haematopoietic cells can be affected by hormone signalling and cell metabolism.

Most of the recent reports investigating the role of HGFs in lineage commitment support a deterministic model of haematopoiesis. Indeed, the study by Rieger *et al.* provides comprehensive evidence for the instructive actions of M-CSF and G-CSF on GMPs due to real-time tracking of cell death and differentiation events, and disputes a selective role for these factors in the GMP population [268]. However, other studies do not provide enough evidence to refute a model in which HGFs act in a selective manner. For example, the studies investigating the effects of M-CSF [267], Epo [269] and IL-1 β [175] on early HSPCs have demonstrated that these factors act on multipotent cells, but it cannot be excluded that HGFs are selectively expressed within these populations. As mentioned previously, the study by Tsapogas *et al.* does not provide enough information to confirm that Flt3L acts on progenitors upstream of MEPs to skew their development towards a GM-lymphoid fate [288]. As such, the role of HGFs in lineage fate is still controversial. To determine whether HGFs truly provide instructive cues, or act to selectively expand distinct haematopoietic subpopulations, it is

important to investigate the expression of HGF receptors by different stem and progenitor cell compartments at the single cell level.

1.3.3 Lineage-bias in the haematopoietic system

A number of lineage-biased HSPC populations have been identified in the mouse BM. These cells are considered to be biased because they disproportionately contribute to particular lineages when compared to the average output of the population. In 2002, Sieburg's group performed long-term reconstitution assays using the progeny derived from single mouse HSCs *in vitro* [291]. These experiments revealed three subpopulations of HSCs that were capable of generating cells with distinct repopulating characteristics; balanced HSCs, which repopulated irradiated mice with normal ratios of myeloid and lymphoid cells (as seen in unmanipulated mice); MyHSCs; and LyHSCs. Characterisation of these populations using serial transplantation assays revealed that MyHSCs had more self-renewal potential than balanced HSCs and LyHSCs [292].

Muller-Sieburg *et al.* demonstrated that the lymphoid progenitors derived from these HSCs express different levels of IL-7R. Lymphoid progenitors derived from MyHSCs expressed *IL7R* at levels approximately 2.2-fold lower than those derived from LyHSCs [292]. When the progeny of MyHSCs were cultured *in vitro*, they failed to respond to IL-7 stimulation. These cells generated the same number of lymphoid cells in culture regardless of whether IL-7 was present. As such the authors concluded that the bias of these MyHSCs and LyHSCs was dependent on varying patterns of HGF receptor expression [292]. Further analysis of aging mice by Cho *et al.* revealed that the MyHSC pool increased at the expense of the LyHSC

population with age. These workers suggested that this process might explain the shift towards myelopoiesis in older mice and humans [293].

In 2010, Challen and colleagues purified mouse MyHSCs and LyHSCs based on their exclusion of Hoechst 33342 [25]. MyHSCs were identified as the lower side population (SP), while LyHSCs represent the upper SP, allowing for isolation and further characterisation of these populations. *In vitro* characterisation revealed that SP^{low} MyHSCs and SP^{low} LyHSCs are differentially regulated by transforming growth factor (TGF) β 1 [25]. TGF- β 1 stimulates the proliferation of SP^{low} MyHSCs, but inhibits the expansion of SP^{low} LyHSCs. Other markers have since been identified for the purification of MyHSCs and LyHSCs. Gekas *et al.* have isolated a population of MyHSCs based on their expression of CD41 [30]. Two independent studies have also demonstrated that MyHSCs are enriched for in the CD150^{hi} fraction of the LSK compartment of the BM [27, 294]. Shimazu and colleagues have identified a LyHSC population that expresses CD86 [31]. Lastly, Oguro *et al.* have reported that CD229 can be used to distinguish between MyHSCs and LyHSCs [34]. Whether these populations are the same as the cells initially isolated by Challen *et al.* remains to be seen [25].

Jacobsen's group recently identified platelet-biased mouse LT-HSCs that are maintained by Tpo [29]. These cells express von Willebrand factor (vWF), a glycoprotein involved in platelet adhesion, and express higher levels of megakaryocyte-associated genes when compared to vWF⁻ HSCs. Using single cell transplantation assays, the authors showed that vWF⁺ HSCs generate significantly more platelets than the balanced vWF⁻ HSCs. Additionally, these experiments revealed that vWF⁺ HSCs are upstream of vWF⁻ HSCs, leading Sanjuan-Pla *et al.* to propose that platelet-biased vWF⁺ HSCs are at the apex of haematopoiesis [29]. HSCs that express high levels of c-Kit have also been shown to be biased towards the megakaryocyte

lineage [32]. However, these c-Kit^{high} HSCs have reduced self-renewal capacity when compared to c-Kit^{lo} and are derived from c-Kit^{lo} cells, suggesting that platelet-biased c-Kit^{high} and vWF⁺ HSCs may define distinct populations.

‘Cellular barcoding’ of single cells also suggests the existence of additional B-lymphocyte-, granulocyte- and DC-biased HSCs in mice [9, 28]. This technique allows for the tagging of individual cells with a unique genetic sequence from a library of randomly generated DNA sequences, and has been used to monitor the differentiation of HSPCs during BM transplantation assays. Donor cells are first transduced with lentiviruses containing sequences from a DNA library, resulting in the labelling of individual cells with a unique barcode. The donor cells are then transplanted into recipients, and high-throughput sequencing of haematopoietic cells is used to determine the contribution of each individual HSPC to the haematopoietic system. The Weissman [28] and Schumacher [9] groups have used this technique to identify lymphoid-, myeloid- and DC-biased populations of HSCs. Notably, lineage-bias is not restricted to HSCs, as LMPPs can also be subdivided into lymphoid-, myeloid- and DC-biased populations [9].

Lineage-restricted cells with long-term repopulating activity have also been identified. Yamamoto *et al.* have identified three long-term repopulating myeloid-restricted progenitor (MyRP) subpopulations within the HSC compartment of the mouse BM [23]. The group isolated CD150⁺ CD41⁻, CD150⁺ CD41⁺ and CD150⁻ CD41⁻ cells from the LSK CD34⁻ compartment of the mouse BM and performed single cell serial transplantation assays. When monitoring the output of these cells over time, the authors noted that each fraction contained some individual cells that were restricted to particular lineages. These cells were capable of long-term reconstitution and displayed lineage potentials similar to MkPs (MkRPs), CMPs

(CMRPs) and MEPs (MERPs).

CMRPs accounted for approximately 24%, 49% and 16% of the CD150⁺ CD41⁻, CD150⁺ CD41⁺ and CD150⁻ CD41⁻ cells within the LSK CD34⁻ compartment, respectively. Approximately 7% of CD150⁺ CD41⁻ cells and 5% of CD150⁺ CD41⁺ cells displayed MERP activity, and these cells were not detected in the CD150⁻ CD41⁻ fraction. Similarly, 24% of CD150⁺ CD41⁻ cells and 28% of CD150⁺ CD41⁺ cells were MkRPs, while MkRPs was not detected in the CD150⁻ CD41⁻ fraction. The authors then performed paired daughter cell analysis of LT-HSCs, and reported that LT-HSCs directly give rise to CMRPs, MERPs and MkRPs. Finally, Yamamoto *et al.* used a similar approach to demonstrate that the MPP and LMPP populations contained a variety of lineage restricted progenitors [23]. The authors concluded that currently defined HSPC populations are not comprised of homogeneous progenitors with similar lineage-potentials. Rather, they contain a number of distinct subpopulations that together contribute to the lineage potential of the whole population.

A number of lineage-biased populations have been identified within the haematopoietic hierarchy, and some of these have been shown to be differentially regulated by HGFs, such as IL-7, Tpo and TGF- β 1. This adds further complexity when trying to determine a model of haematopoiesis. If these lineage-biased progenitors differentially express HGF receptors and respond to particular factors, then this would support a permissive model of haematopoiesis. On the other hand, if HGFs are responsible for driving lineage-biases in multipotent cells, then this suggests that HGFs are instructive. As highlighted in **Section 1.3.2.4**, analysis of HGF receptor expression within different compartments will help to provide clarity on whether such factors selectively regulate the differentiation and/or lineage fate of HSPC subpopulations.

1.4 Aims of project

There are a large number of conflicting studies available regarding the role of HGFs in the lineage specification of HSPCs. Some of the work provides clear evidence that certain HGFs can instruct HSPC fate, while other studies indicate that HGFs act permissively. The exact mechanisms that govern lineage commitment in HSPCs remains unclear. It is also largely unknown how heterogeneous HSPC populations are in regards to their response to HGFs. For example, lineage-biased populations have been shown to be differentially regulated by certain HGFs, and it has been shown that not all cells within the HSC compartment respond to M-CSF [267], Epo [269] and IL-1 β [175]. This suggests that the receptors for these factors are selectively expressed by certain subpopulations within haematopoietic compartments. If such subpopulations of cells exist within the early HSPC compartments, then HGFs would selectively stimulate these subpopulations to drive their differentiation. This would suggest that certain HSPC populations are somewhat primed to repopulate particular lineages, favouring a selective model of haematopoiesis over a deterministic model. On the other hand, some previous studies have reported the co-expression of particular growth factor receptors by early HSPCs, such as *EPOR* and *CSF3R*, suggesting that Epo and G-CSF act to instruct lineage fate in these cells [116]. Additionally, Rieger *et al.* have elegantly demonstrated the instructive properties of G-CSF and M-CSF using GMP progenitors *in vitro*, strongly supporting a deterministic model of haematopoiesis [268].

Previous studies have attempted to define HGFs as either selective or instructive molecules and, as highlighted in **Section 1.3**, have considered these two properties to be mutually exclusive. However, as highlighted in the previous paragraph, there is evidence to suggest

that aspects of both a selective and deterministic model play a role in HSPC development. Therefore, defining lineage specification as either a selective or deterministic process based on the action of HGFs is possibly an oversimplification of an extremely complex process, especially considering the heterogeneity of HSPCs. To further explore this postulate, the analysis of HGF receptor expression at the single cell level is required, with particular focus on the selective expression and co-expression of such receptors within early HSPC populations. Ultimately, this will provide insight into how HGFs regulate HSPC differentiation, and help to determine whether HGFs act in a selective or instructive manner. Understanding such a process will be helpful in the manipulation of HSPCs for clinical purposes, such as the *in vitro* manufacturing of erythrocytes for blood transfusions [295].

The purpose of this project is to investigate the expression of HGFs on single HSPCs. Single cell quantitative RT-PCR (qRT-PCR) assays were first designed and optimised, and then used to examine the expression of HGF transcripts by cells of all major HSPC compartments of the mouse BM. The design of multiplex qRT-PCR assays allowed for the analysis of potential co-expression of HGF receptor genes within the multipotent haematopoietic cell compartments of the BM. Expression of HGF receptor protein within each HSPC compartment was then investigated and the data was compared with the findings from the qRT-PCR studies. Finally, *in vitro* culture experiments were undertaken to examine the responsiveness of particular HSPC compartments to Flt3L. These included analyses of cell signalling pathways and cell differentiation/lineage commitment. The findings generated from this work have identified novel patterns of HGF receptor expression throughout the haematopoietic hierarchy, and add to the debate regarding the role of HGFs in regulating haematopoiesis.

CHAPTER 2: MATERIALS AND METHODS

2.1 Mice

C57/BL6 mice (WT) were purchased from [REDACTED]

[REDACTED] All mice were treated in accordance to guidelines set out by The Home Office (project license numbers 30/2850 and PPL70/8011), and were culled by cervical dislocation between 7-14 weeks of age for this study.

2.2 Analysis of HemaExplorer and BloodSpot databases

Raw values for *FLT3*, *EPOR*, *CSF1R* and *CSF3R* expression by HSPCs were exported from the HemaExplorer and BloodSpot databases [296, 297]. When searching for genes in the databases, the 'Mouse normal haematopoietic system' dataset was selected. This included LT-HSC, ST-HSC, LMPP, CLP, ETP, pro-B-lymphocytes, pre-B-lymphocytes, preGM, GMP, MEP, MkP, preCFU-E, CFU-E and EP populations. Other populations were also included in the dataset but these were excluded, as they were not relevant to this study. Data was downloaded in Microsoft Excel format from the website. Where the data included more than one set of results, all results were averaged and the mean was included in the data analysis. As the data could only be exported in \log_2 format, the data was transformed back to the original expression values using the formula:

$$2^{[Log\ transformed\ expression\ values]} = [Original\ expression\ values]$$

Mean and standard error for expression of each gene by each HSPC population was calculated individually and then plotted for analysis.

2.3 Bone marrow cell preparation

BM cells were isolated from both mouse hindlimbs and forelimbs to ensure high cell numbers were obtained during experiments. To prepare the hindlimb for processing, scissors were used to cut through the pelvis of the mouse, removing the femur, tibia and fibula. This ensured that the femur head remained intact during preparations. The hindpaw was then separated at the ankle and the skin over the limb was removed. To separate the femur from the tibia, the knee was hyperextended and pulled apart. The bones were then cleaned of any excess muscle or fat. To remove the forelimbs from the mouse, the skin around the limb was cut and reflected. The limb was then gently pulled away from the axial skeleton. The scapula, humerus and radius/ulna were then each separated by pulling apart the joints. As before, the bones were cleaned of muscle and fat. Of the forelimb, only the humerus and ulna were retained as the radius and scapula did not contain a significant amount of BM.

Unless otherwise stated, cells were flushed from the BM cavity using a 1mL syringe (BD biosciences, NJ, USA) and 18-gauge needle (Terumo, Leuven, Belgium), and fluorescent activated cell sorting (FACS) buffer. FACS buffer was prepared by adding 2% fetal calf serum (FCS) and 2mM EDTA to Dulbecco's phosphate buffered saline (DPBS) without $\text{Ca}^{+}/\text{Mg}^{+}$ (all Sigma-Aldrich, Haverhill, UK). The 18-gauge needle was inserted into both sides of each bone before all cells from the BM of a single mouse were flushed into 15mL falcon tubes (Thermo Fisher Scientific, Loughborough, UK). Cell suspensions were mixed using a pipette before being strained using 70 μM Cell strainers (Thermo Fisher Scientific) and then centrifuged at 4°C, 394 relative centrifugal force (rcf, g) for 4 minutes. The pellet was resuspended in 500 μL of ACK Lysing Buffer (Gibco, Thermo Fisher Scientific) to lyse erythrocytes and incubated on

ice for 10 minutes. Cells were then diluted to 5mL using FACS buffer and spun down at 4°C, 394 rcf for 4 minutes. The pellet was resuspended in buffer or cell culture medium and processed as required.

2.4 Preparation of bone marrow for flow cytometric analysis

BM cells were prepared from C57/BL6 mice as described in **Section 2.3**. Once the erythrocytes were lysed, cells were resuspended in FACS buffer, divided into multiple samples and transferred to non-sterile v-bottomed 96-well plates (Greiner Bio-One, Gloucestershire, UK). The samples were then pelleted at 4°C, 394 rcf for 4 minutes and the supernatant was removed by rapidly turning the plates upside down over the sink. Unless CD16/32 expression was examined using fluorescently-labelled antibodies (as needed for myeloid progenitor analysis), cells were incubated with anti-CD16/CD32 for 20 minutes to block CD16 (FcγIII) and CD32 (FcγII) receptors, prior to staining. After blocking, samples were then stained in 50-100µL FACS buffer containing antibody cocktails or a single antibody for compensation for at least 1 hour on ice. Following staining, samples were washed twice using FACS buffer, and subsequently resuspended in FACS buffer. Cells were finally filtered using Partec CellTrics sterile filters (Sysmex-Partec, Münster, Germany) and transferred to polypropylene FACS tubes (Thermo Fisher Scientific). Samples were acquired using a CyAN FACS Analyser (Beckman Coulter, High Wycombe, UK) controlled by Summit v4.3 software. Post-experimental analysis was carried out using FlowJo software, version 10.1.

2.5 Preparation of bone marrow for fluorescent activated cell sorting

BM cells were prepared from C57/BL6 mice as described in **Section 2.3**, and the protocol for cell sorting was similar to the protocol used for flow cytometry (**Section 2.4**). However, when BM samples were prepared for FACS, sterile DPBS (without Ca^+/Mg^+) containing 10% FCS was used. After erythrocyte lysis, cell suspensions were resuspended in 500 μL of 10% FCS DPBS and transferred to sterile 1.5 mL Eppendorfs (Eppendorf, Stevenage, UK) before being pelleted at 4°C, 394 rcf for 4 minutes. Unless analysing CD16/32 expression, F_c receptors were blocked as per **Section 2.4**. As most of the cells from a single mouse were processed when sorting single HSCs, cell pellets were resuspended in a volume of 200 μL of 10% FCS DPBS containing antibody cocktails. Samples were then incubated with the antibody cocktails for at least 1 hour on ice. Samples were then washed twice in 10% FCS DPBS, and subsequently resuspended in 10% FCS DPBS. Cells were finally filtered using Partec CellTrics sterile filters (Sysmex-Partec) and transferred to either sterile polypropylene FACS tubes or sterile polystyrene FACS tubes (Thermo Fisher Scientific). All samples were sorted twice to ensure high purity; the first sort was set to 'purify' on the Summit software (Beckman Coulter) and cells were sorted into 500 μL of 10% FCS DPBS. The initial sort was set to 'purify' with a drop envelope of 1. This usually resulted in a good-to-high purity when analysing with strict gates, and it was only a rare occurrence for impurities to fall far outside of the gating strategy. The second sort was set to 'single-cell' with a drop envelope of 0.5 to ensure high purity when sorting. Cells were either sorted into LightCycler 480 384-well plates (Roche) containing 1 μL of H_2O in each well for qRT-PCR analysis, or into buffer/culture medium for further processing.

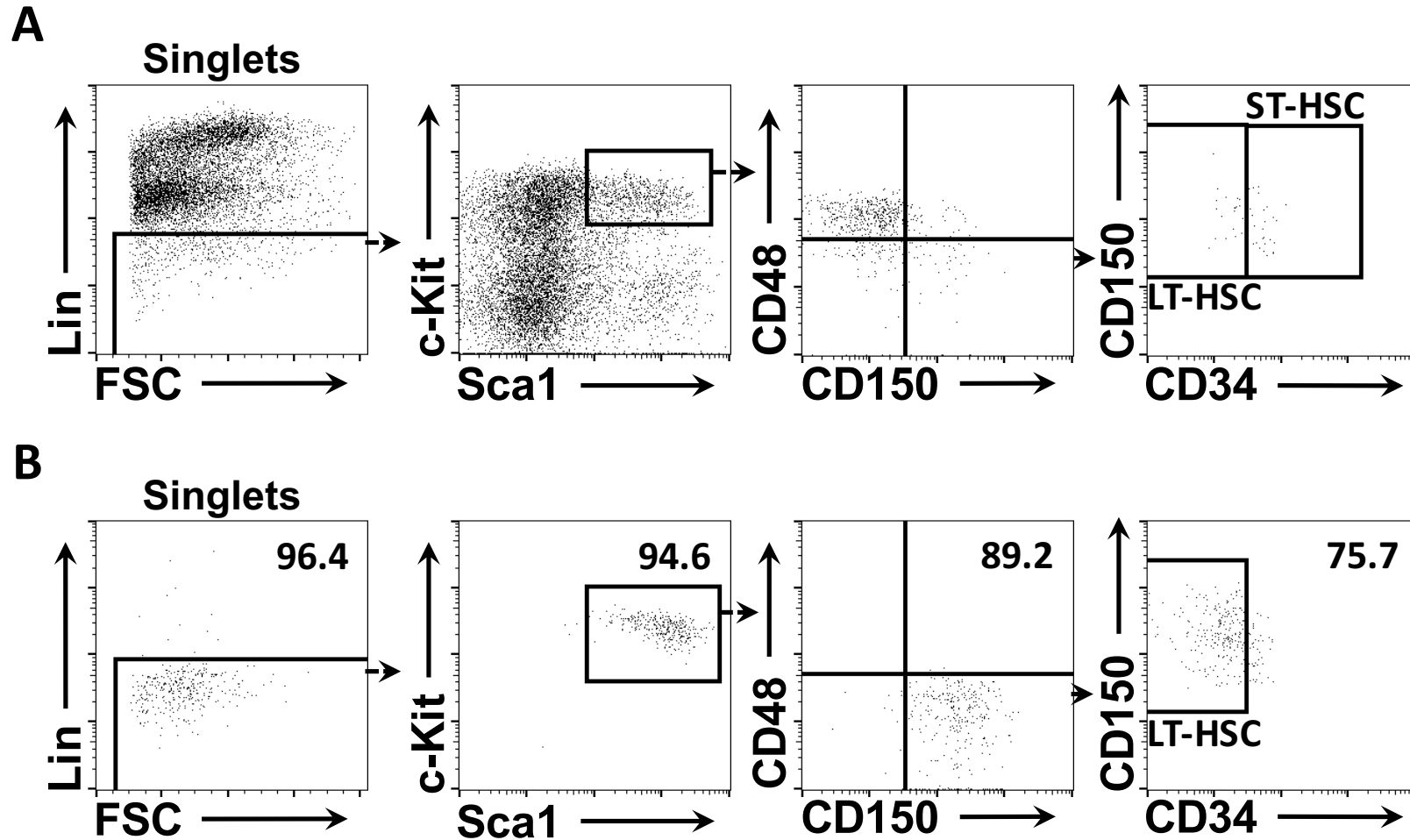


Figure 2.1. Isolation of single LT-HSCs. (A) LT-HSCs were sorted from whole BM into 500µL of phosphate buffered saline supplemented with 10% fetal calf serum. (B) Single LT-HSCs from the initial sort (A) were sorted a second time to ensure high purity. Values depicted in (B) indicate the number of cells within the gate as a percentage of singlets. Lin, lineage markers; LT-HSC, long-term haematopoietic stem cell; ST-HSC, short-term haematopoietic stem cell; BM, bone marrow.

Once sorting was complete, PCR plates were sealed with adhesive PCR film and were immediately frozen and stored at -80°C until required. Sorting was carried out using either a MoFlo High Speed Sorter (Beckman Coulter) or a MoFlo Astrios (Beckman Coulter) controlled by Summit v4.3 or Summit v6.2.3 software, respectively. Post-experimental analysis was carried out using FlowJo software, version 10.1, to ensure quality of sorts. A representative isolation of single LT-HSCs is shown in **Figure 2.1**. Unfortunately, given the small numbers of cells sorted, especially when sorting HSCs, it was not feasible to check the purity after the second sort.

2.6 Antibody titration for fluorescent activated cell sorting and flow cytometric analysis

Antibodies were titrated by staining whole BM cells at different dilutions of the original antibody concentration. Unless a more concentrated dilution was specified by the supplier, the most concentrated dilution that each antibody was tested at was 1/50. Optimum dilutions were chosen as the least concentrated dilution that did not yield a decrease in staining when compared to the most concentrated sample (e.g. 1/50). Where there was an immediate loss in staining following dilution at 1/100, 1/50 was chosen as the optimum concentration. An example of an antibody titration can be seen in **Figure 2.2**.

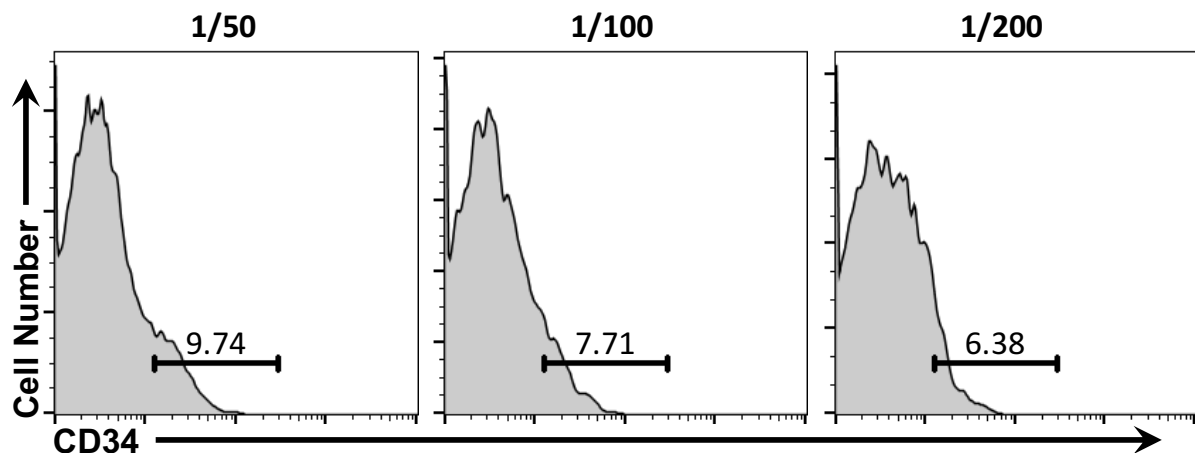


Figure 2.2. Example of an antibody titration used for flow cytometry. An antibody specific for CD34 was titrated at dilutions of 1/50, 1/100 and 1/200 to determine the optimum dilution for flow cytometry. The optimum dilution was chosen as 1/50, as there was a clear decrease in staining when diluting the antibody further. Values indicate the percentage of cells that are within the given gate.

2.7 Preparation of bone marrow cell lysates for testing and optimisation of qRT-PCR assays

Cells were isolated from BM as described in **Section 2.3**. Whole BM cells were transferred to 1.5 mL Eppendorfs, pelleted at 4°C, 394 rcf for 10 minutes, and the supernatant was aspirated. Cells were lysed by adding 20-50µL of H₂O to the pellet before the samples were vortexed and incubated on ice for 5 minutes. The nucleotide concentration of cell lysates was determined by analysing 0.5µL of the sample on a Nanodrop 2000. Samples were then stored at -80°C until required.

2.8 qRT-PCR assay design and optimisation for gene expression analysis

For a brief and succinct summary of the qRT-PCR assay design and optimisation workflow used in this thesis, see **Figure 2.3**.

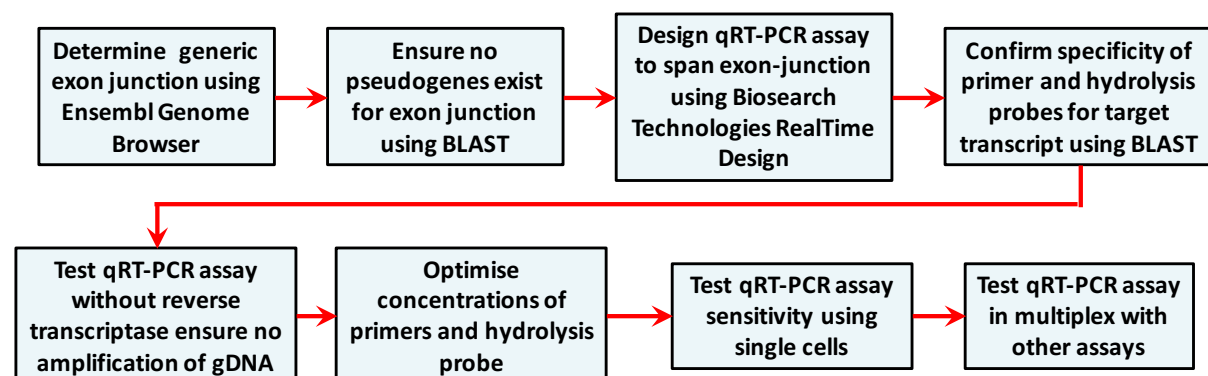


Figure 2.3. Workflow of multiplex qRT-PCR assay design and optimisation for detection of gene expression in single cells. BLAST, Basic Local Alignment Search Tool; gDNA, genomic DNA.

2.8.1 Identification of candidate sequences for the design of qRT-PCR assays

Information regarding a gene of interest was obtained by searching Ensembl Genome Browser (<http://www.ensembl.org/index.html>) using the gene name. Using this database, details about a gene was gathered including the DNA sequence, the mRNA sequence of any protein coding transcripts, and the number of exons present within the gene. To analyse the gene and transcript sequences, the freely available Basic Local Alignment Search Tool (BLAST, <http://blast.ncbi.nlm.nih.gov/Blast.cgi>) was used. BLAST is an algorithm that allows for the

comparison of input protein and nucleotide sequences to known protein and nucleotide sequences within a biological database/library [298].

To ensure accurate analysis of gene expression at the single cell level, qRT-PCR assays were designed to specifically detect mRNA transcripts but not genomic DNA (gDNA). For this reason, qRT-PCR assays were only designed to be specific for regions spanning exon junctions. Additionally, as the qRT-PCR assays were intended to detect all protein coding transcripts within a cell, all protein coding transcripts for a gene of interest were analysed to determine shared exon junctions that could be interrogated using a qRT-PCR assay. This strategy was used for the design of generic mRNA-specific qRT-PCR assays that detected all protein coding transcripts. Once all of the generic exon junctions were identified within a gene, they were analysed using BLAST to ensure that no pseudogenes were present at these sequences. The BLAST mouse genomic database was used to analyse the mRNA sequences flanking the candidate exon-exon junction (20 nucleotides either side of each exon-exon junction) to determine whether similar sequences existed within the mouse genome. For completeness, these sequences were also analysed using the BLAST RefSeq RNA database, which determined if the sequences spanning the exon-exon junctions shared any complementarity to any other transcripts in the mouse transcriptome.

For design of qRT-PCR primers and hydrolysis probes, RealTimeDesign Software, an online interactive program hosted by Biosearch Technologies (California, USA), was used. The RealTimeDesign Software calculates the best primers and hydrolysis probe sequences for a chosen DNA sequence based on melting temperature, length and internal stability. It also allows manual input and modification of these sequences allowing users to tailor any suggested assay sequence to their needs. Hydrolysis probe-based qRT-PCR assays allow for

greater specificity and are required for the combination of assays in duplex/multiplex reactions, so all of the assays that were designed for this thesis were hydrolysis probe-based.

Using the RealTimeDesign Software, sequences (usually containing 100 nucleotides either side of a candidate exon junction) were input and the specific location of an exon-exon junction was marked using the '^' key. This allowed the software to tailor the hydrolysis probe and primer sequences to directly interrogate the specified exon-exon junction. Under the 'Express: qPCR - BHQ Probe' menu, the application was either set to 'qPCR - BHQ' or 'qPCR - BHQ Plus', the mode was set to 'custom', and the software was used in 'Single Plex' mode. Assays were designed to amplify 100-200 nucleotide sequences. Where needed, some assays were designed using BHQplus Probes (Biosearch Technologies), which are designed using duplex stabilizing technology that permits the use of shorter sequences. Hydrolysis probes were covalently attached to FAM, Cal560, Cal610 or Quasar670 fluorophores.

Once the sequences for a qRT-PCR assay (hydrolysis probe, forward primer and reverse primer) were designed, they were analysed using the BLAST database. Firstly, the RefSeq RNA BLAST database was used to analyse the primer and hydrolysis probe sequences to confirm that they were specific for the chosen target mRNA, and also to ensure that the sequences did not share high complementarity with any other regions in the mouse transcriptome. Lastly, the primer and hydrolysis probe sequences were analysed using the genomic BLAST database to ensure that they did not share complementarity with any genomic sequences in the mouse. If the RealTime Design software was unable to design a hydrolysis probe RT-PCR assay for a given exon junction, or the probe and primer sequences designed for a given exon junction shared high sequence homology with another mouse genomic or transcriptomic sequence, another exon junction within the same gene was identified and a qRT-PCR assay

was designed for this sequence using the same protocol. Overall, this design strategy helped to prevent the design of qRT-PCR assays that detected gDNA and/or non-specific targets.

Once primer and probe sequences that suited the parameters described above were selected, assays were ordered from Biosearch Technologies and its sister company, DNA Technology (Risskov, Denmark). All oligonucleotides were shipped as lyophilised powders. The oligonucleotides were resuspended in H₂O as instructed by the manufacturer.

2.8.2 Optimisation of qRT-PCR primer concentrations

Once qRT-PCR assays were designed, they required primer and hydrolysis probe optimisation to ensure accurate and sensitive amplification of transcripts in single cells. Firstly, limiting concentrations of the forward and reverse primers of each qRT-PCR assay were determined. For each assay, both primer sequences were tested in variable combinations. This included final experimental concentrations of 300nM, 200nM, 100nM, 80nM, 60nM and 40nM. All possible combinations of these forward and reverse primer concentrations were assayed, resulting in preparation of 36 reactions that were tested using 3 technical replicates. Mean values for each reaction were calculated from the technical replicates and used for analysis. When preparing the reactions, a dilution of whole BM lysate (approximately 200ng of RNA and DNA) and an excess concentration of hydrolysis probe (250nM) remained constant, ensuring that the only variables in the reactions were the primer concentrations and combinations. A master mix for all reactions was prepared containing Quantitect Master Mix and RT mix (Qiagen, Manchester, UK), H₂O, whole BM lysate and hydrolysis probe but did not contain primers as these were added at a later stage. Using an electronic pipette, 4µL of the

master mix was dispensed into 108 individual wells (36 reactions in triplicate) of a LightCycler 480 384-well plate (Roche, West Sussex, UK). Solutions of both forward and reverse primers were prepared at the following stock concentrations: 1.8 μ M, 1.2 μ M, 600nM, 480nM, 360nM and 240nM. Again, using an electronic pipette, 1 μ L each of the forward and reverse primer stocks were dispensed into the LightCycler 480 384-well plate to bring reactions to a final volume of 6 μ L. An example of the master mix used for primer optimisation protocols is shown in **Table 1**. **Figure 2.4** represents the format used on a 384-well PCR plate to ensure all combinations of primer concentrations were tested for a given qRT-PCR assays.

Table 1: Example of a master mix preparation for the optimisation of qRT-PCR primer concentrations.

Assay Constituent	Volume for x1 reaction	Volume for x125 reactions
Quantitect Master Mix	3 μ L	375 μ L
Quantitect RT Mix	0.06 μ L	7.7 μ L
Hydrolysis probe (5 μ M stock)	0.3 μ L	37.5 μ L
Whole BM lysate	0.2 μ L	25 μ L
H ₂ O	0.44 μ L	55 μ L
Total	4 μ L	500 μ L

BM, bone marrow; RT, reverse transcriptase.

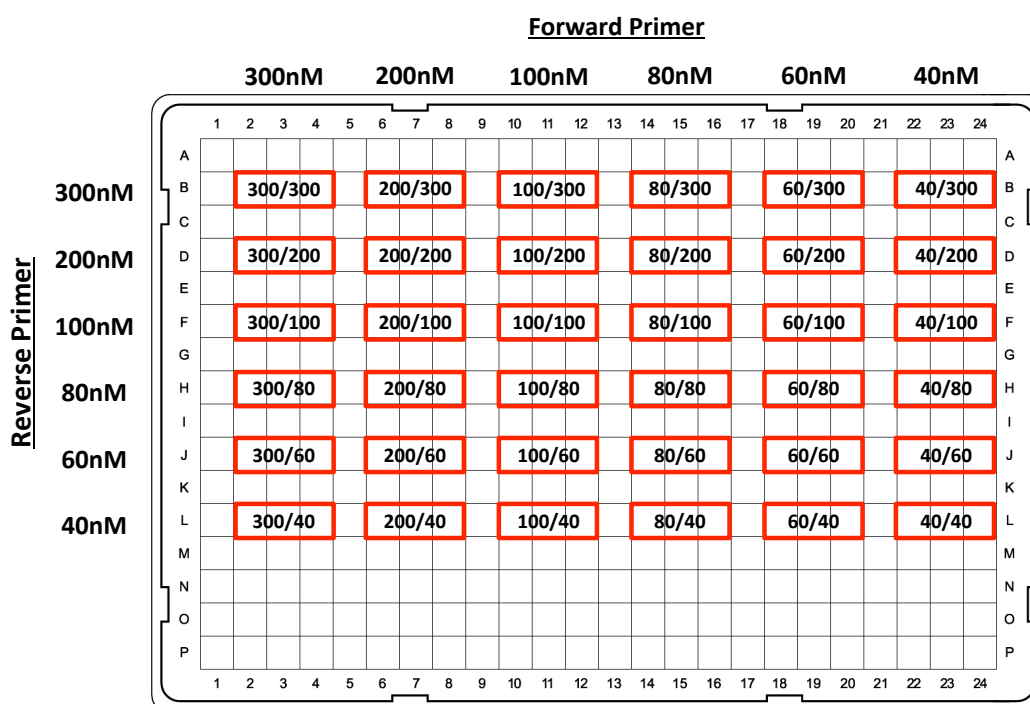


Figure 2.4. 384-well plate format used to determine limiting primer concentrations for qRT-PCR assays. This plate format was used to test all possible combinations of forward and reverse primer concentrations using final primer concentrations of 300nM, 200nM, 100nM, 80nM, 60nM and 40nM. The red boxes represent technical replicates of a specified primer concentration combination in nM. For example, sample '100/80' labels a sample containing 100nM of the forward primer and 80nM of the reverse primer.

To compare primer concentration combinations, reactions with 300nM of forward primer and 300nM of reverse primer were used as a 'reference' reaction (300nM/300nM reaction), as this reaction was considered to have non-limiting amounts of both primers. To select the optimal limiting primer concentrations, two parameters in each reaction were analysed. Firstly, the threshold cycle (Ct) for each reaction was calculated. Any reactions that had a Ct value that was >0.5 cycles greater than the Ct value of the 300nM/300nM reaction were considered to have compromised efficiency, so they were excluded from selection. Secondly, the level of fluorescence at the end of the plateau phase of the reactions was calculated, and this value was termed the 'end fluorescence value'. Amongst the reactions that were considered efficient based on Ct value, the reaction with the lowest end fluorescence value

was identified. The primer concentrations within this reaction were selected as the optimal limiting primer conditions. See **Figure 2.5** for a representative amplification plot showing the reference reaction (300nM/300nM), a reaction containing the optimum primer concentration combination (60nM of forward primer and 300nM of reverse primer; 60nM/300nM), and a reaction that has lost efficiency due to low primer concentrations (60nM of forward primer and 60nM of reverse primer; 60nM/60nM).

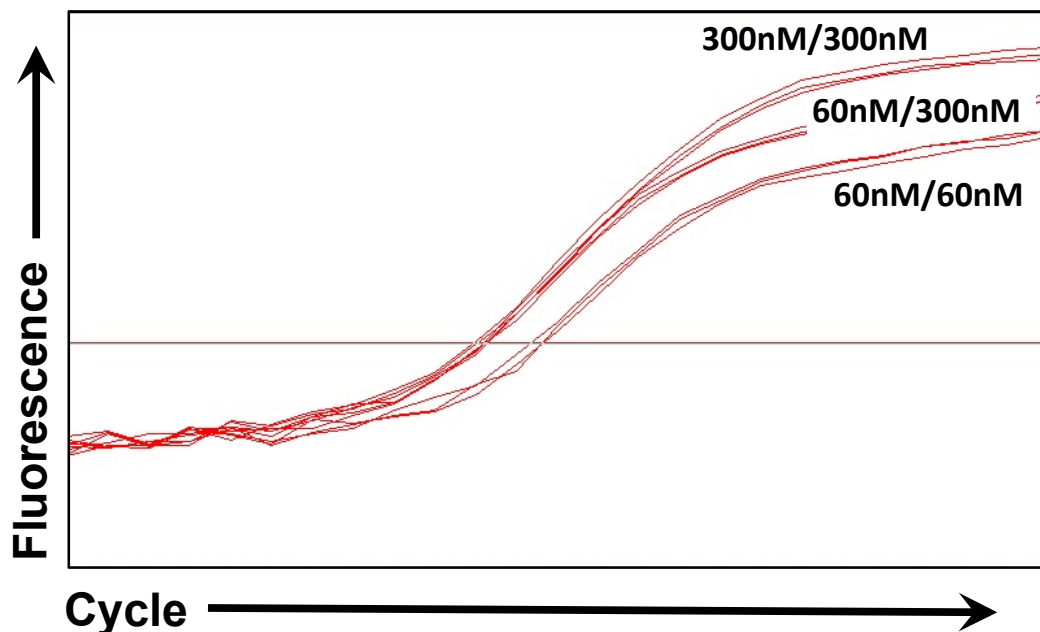


Figure 2.5. Selection of limiting primer concentrations for a qRT-PCR assay. The reference reaction, containing 300nM of forward primer and 300nM of reverse primer (300nM/300nM reaction), was used to select an optimal limiting primer concentration combination. Firstly, reactions that had a Ct value that was >0.5 cycles greater than the Ct value of the reference reaction (300nM/300nM reaction) were not considered efficient (see the reaction containing 60nM of forward primer and 60nM of reverse primer; 60nM/60nM). Of the samples that had a Ct value that was <0.5 cycles greater than the Ct value of the reference reaction (see the reaction containing 60nM of forward primer and 300nM of reverse primer; 60nM/300nM), the reaction with the lowest end fluorescence value was selected to be the optimum primer concentration combination. The horizontal line was used to calculate the Ct. Ct, threshold cycle.

2.8.3 Optimisation of hydrolysis probe concentrations

Optimum hydrolysis probe concentrations for qRT-PCR assays were determined using a similar protocol as described in **Section 2.8.2**. The hydrolysis probes were analysed at concentrations of 250nM, 225nM, 200nM, 175nM, 150nM, 125nM, 100nM, 75nM, 50nM and 25nM. Reactions were performed with 3 technical triplicates, and mean values for each reaction were calculated and used for analysis. When preparing the reactions, the concentration of whole BM lysate (approximately 200ng of RNA and DNA) remained constant and optimal limiting primer concentrations were used, ensuring that the only variable in the reactions was the concentration of hydrolysis probe.

Table 2: Example of a master mix preparation for the optimisation of qRT-PCR hydrolysis probe concentrations.

Assay Constituent	Volume for x1 reaction	Volume for x35 reactions
Quantitect Master Mix	3 µL	105 µL
Quantitect RT Mix	0.06 µL	2.1 µL
Whole BM lysate	0.2 µL	7 µL
Forward primer	1 µL	35 µL
Reverse primer	1 µL	35 µL
H ₂ O	0.44 µL	15.4 µL
Total	5.7 µL	199.5 µL

BM, bone marrow; RT, reverse transcriptase

A master mix was prepared containing qRT-PCR buffer and enzyme solution, H₂O, whole BM lysate and limiting primer concentrations. Using an electronic pipette, 5.7µL of the master mix was dispensed into 30 individual wells (10 reactions in triplicate) of a LightCycler 480 384-well plate. Solutions of the hydrolysis probe were prepared at the following concentrations: 5µM, 4.5µM, 4µM, 3.5µM, 3µM, 2.5µM, 2µM, 1.5µM, 1µM, 0.5µM. Again, using an electronic pipette, 0.3µL of the relevant hydrolysis probe stock solution was dispensed into the LightCycler 480 384-well plate to bring reactions to a final volume of 6µL. A typical master mix preparation used to optimise hydrolysis probe concentrations is shown in **Table 2**.

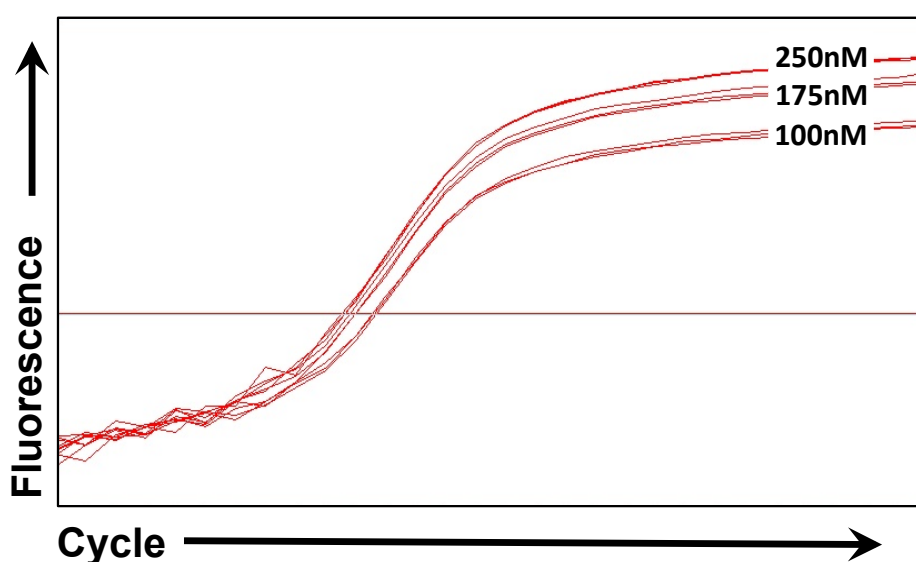


Figure 2.6. Optimisation of hydrolysis probe concentrations for a qRT-PCR assay. The reference reaction, containing 250nM of hydrolysis probe, is used to select a primer concentration combination (250nM reaction). Firstly, reactions that had a Ct value that was >0.5 cycles greater than the Ct value of the reference reaction (250nM reaction) were considered to have compromised efficiency, and were removed from analysis (see the reaction containing 100nM of hydrolysis probe). Of the remaining reactions, the reaction with the lowest hydrolysis probe concentration was selected to be the optimal hydrolysis probe concentration (see the reaction containing 175nM of hydrolysis probe). Ct, threshold cycle.

The reaction containing 250nM of hydrolysis probe was included as a reference reaction as this was considered to be a non-limiting amount of probe. The Ct value of each reaction was

analysed and compared to the Ct value of the reaction containing 250nM of hydrolysis probe. Any reactions that had a Ct value that was >0.5 cycles greater than the Ct value of the reference reaction were considered to have lost efficiency due to low probe concentrations, so they were excluded from selection. Amongst the remaining reactions, the lowest concentration of hydrolysis probe was selected as the optimum concentration. If all reactions produced a Ct value >0.5 cycles greater than the reference Ct value then the optimum hydrolysis probe concentration was chosen as 250nM. Data from a representative hydrolysis probe optimisation experiment is shown in **Figure 2.6**.

2.9 qRT-PCR analysis

2.9.1 Preparation of cells previously sorted into LightCycler 480 384-well plates for qRT-PCR analysis

Gene expression of FACS sorted cells was analysed using a one-step QuantiTect Multiplex RT-PCR Kit (Qiagen) with optimised primer and hydrolysis probe concentrations in LC480 384-well plates. Reactions were prepared on ice, for a final reaction volume of 6uL. No template controls (NTCs) and reactions without reverse transcriptase (-RT) were prepared and loaded into the plate as controls for complementary DNA (cDNA) contamination and gDNA amplification, respectively. For the single-cell samples, a master mix was prepared containing a qRT-PCR buffer and enzyme solution, H₂O, and limiting concentrations of primers and hydrolysis probe. The volume of water in each master mix was adjusted depending on the number of assays included in each reaction. An example of a master mix used to detect the expression of three genes in a single cell is shown in **Table 3**. When preparing reactions using

a LightCycler 480 384-well plate that was previously stored at -80°C, the plate was briefly centrifuged to collect any sample at the bottom of the well before removing the adhesive PCR film. Using an electronic pipette, 5 µL of the master mix was added to each well, which already contained 1 µL of H₂O from when the cell was initially sorted. This resulted in a final reaction volume of 6µL. The PCR plate was then sealed using adhesive PCR film and stored on ice until it was analysed on a LC480 II instrument (Roche).

Table 3: Example of a master mix preparation for the analysis of gene expression in single cells.

Assay Constituent	Volume for x1 reaction	Volume for x30 reactions
Quantitect Master Mix	3 µL	90 µL
Quantitect RT Mix	0.06 µL	1.8 µL
Assay 1 - Forward Primer	0.15 µL	4.5 µL
Assay 1 - Reverse Primer	0.15 µL	4.5 µL
Assay 1 - Hydrolysis probe	0.15 µL	4.5 µL
Assay 2 - Forward Primer	0.15 µL	4.5 µL
Assay 2 - Reverse Primer	0.15 µL	4.5 µL
Assay 2 - Hydrolysis probe	0.15 µL	4.5 µL
Assay 3 - Forward Primer	0.15 µL	4.5 µL
Assay 3 - Reverse Primer	0.15 µL	4.5 µL
Assay 3 – Hydrolysis probe	0.15 µL	4.5 µL
H ₂ O	0.59 µL	17.7 µL
Total	5 µL	150 µL

RT, reverse transcriptase.

2.9.2 Amplification program used on the Roche LC480 II PCR instrument for analysis of gene expression

LightCycler 480 384-well plates were loaded into a LC480 II instrument (Roche) for the analysis of gene expression. The Quantitect RT-PCR kit (Qiagen) allows for single-step amplification of targets and the manual contains detailed protocols for the use of this kit. The program used on the instrument is outlined in **Table 4**. The first step in the amplification process was the conversion of mRNA to cDNA by RT. This step was carried out at 50°C for 20 minutes. The second step in the Quantitect protocol requires an initial activation step of the HotStarTaq DNA polymerase at 95°C for 15 minutes. The remaining steps are part of a 2-step denaturation and annealing/extension cycle. The denaturation step was carried out at 94°C for 45 seconds, followed by 60°C at 45 seconds for the annealing/extension stage. This 2-step cycle was repeated for 40-50 cycles.

Table 4: Amplification program used for the one-step gene expression analysis using the Qiagen Quntitect qRT-PCR kit.

Stage	Length	Temperature	Description
Reverse Transcription	20 minutes	50°C	mRNA > cDNA
Polymerase Activation	15 minutes	95°C	Activation of HotStarTaq DNA polymerase
2-step cycling			
- Denaturation	45 seconds	94°C	X 40-50 cycles
- Annealing/extension	45 seconds	60°C	
cDNA, complementary DNA			

Fluorescence analysis was performed using LC480 SX1.5 software (Roche), and the threshold for analysis was set manually at 0.03 arbitrary units (AU) above the median NTC fluorescence value at cycle 43. This ensured that results were comparable across all experiments as this controlled for background fluorescence.

2.10 Conjugation of purified antibodies to APC using Lightning Link

Innova Biosciences (Babraham, UK) provide Lightning Link kits that allow the conjugation of fluorophores to purified antibodies. The Lightning-Link allophycocyanin (APC) kit was used in an attempt to conjugate APC to a purified anti-CD114 antibody. The method was carried out according to the manufacturer's instructions. Firstly, 100µL of the CD114 antibody was aliquoted into an Eppendorf. Ten µL of the LL-Modifier reagent (1µL of LL-Modifier reagent:10µL of antibody) was added to the antibody and the solution was gently mixed with a pipette. The antibody and LL-Modifier reagent was added to a commercial vial of Lightning Link mix and the lyophilised powder was gently dissolved into the solution using a pipette. The solution was left in the dark at room temperature (20-25°C) for 3 hours. Following incubation, 10µL of the LL-Quencher reagent was added to the mixture. The solution was left to stand at room temperature for 30 minutes and then placed at 4°C for later use.

2.11 Haematopoietic stem cell and multipotent progenitor *in vitro* culture

HSCs and MPPs were sorted from murine BM according to the protocol outlined in **Section 2.5**. Unless otherwise stated, cells were double sorted into Eppendorfs containing 500µL Iscove's Modified Dulbecco's Media (IMDM, Thermo Fisher Scientific) containing 10% FCS, 1,000 U/mL penicillin and 1,000 µg/mL streptomycin (Thermo Fisher Scientific), 50 ng/mL Tpo and 20 ng/mL SCF (Peprotech, London, UK), with and without 100ng/mL Flt3L (Biolegend, London, UK). Cells were then transferred to either sterile 48-well or 96-well culture plates (Greiner Bio-One) and incubated at 37°C in a 5% CO₂ incubator for a defined period of time. After incubation, cells were transferred to FACS tubes for sorting. To reduce loss of cells after transferring the cell suspension, the wells of the culture plates were washed out with cell culture medium and this solution was added to the cell suspension.

2.12 Phosphoflow: Analysis of phosphorylated proteins using flow cytometry

Cells were isolated from BM and stained using specified antibodies as described in **Section 2.3**. However, when BM cells were isolated for phosphoflow analysis, DPBS (without Ca⁺/Mg⁺) containing 0.5% FCS was used to prepare the cells. Once the cells were stained with antibodies, they were washed three times using serum-free DPBS before resuspending the cells in pre-warmed serum-free IMDM. Each cell suspension from 1 mouse was divided into 2 samples and cells were starved in sterile 48-well culture plates at 37°C in a 5% CO₂ incubator

for approximately 3 hours. After starvation, half of each sample was stimulated with 150ng/mL Flt3L for 7.5 minutes. The same volume of serum-free IMDM was added to the other half of each sample (unstimulated control). All samples were promptly fixed in a 1.6% paraformaldehyde (PFA) solution by diluting either 4% PFA prepared in the lab, or 16% commercial electron microscopy-grade (EM-grade) PFA, for 15 minutes at room temperature. Cells were pelleted at 4°C, 394 rcf for 4 minutes and the fixing solution was removed using a pipette. Ice-cold acetone or methanol was added to permeabilise the cells and samples were incubated at -20°C for 15 minutes. Cells were pelleted at 4°C, 394 rcf for 4 minutes and the acetone or methanol was removed by aspiration. The cells were subsequently washed in 2% FCS DPBS. Samples were stained by resuspending cells in 200µL of 2% FCS DPBS containing anti-phospho-ribosomal protein S6 (pS6) and incubated on ice for 1 hour. Cells were washed twice using 2% FCS DPBS before acquisition on a CyAN FACS Analyser (Beckman Coulter) controlled by Summit v4.3 software. Stimulated and unstimulated samples from a single mouse were compared during analysis, which was carried out using FlowJo software, version 10.1.

2.13 Methylcellulose colony forming assays

2.13.1 Plating of haematopoietic stem cells on MethoCult M3434

For analysis of the survival and differentiation of HSCs, MethoCult M3434 (StemCell Technologies, Cambridge, UK) was used. M3434 contains 50ng/mL recombinant mouse (rm)SCF, 10ng/mL rmlL-3, 10ng/mL rmlL-6, 3 units/mL recombinant human Epo and is

optimised for growth of murine macrophage progenitors (CFU-M), granulocyte progenitors (CFU-G), CFU-GM, CFU-GEMM, and CFU-E/BFU-E. During colony forming assays, M3434 was supplemented with Tpo to support growth of megakaryocyte progenitors (CFU-Meg) [299]. M3434 MethoCult medium (StemCell Technologies) was purchased in 100mL bottles. As soon as the medium arrived, the bottle was rigorously vortexed to ensure complete mixing of the contents. The medium was left to sit at room temperature until the bubbles settled at the top of the medium. Once mixed, the entire bottle was divided into 3.5mL aliquots using sterile 5mL polypropylene tubes. Care was taken to ensure there was minimal transfer of bubbles. The aliquots were then stored at -20°C until required.

To assess HSC survival and differentiation, varying numbers of HSCs (LSK CD150⁺ CD48⁻) were sorted into IMDM medium containing 10% FCS, 1,000 U/mL penicillin and 1,000 µg/mL streptomycin. Sorted HSCs were added to M3434 MethoCult medium supplemented with 25ng/mL TPO, 1,000 U/mL penicillin and 1,000 µg/mL streptomycin. Flt3L or equal volumes of IMDM were then added to each sample, and a uniform cell suspension was made by gently vortexing the sample. Cells were plated using a 1mL syringe into a 35mm petri dish and were plated as duplicates. Duplicate plates were placed in 100mm petri dishes with a 35mm petri dish full of water before incubating the cultures at 37°C in a 5% CO₂ incubator. Colony numbers and type were scored on day 11.

2.13.2 Cytospin preparations

Colonies were identified by picking representative colonies with a 10µL pipette tip, resuspending the cells in 100µL of DPBS, and loading them into cytospin funnels (VWR

International, Lutterworth, UK) for centrifugation. Samples were centrifuged at 23g for 8 minutes onto microscope slides (Thermo Fisher Scientific) and then air-dried. Subsequently, cytopsin samples were stained using Diff-Quick staining solutions (Polysciences, Hirschberg an der Bergstrasse, Germany). Samples were dipped 15 times for 1 second into Solution1 (Fixative), Solution2 (Eosin G) and then Solution3 (Thiazine dye), before being washed with distilled water. Square cover slides (Agar Scientific, Stansted, UK) were mounted onto the cytopsin using neutral mounting medium. Images were taken using a Leica DM6000B microscope (Leica Microsystems, Milton Keynes, UK).

2.13.3 Identification of colonies

When colonies were counted and scored in the M3434 medium, colony types were identified based on the phenotype of the cells within the colony and by using the MethoCult technical manual supplied by StemCell Technologies. Colonies that contain CFU-M appear dispersed with large oval or round cells. CFU-G contain cells that are smaller than monocytes. These cells are round and relatively uniform in size. When both of these cell types were present in a highly cellular colony, it was scored as CFU-GM. CFU-GEMM are the largest colonies, and are distinguished from other colonies by their densely populated dark brown cores. There are no distinct borders separating peripheral cells from the core of CFU-GEMM colonies. CFU-Meg were observed as colonies with few round, very large cells. Finally, when these cells were present with other, smaller cells in sparsely populated colonies, the colonies were scored as megakaryocyte-mixed (CFU-MegMix). Only colonies containing more than 50 cells were scored.

To confirm that the colonies were scored correctly, cytopspin preparations of representative colonies were stained with a Differential Quik Stain Kit. Monocytes were identified as cells with abundant dull blue/grey cytoplasms and usually kidney shaped nuclei [300]. Granulocyte progenitors were recognised as cells with pale blue cytoplasms, with high nuclear to cytoplasmic ratio (myeloblast) and dark to pale pink cytoplasms (promyelocytes) [300, 301]. The cytoplasm of promyelocytes appears this way due to the basophilic nature (pale blue staining) of the cytoplasm and magenta staining of cytoplasmic granules [300]. Megakaryocytes and their progenitors were easily distinguished by their size. Promegakaryocytes contain granules which can cause pink/purple staining of the cytoplasm. As these cells differentiate into megakaryocytes, endomitosis occurs to produce highly polyploidy cells with dark blue (basophilic) cytoplasms [300, 302, 303]. Erythroblasts were identified as cells with high nuclei to cytoplasm ratio, and have intensely basophilic purple, sometimes gray, cytoplasms [301, 302].

2.14 Graphing of data and statistical analysis

All data, apart from primer optimisation results, were graphed in and exported from GraphPad Prism version 6. Matlab R2015b was used to create 3 dimensional surface plots to present primer optimisation data. Microsoft PowerPoint 2011, version 14, was used to group graphs into the figures presented in this study. The statistical tests used to analyse the data presented in this study are included in the relevant figure legends. Results were considered statistically significant for p values <0.05 .

2.15 Figure illustration

Adobe Illustrator CC was used to create all illustrated figures for this thesis.

CHAPTER 3: EXPRESSION OF RECEPTORS FOR GROWTH FACTORS DURING HAEMATOPOIESIS

3.1 Introduction

Analysis of a population of cells is not very informative when studying stem and progenitor cells, given the possible heterogeneous nature of these populations. It results in the generation of misleading data that represent an average of an entire population, and does not account for a change in or the presence of rare sub-fractions within the sample. Recent advances in high throughput single cell analysis techniques have been crucial in furthering our understanding of HSPC biology. For example, the LS⁻K compartment of the murine BM is commonly divided into CMP, GMP, and MEP populations using the CD16/32 and CD34 surface markers [67]. However, Paul *et al.* have used index sorting and RNA-sequencing to identify 19 subpopulations within the LS⁻K compartment, indicating that the above surface marker approach does not accurately capture the heterogeneity of myeloid progenitors [304]. Tsang *et al.* have also analysed RNA-sequencing data for single HSCs (LSK CD150⁺ CD48⁻) and reported a large degree of transcriptional heterogeneity. The group found that genes associated with cell cycle activity, protein localisation and transcription were highly variable at the single cell level [305]. Wilson and colleagues have reported similar findings, and identified 4,533 genes that were variably expressed between 92 LT-HSCs (LSK CD150⁺ CD48⁻ CD34⁻ Flt3⁻) using RNA-sequencing analysis [306]. These studies, and many more [294, 307, 308], highlight the heterogeneous nature of HSPC populations.

The heterogeneity observed in HSPC populations is further confounded by the presence of lineage-biased subpopulations. Cellular barcoding has been used to monitor the fate of single LMPPs and HSCs *in vivo*, revealing a number of lineage-biased populations within each compartment. A number of HSC and LMPP subpopulations can be classified based on their granulocyte, B-lymphocyte, DC and monocyte output [9, 28]. Similarly, Benz *et al.* have observed MyHSCs and LyHSCs when transplanting single HSCs into irradiated mice and monitoring their long-term output [309]. These lineage-biased HSCs can also be isolated based on the expression of particular surface or intracellular markers. The Jacobsen group have identified vWF⁺ HSCs that possess increased platelet potential *in vivo* when compared to vWF⁻ HSCs [29], while MyHSCs and LyHSCs can be isolated based on their exclusion of Hoechst stain and expression of CD150, CD86 and CD41 [25-27, 30, 31, 310].

While recent studies have focused on characterising lineage-biased populations of HSPCs, it is still unclear how lineage-bias first arises. As described in **Chapter 1**, there is strong evidence to suggest that HGFs within the BM microenvironment modulate haematopoiesis through instructional cues. M-CSF and Epo upregulate lineage-associated genes in early HSPCs, and stimulate them to differentiate towards a GM or erythroid fate, respectively [267, 269]. Similarly, Reiger *et al.* have shown that M-CSF and G-CSF are capable of instructing a macrophage or granulocytic lineage fate in single GMPs *in vitro*, respectively [268]. There is also evidence to suggest that Flt3L may act on multipotent progenitors to promote GM-lymphoid development at the expense of MegE fate [288]. Given their role in driving lineage decisions, these factors may regulate HSPC lineage-biases. In fact, stimulation of multipotent cells with M-CSF *in vitro* results in a myeloid developmental program that persist for up to 6 weeks after the cells have been transplanted into WT hosts, suggesting an induction of a

temporary GM-bias [267]. Determining the expression patterns of receptors for HGFs by developing haematopoietic cells will be important in understanding how and at what point in the haematopoietic hierarchy ligands might instruct lineage fate.

There is evidence to suggest that HSPCs are heterogeneous as to the expression of receptors for Flt3L, Epo, M-CSF and G-CSF. Following exposure to M-CSF or Epo, some, but not all, HSCs upregulate lineage-associated genes [267, 269]. Additionally, Miyamoto have reported, using single cell gene expression analysis, that *CSF3R* and *EPOR* are selectively expressed by a large proportion of HSCs [116]. These findings suggest the presence of HSC subpopulations that differentially respond to HGFs. In fact, in more mature progenitors, selective expression of particular HGFs has been used to isolate functionally distinct subpopulations. The preGM compartment can be divided into Flt3⁺ and Flt3⁻ fractions that contain T-lymphocyte/myeloid and myeloid-restricted progenitors, respectively [77]. Similarly, co-expression of M-CSFR and Flt3 on the surface of CMPs marks a population of DC progenitors [304]. Given these findings, further investigation into the expression of HGF receptors within other compartments, including the HSC compartment, may identify distinct lineage-biased subpopulations.

As evidence suggests that Flt3, EpoR, M-CSFR and G-CSFR are variably expressed by HSC, it is important to determine whether co-expression of these receptors occurs at this stage. Miyamoto *et al.* have provided insight into this, as they have shown that some single HSCs (LSK CD34⁻ Thy1.1^{lo}) co-express *EPOR* and *CSF3R* [116]. However, single cell analysis has not been carried out to determine if other HGF receptor transcripts are co-expressed by HSCs. Furthermore, it is unclear if Flt3, EpoR, M-CSFR and G-CSFR proteins are co-expression at the surface of HSCs. As the expression of these receptors has not been investigated in the LT-HSC, ST-HSC and MPP compartments, it is unclear if co-expression patterns change as HSCs exit a

quiescent state and begin to differentiate. Understanding this will help to determine if HGFs act on discrete subpopulations of early HSPCs, and if these factors differentially regulate multipotent cells as they mature.

3.1.1 Aims of chapter

Current evidence suggests that HSPCs are heterogeneous in regard to expression of the receptors for Flt3L, Epo, M-CSF and G-CSF. While HSCs have been shown to express these receptors, it is largely unclear whether co-expression of these HGF receptors is commonplace during the early stages of haematopoiesis, or if HSC and MPP subpopulations exclusively express particular receptors. This is an important distinction. If cells within the HSC and MPP compartments are found to exclusively express particular HGF receptors, this would suggest that HGFs act permissively by activating distinct HSPC subpopulations, supporting a selective model of haematopoiesis. On the other hand, if single HSCs and MPPs co-express HGF receptors, this would support a deterministic model of haematopoiesis whereby single cells have the ability to respond to multiple environmental cues. As described in **section 1.4**, there is evidence to suggest that both selective expression and co-expression of HGF receptors occurs during haematopoiesis. If this is the case, then the selective and deterministic models of haematopoiesis are not exclusive. Therefore, HSPC differentiation may be regulated by features of both models. Identifying the expression patterns of multiple HGF receptors by HSPCs will help to investigate whether this is the case, and further our understanding of the mechanisms that regulate HSPC differentiation.

This chapter focused on mapping the expression profiles of the *FLT3*, *EPOR*, *CSF1R* and *CSF3R*

genes, and their encoded proteins, during murine haematopoiesis. As described above, the purpose of this was to determine if distinct subpopulations could be identified within HSPC populations based on expression of these HGF receptors, and to what extent these receptors are co-expressed by early HSPCs. Firstly, freely accessible HSPC gene expression databases were interrogated to investigate the expression of *FLT3*, *EPOR*, *CSF1R* and *CSF3R* by well-defined HSPC populations, and to determine at what point these genes are expressed during haematopoiesis. Secondly, FACS staining strategies and qRT-PCR assays were designed and optimised for the analysis of HGF receptor expression by single LT-HSCs, ST-HSCs, MPPs and lineage-restricted progenitors. Lastly, multiplex analysis was employed to investigate whether these receptors are co-expressed at both the mRNA and protein level within the HSC and MPP compartments.

3.2 Investigation of *FLT3*, *EPOR*, *CSF1R* and *CSF3R* expression during haematopoiesis using the HemaExplorer and BloodSpot databases

In 2013, Bagger *et al.* published a paper describing their HemaExplorer database, terming it “a curated database of processed mRNA Gene expression profiles that provides an easy display of gene expression in haematopoietic cells” [296]. The database provides gene expression data of mouse and human haematopoietic cells, including data for human acute myeloid leukaemia, from 271 microarray-based experiments. More recently, Bagger and co-workers described the BloodSpot database, which greatly expands on the HemaExplorer database in terms of the number of HSPC populations that can be analysed, and includes new

functionalities, such as graphical tree plots that illustrate how genes are differentially expressed during haematopoiesis [297]. As the expression of *FLT3*, *EPOR*, *CSF1R* and *CSF3R* by mouse HSPCs was of interest, the expression data for these particular genes within the haematopoietic hierarchy were extracted from the databases. When the databases were created, the batch effects caused by compilation of studies were estimated and samples were normalised accordingly. As such, the gene expression values obtained from the databases are measured in normalised AU.

Data for expression of HGF receptors by each of the relevant HSPC populations were exported from the database for analysis, as shown in **Figure 3.1**. The cell populations included the LT-HSC, ST-HSC, LMPP, preGM, GMP, MEP, MkP, preCFU-E, CFU-E, EP, CLP, pro-B-lymphocyte, pre-B-lymphocyte and ETP populations. The available information regarding the surface marker profile used to isolate each HSPC population included in the databases is listed in **Table 5** so that the results can be compared to the single cell gene expression analysis carried out later in this chapter [296, 297]. Notably, the studies included in the HemaExplorer and BloodSpot databases isolated LT-HSCs and ST-HSCs as LSK CD34⁻ Flt3⁻ and LSK CD34⁺ Flt3⁻, respectively, instead of their SLAM phenotypes. Unfortunately, the phenotypes used to isolate the MEP, MkP, CLP, pro-B-lymphocyte, pre-B-lymphocyte and ETP populations were not available.

When exporting the data, it became clear that the databases only included 2 data points for some populations, so statistical analysis could not be performed for these samples. Additionally, as can be seen in **Figure 3.1**, the data obtained from the databases show that targets were amplified in all populations. The consistent, but low, levels of expression observed in certain populations suggest that the microarray experiments detected gDNA, and

that the assays were not RNA specific. Despite this, there were clear distinctions between cells that expressed high levels of mRNA, and those that expressed little to none.

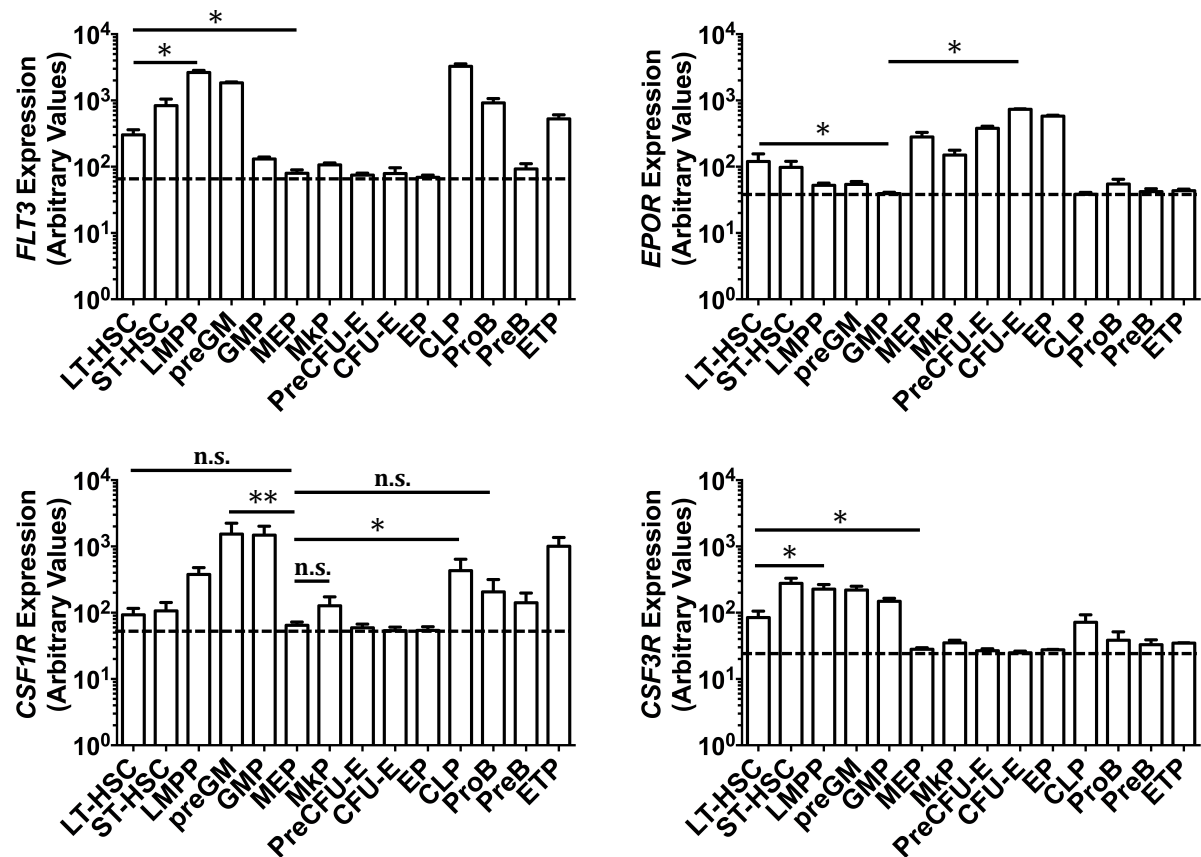


Figure 3.1. Expression of growth factor receptors by HSPCs according to the HemaExplorer and BloodSpot databases. Raw values of *FLT3*, *EPOR*, *CSF1R* and *CSF3R* expression in murine HSPCs were obtained from the HemaExplorer and BloodSpot databases. Values are expressed in arbitrary units, as the data obtained from the databases are normalised using calculated batch effect estimators so that results can be compared across the numerous studies compiled within the databases. Targets were amplified in all populations, suggesting that the assays used during analysis of gene expression detected gDNA. To estimate the gDNA amplification threshold, the dotted lines are included in each bar chart to depict the lowest mean expression value from the analysed populations. Expression is plotted on a log scale. HSPCs, haematopoietic stem and progenitor cells; LT-HSC, long-term haematopoietic stem cell; ST-HSC, short-term haematopoietic stem cell; LMPP, lymphoid-primed multipotent progenitor; preGM, pre-granulocyte-macrophage progenitor; GMP, granulocyte-macrophage progenitor; MEP, megakaryocyte-erythroid progenitor; EP, erythroid progenitor; MkP, megakaryocyte progenitor; CFU-E, erythroid colony forming unit; CLP, common lymphoid progenitor; proB, pro-B-lymphocyte; preB, pre-B-lymphocyte; ETP, early thymic progenitor; gDNA, genomic DNA; *EPOR*, erythropoietin receptor; *FLT3*, fms-like tyrosine kinase 3; *CSF1R*, macrophage-colony stimulating factor receptor; *CSF3R*, granulocyte-colony stimulating factor receptor.

FLT3 was highly expressed by lineage-restricted progenitors that have lymphoid, granulocytic and/or myelomonocytic potential, which is as expected [73, 311]. LMPPs, preGMs and CLPs expressed the highest levels of *FLT3*, with lower levels being expressed by pro-B-lymphocyte and ETP cells. Interestingly, when compared to the remaining populations, ST-HSCs (LSK CD34⁺ Flt3⁻) and, to a lesser extent, LT-HSCs (LSK CD34⁻ Flt3⁻) expressed slightly higher levels of *FLT3*. The expression of *FLT3* by LT-HSCs was significantly lower than the levels expressed by LMPPs [$p=0.0159$], but significantly higher than the levels expressed by the MEP population [$p=0.0286$]. As the MEP population is not considered to express *FLT3* [312], the above indicates that *FLT3* expression is present within the LSK Flt3⁻ HSC compartment.

EPOR expression was much more restricted when compared to *FLT3* expression, as only late progenitors with erythroid potential expressed this gene at a high level (CFU-E, preCFU-E, EP and MEP). This is commensurate with the known association of *EPOR* with the erythroid lineage. LMPPs are known to lack expression of erythroid related genes [73], and the levels of *EPOR* detected in preGMs, GMPs, CLPs, pro-B-lymphocytes, pre-B-lymphocytes and ETPs were similar to those detected in LMPPs, indicating that amplification in these populations were due to gDNA amplification [73]. Indeed, the levels of *EPOR* expressed by CFU-E were significantly more than the levels detected in the LMPP populations [$p=0.0357$]. Significantly higher levels of *EPOR* were detected in LT-HSCs when compared to LMPPs, indicating that *Epor* mRNA is expressed by LSK Flt3⁻ HSCs [$p=0.0159$].

MEPs, CFU-Es, preCFU-Es and EPs expressed *CSF1R* at a very low level. Megakaryocyte and EPs are known to express few myelomonocytic-associated genes and, therefore, amplification in these populations is likely to be due to *CSF1R* gDNA [313, 314]. When compared to the MEP population, there was no significant difference in the levels of *CSF1R* expressed by LT-HSCs

[$p=0.3427$], MkPs [$p=0.495$] and Pro-B-lymphocytes [$p=0.29$], indicating that the levels of *CSF1R* expression in these populations were also due to gDNA amplification. This was interesting, considering that HSCs are known to express M-CSFR protein [267]. Conversely, high levels of *CSF1R* were detected in the preGM, GMP, ETP, LMPP and CLP populations. CLPs [$p=0.0182$] and preGMs [$p=0.002$] also expressed significantly higher levels of *CSF1R* when compared to MEPs, indicating that these populations expressed *Csf1r* transcripts.

Table 5: Surface marker expression profile of the HSPC populations included in the HemaExplorer and BloodSpot databases [296, 297].

HSPC Population	Phenotype
LT-HSC	c-kit ⁺ Lin ⁻ Sca1 ⁺ CD34 ⁻ flt3 ⁻
ST-HSC	c-kit ⁺ Lin ⁻ Sca1 ⁺ CD34 ⁺ flt3 ⁻
LMPP	c-kit ⁺ Lin ⁻ Sca1 ⁺ CD34 ⁺ flt3 ⁺
preGM	c-kit ⁺ Lin ⁻ Sca1 ⁻ CD150 ⁻ FcγR ^{lo} CD105 ^{lo}
GMP	c-kit ⁺ Lin ⁻ Sca1 ⁻ CD150 ⁻ FcγR ^{hi}
MEP	<i>Data not available</i>
MkP	<i>Data not available</i>
preCFU-E	c-kit ⁺ Lin ⁻ Sca1 ⁻ CD150 ⁺ FcγR ^{lo} CD105 ^{hi}
CFU-E	c-kit ⁺ Lin ⁻ Sca1 ⁻ CD150 ⁻ FcγR ^{lo} CD105 ^{hi} TER-119 ⁻
EP	c-kit ⁺ Lin ⁻ Sca1 ⁻ CD150 ⁻ FcγR ^{lo} CD105 ^{hi} CD71 ⁺ TER-119 ⁺
CLP	<i>Data not available</i>
Pro-B-lymphocyte	<i>Data not available</i>
Pre-B-lymphocyte	<i>Data not available</i>
ETP	<i>Data not available</i>

HSPC, haematopoietic stem and progenitor cell; LT-HSC, long-term haematopoietic stem cell; ST-HSC, short-term haematopoietic stem cell; LMPP, lymphoid primed multipotent progenitor; preGM, pre-granulocyte-macrophage progenitor; GMP, granulocyte-macrophage progenitor; MEP, megakaryocyte-erythroid progenitor; EP, erythroid progenitor; MkP, megakaryocyte progenitor; CFU-E, erythroid colony forming unit; CLP, common lymphoid progenitor; ETP, early thymocyte progenitor; Flt3, fms-like tyrosine kinase; Lin, lineage markers.

Finally, expression of *CSF3R* was largely restricted to HSPC populations that had granulocytic potential, such as LMPPs, preGMs and GMPs. Interestingly, the highest level of *CSF3R* expression was found to be in the ST-HSC compartment. However, statistical analysis was not performed on this population as the data included just 2 data points. Again, low levels of *CSF3R* expression by MEPs, CFU-Es, preCFU-Es and EPs indicated amplification due to gDNA, implying that these populations did not express the *CSF3R* gene. LT-HSCs expressed significantly lower levels of *CSF3R* than LMPPs [$p=0.0317$] but significantly higher levels than MEPs [$p=0.0286$], suggesting that *Csf3r* mRNA was present in this population. The CLP population also expressed higher levels of *CSF3R* than MEPs but this could not be confirmed by statistical analysis as the data exported from the database only included 2 data points for the CLP population.

These data indicate that *FLT3*, *EPOR* and *CSF3R* are expressed by HSCs, and that expression of these receptors by cells at later stages of development is largely restricted to progenitor populations that possess the associated lineage potentials. For example, *EPOR* was highly expressed by MEPs, EPs and CFU-Es, but not by LMPPs, CLPs or GMPs, which lack erythroid potential. This analysis provided an insight into where *FLT3*, *EPOR*, *CSF1R* and *CSF3R* genes are expressed during haematopoiesis. The following results obtained from the single cell gene expression analysis studies aim to confirm the validity of the data generated from the HemaExplorer and BloodSpot databases.

3.3 Gating strategy for the isolation and analysis of haematopoietic stem and progenitor cells

In order to analyse the patterns of HGF receptor expression during haematopoiesis, flow cytometry antibody panels were designed for the identification and isolation of HSPCs. The cell surface marker profiles were adapted from recent publications (**Figure 3.2**). When performing flow cytometry or FACS, cells were first gated based on their forward scatter (FSC)/side scatter (SSC) profile to exclude noise and debris. Doublets were then removed by gating for cells with a low pulse width profile. Auto-fluorescent cells were also removed from analysis using a fluorescent channel that was not being used, as these cells were likely to be dead or dying.

A lineage cocktail was created by combining antibodies for CD3 ϵ , CD11b, B220, Gr-1, TER-119 to allow for the exclusion mature haematopoietic cells, such as lymphocytes, monocytes and erythroid cells. Thus, all HSPC populations were first gated as Lin $^{-}$. By staining for Sca1 and c-Kit, the early HSPC populations could be identified. Within the LSK compartment, the Morrison group has shown that CD150 and CD48 allow for the enrichment of HSCs, MPPs and progenitors with varying lineage-potentials [34]. Therefore, this gating strategy was employed to identify HSCs and MPPs as LSK CD150 $^{+}$ CD48 $^{-}$ and LSK CD150 $^{-}$ CD48 $^{-}$ respectively. To distinguish between LT-HSCs (LSK CD150 $^{+}$ CD48 $^{-}$ CD34 $^{-}$) and ST-HSCs (LSK CD150 $^{+}$ CD48 $^{-}$ CD34 $^{+}$) cells, CD34 was added to the panel to identify CD34 $^{-}$ and CD34 $^{+}$ HSCs, respectively [21].

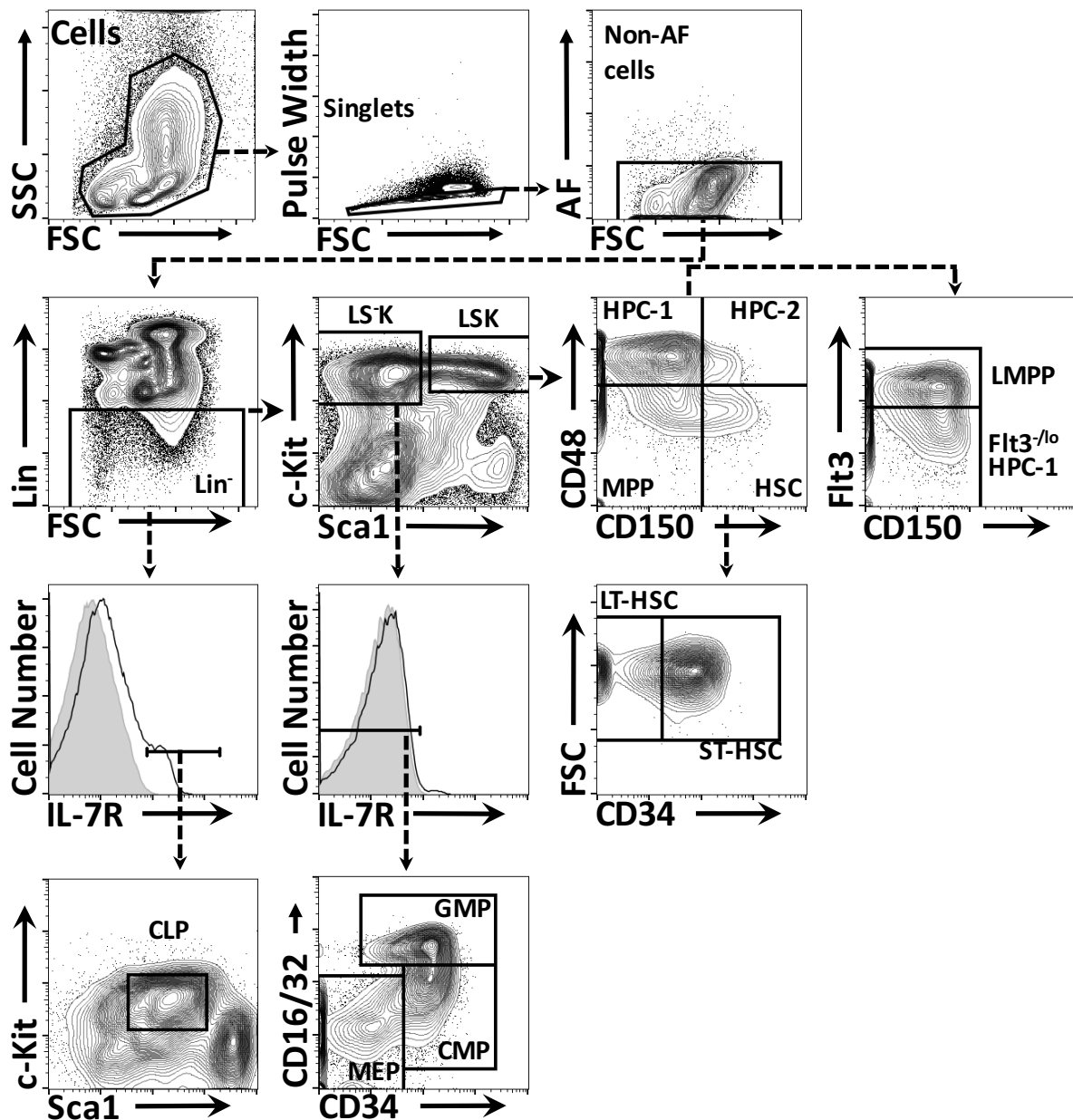


Figure 3.2. Isolation of HSPCs from mouse BM. Cells identified as HSCs, subpopulations of these cells and various progenitors are delineated by the black boxes. Shaded areas in histograms depict the isotype control staining. For the purpose of this figure, flow cytometry plots from a number of staining strategies and experiments have been combined to show a comprehensive gating strategy of all the HSPC populations analysed in this study. After gating for singlet cells, a channel that did not correspond with any staining was used to exclude AF cells, as these were likely to be dead/dying cells. HSPCs, haematopoietic stem and progenitor cells; Lin, lineage markers; LSK⁻, Lin⁻ Sca1⁻ c-Kit⁺; LSK, Lin⁻ Sca1⁺ c-Kit⁺; Flt3, fms-like tyrosine kinase 3; IL-7R, interleukin-7 receptor; HSC, haematopoietic stem cell; MPP, multipotent progenitor; HPC, haematopoietic progenitor cell; LMPP, lymphoid-primed multipotent progenitor; CLP, common lymphoid progenitor; CMP, common myeloid progenitor; GMP, granulocyte-macrophage progenitor; MEP, megakaryocyte-erythroid progenitor; AF, auto-fluorescent; BM, bone marrow.

CD150 and CD48 staining within the LSK compartment also allowed for the identification of maturing progenitors, such as HPC-1 (LSK CD48⁺ CD150⁻), which possesses GM-lymphoid potential and minimal MegE potential, and HPC-2 (LSK CD48⁺ CD150⁺), a population that can give rise to MegE cells and very few GM-lymphoid cells [34]. However, as some HPC-1 are known to express high levels of Flt3, their staining profile overlaps with the LMPP compartment; these cells have been described as LSK Flt3^{hi} by the Jacobsen group [73]. To include this population, the staining strategy was adapted to divide the LSK CD48⁺ CD150⁻ compartment into Flt3^{hi} and Flt3^{-/lo} cells, which were referred to as LMPP and Flt3^{-/lo} HPC-1, respectively, for the purpose of this study.

Table 6: Proportion and phenotype of haematopoietic stem and progenitor cells within the mouse BM

Cell population	Phenotype	% of whole BM
LT-HSC	LSK CD150 ⁺ CD48 ⁻ CD34 ⁻	4.75 ± 0.4 x10 ⁻³
ST-HSC	LSK CD150 ⁺ CD48 ⁻ CD34 ⁺	13.7 ± 0.6 x10 ⁻³
Total HSC	LSK CD150 ⁺ CD48 ⁻	1.85 ± 0.06 x10 ⁻²
MPP	LSK CD150 ⁻ CD48 ⁻	6.1 ± 0.58 x10 ⁻²
Flt3 ^{-/lo} HPC-1	LSK CD150 ⁻ CD48 ⁺ Flt3 ^{-/lo}	8.25 ± 0.8 x10 ⁻²
LMPP	LSK CD150 ⁻ CD48 ⁺ Flt3 ^{hi}	0.1 ± 0.02
HPC-2	LSK CD150 ⁺ CD48 ⁺	7.1 ± 0.9 x10 ⁻³
CLP	Lin ⁻ Sca1 ^{lo} c-Kit ^{lo} IL-7Rα ⁺	7.1 ± 1.7 x10 ⁻²
CMP	LS ⁻ K IL-7Rα ⁻ CD16/32 ^{lo} CD34 ^{hi}	0.41 ± 0.007
GMP	LS ⁻ K IL-7Rα ⁻ CD16/32 ^{hi} CD34 ^{hi}	0.36 ± 0.03
MEP	LS ⁻ K IL-7Rα ⁻ CD16/32 ^{lo} CD34 ^{lo}	0.45 ± 0.006

Percentages are given as mean ± standard error of the values obtained for n=6-9 mice. BM cells were gated according to FSC/SSC and pulse width. BM, bone marrow; AF, auto-fluorescence; LS⁻K, Lineage⁻ Sca1⁻ c-Kit⁺; LSK, Lineage⁻ Sca1⁺ c-Kit⁺; Flt3, fms-like tyrosine kinase 3; IL-7Rα, interleukin-7 receptor α subunit; HSC, haematopoietic stem cell; LT, long-term; ST, short-term; MPP, multipotent progenitor; HPC, haematopoietic progenitor cell; LMPP, lymphoid-primed multipotent progenitor; CLP, common lymphoid progenitor; CMP, common myeloid progenitor; GMP, granulocyte-macrophage progenitor; MEP, megakaryocyte-erythroid progenitor; FSC, forward scatter; SSC, side scatter.

The lymphoid restricted CLP population was identified by first gating for IL-7Rα⁺ cells within the Lin⁻ population. These cells were then gated based on low levels of Sca1 and c-Kit (Lin⁻ Sca1^{lo} c-Kit^{lo} IL-7Rα⁺) according to work published by the Weissman group [66]. Some LMPPs express IL-7Rα [73], so the Sca1 and c-Kit gating strategy for CLP isolation was modified to ensure it did not overlap with the strategy used to isolate LMPPs. Finally, according to Akashi *et al.*, BM myeloid progenitors express c-Kit, but lack expression of Sca1 and IL-7Rα on their surface [67]. As such, myeloid progenitors were identified by gating for LS⁻K IL-7Rα⁻ cells. Within this compartment, expression of CD16/32 and CD34 was used to identify CMPs (LS⁻K IL-7Rα⁻ CD16/32^{lo} CD34^{hi}), GMPs (LS⁻K IL-7Rα⁻ CD16/32^{hi} CD34^{hi}) and MEPs (LS⁻K IL-7Rα⁻ CD16/32^{lo} CD34^{lo}) [67]. **Table 6** lists the proportions and phenotypes of these HSPC populations within the BM.

3.4 Optimisation of qRT-PCR assays for the detection of growth factor receptor gene expression

3.4.1 *ACTB* as an endogenous control gene for qRT-PCR analysis

Once the antibody panels were defined for the isolation of single HSPCs, qRT-PCR assays were designed and optimised for the detection of HGF receptor gene expression in single cells. Prior to designing any assays, a reliable endogenous control gene was selected. *ACTB* encodes the cytoskeletal protein β-actin and is a commonly used control gene. [315-317]. To determine if this gene was homogeneously expressed by the populations that were going to be analysed

during this study, the HemaExplorer and BloodSpot databases were examined to compile data for the HSPC populations of interest. These included the LT-HSC, ST-HSC, LMPP, preGM, GMP, MEP and CLP populations.

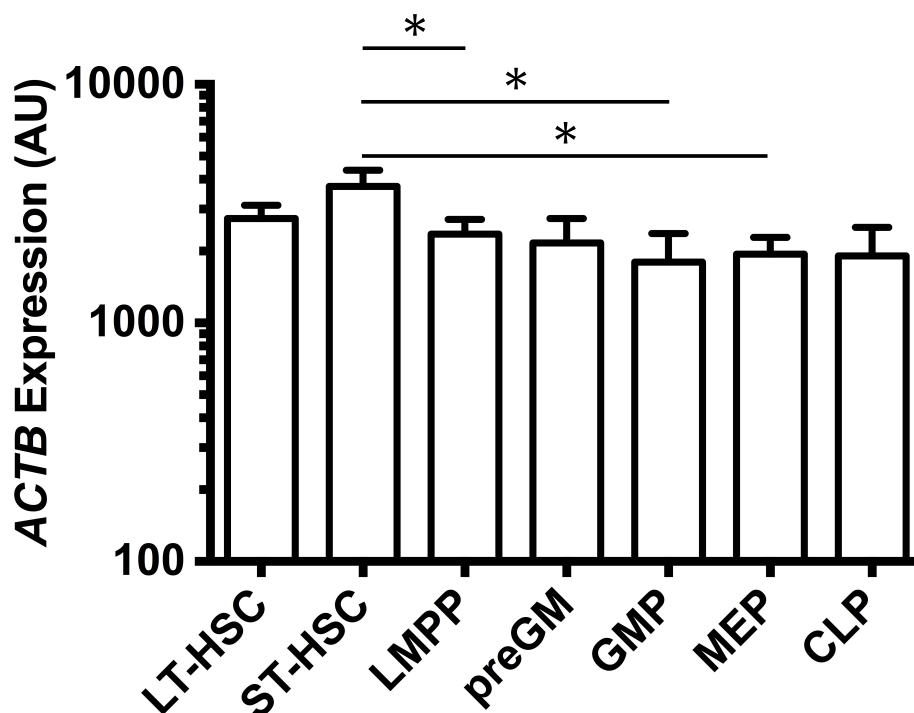


Figure 3.3. Investigation of *ACTB* expression by HSPC populations. The expression of *ACTB* by HSPC populations was analysed using the HemaExplorer and BloodSpot databases. Values are expressed in AU, as the data are normalised using calculated batch effect estimators so that results can be compared across the numerous studies compiled within the databases. Data is plotted on a log scale. HSPCs, haematopoietic stem and progenitor cells; LT-HSC, long-term haematopoietic stem cell; ST-HSC, short-term haematopoietic stem cell; LMPP, lymphoid-primed multipotent progenitor; preGM, pre-granulocyte-macrophage progenitor; GMP, granulocyte-macrophage progenitor; MEP, megakaryocyte-erythroid progenitor; Mkp, megakaryocyte progenitor; CFU-E, erythroid colony forming unit; CLP, common lymphoid progenitor; ProB, pro-B-lymphocyte; Pre, pre-B-lymphocyte cell; ETP, early thymic progenitor; AU, arbitrary units; *ACTB*, β -actin.

All of the cell populations expressed the *ACTB* gene at a high level (**Figure 3.3**). There were significant differences in the expression of *ACTB* between a number of populations. For example, the levels of *ACTB* expressed by ST-HSCs was significantly higher than LMPPs [$p=0.0342$], GMPs [$p=0.0226$] and MEPs [$p=0.0146$]. This indicated that analysing HGF receptor gene expression relative to *ACTB* expression would not allow for accurate comparison between the HSPC populations. However, this would likely be the case with other commonly used endogenous control genes. As the expression of HGF receptor genes was being measured in single cells, the Ct values obtained directly from gene expression analysis could be compared between samples. Thus, the endogenous control gene was only required to confirm the presence of a single cell in each well of a PCR plate during analysis. As *ACTB* was found to be highly expressed by all populations (when compared to *FLT3*, *EPOR*, *CSF1R* and *CSF3R*, according to the HemaExplorer and BloodSpot databases [**Figure 3.1**]), this gene was chosen as an endogenous control.

3.4.2 *ACTB*, *FLT3*, *EPOR*, *CSF1R* and *CSF3R* qRT-PCR assay design

Following endogenous control gene selection, qRT-PCR assays specific for *Actb*, *Flt3*, *Epor*, *Csf1r* and *Csf3r* transcripts were designed. Each gene was examined using the Ensembl genome browser (*FLT3*, ENSMUSG00000042817; *EPOR*, ENSMUSG00000006235; *CSF1R*, ENSMUSG00000024621; *CSF3R*, ENSMUSG00000028859) to determine the sequences of all the possible protein coding splice variants, and from this, generic exon junctions were selected. For a detailed method of how qRT-PCR assays were designed, see **Section 2.8**. To exclude non-specific priming from gDNA, the generic exon junction sequences were analysed

using BLAST to ensure that there were no pseudogenes containing these generic exon-exon junction sequences, and that similar sequences were not present in non-relevant genes in the mouse genome. BLAST analysis revealed that no pseudogenes containing the sequence spanning the junction between the first and second exon in the murine *ACTB* gene exist, so this sequence was selected as the qRT-PCR assay target. Similarly, BLAST analysis did not reveal any sequence homology within the mouse transcriptome and genome for the selected target sequences of the *FLT3*, *EPOR*, *CSF1R* and *CSF3R* genes. For both the *EPOR* and *FLT3* gene, the second exon-exon junction was chosen for qRT-PCR assay design, while the 14th and 3rd exon-exon junctions of the *CSF1R* and *CSF3R* genes were chosen, respectively (see **Table 7** and **Figure 3.4**).

Table 7: Intron size for the interrogated exon-exon junctions in the *ACTB*, *FLT3*, *EPOR*, *CSF1R* and *CSF3R* genes

Assay	Interrogated exon-exon junction	Intron size
<i>ACTB</i>	Exon 1 – Exon 2	959 nt
<i>FLT3</i>	Exon 2 – Exon 3	6,314 nt
<i>EPOR</i>	Exon 2 – Exon 3	337 nt
<i>CSF1R</i>	Exon 14 – Exon 15	2,028 nt
<i>CSF3R</i>	Exon 3 – Exon 4	2,362 nt

ACTB, β -actin; *FLT3*, fms-like tyrosine kinase 3; *EPOR*, erythropoietin receptor; *CSF1R*, macrophage-colony stimulating factor receptor; *CSF3R*, granulocyte-colony stimulating factor receptor nt, nucleotides.

ACTB

```
CAGCTTCT TTGCAGCTCC TTC
CACCAGTT CGCCATGGA
1 CACAGCTTCT TTGCAGCTCC TTGCTTGCCT GTCCACACCC GCCACCACTT CGCCATGGAT
GTGTCGAAGA AACGTCGAGG AAGCAACGGC CAGGTGTGGG CGGTGGTCTA CGCGTACCTA
61 GACGATATCG CTGCGCTGGT CGTCGACAAC GGCT
CTGCTATAGC GACGCGACCA GCAGCTGTTG CCGA
TATAGC GACGCGACCA GC
```

FLT3

```
ATCAGC GGGAAAGCCA TCATC
1 GCTCATCAGC GGGAAAGCCA TCATCGTACC GAATGGTGGC AGGATCCCCA GAAGACCTCC
CGAGTAGTCG CCTTTTCGGT AGTAGCATGG CTTACCAAGC TCCTAGGGGT CTTCTGGAGG
ATGG CTTACCAAGC TCCT
T CTTCTGGAGG
61 AGTGTGCCCC GA
TCACACGGGG CT
TCACACGGG
```

EPOR

```
CTCCGG GATGGACTTC AACTAC
1 CGAGCTCCGG GATGGACTTC AACTACAGCT TCTCATACCA GCTCGAGGGT GAGTCAC
GCTCGAGGCC CTACCTGAAG TTGATGTCGA AGAGTATGGT CGAGCTCCCA CTCAGTGCTT
61 AGTCAATAGT CCTGCACCAG GCT
TCAGTACATC GGACGTGGTC CGA
TCAGTACATC GGACGTGGTC
```

CSF1R

```
AACCTCT TGGGAGCCTG TACTCAG
1 GTCAACCTCT TGGGAGCCTG TACTCACGGA GGACCTGTCC TGGTCATCAC TGAATACTGC
CAGTTGGAGA ACCCTCGGAC ATGAGTGCCT CCTGGACAGG ACCAGTAGTG ACTTATGACC
61 TGCTATGGAG ACCTACTCAA CTTTCTCCGA AGGAAGGCCG AGGCTATGCT AG
ACGATACCTC TGGATGAGTT GAAAGAGGCT TCCTTCCGGC TCCGATACGA TC
T TCCTTCCGGC TCCGATACG
```

CSF3R

```
CTGCA CCTGACTGG AGTTAC
1 GGAGCCTGCA CCTGACTGG AGTTACCTG ATCTTCTTGC TACTCCCCAG AGTCTGGAG
CCTCGGACGT GGGACTGACC TCAATGGGAC TAGAAGAAGC ATGAGGGGTC TTCAGACCTC
TGGAC ACATCGAGAT TTCAC
61 AGCTGTGGAC ACATCGAGAT TTCACCCCT GTTGTCCGCC TGGGGGACCC TGTCCTGGCC
TCGACACCTG TGTAGCTCTA AAGTGGGGG CAACAGGCGG ACCCCCTGGG ACAGGACCGG
G ACAGGACCGG
121 TCITGCACCA T
AGAACGTGGT A
AGAACGTG
```

Figure 3.4. Sequence alignment of *ACTB*, *FLT3*, *EPOR*, *CSF1R* and *CSF3R* qRT-PCR assays within regions of their target genes. The forward primer, reverse primer and hydrolysis probe sequences are shown highlighted in blue, green, and pink, respectively. The red box highlights an exon junction. The numbers to the right of the gene names correspond to the length of the interrogated sequence input into the Biosearch Technologies RealTimeDesign software and do not relate to the true length of the gene. *ACTB*, β -actin; *FLT3*, fms-like tyrosine kinase 3; *EPOR*, erythropoietin receptor; *CSF1R*, macrophage-colony stimulating factor receptor; *CSF3R*, granulocyte-colony stimulating factor receptor.

Table 8: Primer and hydrolysis probe sequence for the *ACTB*, *FLT3*, *EPOR*, *CSF1R* and *CSF3R* qRT-PCR assays

Assay/Target	Forward Primer	Reverse Primer	Hydrolysis Probe
<i>ACTB</i>	5'-CAGCTTCTTTGCAGCTCCTTC-3'	5'-CGACCAGCGCAGCGATAT-3'	5'-CACCAGTTCGCCATGGA-3'
<i>FLT3</i>	5'-ATCAGCGGGAAAGCCATCATC-3'	5'-GGGCACACTGGAGGTCTTCT-3'	5'-TCCTCGCACCATTTCGGTA-3'
<i>EPOR</i>	5'-CATACCAGCTCGAGGGTGAGTCAC-3'	5'-CTCCGGGATGGACTTCAACTAC-3'	5'-CTGGTGCAGGCTACATGACT-3'
<i>CSF1R</i>	5'-ACCTGTCCTGGTCATCACT-3'	5'-AACCTCTTGGGAGCCTGTACTCAC-3'	5'-GCATAGCCTCGGCCTTCCTT-3'
<i>CSF3R</i>	5'-TGGACACATCGAGATTTAC-3'	5'-CTGCACCCTGACTGGAGTTAC-3'	5'-GTGCAAGAGGCCAGGACAG-3'

ACTB, β -actin; *FLT3*, fms-like tyrosine kinase 3; *EPOR*, erythropoietin receptor; *CSF1R*, macrophage-colony stimulating factor receptor; *CSF3R*, granulocyte-colony stimulating factor receptor.

Hydrolysis probe-based qRT-PCR assays specific for the detection of *Actb*, *Flt3*, *Epor*, *Csf1r* and *Csf3r* transcripts were designed to flank each corresponding exon-exon junction using the RealTimeDesign Software (described in **Section 2.8**). Where possible, a probe was designed to directly complement the exon-exon junction itself, especially when short introns were present (**Table 7**) between the chosen exons (see annealing location of hydrolysis probe for the *ACTB*, *FLT3* and *EPOR* assays in **Figure 3.4**). Before purchasing the assays, primers and hydrolysis probes were analysed for complementarity within the mouse transcriptome and genome using BLAST to ensure specificity. It was found that none of the designed primers or probes shared complementarity with any other mouse genomic or transcriptomic sequences. Thus, these primers and hydrolysis probes for the detection of *Actb*, *Flt3*, *Epor*, *Csf1r* and *Csf3r* transcripts were purchased from Biosearch Technologies (California, USA) and DNA Technology (Aarhus, Denmark). Primer and hydrolysis probe sequences for the *ACTB*, *FLT3*, *EPOR*, *CSF1R* and *CSF3R* qRT-PCR assays are listed in **Table 8**.

3.4.3 Optimisation of *ACTB*, *FLT3*, *EPOR*, *CSF1R* and *CSF3R* qRT-PCR assays

Next, the specificity of the *ACTB*, *FLT3*, *EPOR*, *CSF1R* and *CSF3R* qRT-PCR assays was confirmed. As these assays were designed for the detection of mRNA, they were tested to ensure they did not amplify gDNA. To do this, qRT-PCR analysis of whole BM lysate was performed for each assay with (+) and without (-) the RT enzyme, using non-limiting concentrations of primers and probes (900nM of primers and 250nM of hydrolysis probe). As the RNA in -RT samples is not converted to cDNA, amplification in these samples would only

occur if the given assay spans a region within gDNA. The *ACTB*, *FLT3*, *EPOR*, *CSF1R* and *CSF3R* qRT-PCR assays were tested using approximately 200ng of RNA and DNA obtained from whole BM lysate, and amplification was carried out for 45-50 cycles. All assays successfully amplified targets in the +RT but not the -RT reactions, indicating that they were specific for mRNA transcripts, and not gDNA (**Figure 3.5**). This was essential for moving forward with qRT-PCR optimisation, and confirmed that these assays could be used for analysis of gene expression by individual cells without previous DNase digestion.

For accurate analysis of single cell gene expression, each of the *FLT3*, *EPOR*, *CSF1R* and *CSF3R* qRT-PCR assays needed to be combined with the endogenous control gene. This allowed for the discrimination between samples that did not express the target HGF receptor gene and empty wells. To prevent competition occurring between assays in multiplex reactions, primer and probe concentrations needed to be optimised. The use of limiting concentrations of primers ensured that assays reproducibly and efficiently amplified a target to a level that could be detected, but did not impede the amplification of other targets through excessive use of reaction constituents.

Optimum primer concentrations were determined for each qRT-PCR assay by comparing varying concentrations and combinations of forward and reverse primers using constant concentrations of template (approximately 200ng of RNA and DNA from whole BM lysate) and non-limiting hydrolysis probe (250nM). For a detailed protocol for the optimisation of qRT-PCR assay primer concentrations see **Section 2.8**. As a positive control, reactions with unlimiting primer concentrations containing 300nM of forward primer and 300nM of reverse primer were included (reference reaction; 300nM/300nM reaction). Candidate primer combinations were first selected based on their efficiency (any sample with a Ct value of >0.5

cycles greater than the Ct value of the reference reaction was disregarded due to a loss in efficiency) (**Figure 3.6**). Of the remaining primer combinations, the sample with the lowest fluorescence level at the end of the plateau phase of the amplification curve was considered to represent the optimal limiting primer concentrations (**Figure 3.7**).

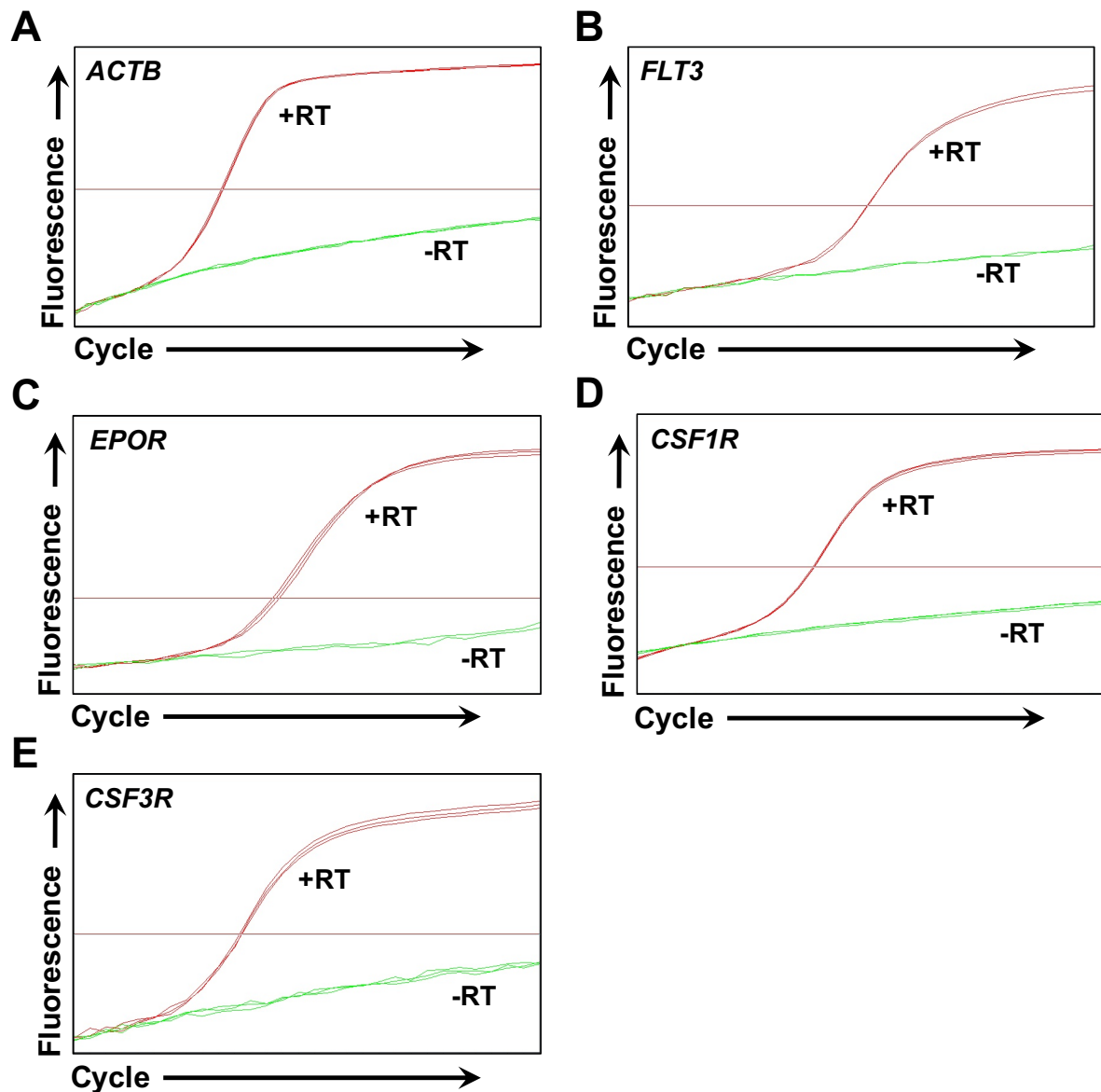


Figure 3.5. Amplification of qRT-PCR assay targets from whole BM lysate with and without reverse transcriptase. The specificity of the qRT-PCR assays was tested to ensure that they did not detect genomic DNA. Amplification of **(A) Actb**, **(B) Flt3**, **(C) Csf1r**, **(D) Epor** and **(E) Csf3r** from whole BM samples with (red amplification curves) and without (green amplification curves) RT. Fluorescence is plotted on a log scale. BM, bone marrow; RT, reverse transcriptase. *ACTB*, β -actin; *FLT3*, fms-like tyrosine kinase 3; *EPOR*, erythropoietin receptor; *CSF1R*, macrophage-colony stimulating factor receptor; *CSF3R*, granulocyte-colony stimulating factor receptor.

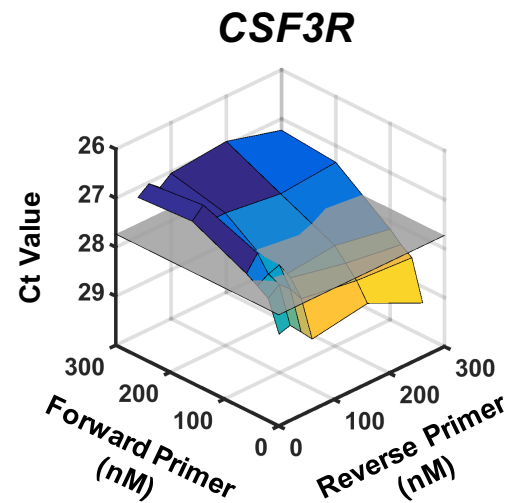
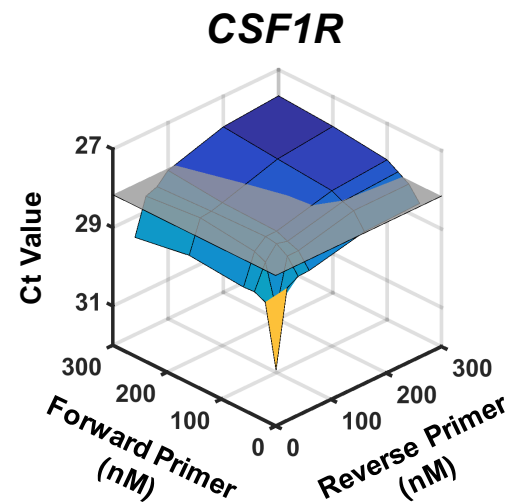
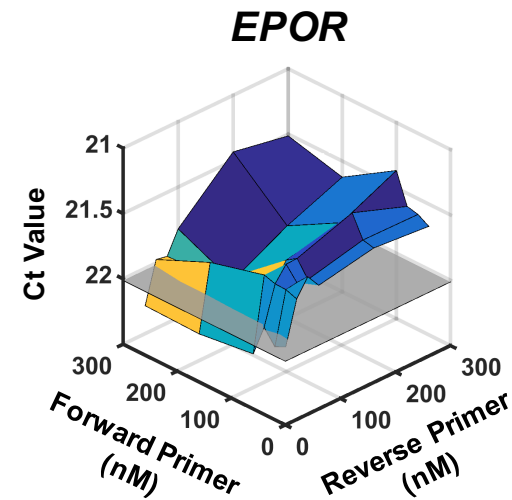
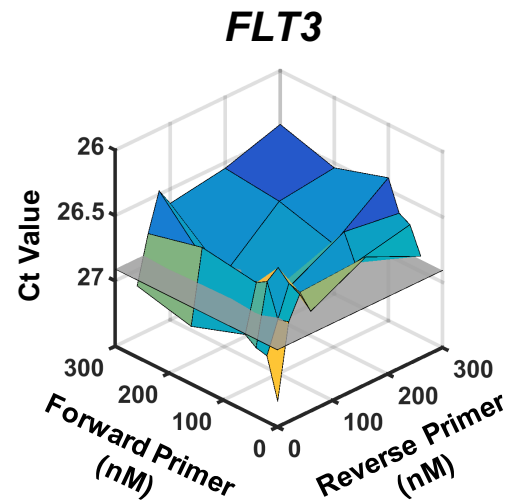
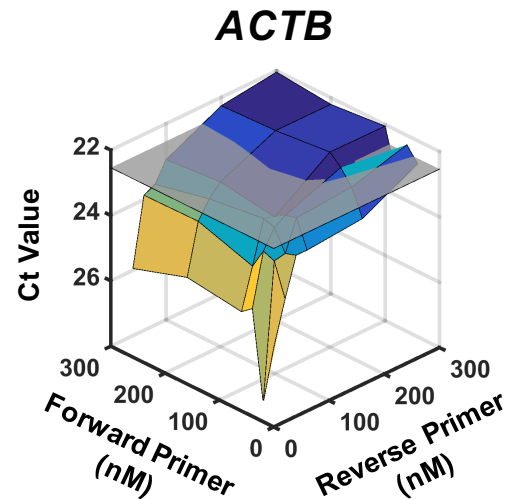


Figure 3.6. Ct values obtained during primer optimisation of qRT-PCR assays. Primers of the *ACTB*, *FLT3*, *EPOR*, *CSF1R* and *CSF3R* qRT-PCR assays were tested in varying concentrations and combinations to determine limiting conditions. Grey transparent panes are set to 0.5 cycles greater than the Ct of the reference reaction (300nM forward primer, 300nM reverse primer). All reactions with a Ct value above this were considered to have maintained efficiency when compared to the reference reaction (note z-axis is in reverse). Each data point represents the mean of 3 technical replicates. Ct, threshold cycle; *ACTB*, β -actin; *FLT3*, fms-like tyrosine kinase 3; *EPOR*, erythropoietin receptor; *CSF1R*, macrophage-colony stimulating factor receptor; *CSF3R*, granulocyte-colony stimulating factor receptor.

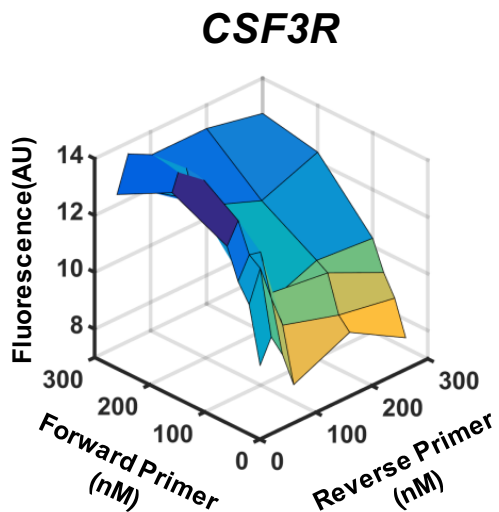
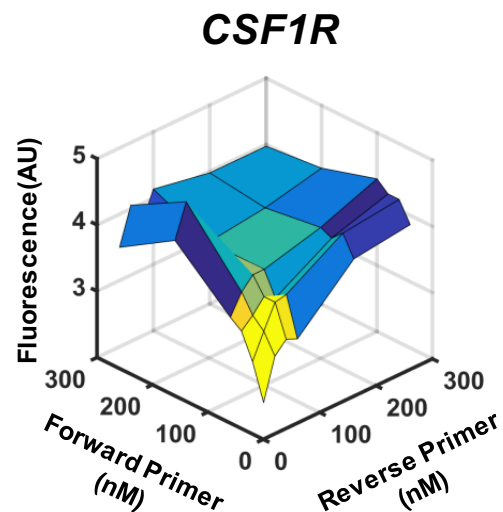
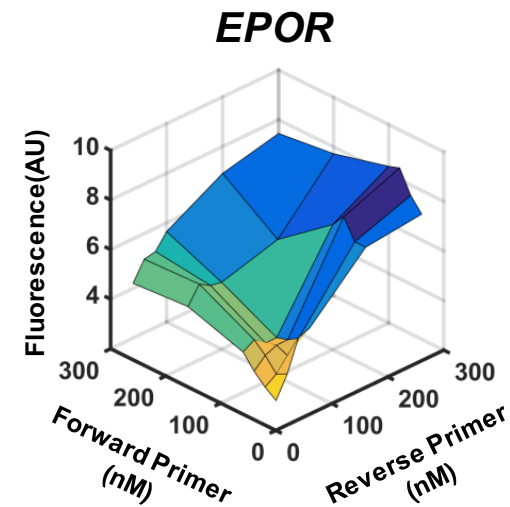
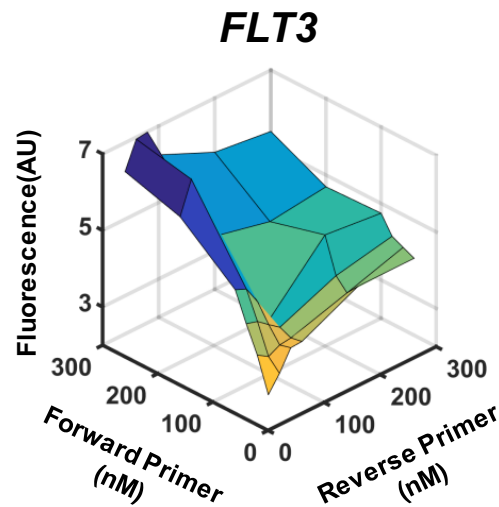
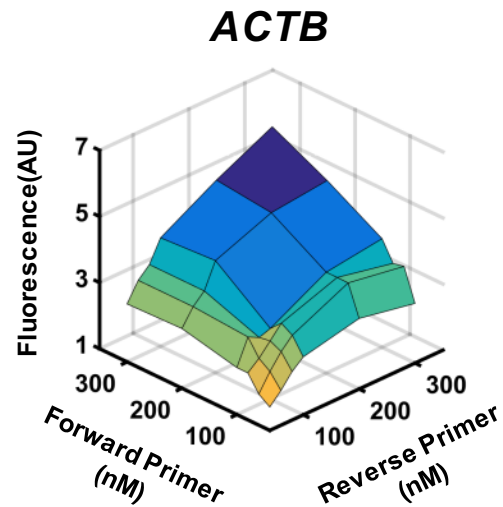


Figure 3.7. Peak fluorescence obtained during primer optimisation of qRT-PCR assay. Primers of the *ACTB*, *FLT3*, *EPOR*, *CSF1R* and *CSF3R* qRT-PCR assays were tested in varying concentrations and combinations to determine limiting conditions. Fluorescence values at the end of the plateau phase were plotted for each primer combination. Each data point represents the mean of 3 technical replicates. AU, arbitrary units; *ACTB*, β -actin; *FLT3*, fms-like tyrosine kinase 3; *EPOR*, erythropoietin receptor; *CSF1R*, macrophage-colony stimulating factor receptor; *CSF3R*, granulocyte-colony stimulating factor receptor.

This method was successful for the *ACTB*, *FLT3*, *EPOR* and *CSF3R* assays. However, when analysing the *CSF1R* primer optimisation data, all of the primer combinations that resulted in a Ct value of <0.5 cycles greater than the reference reaction Ct value had either equal or greater end fluorescence values. Even minor decreases in peak fluorescence values were accompanied by an increase in Ct values (**Figure 3.6** and **Figure 3.7**). Thus, the primer concentrations in the reference reaction (300nM/300nM) were used for all future *CSF1R* assays. The optimum primer concentrations for each assay are listed in **Table 8**.

Using the optimum concentrations of primers for each assay, the probe concentrations for the *ACTB*, *FLT3*, *EPOR*, *CSF1R* and *CSF3R* qRT-PCR assays were subsequently optimised. Reactions were set up using varying concentrations of hydrolysis probe to amplify a constant concentration of template (approximately 200ng of RNA and DNA from whole BM lysate). Again, a detailed protocol is described in **Section 2.8**. A reaction containing 250nM of hydrolysis probe was included as a reference reaction as this was considered to contain excessive amounts of probe. As with the primer optimisation protocol, candidate hydrolysis probe concentrations were considered to have lost efficiency if they yielded a Ct value of >0.5 cycles greater than the Ct value of the reference reaction. Of the reactions that had retained efficiency, the lowest concentration of probe was selected as the optimal probe concentration (**Figure 3.8**). Probe optimisation was successful for all of the assays. Therefore, the *ACTB*, *FLT3*, *EPOR*, *CSF1R* and *CSF3R* qRT-PCR assays were fully optimised, and all future reactions were carried out using the optimum conditions for each assay. The optimum hydrolysis probe concentration for each assay is listed in **Table 8**.

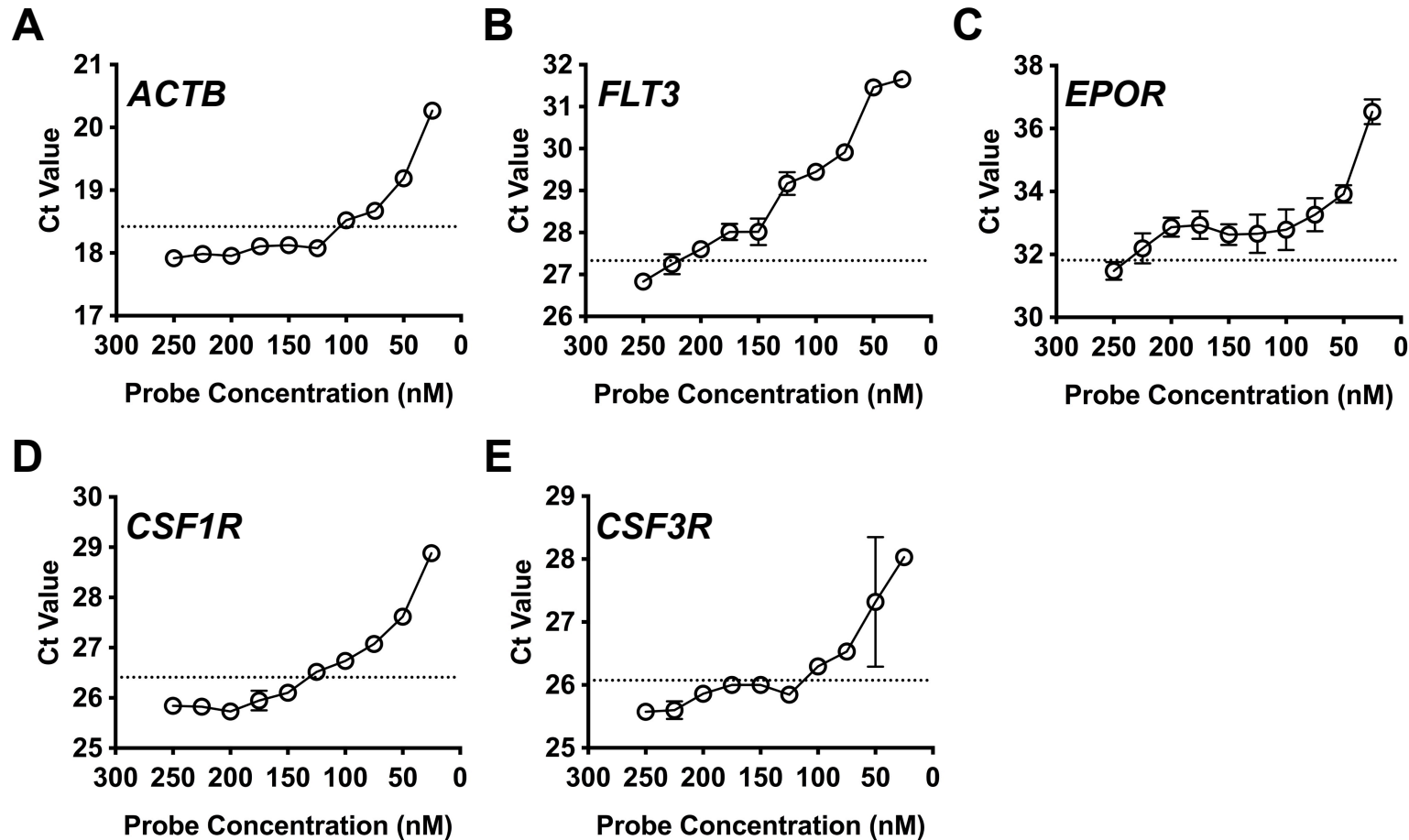


Figure 3.8. Optimisation of hydrolysis probe concentration for *ACTB*, *FLT3*, *EPOR*, *CSF1R* and *CSF3R* qRT-PCRs. Varying concentrations of hydrolysis probe were used to determine the optimum concentration for the detection of (A) *ACTB*, (B) *FLT3*, (C) *EPOR* (D) *CSF1R* and (E) *CSF3R* expression. All reactions contained limiting primer concentrations and a constant concentration of RNA/DNA from whole BM lysate. Dotted lines are set to 0.5 cycles greater than the reference reaction (reaction containing 250nM of hydrolysis probe). All reactions below this line were considered to have maintained efficiency when compared to the reference reaction. Data represents mean \pm standard error from at least 3 technical replicates at each point. Ct, threshold cycle; *ACTB*, β -actin; *FLT3*, fms-like tyrosine kinase 3; *EPOR*, erythropoietin receptor; *CSF1R*, macrophage-colony stimulating factor receptor; *CSF3R*, granulocyte-colony stimulating factor receptor.

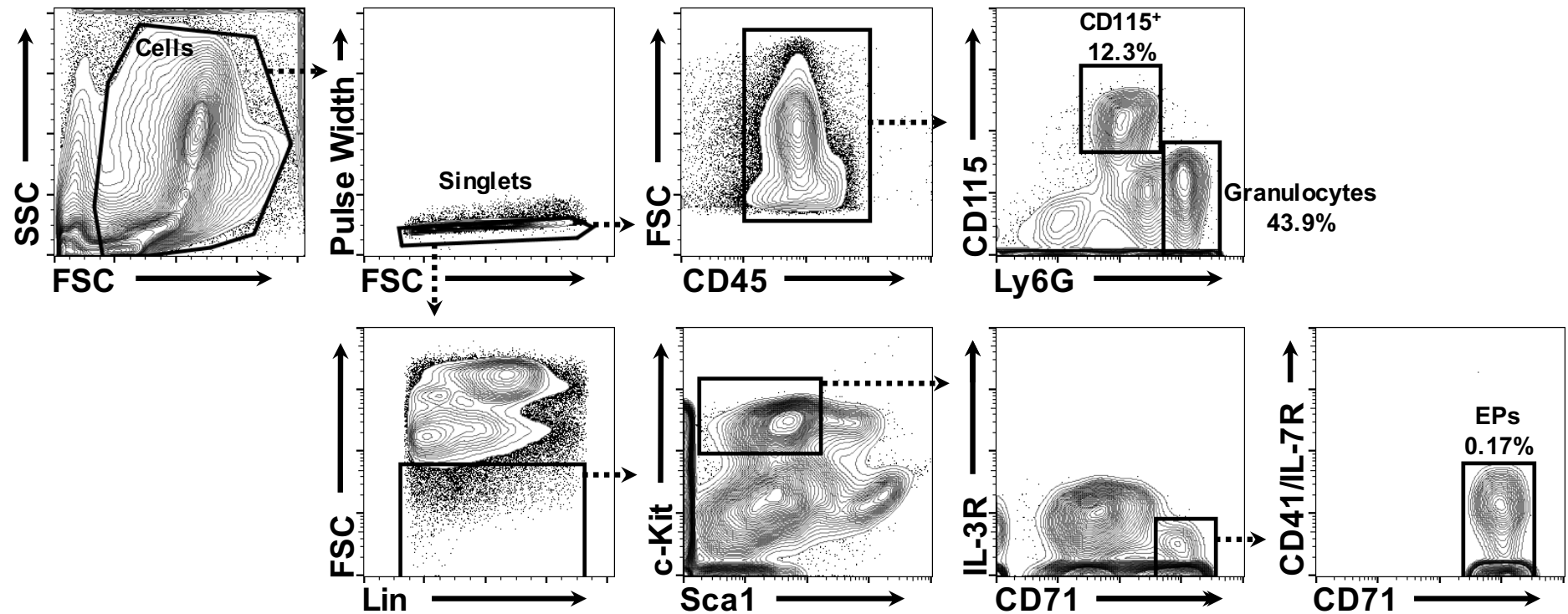


Figure 3.9. Isolation of CD115⁺ leukocytes, Ly6G⁺ granulocytes and EPs from mouse BM to test the single cell sensitivity of the *CSF1R*, *CSF3R* and *EPOR* qRT-PCR assays. Populations are delineated by the black boxes. Cells were first gated based on their FSC/SSC profile, and then doublets were excluded by gating for cells with a low pulse width value. Values shown represent the percentage of singlet events within the given gate. FSC, forward scatter; SSC, side scatter; Lin, lineage markers; IL-3R, interleukin-3 receptor; EP, erythroid progenitor; BM, bone marrow.

Once the qRT-PCR assays were optimised, they were tested to determine if they were sensitive enough to detect gene expression by single cells. To do this, single cells that were known to express the gene of interest were sorted and analysed using the optimised assays. By sorting 1, 2, 4, 8, 16, 32 and 64 cell(s) into single wells of 384-well PCR plates, the efficiency of the qRT-PCR assays could also be determined as, on average, a decrease of 1 Ct per cell number doubling would indicate efficient amplification of target sequences (see dotted lines in Figure 3.10).

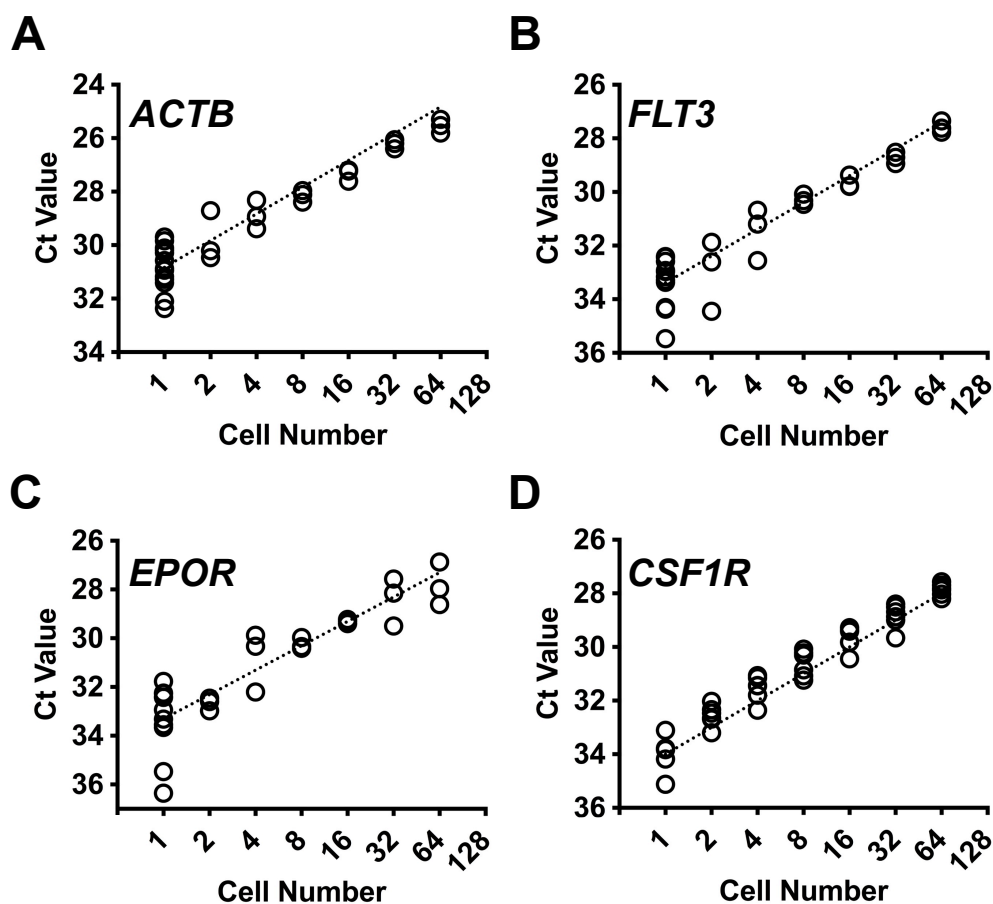


Figure 3.10. Detection of *ACTB*, *FLT3*, *EPOR* and *CSF1R* gene expression in single cells. Detection of gene expression in varying cell numbers using (A) *ACTB*, (B) *FLT3*, (C) *EPOR* and (D) *CSF1R* qRT-PCR assays at optimised primer and probe concentrations. For comparison, the dotted lines represent an efficient amplification with a decrease in 1 cycle per cell number doubling. Common lymphoid progenitors, lymphoid-primed multipotent progenitors, erythroid progenitors and CD115+ leukocytes were sorted to test the efficiency of the (A) *ACTB*, (B) *FLT3*, (C) *EPOR* and (D) *CSF1R* qRT-PCR assays, respectively. Data represents mean \pm standard error from at least 3 samples. Ct, threshold cycle; *ACTB*, β -actin; *FLT3*, fms-like tyrosine kinase 3; *EPOR*, erythropoietin receptor; *CSF1R*, macrophage-colony stimulating factor receptor; *CSF3R*, granulocyte-colony stimulating factor receptor.

ACTB is expressed by all cells, so CLPs were sorted to test the sensitivity of the *ACTB* qRT-PCR assay due to their simple staining profile. LMPPs were identified based on the presence of Flt3 on their surface, so variable numbers of these cells were sorted to determine if the *FLT3* qRT-PCR assay could detect single cell gene expression [73]. CLPs and LMPPs were purified using the gating strategy depicted in **Figure 3.2**. To test the sensitivity of the *CSF1R* and *CSF3R* qRT-PCR assays, single BM CD45⁺ CD115⁺ (M-CSFR⁺) leukocytes and CD45⁺ Ly6G⁺ granulocytes were sorted, respectively (**Figure 3.9**) [318, 319]. Finally, to verify the sensitivity of the *EPOR* qRT-PCR assay, LS⁻K IL-3R⁻ IL-7Rα⁻ CD41⁻ CD71⁺ EPs were purified (**Figure 3.9**) [313].

Table 9: Optimum primer and hydrolysis probe concentrations of qRT-PCR assays for the detection of gene expression by single cells

Assay Target	Optimum Forward Primer Conc. (nM)	Optimum Reverse Primer Conc. (nM)	Optimum Hydrolysis Probe Concentration	Single-cell gene expression detected
<i>ACTB</i>	60	300	125	Yes
<i>FLT3</i>	80	60	225	Yes
<i>EPOR</i>	80	100	150	Yes
<i>CSF1R</i>	300	300	125	Yes
<i>CSF3R</i>	300	60	175	No

ACTB, β-actin; *FLT3*, fms-like tyrosine kinase 3; *EPOR*, erythropoietin receptor; *CSF1R*, macrophage-colony stimulating factor receptor; *CSF3R*, granulocyte-colony stimulating factor receptor.

Using the *ACTB*, *FLT3*, *EPOR* and *CSF1R* qRT-PCR assays, expression of the respective transcripts in single cells were successfully detected. On average, a decrease of 1 Ct was observed for each cell number doubling, indicating that the assays were amplifying target mRNA in an efficient manner (**Figure 3.10**, dotted lines). However, when the expression of *CSF3R* was analysed, the amplification curves began to diminish as the cell number decreased. By comparing the amplification data of the *CSF3R* assay to that of the *CSF1R* assay, it was clear

that the *CSF3R* assay was not sensitive when assaying single cells (**Figure 3.11**). Thus, this assay was not used to analyse *CSF3R* expression in HSPCs in future experiments. The ability of the *ACTB*, *FLT3*, *EPOR*, *CSF1R* and *CSF3R* qRT-PCR assays to detect single cell gene expression is listed in **Table 8**.

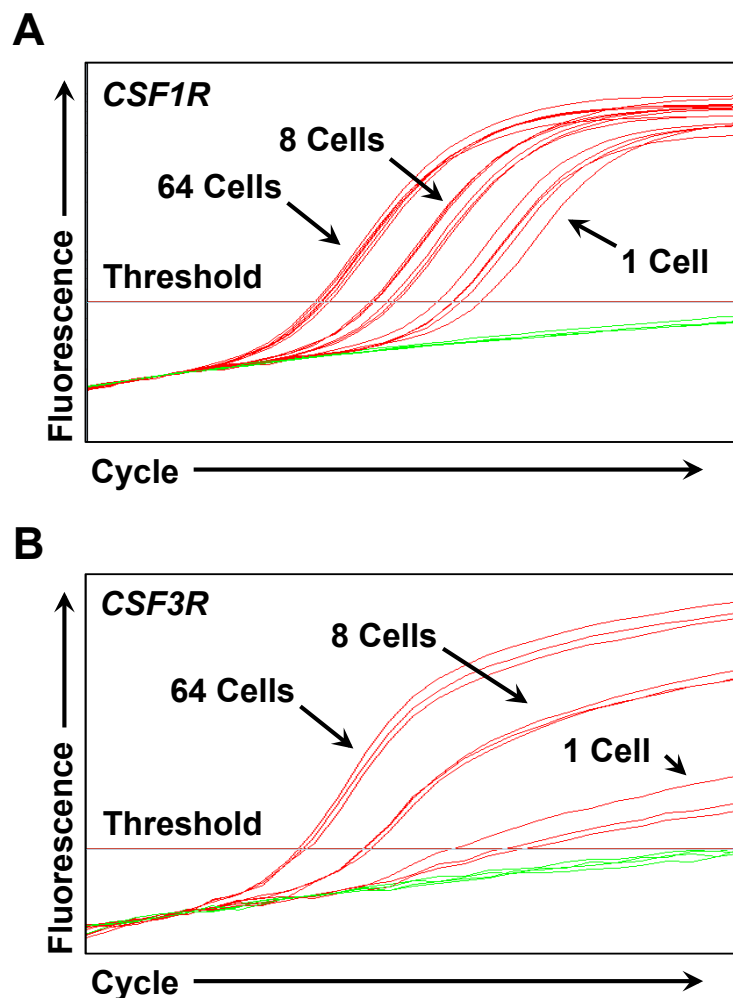


Figure 3.11. Amplification of *Csf1r* and *Csf3r* from single cells. The **(A)** *CSF1R* qRT-PCR assay detected gene expression by single CD115⁺ leukocytes, which was clearly distinguished from background (no-template controls; green curves). On the other hand, the **(B)** *CSF3R* qRT-PCR did not efficiently amplify *Csf1r* transcripts when analysing single Ly6G⁺ neutrophils. The logarithmic phase of the *Csf3r* amplification curves begin to diminish as cell number decreases. Each red curve represents amplification of the given gene from 1, 8 or 64 cell(s). Green amplification curves represent background fluorescence seen in control reactions with no template. Fluorescence is plotted on a log scale. *CSF1R*, macrophage-colony stimulating factor receptor; *CSF3R*, granulocyte-colony stimulating factor receptor.

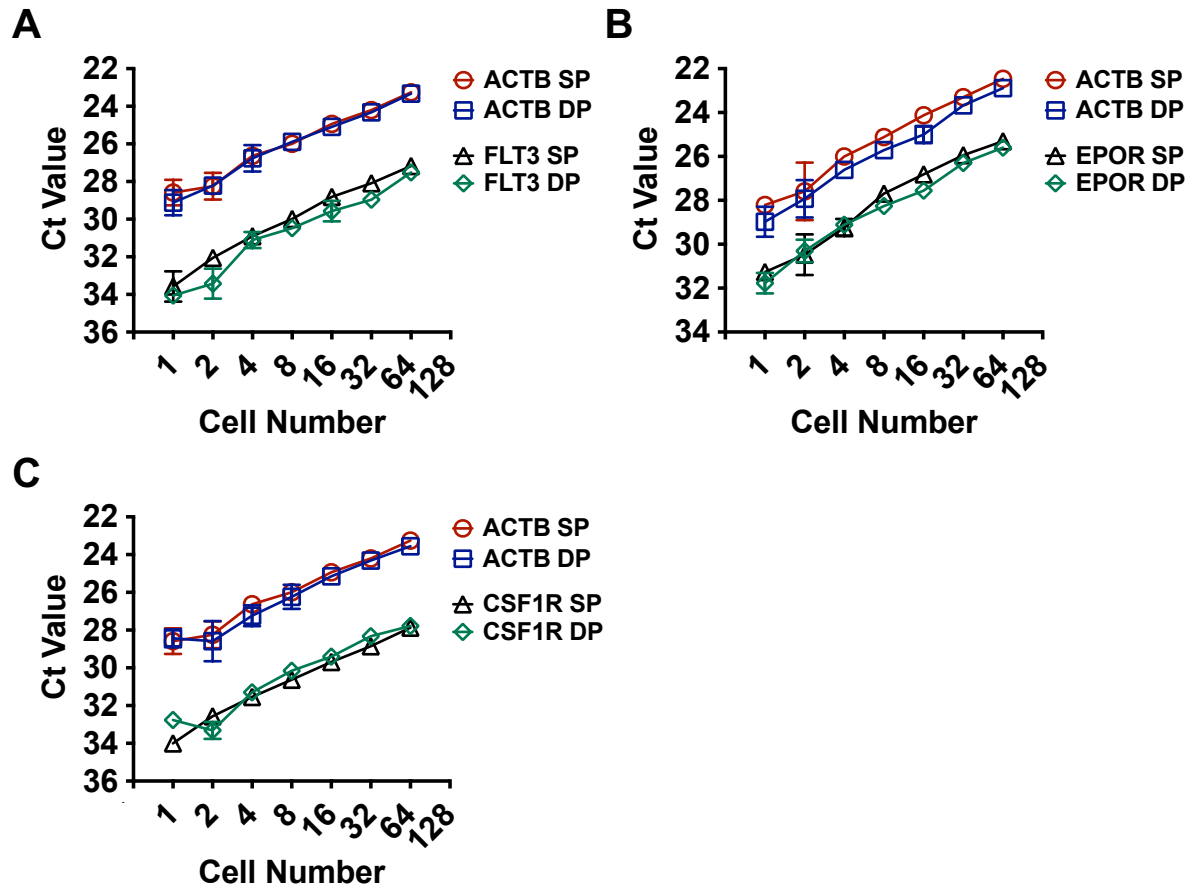


Figure 3.12. Validation of *FLT3*, *EPOR* and *CSF1R* qRT-PCR assays in duplex with *ACTB* using single cells. (A) Amplification of *Actb* and *Flt3* in varying numbers of LMPPs using singleplex and duplex reactions. (B) Amplification of the *Actb* and *Epor* genes in varying numbers of EPs using singleplex and duplex reactions. (C) Amplification of *Actb* and *Csf1r* in varying numbers of CD115⁺ leukocytes using singleplex and duplex reactions. Each data point represents mean \pm standard error from at least 3 samples. SP, singleplex; DP, duplex; LMPP, lymphoid-primed multipotent progenitor; EP, erythroid progenitor; Ct, threshold cycle; *ACTB*, β -actin; *FLT3*, fms-like tyrosine kinase 3; *EPOR*, erythropoietin receptor; *CSF1R*, macrophage-colony stimulating factor receptor.

As mentioned previously, in order to accurately determine the percentage of cells that express a HGF receptor within a cell population, the *FLT3*, *EPOR* and *CSF1R* qRT-PCR assays needed to be combined with *ACTB* which was used to confirm the presence of a cell within each well of a PCR plate during analysis. To ensure that no efficiency was lost when combining assays, the sensitivity of the duplex assays was tested using varying numbers of single cells as before. The single-cell sensitivity of the *ACTB* + *FLT3*, *ACTB* + *EPOR* and *ACTB* + *CSF1R* duplex

qRT-PCR reactions was tested by analysing 1, 2, 4, 8, 16, 32 and 64 LMPP(s), EP(s) and CD115⁺ leukocyte(s), respectively. Singleplex reactions of each assay were carried out in parallel to determine if there was any loss efficiency when assays were combined. When compared to the singleplex reactions, it was clear that the *FLT3*, *EPOR* and *CSF1R* qRT-PCR assays maintained efficiency and Ct values when performed in duplex with *ACTB* (**Figure 3.12**).

Of particular interest was the possible co-expression of HGF receptor genes during the early stages of haematopoiesis. Hence, some qRT-PCR assays were combined in triplex reactions and efficiencies were tested as before. One reaction combined the *ACTB*, *FLT3* and *EPOR* assays (*ACTB* + *FLT3* + *EPOR* triplex qRT-PCR assay), and a second combined the *ACTB* + *EPOR* + *CSF1R* assays (*ACTB* + *EPOR* + *CSF1R* triplex qRT-PCR assay). As there are not any well-defined cells that constitutively express both *FLT3* and *EPOR*, the *ACTB* + *FLT3* + *EPOR* triplex qRT-PCR assay was tested by sorting both LMPPs and EPs into the same wells of a PCR plate. Similarly, there are no well-defined cells that constitutively express *EPOR* and *CSF1R*, so the *ACTB* + *EPOR* + *CSF1R* triplex qRT-PCR assay was tested by sorting both EPs and CD115⁺ leukocytes into the same wells of a PCR plate.

Unfortunately, while the Ct values for the *ACTB* + *FLT3* + *EPOR* and *ACTB* + *EPOR* + *CSF1R* triplex reactions were comparable to singleplex reactions (**Figure 3.13**), the amplification curves of the assays in triplex showed a loss in efficiency of at least one of the assays (**Figure 3.14** and **Figure 3.15**). As this may cause issues when assaying cells with a very low level of gene expression, all HSPCs were first assayed for HGF gene expression of *FLT3*, *EPOR* and *CSF1R* by performing qRT-PCR duplex assays in combination with the *ACTB* assay. Any potential signs of gene co-expression in early HSPCs were investigated at a later stage.

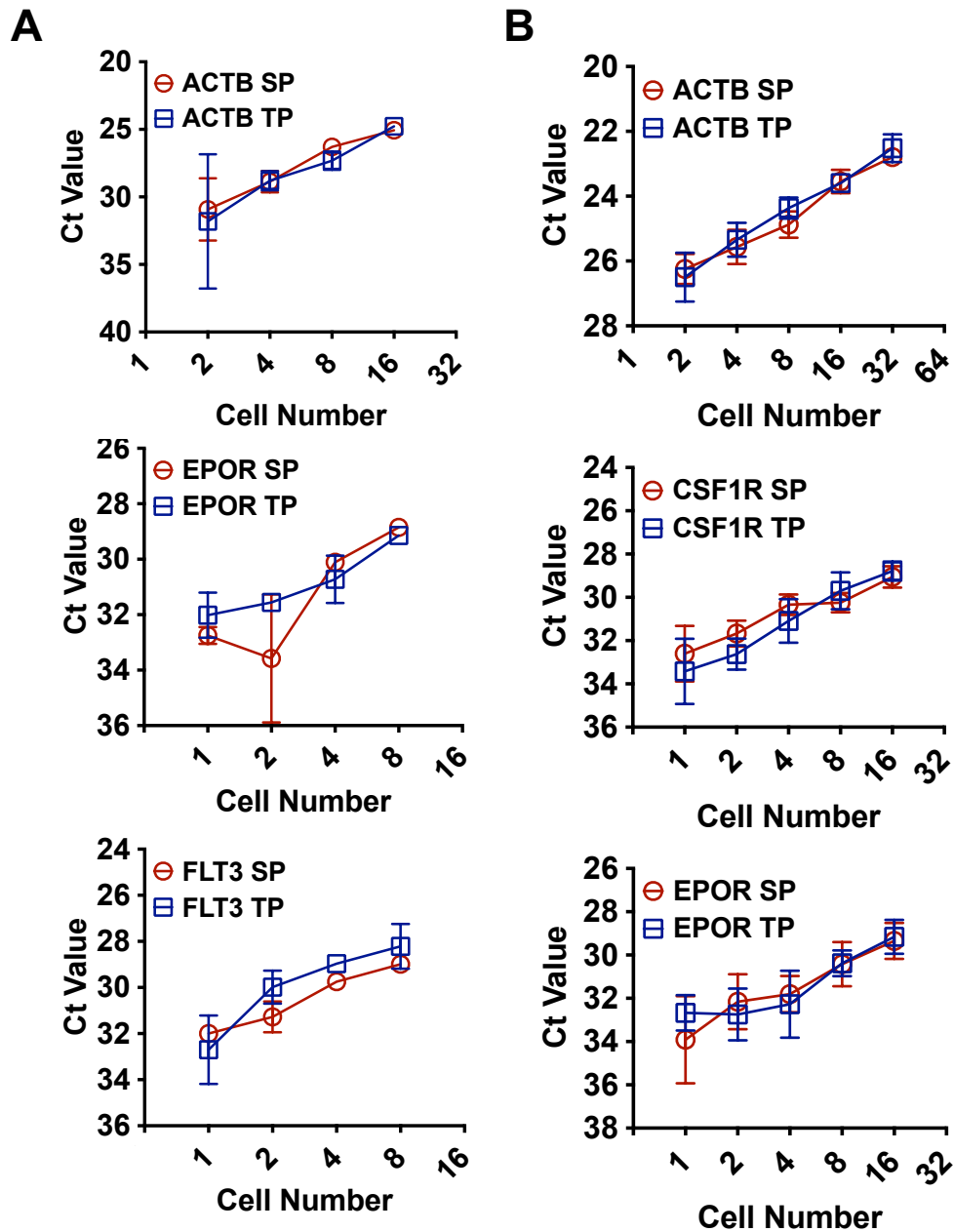


Figure 3.13. Validation of triplex qRT-PCR assays using single cells. (A) Detection of *ACTB*, *FLT3* and *EPOR* expression in varying numbers of LMPPs and EPs using singleplex and triplex reactions. Cell number values for *FLT3* and *EPOR* assays are representative of the number of LMPPs or EPs that are present in the sample, respectively. Cell number values for the *ACTB* assay are representative of the combined number of LMPPs and EPs that are present in the sample. **(B)** Detection of *ACTB*, *CSF1R* and *EPOR* expression in varying numbers of CD115⁺ leukocytes and EPs using singleplex and triplex reactions. Cell number values for *CSF1R* and *EPOR* assays are representative of the number of CD115⁺ leukocytes or EPs that are present in the sample, respectively. Cell number values for the *ACTB* assay are representative of the combined number of CD115⁺ leukocytes and EPs that are present in the sample. Each data point represents mean \pm standard error from at least 3 samples. LMPP, lymphoid primed multipotent progenitor; EP, erythroid progenitor; SP, singleplex; TP, triplex; Ct, threshold cycle; *ACTB*, β -actin; *FLT3*, fms-like tyrosine kinase 3; *EPOR*, erythropoietin receptor; *CSF1R*, macrophage-colony stimulating factor receptor.

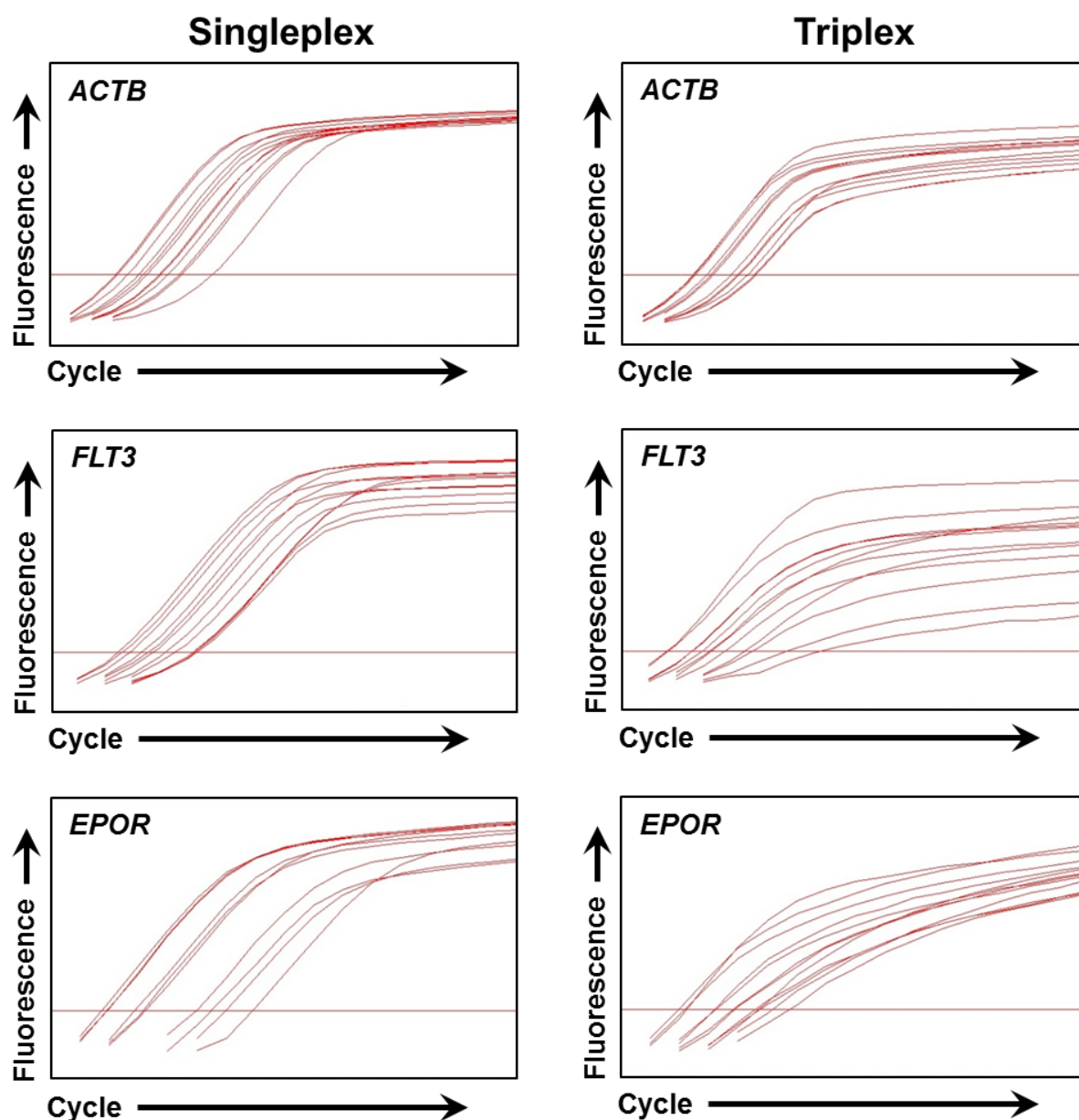


Figure 3.14. Amplification of *Actb*, *Flt3* and *Epor* in single cells using triplex qRT-PCR reactions. Comparison of amplification of *Actb*, *Flt3* and *Epor* in varying numbers of cells using singleplex reactions to triplex reactions. The amplification of *Flt3* was not efficient in triplex reactions, as revealed by the diminishing amplification curves. Lymphoid-primed multipotent progenitors and erythroid progenitors were sorted to test the efficiency of the *ACTB*, *FLT3* and *EPOR* qRT-PCR assays. Fluorescence is plotted on a log scale. *ACTB*, β -actin; *FLT3*, fms-like tyrosine kinase 3; *EPOR*, erythropoietin receptor.

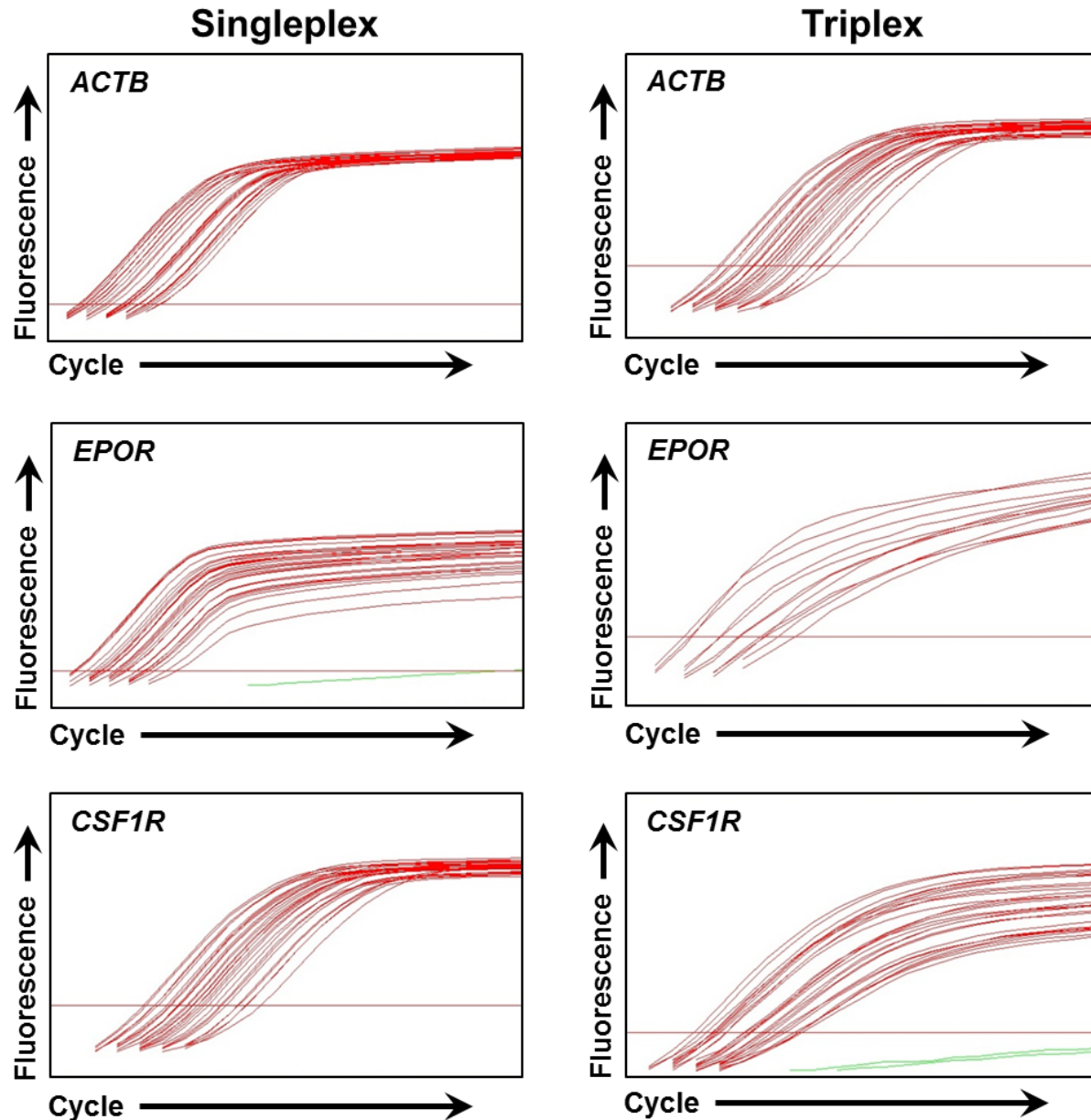


Figure 3.15. Amplification of *Actb*, *Epor* and *Csf1r* in single cells using triplex qRT-PCR reactions. Comparison of amplification of *Actb*, *Epor* and *Csf1r* in varying numbers of cells using singleplex reactions to triplex reactions. The *EPOR* and *CSF1R* qRT-PCR assays lost efficiency when in triplex reactions, as depicted by the diminishing amplification curves. CD115⁺ leukocytes and erythroid progenitors were used to test the efficiency of the *ACTB*, *EPOR* and *CSF1R* qRT-PCR assays. Fluorescence is plotted on a log scale. *ACTB*, β -actin; *EPOR*, erythropoietin receptor; *CSF1R*, macrophage-colony stimulating factor receptor.

3.5 Expression of growth factor receptor transcripts during haematopoiesis

3.5.1 Expression of *Flt3*, *Epor* and *Csf1r* transcripts by haematopoietic stem and progenitor cells

Having successfully designed and optimised the qRT-PCR assays, it was possible to investigate the expression of *FLT3*, *EPOR* and *CSF1R* genes within HSPC populations. For single cell analysis, cells from 3-6 mice were analysed and approximately 20-40 cells were obtained from each mouse. As such, all data from this section are represented in two ways; *i*) percentages as mean \pm standard error of the values obtained from 3-6 mice, and; *ii*) percentages as calculated from the total number of cells that were assayed. Any wells that did not produce amplification of *Actb* were excluded from the analysis as they were considered to be empty. The number of single cells sorted into wells of a PCR plate according to the sorting software, and the number of these wells that produced successful amplification of *Actb*, is listed in **Table 10**. For all populations and assays, sorting efficiency never dropped below 90%. Throughout the analysis of HGF receptor gene expression, single cells expressing these receptors could clearly be distinguished from those that did not, as can be seen in **Figure 3.16**. In total, more than 3,000 single cells were assayed for gene expression analysis.

Firstly, to investigate the expression of HGF receptors in the early, multipotent HSPC compartments, the number of cells expressing *FLT3*, *EPOR* and *CSF1R* genes by within the LT-HSC, ST-HSC and MPP compartments was investigated (**Figure 3.17A**). Analysis revealed *FLT3* expression within a small subpopulation of LT-HSCs ($n=6$ mice) and ST-HSCs ($n=6$ mice). Of the

LT-HSCs that were analysed, $11.6\% \pm 2.19$ (28/248 cells; 11.3% of total) expressed *Flt3* transcripts, and $21\% \pm 3.4$ of cells in the ST-HSC compartment (56/252 cells; 22.2% of total) also expressed this gene. There was a significant increase in the number of *FLT3* expressing cells in the ST-HSC population when compared to the LT-HSC population [$p=0.0476$]. The number of cells within the MPP ($n=6$ mice) compartment expressing *FLT3* ($64\% \pm 2.2$ of cells; 190/297 cells [64% of total]) was greatly increased when compared to ST-HSC [$p=0.0022$] (Figure 3.17A).

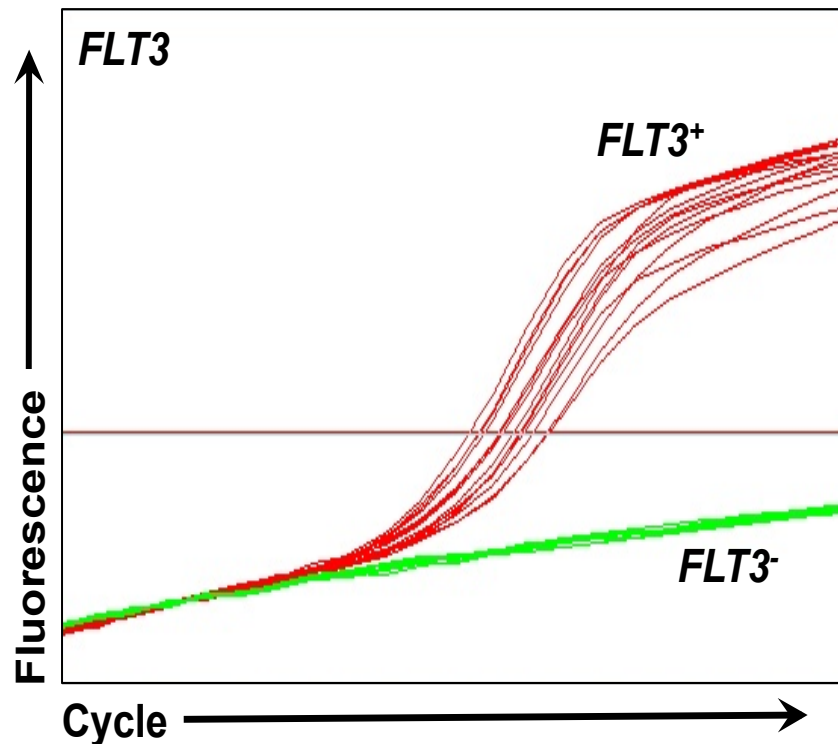


Figure 3.16. Analysis of *FLT3* expression by single LT-HSCs. A representative amplification curve showing positive (red) and negative (green) detection of *FLT3* expression by LT-HSCs. *Flt3*⁺ and *Flt3*⁻ cells are clearly distinguished from each other. *FLT3*, fms-like tyrosine kinase 3; LT-HSC, long-term haematopoietic stem cell.

A small number of cells expressing *EPOR* within the LT-HSC ($n=6$ mice) and ST-HSC ($n=6$ mice) compartments were detected, and these values reflect previous findings [115, 320]. *EPOR* was expressed by $12.8\% \pm 1.46$ (31/245 cells; 12.7% of total) of LT-HSCs and $19.3\% \pm 4.6$ (42/237 cells; 17.7% of total) of ST-HSCs, and these values were not significantly different [$p=0.2188$]. Of the MPPs ($n=6$ mice) analysed, only $8.2\% \pm 4.6$ (25/300 cells; 8.3% of total) expressed *EPOR*. While this was lower than the number of ST-HSCs expressing *EPOR*, the difference was not significant [$p=0.0628$] (**Figure 3.17B**).

CSF1R expression was rarely detected within these populations. *Csf1r* transcripts were detected in $0.9\% \pm 0.9$ (1/122 cells; 0.8% of total) of LT-HSCs ($n=3$ mice), $2.14\% \pm 1.3$ (2/118 cells; 1.7% of total) of ST-HSCs ($n=3$ mice), and $4.8\% \pm 3.8$ (7/145 cells; 4.8% of total) of MPPs ($n=3$) (**Figure 3.17C**). Given the few HSCs that expressed *CSF1R*, it is possible that these *Csf1r*⁺ cells were due to impurities during sorting. However, as M-CSF is known to instruct HSCs towards myeloid fates by stimulating its receptor, *CSF1R* expression would be expected in this compartment [267]. The qRT-PCR assay used here may not have been sensitive enough to detect *CSF1R* expression in single HSCs. Mossadegh-Keller *et al.* have also failed to detect *CSF1R* expression in single LT-HSCs (LSK CD150⁺ CD48⁻ CD34⁻) [267]. In this regard, the *CSF1R* gene may not need to be continuously transcribed to maintain expression of M-CSFR on the surface of HSCs, and so *CSF1R* expression may only occur very rarely.

Table 10: Percentage of wells assayed that produced successful amplification of *Actb* for each HSPC population

	<i>FLT3</i> qRT-PCR assay			<i>EPOR</i> qRT-PCR assay			<i>CSF1R</i> qRT-PCR assay		
	<i>Total number of wells assayed</i>	<i>Actb</i> ⁺	% <i>Actb</i> ⁺	<i>Total number of wells assayed</i>	<i>Actb</i> ⁺	% <i>Actb</i> ⁺	<i>Total number of wells assayed</i>	<i>Actb</i> ⁺	% <i>Actb</i> ⁺
LT-HSC	248	248	100	258	245	94.96	122	122	100
ST-HSC	269	252	93.68	266	237	89.10	122	118	96.72
MPP	305	297	97.38	306	300	98.04	151	145	96.03
HPC1	101	101	100	104	100	96.15	101	101	97.12
HPC2	58	56	96.55	59	58	98.31	57	56	98.25
LMPP	99	97	97.98	99	99	100	99	97	97.98
CLP	95	94	98.95	97	94	96.91	91	90	98.90
CMP	86	81	94.19	87	79	90.80	88	81	92.05
GMP	102	98	96.08	102	96	94.12	104	99	95.19
MEP	102	92	90.20	102	98	96.08	102	96	94.12

LT-HSC, long-term haematopoietic stem cell; ST-HSC short-term haematopoietic stem cell; MPP, multipotent progenitor; HSPC, haematopoietic stem and progenitor cell LMPP, lymphoid-primed multipotent progenitor; CLP, common lymphoid progenitor; CMP, common myeloid progenitor; GMP, granulocyte-macrophage progenitor; MEP, megakaryocyte-erythroid progenitor; *ACTB*, β -actin; *FLT3*, fms-like tyrosine kinase 3; *EPOR*, erythropoietin receptor; *CSF1R*, macrophage-colony stimulating factor receptor.

Next, the expression of *FLT3*, *EPOR* and *CSF1R* by more mature BM progenitors was investigated, and the analysis revealed a clear association between the presence of HGF receptor transcripts and the lineage potential of the populations. A large number of cells within the LMPP ($n=3$ mice) ($92.8\% \pm 2.04$; 90/97 cells [92.8% of total]) compartment expressed *FLT3*, and this was significantly more than the number of *Flt3*⁺ cells present in the MPP compartment [$p=0.0119$]. This was to be expected given the high levels of Flt3 receptor within this compartment [73]. Of the 94 CLPs ($n=3$ mice) analysed, a $66.2\% \pm 3.8$ (62/94 cells; 66% of total) expressed *FLT3*. Again, given that CLPs are regulated by Flt3L this was not surprising [321]. When *Flt3*^{-/-} HPC-1 ($n=3$ mice) were analysed, $57.2\% \pm 14.1$ (57/101 cells; 56.4% of total) of cells expressed *FLT3*. The number of cells that expressed *FLT3* significantly decreased as MPPs committed to the myeloid lineage and differentiated into CMPs [$p=0.0119$]. Of the CMPs ($n=3$ mice) and GMPs ($n=3$ mice) assayed, $24.9\% \pm 5.4$ (21/81 cells; 25.9% of total), and $21.4\% \pm 2.8$ (21/98 cells; 21.4% of total) expressed detectable levels of *FLT3*, respectively. The number of GMPs that expressed *FLT3* was similar to reported findings, as Böiers *et al.* previously showed that *FLT3* expression was detectable in $22\% \pm 9$ GMPs [322]. Furthermore, $9.9\% \pm 5.95$ of HPC-2 ($n=3$ mice) (8/56 cells; 14.3% of total) were found to express *FLT3*. Finally, *FLT3* expression was only detected in 1 of 98 MEPs ($n=3$ mice) ($1\% \pm 1$; 1/98 cells [1% of total]). Mouse MegE progenitors have been reported to lack Flt3 expression [323], and mouse MEPs have been shown to lack Flt3 transcriptional activity [312]. Given that purity rarely reaches 100% when sorting, the *Flt3*⁺ cell purified with the single MEPs was likely due to contamination (**Figure 3.17A**). When compared, the LT-HSC compartment contained significantly more *Flt3*⁺ cells than the MEP compartment [$p=0.0238$], indicating that the *FLT3* expression observed in the LT-HSC population was not an artefact of analysis or due to impurities.

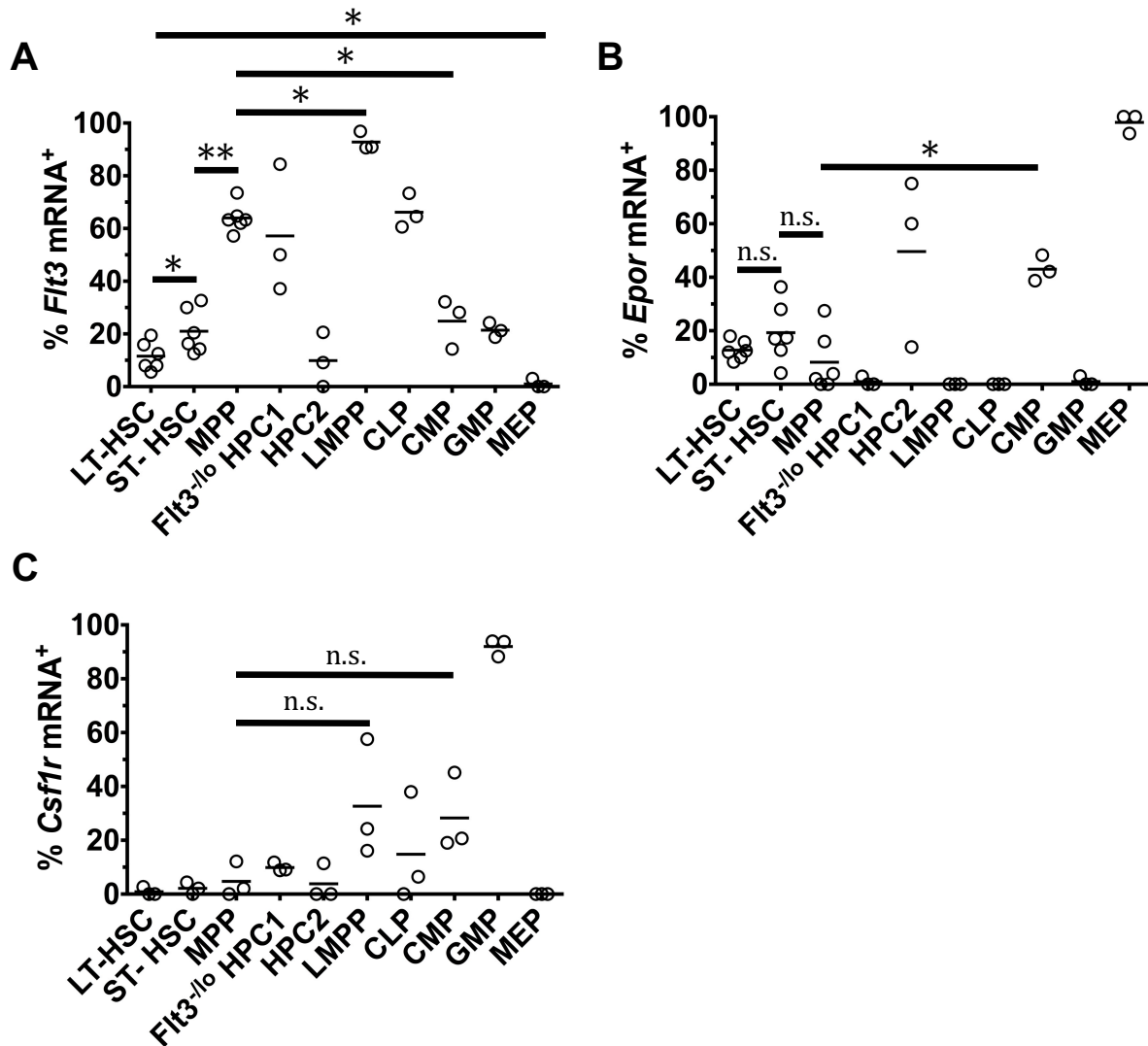


Figure 3.17. Expression of *Flt3*, *Epor* and *Csf1r* transcripts by HSPCs. The percentage of cells within each HSPC population that express (A) *Flt3*, (B) *Epor* and (C) *Csf1r* mRNA when analysed at the single cell level are shown. Each individual point represents a single mouse. Assays were carried out in duplex with a qRT-PCR assay specific for *Actb* transcripts, and reactions that did not give rise to detectable amplification of *Actb* were removed from analysis as this indicated an empty well. Data are the mean of the values obtained for single cells from 3-6 mice (approximately 20-40 cells/mouse). *p* values obtained by two-tailed non-parametric student's t-test where; *, *p* < 0.05; **, *p* < 0.01. LT-HSC, long-term haematopoietic stem cell; ST-HSC short-term haematopoietic stem cell; MPP, multipotent progenitor; HSPC, haematopoietic stem and progenitor cell; HPC, haematopoietic progenitor cell; LMPP, lymphoid-primed multipotent progenitor; CLP, common lymphoid progenitor; CMP, common myeloid progenitor; GMP, granulocyte-macrophage progenitor; MEP, megakaryocyte-erythroid progenitor; *Actb*, β -actin; *Epor*, erythropoietin receptor; *Flt3*, fms-like tyrosine kinase 3; *Csf1r*, macrophage-colony stimulating factor receptor; n.s., not significant.

EPOR expression was more restricted in regard to different HSPC populations when compared to the expression of *FLT3*. Almost all of the MEPs ($n=3$ mice) that were analysed expressed *EPOR* ($97.9\% \pm 2.1$; 96/98 cells [98% of total]). This was similar to the findings of Miyamoto *et al.*, as these authors reported that >90% of single MEPs express *EPOR* [116]. *EPOR* was also expressed by $43\% \pm 2.8$ of CMP ($n=3$) (34/79 cells [43% of total]), and this was significantly more than the number of *Epor*⁺ MPPs [$p=0.0238$]. Again, the number of CMPs that were found to express *EPOR* was similar to the number reported by Miyamoto and co-workers [116]. Notably, the proportion of cells expressing *EPOR* within the HPC-2 ($n=3$) compartment was quite variable between mice, as $49.6\% \pm 18.4$ of HPC-2 (20/58 cells [34.5% of total]) expressed detectable levels of the gene (**Figure 3.17B**). *Epor* mRNA was only detected in 1 of 100 *Flt3*^{-/^{lo}} HPC-1 ($n=3$) ($0.98\% \pm 1$; 1/100 cells [1% of total]) and 1 of 96 GMP ($n=3$) ($1\% \pm 1$; 1/96 cells [1% of total]) (**Figure 3.17B**). While the expression of *EPOR* by *Flt3*^{-/^{lo}} HPC-1 has not been previously investigated, these LSK CD150⁻ CD48⁺ cells possess little erythroid potential [34]. Similarly, single GMPs have been shown to lack *EPOR* expression [116]. These data suggest that the single *Flt3*^{-/^{lo}} HPC-1 and GMP that expressed *EPOR* were due to contamination during sorting. Finally, *EPOR* expression was not detected in any LMPPs (0/99 cells) or CLPs (0/94). This was to be expected, as LMPPs have been shown to lack *EPOR* expression [73], and CLPs lack erythroid potential and do not respond to Epo *in vitro* [66].

Csf1r transcripts were most commonly detected in GMPs ($n=3$), as $92\% \pm 3.2$ (91/99 cells; 91.9% of total) of these cells expressed the gene (**Figure 3.17C**). Approximately one third of LMPPs ($n=3$ mice) ($32.6\% \pm 12.7$; 32/97 cells [33% of total]), and $28.3\% \pm 8.4$ of CMPs ($n=3$) (24/81 cells; 29.6% of total) also expressed *CSF1R*. When compared to the MPP population, the number of cells expressing *Csf1r*⁺ cells in the LMPP [$p=0.1$] and CMP [$p=0.1$]

compartments were not significantly different. *Csf1r* transcripts were also detected in $14.8\% \pm 11.7$ of CLPs ($n=3$ mice) (13/90 cells; 14.4% of total). A small percentage of cells within the $Flt3^{-/lo}$ HPC-1 ($n=3$ mice) compartment ($9.9\% \pm 0.9$; 10/101 cells [9.9% of total]) expressed *CSF1R*, and this proportion fell even lower when analysing HPC-2 ($n=3$ mice) ($3.8\% \pm 3.8$; 4/56 cells [7.14% of total]). *CSF1R* expression was not detected in any of the MEPs ($n=3$ mice) analysed (0/96 cells) (**Figure 3.17C**), which is as expected considering the low level of myelomonocytic-associated genes expressed by this population [314].

Levels of HGF gene expression were variable across and within HSPC populations at the single cell level (**Figure 3.18**). When *FLT3* expression was compared across the HSPC compartments there were slight differences in the mean expression levels of this gene (**Figure 3.18A**). $Flt3^{+}$ LMPPs (Mean Ct: 34.32) expressed the highest mean levels of *FLT3* when compared to the other populations, and this level was significantly increased when compared to the $Flt3^{+}$ MPPs population (Mean Ct: 34.76) [$p=0.0066$]. As LMPPs are identified due to their high levels of *Flt3* at the surface, this was not surprising. Interestingly, despite the large difference between the number of cells expressing *FLT3* in the LMPP ($92.8\% \pm 2.04$) and CMP ($21.4\% \pm 2.8$) populations, the mean levels of *FLT3* expressed by these cells were not statistically different [$p=0.1071$] (**Figure 3.18A**). However, there was a decrease in mean expression of *FLT3* in the more mature $Flt3^{+}$ GMP (Mean Ct: 35.4) population when compared to $Flt3^{+}$ CMPs (Mean Ct: 34.74) [$p=0.0299$]. Furthermore, the $Flt3^{+}$ HPC-2 population expressed the lowest mean level of *FLT3*, and the mean level was significantly decreased when compared to the $Flt3^{+}$ MPP population (Mean Ct: 36.24) [$p=0.0039$]. As the HPC-2 population largely contains MegE primed progenitors [34], this was expected (**Figure 3.18A**). Lastly, the mean expression of *FLT3* in the $Flt3^{+}$ MPP (Mean Ct: 34.76) compartment was not significantly different when

compared to the *Flt3*⁺ ST-HSCs (Mean Ct: 35.5) [$p=0.0547$]. There was further variability when comparing *FLT3* expression within HSPC populations. The expression of *FLT3* by single cells in the *Flt3*⁺ MPP, *Flt3*⁺ LMPP, *Flt3*⁺ CLP and *Flt3*⁺ HPC-1 populations differed by as much as 6 doublings, or 64-fold (Ct 32-38) (**Figure 3.18A**). Within other populations (*Flt3*⁺ LT-HSC, *Flt3*⁺ ST-HSC, *Flt3*⁺ HPC-2, *Flt3*⁺ CMP and *Flt3*⁺ GMP), expression of *FLT3* by individual cells differed by up to 4 doublings, or 16-fold.

Mean levels of *EPOR* expression were comparable between the *Epor*⁺ LT-HSCs (Mean Ct: 34.3) and *Epor*⁺ ST-HSCs [$p=0.3161$]. Additionally, while *Epor*⁺ MPPs (Mean Ct: 33.1) expressed higher mean levels of *EPOR* than *Epor*⁺ ST-HSCs (Mean Ct: 34.38), this was not significant [$p=0.2564$] (**Figure 3.18B**). There was also no significant change in the mean expression of *EPOR* when comparing the *Epor*⁺ MPP and CMP (Mean Ct: 34.07) [$p=0.3689$]. However, there was a very significant increase in mean *Epor* mRNA levels when comparing the *Epor*⁺ MEP population (Mean Ct: 31.4) to the *Epor*⁺ CMP population [$p<0.0001$]. Interestingly, a large variation of *EPOR* gene expression was observed amongst single MPPs. Some cells expressed *EPOR* at levels differing by up to 10.82 doublings, or 1,807-fold (**Figure 3.18B**). MPPs have been divided into subpopulations based on their expression of VCAM and *Flt3*, and this has revealed the varying levels of erythroid potential possessed by cells within the MPP population [324]. Additionally, analysis of PU.1 and GATA-1 expression in MPPs using GFP transgenic mice allows for the purification of PU.1⁺ and GATA-1⁺ LSK CD34⁺ that are lymphoid- and MegE-primed, respectively [325]. Thus, it is possible that the large variation in *EPOR* expression reflects the heterogeneous nature of the erythroid potential of the MPP compartment. Finally, the expression of *EPOR* within the *Epor*⁺ LT-HSC, ST-HSC, HPC-2, CMP and MEP populations was less variable when compared to the *Epor*⁺ MPP population, and the

levels at which these single cells expressed *EPOR* differed by up to 6 doublings (64-fold).

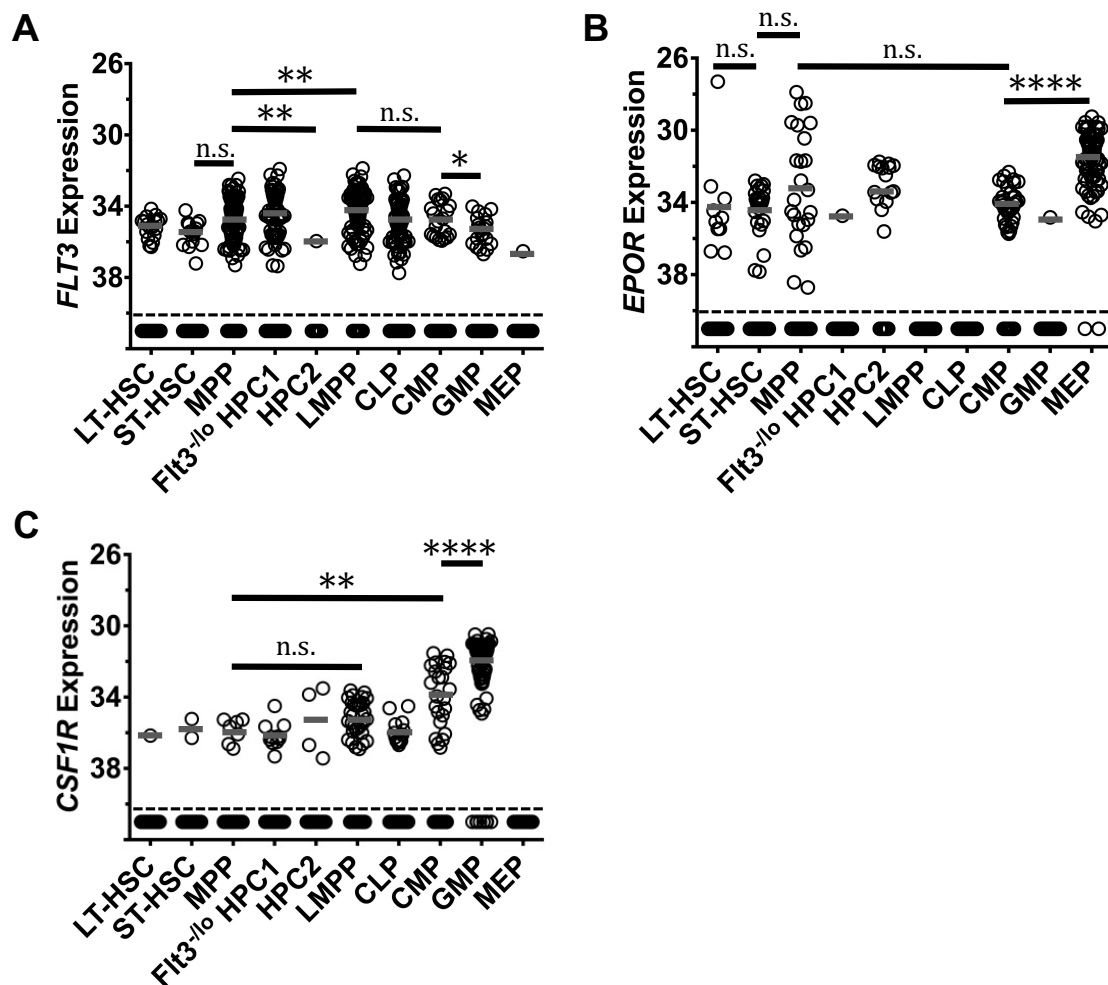


Figure 3.18. Levels of *FLT3*, *EPOR* and *CSF1R* expression within HSPC populations. Expression of (A) *Flt3*, (B) *Epore* and (C) *Csf1r* mRNAs as detected within single cells. The expression levels of target mRNAs are depicted as the threshold cycle (Ct) value and each individual cell is represented by a single data point. Assays were carried out in duplex with a qRT-PCR assay specific for *Actb* transcripts, and reactions that did not give rise to detectable amplification of *Actb* were removed from analysis as this indicated an empty well. Single cells that gave rise to a detectable amplification of *Actb*, but not target mRNAs, are plotted below the dotted lines. Mean values were calculated from all cells that had successful amplification of the target mRNA. *p* values obtained by two-tailed non-parametric student's t-test where; *, *p* < 0.05; **, *p* < 0.01; ***, *p* < 0.001; ****, *p* < 0.0001. LT-HSC, long-term haematopoietic stem cell; ST-HSC short-term haematopoietic stem cell; MPP, multipotent progenitor; HSPC, haematopoietic stem and progenitor cell; HPC, haematopoietic progenitor cell; LMPP, lymphoid-primed multipotent progenitor; CLP, common lymphoid progenitor; CMP, common myeloid progenitor; GMP, granulocyte-macrophage progenitor; MEP, megakaryocyte-erythroid progenitor; *Actb*, β -actin; *Epore*, erythropoietin receptor; *Flt3*, fms-like tyrosine kinase 3; *Csf1r*, macrophage-colony stimulating factor receptor; n.s., not significant.

Mean expression levels of *CSF1R* gradually increased as progenitors committed to a GM fate (**Figure 3.18C**). The mean level at which single *Csf1r*⁺ MPPs (Mean Ct: 35.88) expressed *CSF1R* was lower than the level expressed by *Csf1r*⁺ LMPPs (Mean Ct: 35.17), but this was not significant [*p*=0.0804]. However, when compared to the *Csf1r*⁺ CMP population (Mean Ct: 33.91), *Csf1r*⁺ MPPs expressed significantly lower mean levels of *CSF1R* [*p*=0.0055]. Furthermore, the mean levels of *CSF1R* expressed by *Csf1r*⁺ GMPs (Mean Ct: 31.9) was very significant when compared to the levels expressed by the *Csf1r*⁺ CMP compartment [*p*<0.0001]. The *Csf1r*⁺ Flt3^{-/lo} HPC-1 (Mean Ct: 36.1) and *Csf1r*⁺ CLP (Mean Ct: 35.92) populations expressed the lowest mean levels of *CSF1R*. Considering that the CLP and HPC-1 populations are largely lymphoid-primed progenitors, this was not surprising. Single *Csf1r*⁺ MPPs and Flt3^{-/lo} HPC-1 expressed levels of *CSF1R* that differed by up to 3 doublings, or 8-fold. As cells differentiated towards CMPs and GMPs, expression of *CSF1R* became more variable. Single cells within the *Csf1r*⁺ CMP and *Csf1r*⁺ GMP compartments expressed *CSF1R* at levels differing by up to 5.3 or 4.4 doublings (39.4- or 21-fold), respectively (**Figure 3.18C**).

3.5.2 Analysis of *FLT3* and *EPOR* co-expression within the haematopoietic stem cell and multipotent progenitor compartments

Single cells within the LT-HSC, ST-HSC and MPP compartments expressed detectable levels of *FLT3* and *EPOR* (**Section 3.5.1**). If Flt3L and Epo instruct cells within LT-HSC, ST-HSC and MPP HSPC populations, it is important to investigate whether co-expression of the *FLT3* and *EPOR* genes occurs at this level. This would help to determine whether these factors act on the

same populations of cells, or if there are distinct populations that are primed to respond to either Flt3L or Epo. To investigate the possible co-expression of these genes by single LT-HSCs, ST-HSCs and MPPs, a triplex qRT-PCR assay was designed to detect *EPOR* and *FLT3* expression. Unfortunately, as described in **Section 3.4.3**, the efficiency of the *FLT3* qRT-PCR assay decreased when it was combined in a multiplex reaction with the *ACTB* and *EPOR* assays (**Figure 3.14**). Thus, a new *EPOR* qRT-PCR assay, termed *EPOR-2*, was designed. This time, when designing the assay, an attempt was made to try and minimise the complementarity between the *EPOR-2* qRT-PCR assay and the *FLT3* and *ACTB* qRT-PCR assays by comparing primer, probe and target sequences. The alignment of the *EPOR-2* primers and probe can be seen in **Figure 3.19**. Details of the *EPOR-2* qRT-PCR assay, including primer and hydrolysis probe sequences, are shown in **Table 11**.

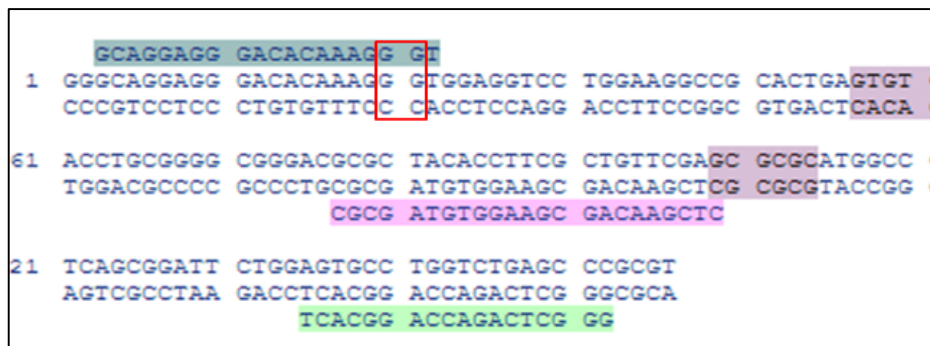


Figure 3.19. Sequence alignment of *EPOR-2* qRT-PCR assay within a region of the *EPOR* gene. The forward primer, reverse primer and probe sequences are shown highlighted in blue, green and pink, respectively. The red box highlights an exon junction. *EPOR*, erythropoietin receptor.

As before, the *EPOR-2* qRT-PCR assay was tested and optimised to ensure efficient amplification of gene targets. Analysis showed that it was specific for *Epor* mRNA, and did not detect gDNA (**Figure 3.20A**). The assay conditions were optimised as before, and the optimum forward primer, reverse primer and hydrolysis probe concentrations were found to be

100nM, 200nM and 50nM, respectively (**Figure 3.20B-D**). When tested using single EPs, the assay efficiently detected single-cell *EPOR* expression (**Figure 3.20E**).

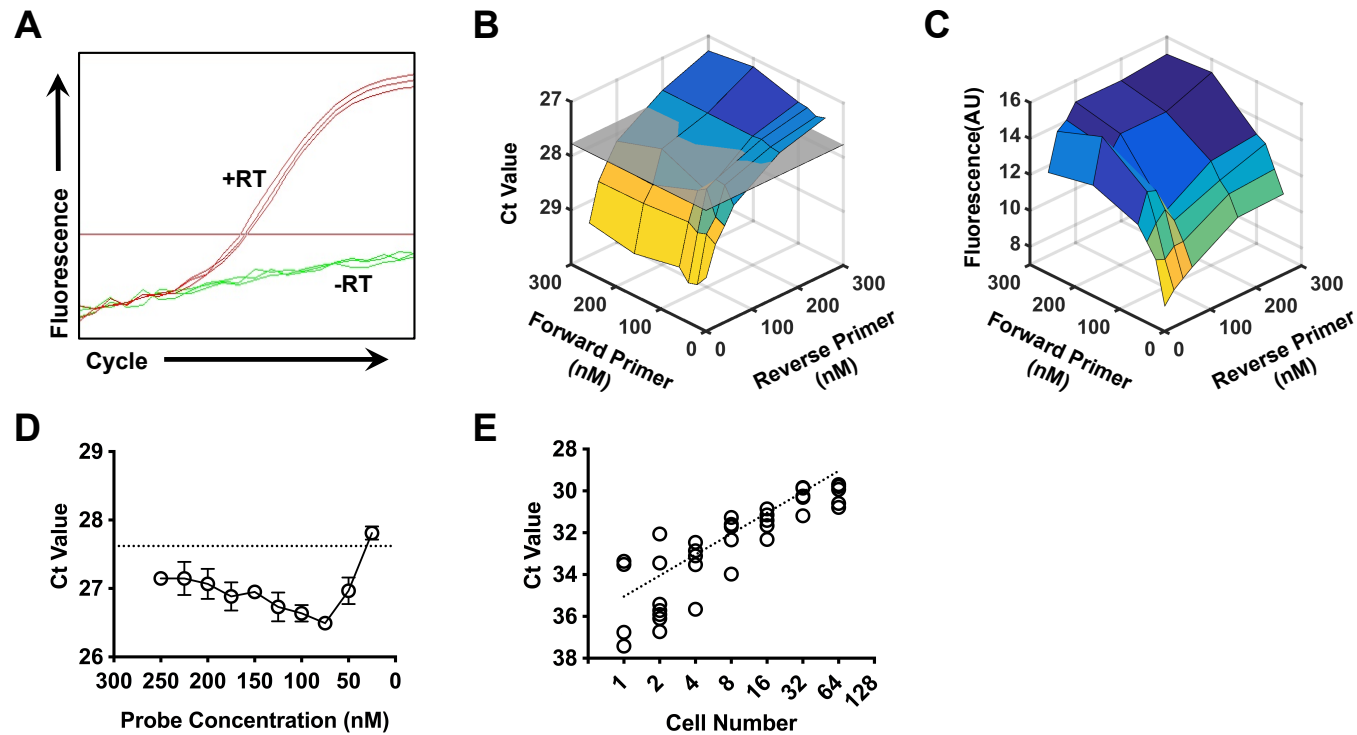


Figure 3.20. Optimisation of *EPOR-2* qRT-PCR assay for detection of single cell gene expression. (A) The *EPOR-2* assay was tested with (+) and without (-) RT to ensure that the assay amplified mRNA (red curves) but not gDNA (green curves). (B, C) Limiting primer concentrations were determined by testing multiple primer concentration combinations. (B) Any sample with a Ct value of >0.5 cycles greater than the Ct value of the reference reaction (300nM forward primer/300nM reverse primer) was disregarded due to a loss of efficiency (below the transparent grey plane). (C) Of the remaining samples, the primer combination with the lowest peak fluorescence value was selected as the limiting reaction. (D) Multiple probe concentrations were tested, and of the reactions with a Ct value that was not >0.5 cycles greater than the Ct value of the reference reaction (250nM hydrolysis probe), the lowest probe concentration was selected as the optimum (below the dotted line). (E) When tested using single cells, the assay clearly amplified expression of *EPOR* by single EPs, and there was an average increase in 1 cycle per cell number doubling (dotted line represents 1 Ct per cell number doubling, for reference). Optimum forward primer, reverse primer and hydrolysis probe concentrations were found to be 100nM, 200nM and 50nM, respectively. gDNA, genomic DNA; RT, reverse transcriptase; Ct, threshold cycle; AU, arbitrary units; EP, erythroid progenitor; *EPOR*, erythropoietin receptor.

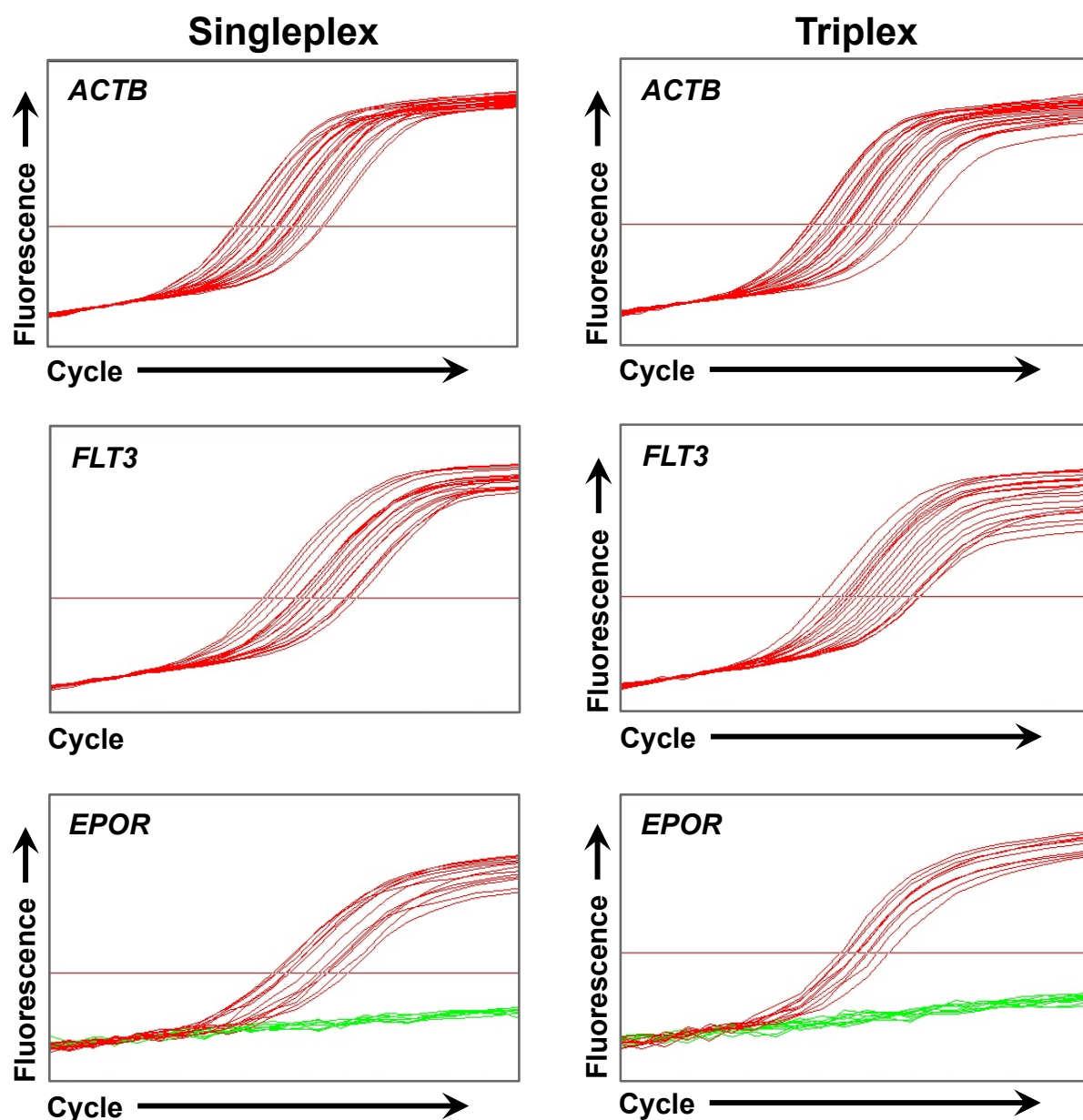


Figure 3.21. Amplification of target transcripts using the *ACTB*, *FLT3* and *EPOR*-2 qRT-PCR assays in singleplex and triplex. Comparison of amplification of *Actb*, *Flt3* and *Epor* in single cells using singleplex reactions and triplex reactions. The amplification curves of all three assays were comparable when comparing singleplex to triplex reactions. Lymphoid-primed multipotent progenitors and erythroid progenitors were sorted to test the efficiency of the *ACTB*, *FLT3* and *EPOR* qRT-PCR assays. Fluorescence is plotted on a log scale. *ACTB*, β -actin; *FLT3*, fms-like tyrosine kinase 3; *EPOR*, erythropoietin receptor.

Table 11: Details of the *EPOR-2* qRT-PCR assay.

<i>EPOR-2</i> qRT-PCR assay	
Forward Primer	5'-GCAGGAGGGACACAAAGGGT-3'
Reverse Primer	5'-GGGCTCAGACCAGGCACT-3'
Hydrolysis Probe	5'-CTCGAACAGCGAAGGTGTAGCGC-3'
Interrogated exon-exon junction	Exon 4 – exon 5
Intron size	604 nt

EPOR, erythropoietin receptor; nt, nucleotides.

To ensure that the new *EPOR* qRT-PCR assay did not interact or compete with the *ACTB* or *FLT3* assays, the three assays were tested in triplex using single cells. As before, varying numbers of LMPPs and EPs were sorted into wells of a PCR plate, and the qRT-PCR assays were tested individually and in triplex (**Figure 3.21** and **Figure 3.22**). When comparing the levels of amplification of *Flt3* and *Epor* transcripts in the triplex reaction to the individual assays, there was no clear difference. The amplification curves of the assays in triplex were also comparable to those seen when singleplex assays were used (**Figure 3.21**). However, the level of *ACTB* expression in the triplex reaction dropped by roughly 3 cycles when compared to the singleplex *ACTB* assay (**Figure 3.22**). As *ACTB* was included as an endogenous positive control to test the presence of cells in the wells of a PCR plate, but not used to quantify gene expression, this was not considered to be an issue.

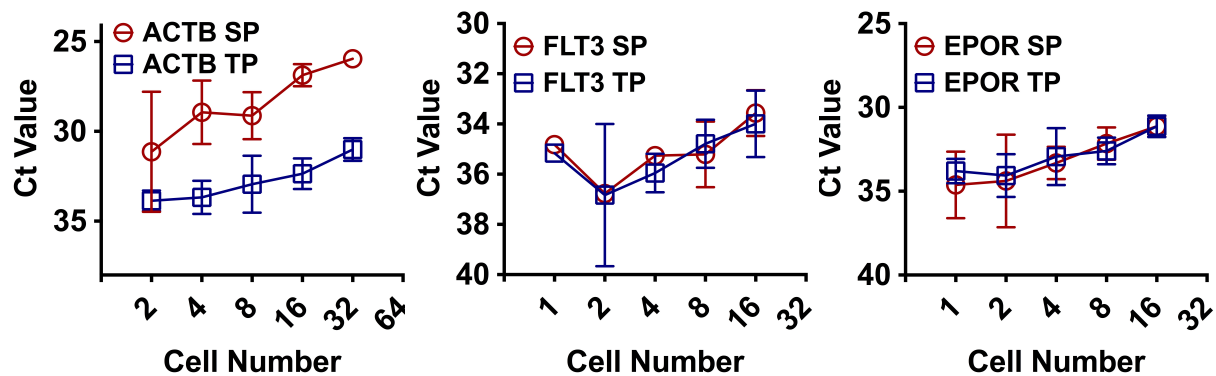


Figure 3.22. Single-cell sensitivity of *ACTB*, *FLT3* and *EPOR-2* qRT-PCR assays in triplex. The *ACTB*, *FLT3* and *EPOR-2* qRT-PCR assays were used in triplex to amplify target genes in varying numbers of LMPPs and EPs. The individual assays were included for comparison to ensure efficiency was not compromised when the assays were combined in the same reaction. Cell number values for *FLT3* and *EPOR* assays are representative of the number of LMPPs or EPs that are present in the sample, respectively. Cell number values for the *ACTB* assay are representative of the number of LMPPs and EPs that are present in the sample. Data represents mean \pm standard mean from at least 3 samples. LMPP, lymphoid-primed multipotent progenitor; EP, erythroid progenitor; SP, singleplex; TP, triplex: *ACTB*, β -actin; *FLT3*, fms-like tyrosine kinase 3; *EPOR*, erythropoietin receptor.

To investigate the possible co-expression of *FLT3* and *EPOR* within the primitive compartments of the BM, 136 single LT-HSCs, 139 single ST-HSCs and 148 single MPPs were purified and assayed using the *ACTB* + *FLT3* + *EPOR* triplex qRT-PCR assay. When analysing the results, there was a clear distinction between cells that expressed the target gene, and those that did not (**Figure 3.23**). None of the LT-HSCs or MPPs that were analysed were found to co-express both *FLT3* and *EPOR* (**Figure 3.24A**). However, co-expression of both *FLT3* and *EPOR* was detected in 2 of the 139 ST-HSC samples during analysis (1.45% of total) (**Figure 3.24**). The data in **Figure 3.24A** was combined with the previous *FLT3* and *EPOR* expression data generated in **Section 3.5.1**.

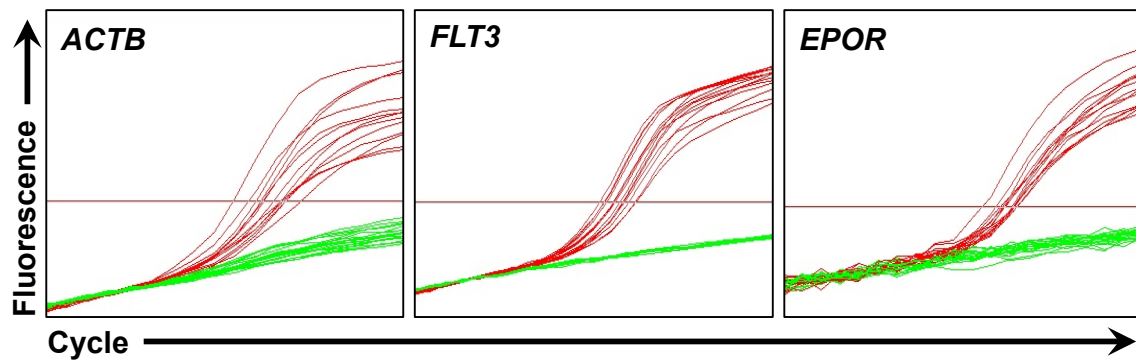


Figure 3.23. Amplification of *Actb*, *Flt3* and *Epor* transcripts in single ST-HSCs using a triplex qRT-PCR assay. The amplification curves are representative of amplification of *Actb*, *Flt3* and *Epor* mRNA in single ST-HSCs using a triplex qRT-PCR assay to investigate *FLT3* and *EPOR* co-expression. Red amplification curves depict single cells that expressed detectable levels of the given gene, while the green amplification curves depict 'no template controls' and single cells that did not express detectable levels of the given gene. As can be seen in the figure, cells expressing these genes were easily identified. Fluorescence is plotted on a log scale. *ACTB*, β -actin; *FLT3*, fms-like tyrosine kinase 3; *EPOR*, erythropoietin receptor; ST-HSC, short-term haematopoietic stem cell.

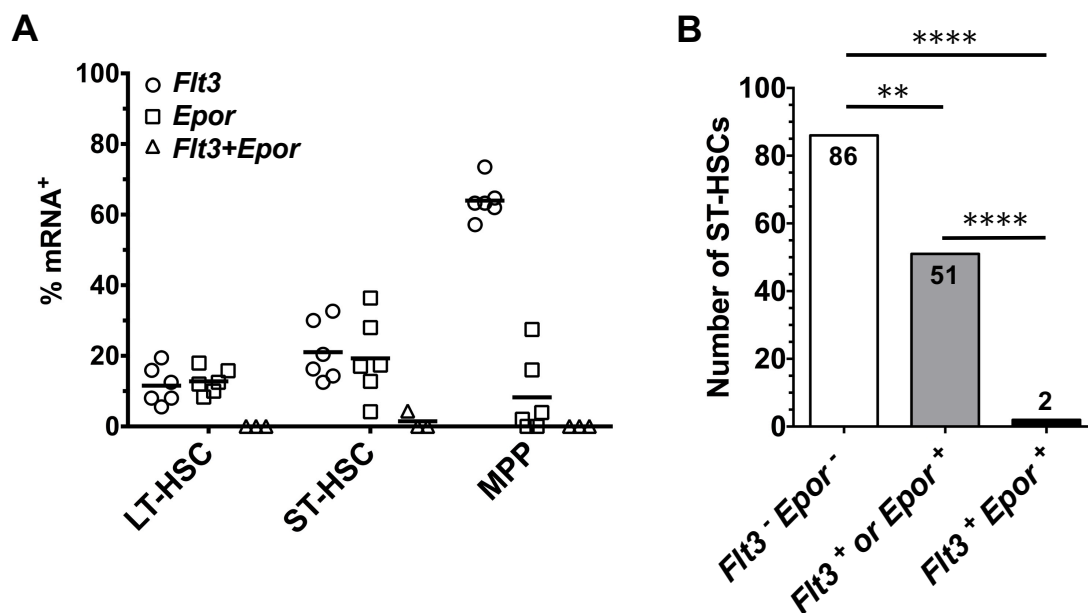


Figure 3.24. Co-expression analysis of *Flt3* and *Epor* transcripts by haematopoietic stem and progenitor cells. (A) The percentages of LT-HSC, ST-HSC and MPP that co-expressed mRNAs for *FLT3* and *EPOR* are compared to the total number of cells that expressed either mRNA. (B) shows the absolute number of ST-HSCs that did not express *FLT3* or *EPOR* (clear column), expressed either *FLT3* or *EPOR* exclusively (shaded column), or co-expressed both *FLT3* and *EPOR* (black column). Reactions were carried out in triplex with an assay specific for *ACTB* expression. Data in (A) are the mean \pm standard error of the values obtained for single cells from 3-6 mice. *p* values in (B) obtained by McNemar's test where; **, $p < 0.01$; ****, $p < 0.0001$. LT-HSC, long-term haematopoietic stem cell; ST-HSC, short-term haematopoietic stem cell; MPP, multipotent progenitor; *ACTB*, β -actin; *FLT3*, fms-like tyrosine kinase 3; *EPOR*, erythropoietin receptor.

One of the ST-HSCs that co-expressed *FLT3* and *EPOR* expressed these genes at levels that were comparable to the levels expressed by cells that exclusively expressed either receptor, while the other cell expressed relatively low levels of *FLT3* and *EPOR* (**Figure 3.25**). Of the remaining ST-HSCs, 86 cells did not express either *FLT3* or *EPOR* and 51 cells exclusively expressed either *FLT3* or *EPOR*. The ST-HSC population mostly contained cells that were *Flt3*⁻ *Epor*⁻, and there was significantly more *Flt3*⁻ *Epor*⁻ ST-HSCs when compared to the number of ST-HSCs that expressed only one of the receptors [$p=0.0037$], or the number of ST-HSCs that co-expressed *FLT3* and *EPOR* [$p<0.0001$] (**Figure 3.24B**). Furthermore, there were significantly more cells that expressed either *FLT3* or *EPOR* when compared to the number of ST-HSCs that co-expressed both genes [$p<0.0001$] (**Figure 3.24B**).

Given the low percentage of co-expression detected in the ST-HSC compartment, it is possible that these positive events were due to the presence of more than one cell in the wells. However, the parameters of the sorting experiments were modified to minimise the chance of sorting doublets. Firstly, the drop envelope was set to 0.5 during sorting. Secondly, as the ST-HSCs were initially sorted into an Eppendorf before being sorted into PCR plates, the secondary single cell isolation sort rate was very slow (from observation). Finally, as cells expressing *FLT3* or *EPOR* represent such a small number of ST-HSCs (approximately 21% and 19%, respectively), if these genes were expressed exclusively, the likelihood of a doublet event being due to a *Flt3*⁺ ST-HSC and a *Epor*⁺ ST-HSC is small (3.99 in 100). Ultimately, it is impossible to determine whether the amplification of *Flt3* and *Epor* in a well was due to impurities during sorting or the presence of a ST-HSC that co-expressed these genes. However, a total of 413 early HSPCs were assayed and there were only 2 instances of *Flt3* and *Epor* amplification in the same well, indicating that even if *FLT3* and *EPOR* co-expression does

occur during early haematopoiesis, it occurs extremely rarely. Thus, these results suggest that *FLT3* and *EPOR* are largely expressed by distinct but separate populations within the LT-HSCs, ST-HSC and MPP compartments.

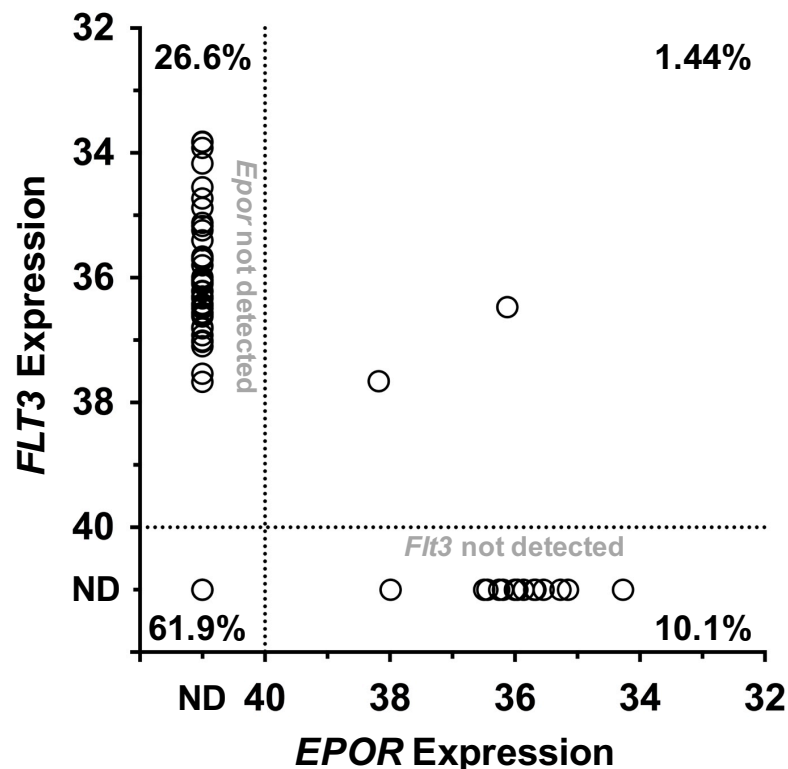


Figure 3.25. Levels of *FLT3* and *EPOR* co-expression by ST-HSCs. Co-expression of *FLT3* and *EPOR* was analysed in 139 individual ST-HSCs. *FLT3* expression was detected in 38 cells, *EPOR* expression was detected in 16 cells, and 87 of these cells did not express detectable levels of either gene. Co-expression of both genes was detected in 2 of 139 cells. Each data point represents a single cell. Assays were carried out in triplex with a qRT-PCR assay specific for *Actb* transcripts, and reactions that did not give rise to detectable amplification of *Actb* were removed from analysis as this indicated an empty well. *Actb*⁺ samples that did not give rise to amplification of the given gene target are plotted arbitrarily below 40 cycles, marked by the dotted lines, and were not considered to express the gene. Data were generated from single cells that were purified from *n*=3 mice. Gene expression is depicted in Ct values. ST-HSC, short-term haematopoietic stem cell; Ct, threshold cycle; ND, not detected; *FLT3*, fms-like tyrosine kinase 3; *EPOR*, erythropoietin receptor.

3.6 Expression of growth factor receptor protein during haematopoiesis

3.6.1 Flt3 and M-CSFR protein expression on the surface of single haematopoietic stem and progenitor cells

Single cell gene expression analysis revealed heterogenic expression patterns of *FLT3*, *EPOR* and *CSF1R* within HSPC populations. However, gene expression does not accurately represent the levels of functional receptor expressed by a cell [326]. In fact, the correlation between mRNA levels and protein in some systems can be as low as 40% [327]. As such, the expression of a HGF receptor gene does not provide an accurate indication of how many cells within a given population are responsive to its ligand. To address this, flow cytometric analysis was used to investigate the expression of HGF receptors on the surface of HSPCs.

Flow cytometry antibodies specific for Flt3 (CD135) and M-CSFR (CD115) were readily available, as they had been used to isolate cells for qRT-PCR assay optimisation and analysis of HGF receptor gene expression. However, sourcing a commercial antibody specific for EpoR that was suitable for flow cytometry proved unsuccessful. Additionally, no fluorescently conjugated anti-G-CSFR (CD114) antibodies could be obtained, so a purified rat anti-mouse antibody was obtained. As most of the antibodies that were used in this study were derived from rat, it was not desirable to use an anti-rat secondary antibody for the detection of G-CSFR. To avoid using a secondary rat antibody, the anti-G-CSFR antibody was conjugated to APC using a Lightning-Link APC kit. The specificity of the antibody was tested.

As specified in **Section 3.4.2**, Ly6G is a surface marker for the identification of granulocytes, and G-CSFR is highly expressed by this population of cells [328]. By staining whole BM cells for G-CSFR and Ly6G the staining profile of the anti-G-CSFR antibody could be compared against BM Ly6G⁺ neutrophils (**Figure 3.26**). By gating Ly6G⁺ and Ly6G⁻ cells and comparing the staining of G-CSFR within these compartments, it was clear that the anti-G-CSFR antibody was not specific for the desired target. There was no clear Ly6G⁺ G-CSFR⁺ population present in the sample, suggesting that the anti-G-CSFR antibody did not mark neutrophils, and therefore did not specifically bind to G-CSFR. Thus, the flow cytometric analysis was limited to the investigation of Flt3 and M-CSFR on the surface of HSPCs. All of the histograms and values for Flt3 and M-CSFR staining in all HSPC populations are depicted in **Figure 3.27**. The LMPP population was identified based on high levels of Flt3 expression. Thus, the histogram depicting Flt3 expression for LMPPs does not show a Flt3 isotype control, as no Flt3^{hi} LMPPs could be gated in the isotype control sample.

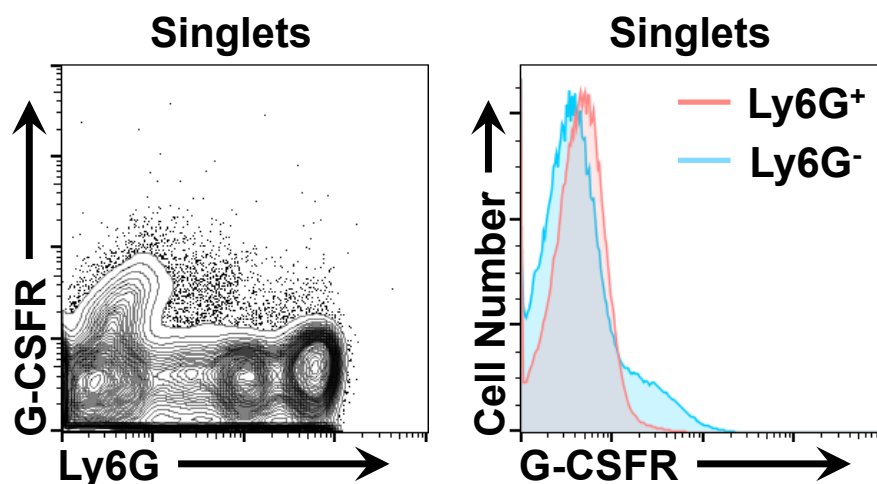


Figure 3.26. Specificity of anti-G-CSFR antibody after APC conjugation. A commercially available purified anti-G-CSFR (CD114) antibody was purchased and conjugated with the fluorophore, APC. Whole BM was stained with the conjugated anti-G-CSFR antibody and an anti-Ly6G antibody to identify granulocytes. As Ly6G stains granulocytes, it was used to determine the specificity of the anti-G-CSFR antibody. The G-CSFR staining was analysed alongside Ly6G staining (left plot), and also within Ly6G⁺ and Ly6G⁻ populations to determine the distribution of G-CSFR staining (right plot). G-CSFR, granulocyte-colony stimulating factor receptor; BM, bone marrow; APC, allophycocyanin.

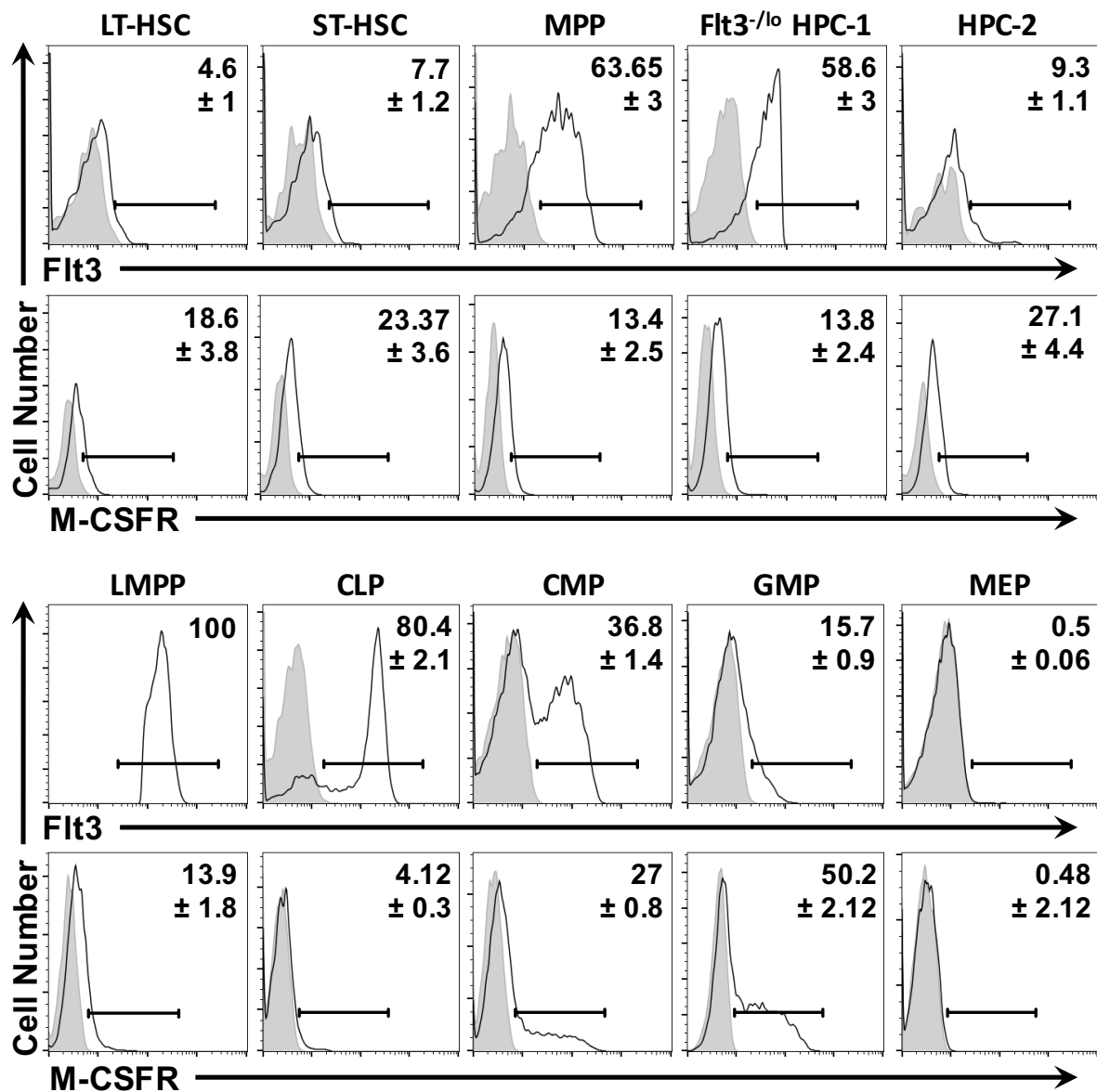


Figure 3.27. Flt3 and M-CSFR expression profiles of haematopoietic stem and progenitor cells. Representative histograms showing the presence of Flt3 and M-CSFR on the surface of haematopoietic stem and progenitor cell populations (solid black line) compared to an isotype control (shaded histogram). Percentages of cells within the given population that stained positive for the HGF receptors are depicted in the upper right corner of each histogram. Data are the mean \pm standard error of values obtained from $n = 3-6$ mice. LT-HSC, long-term haematopoietic stem cell; ST-HSC short-term haematopoietic stem cell; MPP, multipotent progenitor; HPC, haematopoietic progenitor cell; LMPP, lymphoid-primed multipotent progenitor; CLP, common lymphoid progenitor; CMP, common myeloid progenitor; GMP, granulocyte-macrophage progenitor; MEP, megakaryocyte-erythroid progenitor; LSK, Lineage⁻ Sca1⁺ c-Kit⁺; Flt3, fms-like tyrosine kinase 3; M-CSFR, macrophage-colony stimulating factor receptor.

Firstly, the presence of Flt3 protein within the HSC compartment was investigated (**Figure 3.28A**). Low levels of surface Flt3 expression were consistently detected on LT-HSCs ($n=6$ mice) ($4.6\% \pm 1$). There was a slight increase in Flt3 expression within the ST-HSC compartment ($n=6$ mice) ($7.7\% \pm 1.2$) when compared to LT-HSCs, although this was not significant [$p=0.1797$]. For each experiment, the gating was set according to the Flt3 isotype control samples. When setting the gates, the Flt3⁺ values for LT-HSCs and ST-HSCs in the isotype control samples ($n=2$) only accounted for $0.59\% \pm 0.37$ and $0.45\% \pm 0.07$, respectively, indicating that levels of Flt3 observed in the HSC compartment were due to staining of Flt3 protein. The number of cells expressing Flt3 within the HSC compartments was similar to previously published findings. The Jacobsen group has reported that Flt3 is present on the surface of approximately 6% of LSK CD150⁺ CD48⁻ cells [323]. Similarly, Chu *et al.* have reported that Flt3 is present on the surface of <5% of LSK CD150⁺ CD48⁻ cells [329]. While a value was not included in the article, Oguro *et al.* detected a small number of HSC-1 and HSC-2 cells that expressed Flt3 when describing the use of SLAM markers to purify early HSPC populations [34]. Furthermore, when HSCs were stained for IL-7R α , a marker that is known to be absent on the surface of these cells [66], there were no IL-7R α ⁺ cells detected within this compartment. This indicated that the Flt3 signal in the HSC compartment was not due to an artefact of the protocol (**Figure 3.29**).

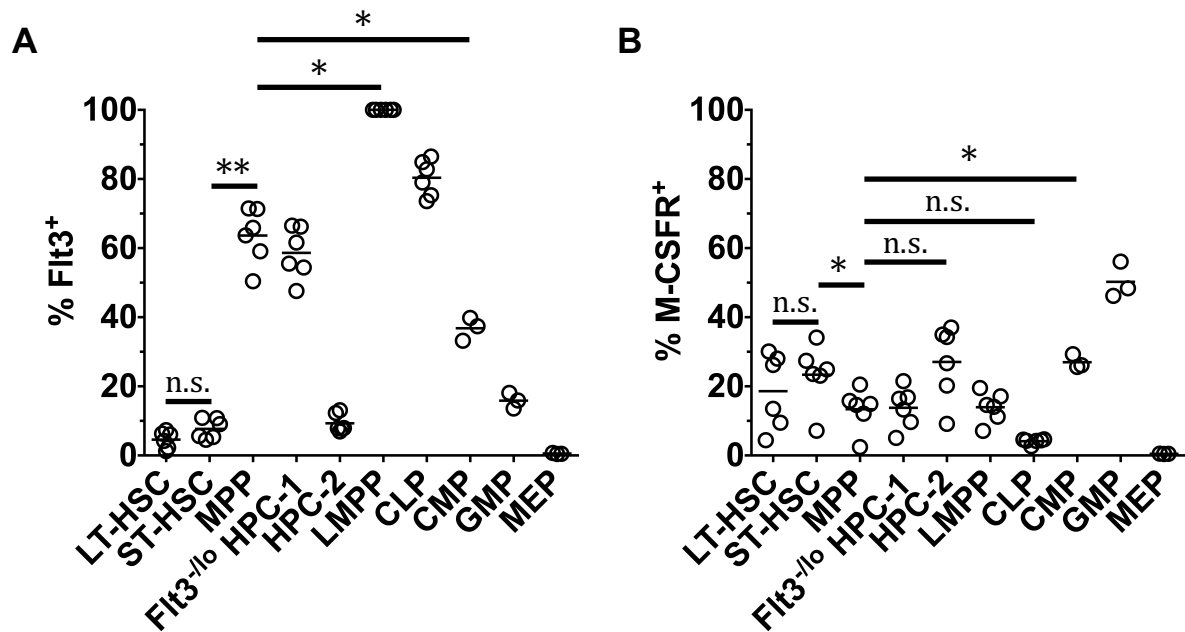


Figure 3.28. Cell surface expression of Flt3 and M-CSFR by haematopoietic stem and progenitor cells. The expression of Flt3 and M-CSFR on the surface of HSPCs was measured by flow cytometry. Data are the mean \pm standard error of values obtained from $n = 3-6$ mice. Each data point represent an individual mouse. p values were obtained by performing two-tailed non-parametric student's t-test where; *, $p < 0.05$. LT-HSC, long-term haematopoietic stem cell; ST-HSC long-term haematopoietic stem cell; MPP, multipotent progenitor; HPC, haematopoietic progenitor cell; LMPP, lymphoid-primed multipotent progenitor; CLP, common lymphoid progenitor; CMP, common myeloid progenitor; GMP, granulocyte-macrophage progenitor; MEP, megakaryocyte-erythroid progenitor; LSK, Lineage⁻ Sca1⁺ c-Kit⁺; Flt3, fms-like tyrosine kinase 3; M-CSFR, macrophage-colony stimulating factor receptor; n.s., not significant.

There was a large and significant increase in the number of cells expressing Flt3 ($63.65\% \pm 3$) when MPPs were compared to the ST-HSC population ($n=6$ mice) [$p=0.0022$] (**Figure 3.28A**). LSK CD150⁻ CD48⁻ MPPs are known to express high levels of Flt3, so this was not surprising [34]. As the LMPP ($n=6$ mice) population is distinguished as Flt3^{hi}, all of the cells in this population were Flt3⁺ ($100\% \pm 0$). Conversely, the number of Flt3 expressing cells was significantly lower in the CMP compartment ($36.8\% \pm 1.4$) when compared to MPPs [$p=0.0022$]. Interestingly, Karsunky *et al.* have observed Flt3 expression on the surface of 50-65% CMPs, and these values differ from the findings reported here [311]. When analysing the remaining populations, Flt3 was found to be expressed by a high proportion of CLPs ($n=6$)

($80.4\% \pm 2.1$), and this was significantly higher when compared to the MPP population [$p=0.0022$]. Within the $\text{Flt3}^{-/\text{lo}}$ HPC-1 ($n=6$) compartment, $58.6\% \pm 3$ of cells were Flt3^+ , while a lower percentage of Flt3 was present on the surface of GMPs ($n=3$) ($15.7\% \pm 0.9$). The percentage of Flt3^+ cells within the CLP and GMP populations shown here are different from what has been previously published. The Jacobsen group has detected Flt3 on the surface of $13\% \pm 4$ of GMPs [322], and it has been reported that 60-70% of CLPs are Flt3^+ [311]. Finally, Flt3 was only detected on a small population of HPC-2 ($n=6$) ($9.3\% \pm 1.1$) and virtually all MEPs were Flt3^- ($n=3$) ($0.4\% \pm 0.1$) (**Figure 3.28A**).

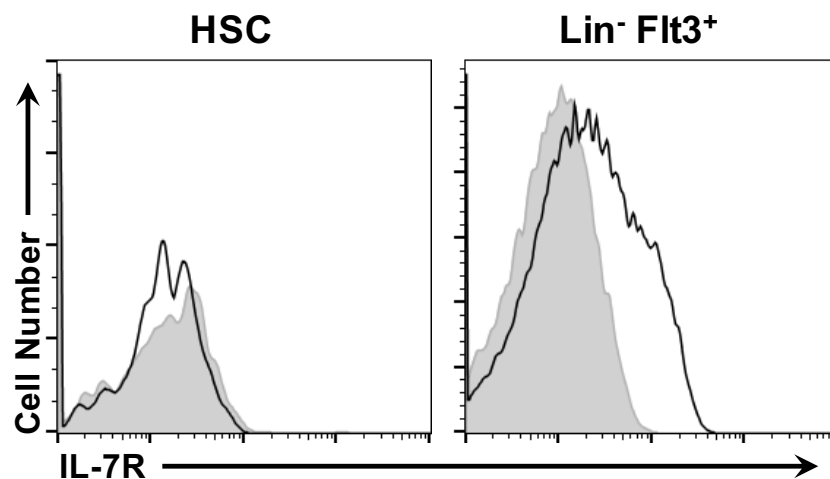


Figure 3.29. Cell surface expression of IL-7R α by BM haematopoietic stem and progenitor cells. Representative histogram showing the absence of IL-7R α on the surface of BM HSCs (LSK CD150⁺ CD48⁻) compared to BM Lin⁻ Flt3⁺ cells. The solid black lines depict staining with the IL-7R α antibody and the shaded histograms depict the isotype control. HSC, haematopoietic stem cell; Lin, lineage markers; Flt3, fms-like tyrosine kinase 3; BM, bone marrow; IL-7R α , interleukin-7 receptor α subunit.

Although *Csf1r* transcripts were only rarely expressed within the LT-HSC and ST-HSC compartments, M-CSFR protein was consistently detected on the surface of a fraction of LT-HSCs ($n=6$ mice) and ST-HSCs ($n=6$ mice) (**Figure 3.28B**). Within the HSC compartment, $18.6\% \pm 3.8$ of LT-HSCs and $23.4\% \pm 3.6$ of ST-HSCs were M-CSFR⁺, and the difference between these

two values was not significant [$p=0.3125$]. Again, the percentage of LT-HSCs and ST-HSCs that stained positive in the M-CSFR isotype controls ($n=2$) were $0.41\% \pm 0.41$ and $0.3\% \pm 0.07$, respectively. There were significantly less MPPs ($n=6$ mice) ($13.4\% \pm 2.46$) expressing M-CSFR when compared to the ST-HSC population [$p=0.0313$]. The number of M-CSFR⁺ Flt3^{-/lo} HPC-1 ($n=6$ mice) ($13.8\% \pm 2.4$) and LMPPs ($n=6$) ($13.9\% \pm 1.8$) was comparable to the number of M-CSFR⁺ MPPs. Although, not a significant when compared to the MPP population [$p=0.0625$], there was a decrease in the number of cells expressing M-CSFR as cells committed to the lymphoid lineage, as only $4.12\% \pm 0.3$ of the CLP ($n=6$ mice) population were M-CSFR⁺ (**Figure 3.28B**). Conversely, there was an increase in the number of M-CSFR⁺ cells as cells differentiated towards the myelomonocytic-granulocytic lineages. When compared to the MPP population, the HPC-2 compartment ($n=6$) ($27.1\% \pm 4.4$) contained significantly more M-CSFR⁺ cells [$p=0.0313$]. Additionally, there was an increase in the number of cell express M-CSFR in the CMP population ($n=3$) ($27\% \pm 0.8$) when compared to MPPs, but this was not significant [$p=0.25$]. Furthermore, the GMP compartment ($n=3$) ($50.2\% \pm 2.12$) contained the highest fraction of M-CSFR⁺ cells when compared to all other populations. Virtually all MEPs ($n=3$) were M-CSFR⁻, which was to be expected given their lack of myelomonocytic-granulocytic potential [67] (**Figure 3.28B**).

For both Flt3 and M-CSFR, there were slight variations when comparing transcript and protein expression. There were more than double the number LT-HSCs and ST-HSCs expressing *FLT3* when compared to the number of cells that expressed Flt3 protein on their surface. Flt3 was detected on the surface of $4.6\% \pm 1$ ($n=6$) LT-HSCs, while *FLT3* expression was detected in $11.6\% \pm 2.19$ ($n=6$) of these cells. Similarly, $21\% \pm 3.4$ ($n=6$) of ST-HSCs expressed *Flt3* transcripts, and $7.7\% \pm 1.1$ ($n=6$) expressed Flt3 on their surface. This suggests that a number

of HSCs express *FLT3* but do not transcribe the Flt3 protein, which is supported by previous studies [312, 323]. Conversely, some populations contained more Flt3⁺ cells than *Flt3*⁺ cells. *Flt3* transcripts were detected in 24.9% ± 5.4 of CMPs (*n*= 3), while 36.8% ± 1.93 of CMPs were Flt3⁺. Additionally, 91.5% ± 1 of CLPs (*n*= 3) were Flt3⁺, but only 66.2% ± 3.8 (*n*= 3) expressed detectable levels of *FLT3* when analysed. For the other populations, the number of cells expressing Flt3 protein or *Flt3* transcripts were similar. For example, 63.65% ± 3 (*n*=6) of MPPs expressed Flt3 on their surface, and 64% ± 2.2 (*n*=6) expressed detectable levels of *FLT3*. Similarly, there isn't a correlation between the expression of M-CSFR and the *CSF1R* gene when comparing gene expression between HSPC populations. *CSF1R* expression was rarely detected in the HSC compartment, but when M-CSFR expression was investigated, 18.6% ± 3.8 of LT-HSCs and 23.4% ± 3.6 of ST-HSCs were M-CSFR⁺. Conversely, almost all of the GMPs analysed expressed detectable levels of *CSF1R* (*n*=3) (92% ± 3.2) but only 50.2% ± 2.12 (*n*=3) were M-CSFR⁺. These results indicated that expression of *FLT3* and *CSF1R* by single HSPCs do not correlate with the presence of Flt3 and M-CSFR on the cell surface.

3.6.2 Investigation of Flt3 and M-CSFR co-expression by haematopoietic stem cells and multipotent progenitors

Both Flt3 and M-CSFR were detected on the surface of LT-HSCs, ST-HSCs and MPPs. As previously described, it was important to determine whether Flt3 and M-CSFR are co-expressed by these cells. As such, the presence of Flt3⁺ M-CSFR⁺ cells within the HSC and MPP compartments was investigated. The gating strategy used for this analysis is shown in **Figure 3.30**.

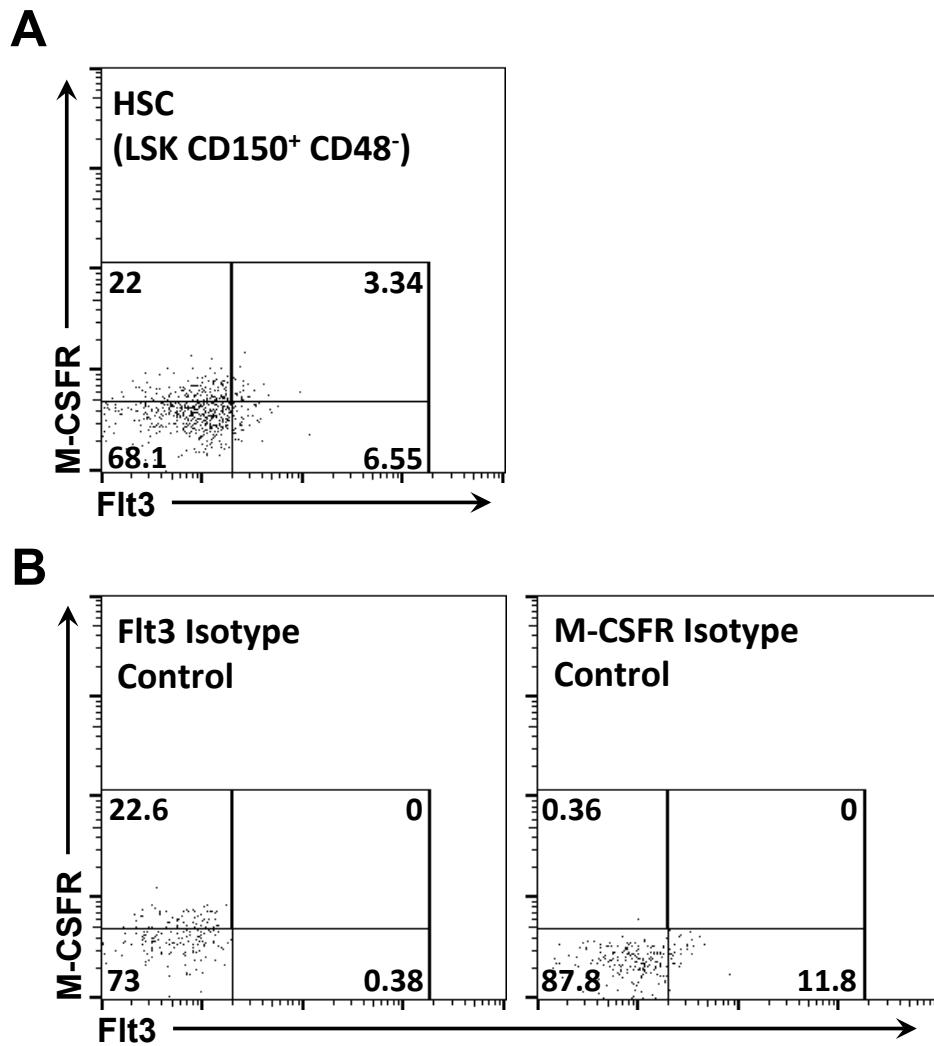


Figure 3.30. Gating strategy used to investigate the co-expression of Flt3 and M-CSFR on the surface of HSCs. (A) Representative flow cytometry plots showing the co-expression of the Flt3 and M-CSFR on the surface of HSCs (LSK CD150⁺ CD48⁻). (B) Staining profiles of HSCs stained with the Flt3 (left) or M-CSFR (right) isotype controls. Values displayed represent the percentage of HSCs within the given gate. HSC, haematopoietic stem cell; LSK, Lineage⁻ Sca1⁺ c-Kit⁺; Flt3, fms-like tyrosine kinase 3; M-CSFR, macrophage-colony stimulating factor receptor.

Co-expression of both Flt3 and M-CSFR was rarely observed when analysing the HSC compartment. Only $1.12\% \pm 0.48$ of LT-HSCs ($n=6$ mice) expressed both genes, and there was a slight, but significant, increase in the number of ST-HSCs ($n=6$ mice) co-expressing Flt3 and M-CSFR ($2.8\% \pm 0.7$) (**Figure 3.31A**) [$p=0.0313$]. Additionally, there was an increase in the percentage of MPPs ($n=6$) ($9.9\% \pm 1.9$) co-expressing the receptors when compared to the ST-HSC compartment (**Figure 3.31A**) [$p=0.0313$]. As Flt3 is only expressed by a small number of

HSCs, co-expression was also calculated as a percentage of Flt3⁺ cells within the LT-HSC and ST-HSC compartments (**Figure 3.31B**). Of the Flt3⁺ LT-HSCs and Flt3⁺ ST-HSCs, 20.1% ± 6.87 and 34.47% ± 5.35 of them co-expressed M-CSFR. The difference between these two groups was not significant [$p=0.0938$].

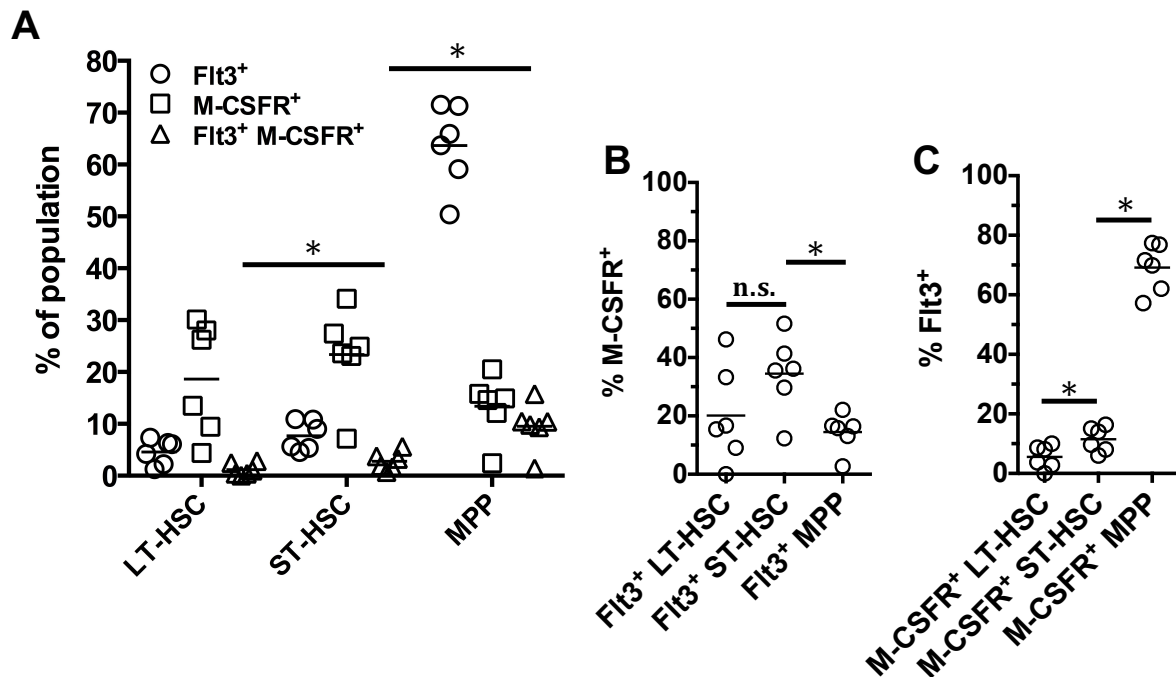


Figure 3.31. Co-expression of Flt3 and M-CSFR on the surface of HSCs and MPPs. (A) The co-expression of Flt3 and M-CSFR on the surface of LT-HSCs, ST-HSCs and MPPs was investigated using flow cytometry. The percentage of cells within each population that express Flt3 or M-CSFR on their surface is included for comparison. **(B)** As Flt3⁺ cells account for such a small proportion of HSCs, the percentage of Flt3⁺ LT-HSCs, ST-HSCs and MPPs that also express M-CSFR on their surface is depicted. **(C)** The percentage of M-CSFR⁺ LT-HSCs, ST-HSCs and MPPs that also express Flt3 on their surface is depicted. Data are the mean ± standard error of values obtained from $n = 6$ mice. p values were obtained by performing two-tailed non-parametric student's t -test where; *, $p < 0.05$. Flt3, fms-like tyrosine kinase; M-CSFR, macrophage-colony stimulating factor; LT-HSC, long-term haematopoietic stem cell; ST-HSC long-term haematopoietic stem cell; MPP, multipotent progenitor; n.s., not significant.

When compared to Flt3⁺ ST-HSCs, there was a decrease in the number of Flt3⁺ MPPs expressing M-CFR (14.46% ± 2.62) [$p=0.0313$]. This decrease can be explained by the large increase in the number of MPPs expressing Flt3 when compared to ST-HSCs. Additionally,

5.55% \pm 1.61 of M-CSFR⁺ LT-HSCs co-expressed both Flt3 and M-CSFR, and this significantly increased to 11.52% \pm 1.71 when analysing the M-CSFR⁺ ST-HSCs population [$p=0.0313$] (**Figure 3.31C**). There was large increase in M-CSFR⁺ MPPs expressing Flt3 (69.17% \pm 3.29) when compared to the ST-HSC population [$p=0.0313$], indicating that as M-CSFR⁺ cells transition from the ST-HSC stage, a large number of them acquire Flt3 expression.

To statistically analyse how often exclusive expression of a single receptor or co-expression of both receptors occurred within the HSC and MPP compartments, the absolute number of cells expressing neither receptor (Flt3⁻ M-CSFR⁻), exclusively expressing one of the receptors (Flt3⁺ or M-CSFR⁺), or co-expressing both receptors (Flt3⁺ M-CSFR⁺) was determined (**Figure 3.32**). This revealed that the majority of cells within both the LT-HSC and ST-HSC compartments were Flt3⁻ M-CSFR⁻. In the LT-HSC compartment, 821 of 1,000 cells were Flt3⁻ M-CSFR⁻, and this was significantly higher than the number of cells that were either Flt3⁺ or M-CSFR⁺ (170 of 1,000 LT-HSCs) [$p<0.0001$] (**Figure 3.32A**). Similarly, there were significantly more Flt3⁻ M-CSFR⁻ cells in the ST-HSC compartment (718 of 1,000 ST-HSCs) than cells that expressed either Flt3 or M-CSFR (254 of 1,000 ST-HSCs) [$p<0.0001$] (**Figure 3.32B**). Only 9 of 1,000 LT-HSCs and 27 of ST-HSCs were Flt3⁺ M-CSFR⁺ cells, and these cells were significantly less frequent than cells that expressed either Flt3⁺ or M-CSFR⁺ [LT-HSC, $p<0.0001$; ST-HSC, $p<0.0001$] (**Figure 3.32A, B**). Most MPPs exclusively expressed either Flt3 or M-CSFR. Of 1,000 MPPs, 577 expressed one of these receptors exclusively and this was significantly more than the number of Flt3⁻ M-CSFR⁻ cells (321 of 1,000 MPPs) in this compartment [$p<0.0001$] (**Figure 3.32C**). As observed in the HSC compartments, cells co-expressing both Flt3⁺ or M-CSFR⁺ accounted for the smallest proportion of MPPs (102 of 1,000 MPPs), and this was significantly less than the number of Flt3⁻ M-CSFR⁻ cells [$p<0.0001$] (**Figure 3.32C**).

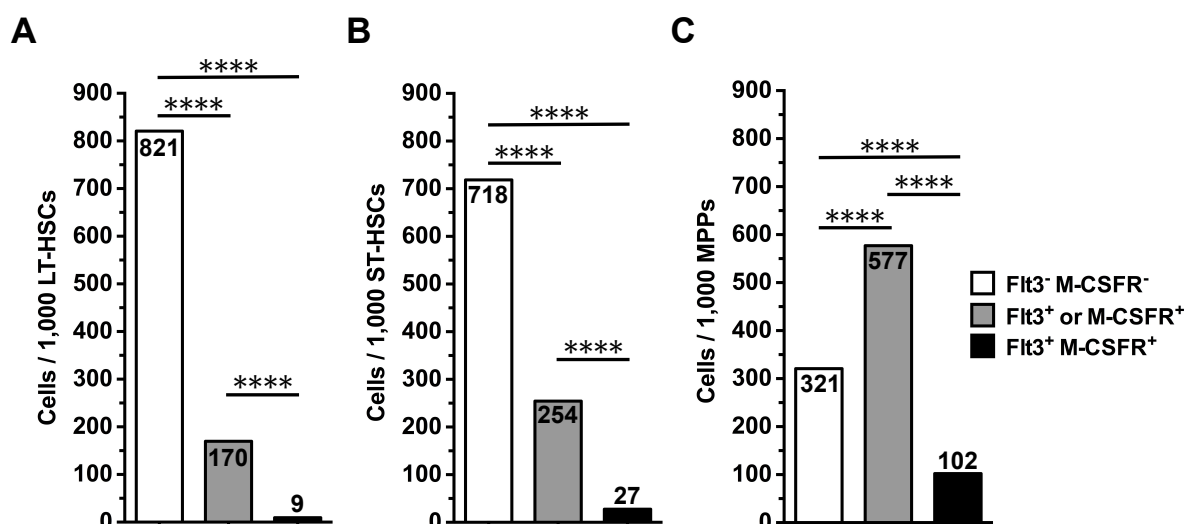


Figure 3.32. Expression of Flt3 and M-CSFR within the LT-HSC, ST-HSC and MPP compartments. The (A) LT-HSC, (B) ST-HSC and (C) MPP populations were divided into cells that lacked expression of Flt3 and M-CSFR (Flt3⁻ M-CSFR⁻, white columns), cells that exclusively expressed either Flt3 or M-CSFR (Flt3⁺ or M-CSFR⁺, grey columns), and cells that co-expressed both receptors (Flt3⁺ M-CSFR⁺, black columns). The absolute number of cells within each of these groups was calculated per 1,000 (A) LT-HSCs, (B) ST-HSCs or (C) MPPs and rounded to the nearest whole number. The graphs represents data from 6 mice, and 2 independent experiments. *p* values obtained by McNemar's test where; ****, *p* < 0.0001. Flt3, fms-like tyrosine kinase; M-CSFR, macrophage-colony stimulating factor; LT-HSC, long-term haematopoietic stem cell; ST-HSC, long-term haematopoietic stem cell; MPP, multipotent progenitor.

3.6.3 Correlation between the presence of Flt3 and the levels of CD150 expressed on the surface of haematopoietic stem cells

HSCs are routinely subdivided into functionally distinct compartments based on the expression of particular surface and cytoplasmic markers. Varying levels of CD150 expression have been used to divide HSCs into CD150 high (CD150^{hi}) myeloid-biased cells and CD150 intermediate (CD150^{int}) cells, which possess less self-renewal capacity and MegE potential in comparison [25, 26]. To investigate if Flt3 or M-CSFR associated with either of these subpopulations, CD150^{hi} and CD150^{int} cells were gated in both the Flt3⁺ and M-CSFR⁺ fractions

of the HSC compartment (**Figure 3.33**). During flow cytometric analysis, very few Flt3⁺ and M-CSFR⁺ cells were present within the LT-HSC and ST-HSC populations (approximately 20-100 cells). This was considered too few for accurate analysis, so the correlation between the presence of Flt3 and/or M-CSFR and the levels of CD150 expression was investigated by analysing the whole HSC compartment (LSK CD150⁺ CD48⁻). Representative plots of CD150^{high} and CD150^{int} expression in Flt3⁺, Flt3⁻, M-CSFR⁺ and M-CSFR⁻ HSC fractions are depicted in **Figure 3.33B**.

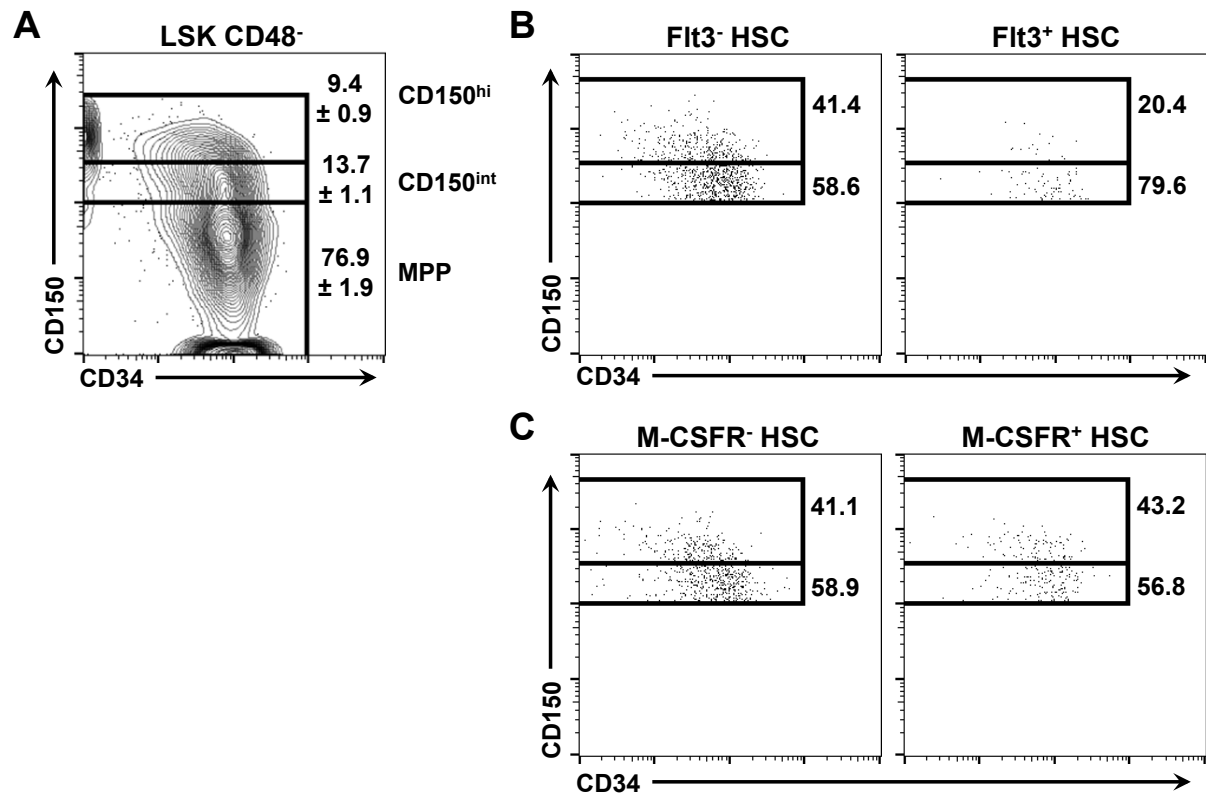


Figure 3.33. Analysis of CD150 expression levels on the surface of HSCs. CD150^{hi} and CD150^{int} cells were gated when analysing Flt3 and M-CSFR expression on the surface of HSCs. **(A)** Gating of CD150^{hi} and CD150^{int} cells within the LSK CD48⁻ population. **(B)** Representative plot showing levels of CD150 expressed on the surface of Flt3⁻ HSCs and Flt3⁺ HSCs. **(C)** Representative plot showing levels of CD150 expressed on the surface of M-CSFR⁻ HSCs and M-CSFR⁺ HSCs. Values displayed represent the percentage of the parent population within the given gate. Data for **(A)** are the mean ± standard error of values obtained from $n = 6$ mice. Flt3, fms-like tyrosine kinase; M-CSFR, macrophage-colony stimulating factor; HSC, haematopoietic stem cell; MPP, multipotent progenitor; LSK, Lineage markers⁻ Sca1⁺ c-Kit⁺.

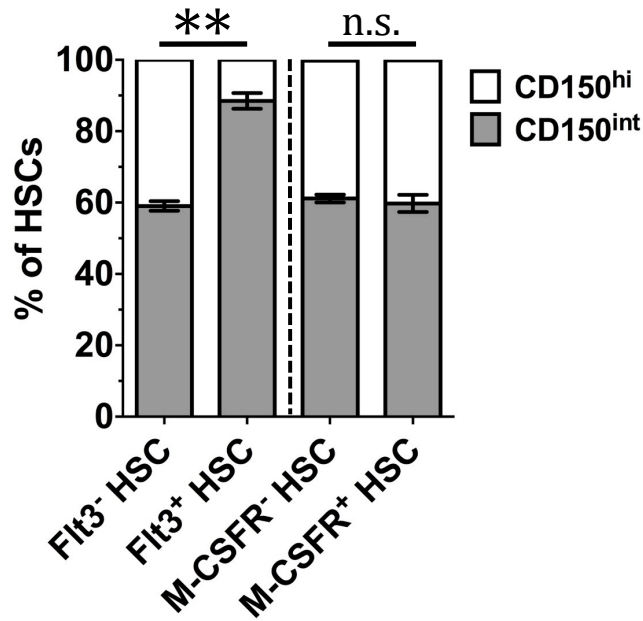


Figure 3.34. Levels of CD150 expressed by Flt3⁺ and M-CSFR⁺ HSCs. Flt3⁺ and M-CSFR⁺ HSCs (LSK CD150⁺ CD48⁻) were analysed according to high (CD150^{hi}) or intermediate (CD150^{int}) levels of CD150 expressed on their surface. Data are the mean \pm standard error of values obtained from $n = 6$ mice, from 2 independent experiments. p values were obtained by performing two-tailed non-parametric student's t-test where; **, $p < 0.01$. HSC, haematopoietic stem cell; LT, long-term; ST, short-term; Flt3, fms-like tyrosine kinase 3; M-CSFR, macrophage-colony stimulating factor receptor; LSK; Lineage⁻ Sca1⁺ c-Kit⁺; n.s., not significant.

Within the LSK CD150⁺CD48⁻ compartment ($n=6$), 88.5% \pm 2.18 of the Flt3⁺ cells expressed intermediate levels of CD150 on their surface, while 59.05% \pm 1.35 of the Flt3⁻ fraction were CD150^{int} in comparison (**Figure 3.34**). This difference was highly significant [$p=0.0022$], indicating an association between the presence of Flt3 on the cell surface and intermediate levels of CD150. On the other hand, there was no significant difference in CD150 distribution when M-CSFR⁺ and M-CSFR⁻ HSCs ($n=6$) [$p=0.5174$] were compared (**Figure 3.34**). Intermediate levels of CD150 expression were detected the surface on 59.76% \pm 2.4 of M-CSFR⁺ and 61.15% \pm 1.08 of M-CSFR⁻ cells. Thus, these findings suggest that Flt3, but not M-CSFR, can be used for enrichment of a functionally distinct subpopulation of LSK CD150⁺CD48⁻ cells.

3.7 Discussion

3.7.1 Flt3, EpoR and M-CSFR mark distinct subpopulations of haematopoietic stem cells and multipotent progenitors and these receptors are rarely co-expressed

Previous studies have provided evidence to suggest that HGF receptors are differentially expressed by cells within the HSC compartment. Epo and M-CSF have been reported to influence lineage fate in some, but not all, HSCs [267, 269] indicating that a subpopulation of HSCs possess the receptors for these factors. Similarly, single cell analysis has shown that the *EPOR* and *CSF3R* genes, and Flt3 protein, are selectively expressed by single HSCs [34, 116, 320, 329]. However, it is largely unclear as to the extent the expression of HGF receptors changes as single HSCs exit a quiescent state and begin to differentiate. To address this, the experiments outlined in this chapter utilised single cell gene expression analysis and flow cytometry to investigate the expression of the above receptors by single HSPCs during early haematopoiesis. The findings presented here show novel patterns of Flt3, M-CSFR and EpoR expression within the LT-HSC, ST-HSC and MPP compartments, and reveal that these receptors are differentially regulated during multipotent cell maturation.

The percentage of cells expressing *Flt3*, *Epor*, *Csf1r* mRNA within each analysed HSPC population is illustrated using the pairwise model in **Figure 3.35**, while the percentage of cells expressing Flt3 and M-CSFR protein within each population is depicted in **Figure 3.36**. It is difficult to map the HPC-1 and HPC-2 compartments to the pairwise model as they represent heterogeneous populations that have not been well characterised [34]. HPC-1 primarily give

rise to GM and lymphoid cells, but have limited MegE potential. Similarly, HPC-2 predominantly produce MegE cells *in vivo*, but are also capable of generating a small number of GM cells and B-lymphocytes. For simplicity, the HPC-1 and HPC-2 populations have been mapped to the pairwise model based on their efficiency in repopulating the GM-lymphoid and MegE lineages, respectively.

Both Flt3 protein and *Flt3* transcripts were detected in the LT-HSC, ST-HSC and MPP compartments. *FLT3* was expressed by $11.6\% \pm 2.19$ of LT-HSCs, $21\% \pm 3.4$ of ST-HSCs and $64\% \pm 2.2$ of MPPs (**Figure 3.17A**), while Flt3 protein was detected on the surface of $4.6\% \pm 1$ LT-HSCs, $7.7\% \pm 1.1$ ST-HSCs and $63.65\% \pm 5$ MPPs (**Figure 3.27A**). These data were consistent with previously published work. The Jacobson group created a *FLT3-Cre* transgenic mouse that contained a loxP-flanked *eYFP* gene (*FLT3-Cre:loxP-eYFP*), and reported that 23% of HSCs (LSK CD150⁺ CD48⁻) were *eYFP*⁺ [323]. The group also detected Flt3 protein on the surface of approximately 6% of HSCs. Other studies have also confirmed the expression of the Flt3 receptor on the surface of a small population of HSCs [34, 329]. However, as these studies did not distinguish HSC subsets using CD34, they did not investigate the expression of the *FLT3* gene and Flt3 protein by LT-HSCs and ST-HSCs. Analysis of the data presented here revealed a slight increase in *FLT3* and Flt3 expression as LT-HSCs differentiate into ST-HSCs (*FLT3*, [$p=0.3125$]; Flt3, [$p=0.0022$]) and a greater increase as ST-HSCs transition to the MPP stage (*FLT3*, [$p=0.0313$]; Flt3, [$p=0.0313$]), supporting proposals that Flt3 is upregulated at the expense of self-renewal ability [19, 20, 323]. Notably, the mean levels of *FLT3* expressed by the *Flt3*⁺ cells within these compartments were not different (**Figure 3.18A**), indicating that the number of cells expressing Flt3, but not the levels at which these cells express *FLT3*, increases as LT-HSCs mature towards MPPs.

EPOR expression was also detected in a small proportion of the HSCs analysed (**Figure 3.17B**). *EPOR* was expressed by $12.8\% \pm 1.46$ of LT-HSCs, and there was a slight increase in the number of *Epor*⁺ ST-HSCs ($19.3\% \pm 4.6$), [$p=0.2188$]. These data were similar to the findings published by Karlsson and co-workers. Karlsson *et al.* have defined HSCs as LSK CD34⁻ Flt3⁻ CD9^{high} based on long-term reconstitution assays, and found that only a small number of these cells expressed *EPOR* (the percentage was not included in the text) [320]. As ST-HSCs differentiated into MPPs, there was a 2-fold, although non-significant, decrease in the expression of *EPOR* ($8.2\% \pm 4.6$) [$p=0.0628$]. Additionally, the levels at which *EPOR* was expressed within the MPP compartment varied greatly when compared to the ST-HSC compartment, giving further indication that regulation of the *EPOR* gene changes during the ST-HSC to MPP transition. Previous studies have also shown a decrease in *EPOR* expression as HSCs mature and support the findings presented here. Lai *et al.* have reported a decrease in *EPOR* expression by the MPP population (LSK Thy1.1⁻) when compared to the HSC population (LSK Thy1.1^{lo}) [324], while Månsson *et al.* have shown that *EPOR* expression is decreased when comparing ST-HSCs (LSK CD34⁺ Flt3⁻) to LT-HSCs (LSK CD34⁻ Flt3⁻) [330].

M-CSFR was expressed by $18.6\% \pm 3.8$ of LT-HSCs and $23.4\% \pm 3.6$ of ST-HSCs, and the number of cells expressing M-CSFR significantly decreased as ST-HSCs matured into MPPs ($13.4\% \pm 2.46$) [$p=0.0313$] (**Figure 3.28B**). Interestingly, *CSF1R* expression was very rarely expressed by cells in the LT-HSC, ST-HSC and MPP compartments despite the presence of M-CSFR protein on the surface of these cells (**Figure 3.17C**). It is possible that the levels of *CSF1R* expressed by these cells were below the detection threshold for the *CSF1R* qRT-PCR assay. Alternatively, HSCs and MPPs may only need to transcribe the *CSF1R* gene rarely to maintain M-CSFR on the surface of these cells. Surprisingly, when comparing the HSC compartment to the LMPP

compartment, which contained fewer M-CSFR⁺ cells (13.9% ± 1.8), *CSF1R* was more regularly detected in LMPPs. As LMPPs are more proliferative than HSCs [73], it is possible that these cells need to continuously transcribe the *CSF1R* gene to maintain M-CSFR on their surface as they divide.

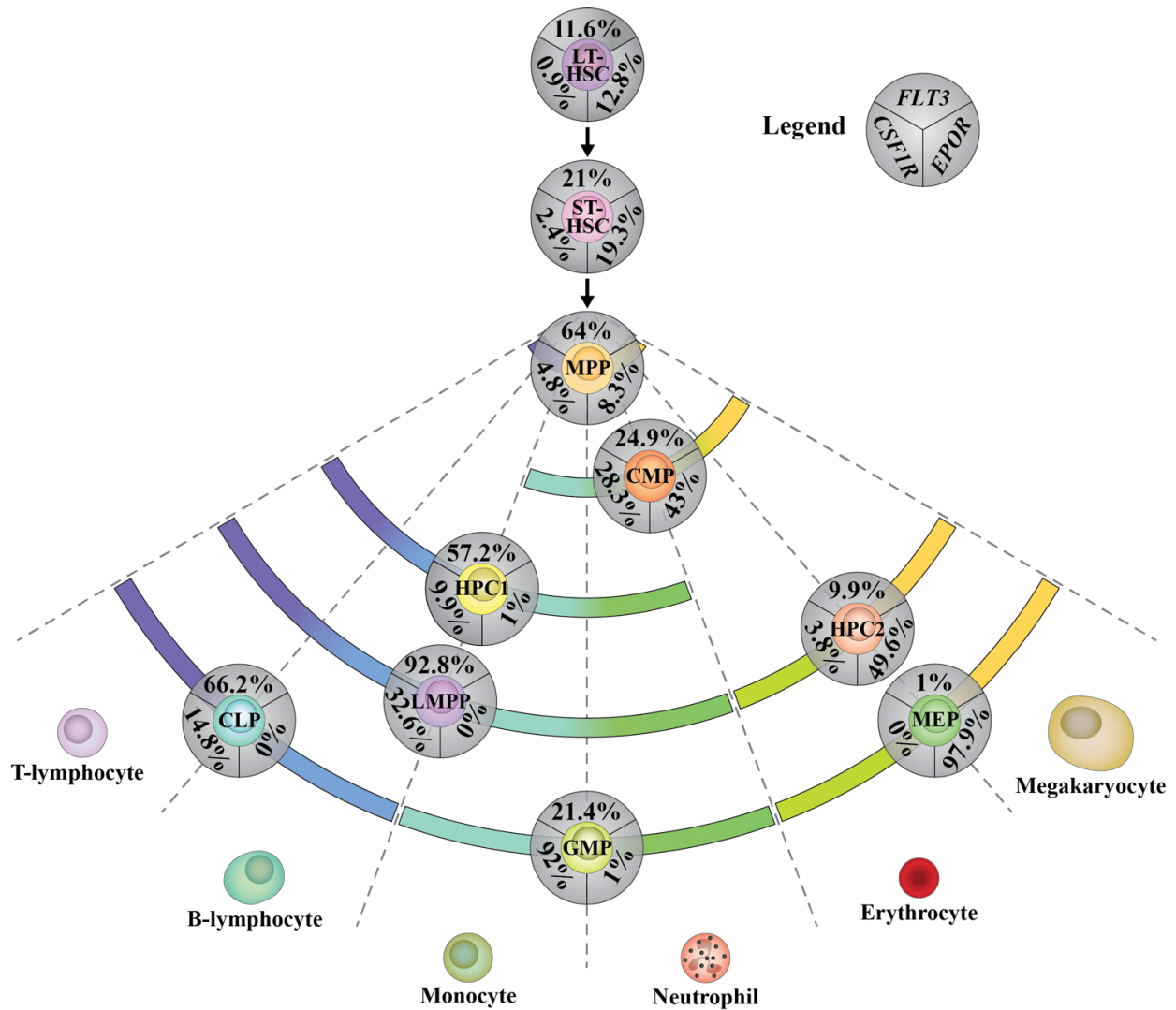


Figure 3.35. Mapping of *FLT3*, *CSF1R* and *EPOR* gene expression to the pairwise model. Values shown correspond to the percentage of cells within the given HSPC population that were found to express *FLT3*, *CSF1R* and *EPOR*. The legend is shown in the top right corner. For these experiments, HPC-1 was isolated as LSK CD48⁺ CD150⁻ Flt3^{-/-}. LT-HSC, long-term haematopoietic stem cell; ST-HSC short-term haematopoietic stem cell; MPP, multipotent progenitor; HSPC, haematopoietic stem and progenitor cell; HPC, haematopoietic progenitor cell; LMPP, lymphoid-primed multipotent progenitor; CLP, common lymphoid progenitor; CMP, common myeloid progenitor; GMP, granulocyte-macrophage progenitor; MEP, megakaryocyte-erythroid progenitor; *EPOR*, erythropoietin receptor; *FLT3*, fms-like tyrosine kinase 3; *CSF1R*, macrophage colony-stimulating factor receptor.

These data revealed that Flt3, M-CSFR and *EPOR* were only expressed by a small number of HSCs and that these receptors are differentially regulated following transition of HSCs to MPPs. To determine if the HSC and MPP subpopulations expressing these receptors overlapped, the co-expression of Flt3, M-CSFR and EpoR by HSCs and MPPs was investigated. First, qRT-PCR analysis revealed that of 136 single LT-HSCs, 139 single ST-HSCs and 148 single MPPs assayed, co-expression of *FLT3* and *EPOR* was only detected in 2 ST-HSC samples. As discussed in **section 3.5.2**, it was difficult to discern whether these events were real or due to contamination of a doublet during sorting. However, the results clearly indicate that co-expression of *FLT3* and *EPOR* rarely occurs during the early stages of haematopoiesis.

The co-expression of Flt3 and M-CSFR protein on the surface of single LT-HSCs, ST-HSCs and MPPs was then investigated using flow cytometry. Flt3 and M-CSFR co-expression was detected on the surface of a very small number of LT-HSCs ($1.12\% \pm 0.48$) and ST-HSCs ($2.8\% \pm 0.7$) (**Figure 3.31A**). Even when represented as a percentage of Flt3⁺ or M-CSFR⁺ cells, these receptors were mostly found to be exclusively expressed by HSCs (**Figure 3.31B, C**). Indeed, analysis of absolute numbers showed that Flt3⁺ M-CSFR⁺ cells represented the smallest fraction of LT-HSCs, ST-HSCs when compared to Flt3⁻ M-CSFR⁻ cells and cells that exclusively expressed one of the receptors (Flt3⁺ or M-CSFR⁺) (**Figure 3.32A, B**). When analysing the MPP population, it was clear that there was a large increase in the co-expression of Flt3 and M-CSFR ($9.5\% \pm 1.9$) when compared to ST-HSCs [$p=0.0313$]. Although Flt3⁺ M-CSFR⁺ were the rarest cells within this population (**Figure 3.32C**), a high proportion of M-CSFR⁺ MPPs co-expressed Flt3 ($69.17\% \pm 3.29$) indicating that M-CSFR expression was commonly associated with the presence of Flt3 at this stage. From these results, it was evident that a rare population of Flt3⁺ M-CSFR⁺ cells exist in the HSC compartment, and that there is a gradual

increase in the co-expression of these receptors as HSCs mature towards the MPP stage. However, with the exception of M-CSFR in the MPP compartment, these receptors are more commonly expressed exclusively rather than together during early haematopoiesis.

CSF1R was only rarely expressed by HSCs, and an antibody for EpoR could not be sourced, so it was not possible to determine the relationship between EpoR/*EPOR* and M-CSFR/*CSF1R* expression. However, given that *FLT3-EPOR* and Flt3-M-CSFR co-expression rarely occurred within the HSC compartment, the findings do not support the presence of single HSCs/MPPs that express all three receptors. Instead, the data indicates that the HSC and MPP compartments contain distinct subpopulations that selectively express HGF receptors. This process of selective expression would sensitise HSCs to particular environmental cues and, therefore, prime them to generate specific lineages when activated by particular HGFs.

Conventionally, HSCs are thought to gradually commit to mature cell fates by transitioning through various intermediate progenitor states. However, previous studies have shown that lineage commitment occurs within the early HSPC compartments. For example, long-term repopulating cells that are committed to mature cell fates have been identified within the LSK CD34⁻ population of the mouse BM. As described in **Section 1.3.3**, Yamamoto *et al.* have enriched for MkRPs, CMRPs and MERPs within this compartment using CD150 and CD41 staining [23]. Similarly, Notta and colleagues have reported that restricted MkPs are primarily found within the CD34⁺ CD38⁻ Thy1⁻ CD45RA⁻ CD49f⁺ HSC compartment of the human BM, and that these cells are rarely generated by CMPs and MEPs [24]. By dividing the MPP, CMP and MEP compartments using CD71 and Mpl, the authors also reported that HSPC compartments are largely comprised of unilineage progenitors, rather than multilineage progenitors, during adult haematopoiesis. Additionally, the existence of lineage-biased

populations, such as MyHSCs and LyHSCs, further support a model whereby HSCs begin to commit towards lineage fates during the early stages of differentiation [9, 29-31, 309, 331]. The selective expression of particular HGF receptors, as seen in **Section 3.5.2** and **3.6.2**, may represent an early stage in this process.

Recent studies that have characterised progenitor populations using single cell analysis also provide evidence for the early lineage commitment of HSPCs. Using lentiviral barcodes to tag individual CMPs, Perié *et al.* monitored the cellular output of CMPs following transplantation into irradiated hosts and reported that few cells possessed oligopotent properties [332]. The CMP compartment was divided into multiple subpopulations that were already committed to the DC, megakaryocyte, erythroid and GM lineages. Paul and co-workers have reported similar findings by analysing RNA sequencing data from 2,730 single index sorted myeloid progenitors (LS⁻K cells) [304]. The group identified 19 transcriptionally homogeneous cell populations in the LS⁻K compartment that could not be defined using conventional CD34 and CD16/32 staining. Within the CMP gating strategy (LS⁻K CD34^{lo} CD16/32^{lo}), progenitors with distinct erythrocyte, megakaryocyte, basophil, monocyte and DC transcriptional profiles were identified, suggesting that commitment towards these lineages occurs upstream of the CMP compartment.

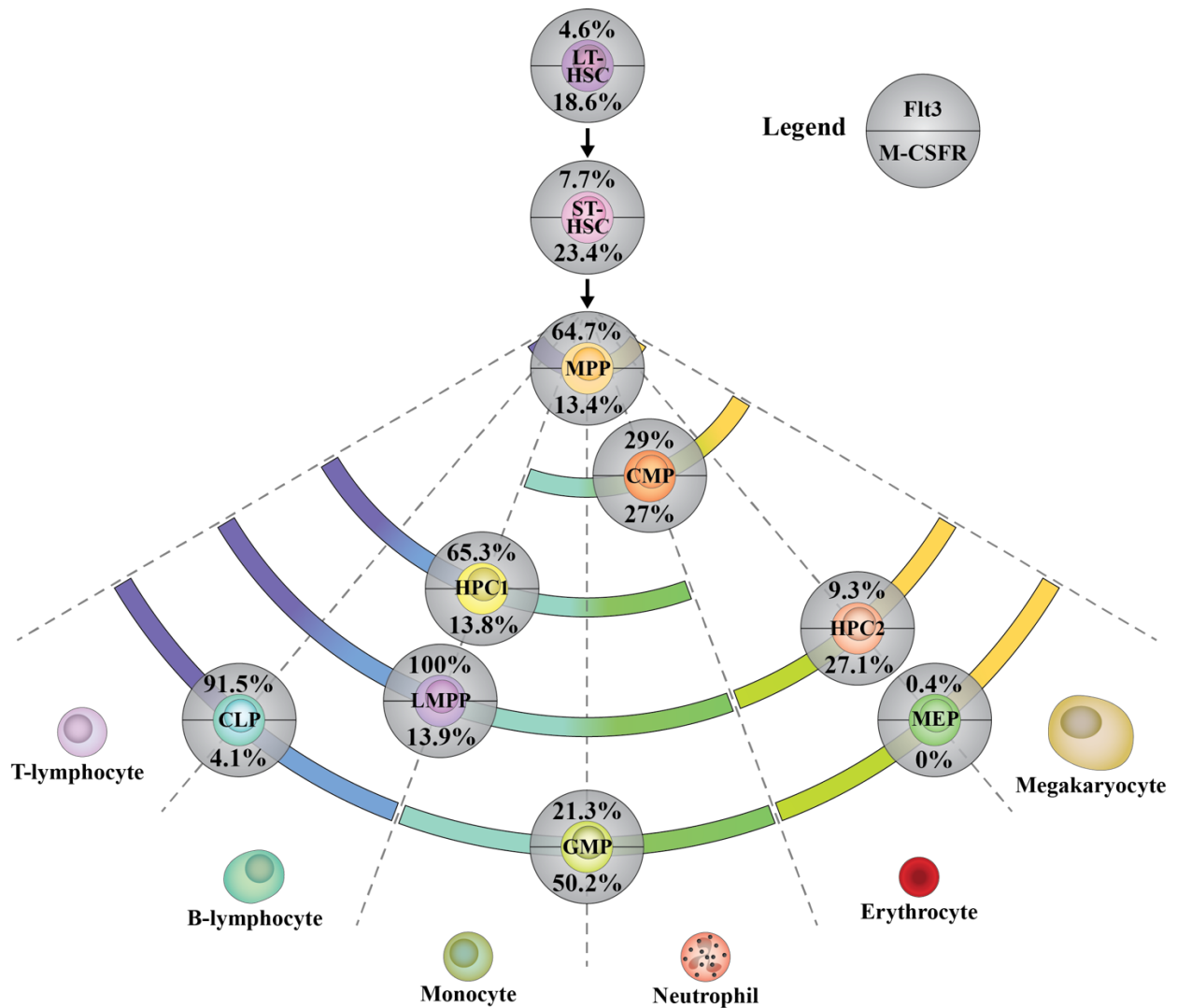


Figure 3.36. Mapping of Flt3 and M-CSFR protein expression to the pairwise model. Values shown correspond to the percentage of cells within the given HSPC population that were found to express Flt3 and M-CSFR protein. The legend is shown in the top right corner. For these experiments, HPC-1 was isolated as LSK CD48⁺ CD150⁻ Flt3^{-/lo}. LT-HSC, long-term haematopoietic stem cell; ST-HSC short-term haematopoietic stem cell; MPP, multipotent progenitor; HSPC, haematopoietic stem and progenitor cell; HPC, haematopoietic progenitor cell; LMPP, lymphoid-primed multipotent progenitor; CLP, common lymphoid progenitor; CMP, common myeloid progenitor; GMP, granulocyte-macrophage progenitor; MEP, megakaryocyte-erythroid progenitor; Flt3, fms-like tyrosine kinase 3; M-CSFR, macrophage colony-stimulating factor receptor.

These reports provide evidence to suggest that HSCs are primed towards myeloid-lineages at an early stage of their maturation. Indeed, MyHSCs are upstream of LyHSCs [25, 26], and studies that have investigated transcriptional lineage priming in HSCs have shown that

myeloid-related genes are enriched in the most primitive haematopoietic compartments prior to onset of lymphoid-associated gene expression. In 2007, Månsson *et al.* used multiplex single cell gene expression analysis to investigate lineage priming in single LT-HSCs (LSK CD34⁺Flt3⁻) and ST-HSCs (LSK CD34⁺Flt3⁻). They reported that of the single LT-HSCs analysed, 37% were MegE primed, 33% were GM primed and virtually none were lymphoid primed. When analysing single ST-HSCs, 23% were MegE primed, 81% were GM primed and, again, lymphoid priming was rarely observed. Similarly, Akashi *et al.* have shown that most single HSCs, isolated as LSK Thy1.1^{lo} cells that retain low levels of rhodamine 123 (Rh), express a high level of MegE- or GM-associated genes but few lymphoid-associated genes [333]. As HSCs progressed to the LSK Thy1.1^{lo} Rh^{high} MPP stage, fewer cells were MegE or GM primed, and lymphoid priming was detected in approximately 30% of cells. These studies might explain the differential regulation of Flt3, M-CSFR and *EPOR* as HSCs make the transition to MPPs. Flt3 was upregulated during this transition, while *EPOR* and M-CSFR were downregulated (**Figure 3.17**). EpoR and M-CSFR may be preferentially expressed in more primitive cells during MegE and GM priming to sensitise the cells to Epo and M-CSF, respectively [267, 269], while Flt3 may be upregulated as the cells transition through a more mature GM-lymphoid primed state, allowing Flt3L to drive myelomonocytic, granulocytic and lymphoid production from this compartment [288].

In support of this, flow cytometric analysis revealed that expression of the Flt3 receptor was strongly correlated with a functional subpopulation of HSCs (**Figure 3.34**). High levels of CD150 expression on the surface of HSCs are associated with increased self-renewal capacity and a bias towards the myeloid lineage [25, 26]. These cells are capable of giving rise to CD150^{int} cells that possess decreased MegE potential and self-renewal capacity. When Flt3⁺

HSCs were divided into CD150^{hi} and CD150^{int} fractions, significantly more Flt3⁺ cells expressed intermediate levels of CD150 on their surface when compared to Flt3⁻ cells [$p=0.0022$]. This finding suggests that Flt3 is upregulated upon transition of HSCs towards a GM-lymphoid primed state (See **section 3.7.2** for further discussion).

Altogether, this study has identified a number of subpopulations within the HSC and MPP compartments based on expression of Flt3, M-CSFR and *EPOR*. These receptors are rarely co-expressed, and are differentially regulated as HSCs begin to mature, suggesting that expression of these receptors mark different stages of lineage priming during early haematopoiesis. Isolation and characterisation of Flt3⁺, M-CSFR⁺ and *Epor*⁺ HSCs will help to determine if there is a hierarchical relationship between these populations and provide further insight into how HGFs regulate early haematopoiesis. Furthermore, identifying the factors that regulate the expression of these receptors in HSCs will likely help to discern how lineage commitment first occurs during haematopoiesis.

3.7.2 Expression of Flt3 within the haematopoietic stem cell compartment is associated with decreased self-renewal capacity

As mentioned in the previous section, Flt3 expression within the HSC compartment was associated with a functional subpopulation of HSCs that express intermediate levels of CD150 on their surface [$p=0.0022$]. In comparison to the more mature CD150^{hi} HSCs, CD150^{int} cells are not as efficient at producing MegE cells, and are less able to self-renew [25, 26]. In line with previous findings [19-21], this result indicates that Flt3 upregulation within the HSC

compartment is associated with a decrease in MegE potential and self-renewal capacity. As such, it is possible that the LSK CD150⁺ CD48⁻ cells expressing the Flt3 receptor represent a population of short-term/transiently repopulating GM-lymphoid-biased progenitors, rather than true HSCs.

The Jacobsen group has performed a number of studies to investigate if self-renewing cells within the HSC compartment express Flt3. In 2001, Adolfsson *et al.* transplanted LSK Flt3⁺ and LSK Flt3⁻ cells into irradiated hosts and compared the multilineage reconstitution of each population [19]. The authors reported that LSK Flt3⁺ failed to support long-term myelopoiesis, and proposed that Flt3 was upregulated as cells lost self-renewal ability and differentiated towards the lymphoid lineage. In a following study, Yang *et al.* added CD34 to the above staining strategy and performed a similar investigation [21]. LSK cells were divided into CD34⁻ Flt3⁻, CD34⁺ Flt3⁻ and CD34⁺ Flt3⁺ fractions and assessed for their ability to reconstitute the haematopoietic system *in vivo*. In agreement with the previous study, the LSK CD34⁺ Flt3⁺ cells were inefficient at reconstituting myeloid cells when compared to the LSK CD34⁻ Flt3⁻ and LSK CD34⁺ Flt3⁻ compartments, and the authors identified these cells as MPPs with limited self-renewal potential. More recently, Buza-Vidas *et al.* have used *FLT3-Cre:loxP-eYFP* mice to investigate if *FLT3* gene expression is initiated in self-renewing cells present in the HSC compartment [323]. Again, the group performed BM transplantation assays and monitored the output of LSK eYFP⁺ and LSK eYFP⁻ *in vivo*. eYFP⁻ cells but not eYFP⁺ cells robustly reconstituted the myeloid lineage in secondary recipients after 6 months, and the Jacobsen group concluded that *FLT3* expression did not mark self-renewing HSCs [323].

The studies performed by the Jacobsen group provide evidence to suggest that *FLT3* and its encoded protein are not expressed by self-renewing LSK CD150⁺ CD48⁻ cells. However, the

experimental approaches used in these studies may not have been sensitive enough to detect a rare population of self-renewing $\text{Flt3}^+/\text{Flt3}^+$ cells [323]. Firstly, the above studies did not assess the ability of LSK $\text{CD34}^- \text{Flt3}^+$ cells to reconstitute irradiated hosts. Additionally, as Buza-Vidas *et al.* used the same number of LSK eYFP^+ and LSK EFYP^- in their transplantation experiments, then unequal numbers of $\text{Flt3}^+/\text{Flt3}^+$ and $\text{Flt3}^-/\text{Flt3}^-$ HSCs would have been compared during the experiments, as $\text{Flt3}^+/\text{Flt3}^+$ cells represent such a small fraction of the HSC compartment. Secondly, self-renewal capacity was evaluated based on the ability of cells to reconstitute the myeloid lineage in all three studies, so the analysis did not consider that Flt3^+ and Flt3^- HSCs may have different lineage potentials. To address these shortcomings, it will be important in future studies to perform single-cell reconstitution assays using single Flt3^+ and Flt3^- LSK $\text{CD150}^+ \text{CD48}^- \text{CD34}^-$ cells in order to comprehensively investigate if Flt3 is present on the surface of a rare subpopulation of self-renewing LSK $\text{CD150}^+ \text{CD48}^- \text{CD34}^-$ cells.

3.7.3 Heterogenic patterns of Flt3 , EpoR and M-CSFR expression identify distinct subpopulations within maturing progenitor compartments.

The expression of Flt3 , EpoR and M-CSFR by haematopoietic progenitors was also investigated to determine if these receptors were differentially expressed at later stages during haematopoiesis. As can be seen from **Figure 3.35** and **Figure 3.36**, HGF receptor gene and protein expression within the HSPC compartments changes as cells mature towards particular cell fates. For example, as cells mature towards the erythroid lineage via the MPP, CMP, HPC-2 and MEP compartments, the number of cells expressing *EPOR* within each subsequent

population steadily increases. Conversely, populations that are primed towards non-erythroid fates contain little to no cells that express *EPOR*. A similar pattern can be seen when considering *CSF1R* and M-CSFR expression. Interestingly, expression of Flt3 protein and its gene followed a biphasic pattern. Only a small number of cells within the HSC compartments expressed *FLT3*, but by the LMPP stage, almost all cells were *FLT3*⁺. The number of cells expressing *FLT3* then decreased upon transition from the LMPP stage to the CLP and GMP compartments. The pattern of Flt3 protein expression is similar, though the decrease in Flt3⁺ cells upon transition from the LMPP to CLP compartment is marginal. As M-CSFR and EpoR are associated with the GM and erythroid lineages, the expression patterns seen in **Figure 3.35** and **Figure 3.36** are unremarkable. However, it is interesting that Flt3 is primarily expressed by progenitors, such as the LMPP. Flt3 is strongly associated with the DC lineage, so it is likely that Flt3 marks progenitors with DC potential (further discussed below). These findings indicate that Flt3 primarily acts to regulate progenitor populations rather than mature cell populations.

Notably, the single-cell analysis of HGF receptor gene and protein expression revealed distinct subpopulations within all progenitor compartments. Most populations could be clearly divided based on the expression of a particular HGF receptor (**Figure 3.17** and **Figure 3.27B**), and some populations expressed highly variable levels of each gene (**Figure 3.18**). The CMP population is a prime example of this. Flt3 and M-CSFR proteins were expressed by 29% ± 3.6 and 27% ± 0.8 of CMPs, respectively, while 43% ± 2.8 of CMPs expressed *EPOR*. Even when comparing *CSF1R* expression levels between individual cells there were disparities, as some *Csf1r*⁺ CMPs expressed levels that were 40-fold higher than other *Csf1r*⁺ CMPs. The data presented here identify a large number of lineage-associated sub-fractions within

haematopoietic progenitor compartments based on the expression of HGF receptors, underscoring the heterogeneous nature of these populations.

As outlined in **Section 3.7.1**, a number of recent studies have indicated that currently defined oligopotent HPC compartments contain a heterogeneous mixture of lineage committed progenitors, rather than a uniform population of oligopotent progenitors [24, 304, 332]. Current evidence also suggests that a number of oligopotent haematopoietic progenitor compartments can be subdivided into lineage committed subpopulations based on the expression of HGF receptors. Within the CMP compartment, DC committed progenitors can be isolated based on their expression of M-CSF and Flt3 [304]. Similarly, the DC potential of the CLP compartment is restricted to the Flt3⁺ compartment [311]. Chi *et al.* have also used Flt3 to isolate unipotent T-lymphocyte progenitors from the preGM population [77]. Finally, the limited megakaryocyte potential of the LSK Flt3^{hi} compartment is restricted to the Mpl⁺ fraction of this population [334].

These studies indicate that the HGF receptor expression patterns identified in this study likely distinguish functionally distinct subpopulations within the Flt3^{-/lo} HPC-1, HPC-2, LMPP, CLP, CMP and GMP compartments. For example, isolation of LMPPs based on the expression of the M-CSFR may allow for enrichment of the GM potential within this compartment, while it is possible that *EPOR* expression within the CMP compartment marks EPs. If these subpopulations identify restricted progenitors, then this would provide further evidence to suggest that lineage commitment occurs in early HSPC compartments, such as the HSC or MPP compartment (see **Section 3.7.1** for further discussion). Isolation and characterisation of the HPC subpopulations identified in this study will be required to confirm this. Furthermore, lineage fate mapping analysis of these populations would help to elucidate

when lineage commitment occurs during haematopoiesis, and how *Flt3*, M-CSFR and EpoR play a role in this process.

3.7.4 The HemaExplorer and BloodSpot databases provide accurate information regarding the expression of *FLT3*, *EPOR* and *CSF1R* during haematopoiesis.

The data extracted from the HemaExplorer and BloodSpot databases revealed that the expression of *FLT3*, *EPOR*, *CSF1R* and *CSF3R* was largely restricted to cells that possessed GM-lymphoid, erythroid, GM and granulocytic potential, respectively, and this was comparable to the data generated from the single cell gene expression analysis (**Figure 3.1**). According to the HemaExplorer and BloodSpot databases, *FLT3* expression was the highest in the CLP and LMPP populations. It was also expressed by LT-HSCs, ST-HSCs, LMPPs, preGMs, CLPs, Pro-B-lymphocytes and ETPs, and to a lesser extent, the GMP population (**Figure 3.1**). The erythroid and megakaryocyte progenitors expressed levels of *FLT3* that suggested amplification of contaminating gDNA, indicating that these cells do not express *Flt3* mRNA. A similar pattern was seen when HSPCs were analysed using single cell qRT-PCR analysis. Both the LMPP and CLP population contained a high number of *Flt3*⁺ cells, reflecting the high levels of *FLT3* expression observed when analysing the databases. *Flt3* was also regularly detected in the LT-HSC, ST-HSC, CMP and GMP compartments, but was absent from the MEP population (**Figure 3.17A**).

Similarly, the patterns of *EPOR* expression observed from single cell gene expression analysis was analogous to the HemaExplorer and BloodSpot databases. As can be seen from the data

extracted from the databases (**Figure 3.1**), *EPOR* was highly expressed in the CFU-E, EP, preCFU-E and MEP populations. *Epor* was also detected in the LT-HSC and ST-HSC compartments. On the other hand, the GMP, CLP and LMPP compartments expressed levels of *EPOR* that suggested amplification of gDNA, indicating that these cells did not express *Epor* mRNA. Although the single cell gene expression analysis used in this study was not performed on CFU-E, EP and preCFU-E populations, almost all MEPs expressed *EPOR* (**Figure 3.17B**), and these cells expressed the highest mean levels of *EPOR* when compared to the other HSPC populations that were analysed (**Figure 3.18B**). On the other hand, *EPOR* expression was not detected in the LMPP or CLP compartments, and was only detected in 1 of 96 GMPs. When analysing the LT-HSC and ST-HSC compartments, *EPOR* expression was detected in a small number of cells, further supporting the accuracy of the databases in regard to *EPOR* expression patterns.

The *CSF1R* gene expression data acquired from the HemaExplorer and BloodSpot databases also accurately reflected the findings from the single cell gene expression analysis. According to the HemaExplorer and BloodSpot databases, GMPs expressed high levels of *CSF1R*, while lower levels were expressed by CLPs and LMPPs. Again, the levels at which *CSF1R* expression was detected within the MegE progenitor populations suggested contamination of gDNA and therefore, that these cells do not express *Csf1r* mRNA. The LT-HSC and ST-HSC compartments expressed slightly higher levels of *CSF1R* than the MEP, so it was unclear whether this was due to contaminating gDNA or low levels of *Csf1r* mRNA expression. When analysing single cells, a high proportion of GMPs were *Csf1r*⁺ (**Figure 3.17C**), and this population expressed the highest mean levels of *CSF1R* when compared to the other HSPC populations (**Figure 3.18C**). A small number of CLPs and LMPPs were found to express *CSF1R*, so this would have

accounted for the low levels of *CSF1R* expression observed when analysing the HemaExplorer and BloodSpot databases. *CSF1R* was not expressed by single MEPs, confirming the findings generated from the database. Lastly, expression of *CSF1R* was only detected in very few single HSCs, so this was in agreement with the slightly increased levels of *CSF1R* expression in LT-HSCs and ST-HSCs when compared to the MEP population in the database values.

Overall, the data presented here indicate that, although the HemaExplorer and BloodSpot databases do not provide information regarding single cell gene expression, they provide an accurate source for data regarding the expression of *FLT3*, *EPOR* and *CSF1R* within whole HSPC populations.

CHAPTER 4: INVESTIGATION OF FUNCTIONAL FLT3 RECEPTOR EXPRESSION WITHIN THE HAEMATOPOIETIC STEM CELL COMPARTMENT

4.1 Introduction

The studies undertaken in **Chapter 3** investigated the expression of the Flt3 and M-CSFR proteins, and the *FLT3*, *EPOR* and *CSF1R* genes by HSPCs to determine the extent to which these receptors are heterogeneously expressed within HSPC compartments, and whether early HSPCs co-express these receptors. Expression of the *FLT3* and *EPOR* genes, and Flt3 and M-CSFR proteins, were detected in subpopulations within the LT-HSC, ST-HSC and MPP compartments. Early HSPCs have been shown to respond to M-CSF and Epo by upregulating lineage-associated genes and acquiring a GM and erythroid fate, respectively [267, 269]. However, while past studies have reported the expression of *FLT3* and its encoded protein within the LSK CD150⁺ CD48⁻ compartment [34, 323, 329], the influence of Flt3L on these cells is unclear.

Tsapogas *et al.* recently reported that a substantial increase in the level of Flt3L *in vivo* causes a dramatic expansion of myelomonocytic, granulocytic and lymphoid progenitors, and a decrease in the number of MEPs and EPs in the BM [288]. Intraperitoneal injection of Flt3L into mice resulted in a rapid reduction of EPs and MEPs, and the kinetics of this response led the authors to hypothesise that Flt3L instructs LSK CD150⁻ CD48⁺ cells towards a GM-lymphoid fate at the expense of a MegE fate [288]. As Flt3 expression is present within the

LSK CD150⁺ CD48⁻ and LSK CD150⁻ CD48⁻ compartments (**Figure 3.27**), Flt3L may drive lineage fate in the most primitive compartments of the BM. In this regard, it is important to determine if these compartments are able to respond to Flt3L.

4.1.1 Role of Flt3 during early haematopoiesis

hHSCs have been shown to reside within the Lin⁻ CD34⁺ CD38⁻ compartment of BM and cord blood [47, 50], and over 90% of Lin⁻ CD34⁺ CD38⁻ hHSCs express Flt3 [335, 336]. Additionally, culture of Lin⁻ CD34⁺ CD38⁻ hHSCs with Flt3L increases their survival *in vitro* [336]. Although the Lin⁻ CD34⁺ CD38⁻ BM and cord blood compartment in humans is heterogeneous, these studies suggest that Flt3L is important for the function of hHSCs. On the other hand, the role of Flt3 during the early stages of murine haematopoiesis is not as clear. In 1994, Zeigler *et al.* were the first to propose that Flt3 was absent from the most primitive mouse haematopoietic compartment of the BM [337]. They isolated Flt3⁺ Lin^{-/low} Sca1⁺ and Flt3⁻ Lin^{-/low} Sca1⁺ BM cells and performed reconstitution assays using these populations. The Flt3⁻ Lin^{-/low} Sca1⁺ cells more efficiently reconstituted irradiated recipients when compared to the Flt3⁺ Lin^{-/low} Sca1⁺ population, and the authors concluded that Flt3 was upregulated as stem cells began to mature. In later studies, both the Jacobsen and Weissman groups used BM transplantation assays to characterise the mouse Flt3⁺ LSK and Flt3⁻ LSK BM populations, and reported that Flt3 expression within the LSK compartment marked a population of stem cells with decreased self-renewal capacity when compared to the Flt3⁻ population [19, 20].

In 2005, the Jacobsen group provided further evidence that Flt3 is absent from mouse HSCs, and also reported that Flt3 is upregulated at the expense of MegE potential [21, 73]. In the

first study, Yang *et al.* characterised the LSK compartment based on Flt3 and CD34 expression, and proposed a haematopoietic hierarchy in which LT-HSCs and ST-HSCs are Flt3⁻, and Flt3 is upregulated as ST-HSCs make the transition to a transiently reconstituting MPP state [21]. Subsequently, Adolfsson *et al.* assessed the ability of LSK subpopulations to give rise to erythrocytes and platelets, and reported that the Flt3⁺ LSK compartment failed to generate MegE progenitors *in vitro* and *in vivo* [73].

Initial studies of Flt3^{-/-} and Flt3L^{-/-} mice also support an association between Flt3 expression, decreased self-renewal, and a loss of MegE potential. In 1995, Mackarechtschian *et al.* generated a transgenic mouse model which lacks Flt3 expression, and reported that these mice show decreased levels of B-lymphocyte progenitors, when compared to WT mice [338]. When transplanted into irradiate hosts, Flt3^{-/-} cells showed a deficiency in T-lymphocyte, B-lymphocyte, monocyte and granulocyte production over 39 weeks. Similarly, McKenna and co-workers have shown that Flt3L^{-/-} mice have less B-lymphocytes, DCs, NK lymphocytes, granulocytes and monocytes when compared to WT mice [339]. The Jacobsen group has also generated Flt3^{-/-} and Flt3L^{-/-} mice, and has characterised them in parallel [321, 340]. In two separate studies, the group reported that Flt3 and its ligand are not required for expansion of myeloid progenitors during steady-state haematopoiesis or following transplantation of whole BM. Notably, HSCs (LSK CD34⁻ [321]/LSK CD150⁺ [340]) were not significantly altered in these mice, or when used to reconstitute primary or secondary hosts, when compared to WT mice. While these studies provided contradicting evidence regarding the role of Flt3 in the generation of myelomonocytic and granulocytic cells, none of these studies suggest a role for Flt3 or its ligand in the maintenance of HSCs, or the generation of erythrocytes and platelets.

Other studies have challenged the association between Flt3 and the loss of MegE potential,

suggesting that multipotent cells express Flt3. In 2006, Forsberg *et al.* observed that Flt3⁺ progenitors gave rise to very small number of platelets when transplanted into irradiated hosts, albeit with lower efficiency than Flt3⁻ cells [341]. Shortly after, Lai *et al.* divided LSK Thy-1.1⁻ Flt3⁺ cells into Flt3^{hi} and Flt3^{low} fractions, and reported that Flt3^{low} cells could generate MEPs *in vivo* [324]. These findings prompted the Jacobsen group to further investigate the ability of LMPPs to contribute to the MegE lineage [334]. They identified a small number (1-2%) of BM LMPPs cells that expressed Mpl, and reported that these cells are capable of producing megakaryocytes and platelets when transplanted into irradiated hosts.

Recent lineage fate mapping experiments also indicate that all lineages, including the erythroid and megakaryocyte lineages, can be derived from a FLT3⁺ multipotent progenitor. Buza-Vidas *et al.* generated a FLT3-Cre:loxP-eYFP transgenic mouse model and showed that over 70% of lymphoid, GM and MegE progenitors were eYFP⁺ [323]. Similarly, Boyer *et al.* created a FLT3-Cre “FlkSwitch” mouse model in which all FLT3⁻ cells that are not derived from a FLT3⁺ progenitor express the red fluorophore, Tomato [342]. Upon upregulation of FLT3, Tomato is irreversibly excised and GFP expression is induced, allowing for GFP labelling of all progeny. With this mouse model, the authors reported that up to 98% of erythroid cells and platelets were GFP⁺, indicating a FLT3⁺ ancestor of these cells. Finally, the Forsberg group has recently reported contradictory findings to other Flt3 knockout studies. The group showed that Flt3^{-/-} mice have impaired development of lymphoid, GM and MegE progenitors [343], further supporting the findings reported by FLT3 lineage fate mapping.

From these studies, there is strong evidence to suggest that MegE potential is not exclusive to cells that lack Flt3 expression. However, the relationship between the upregulation of Flt3 and loss of self-renewal ability may still hold true. Indeed, as was shown in **Figure 3.34**, Flt3

expression within the LSK CD150⁺ CD48⁻ compartment of the BM correlates with a subpopulation of cells that express intermediate levels of CD150 on their surface and have decreased self-renewal ability when compared to CD150^{hi} cells. Thus, it is possible that Flt3⁺ cells in the LSK CD150⁻ CD48⁻ and LSK CD150⁺ CD48⁻ compartments represent multipotent cells that lack self-renewal capacity. This would fit with the model proposed by Tsapogas *et al.* whereby Flt3L instructs MPPs, and not HSCs [288].

4.1.2 Flt3 signalling in haematopoietic stem and progenitor cells

Although Flt3L acts on Flt3⁺ HSPCs to drive GM-lymphoid production [288], the cell-intrinsic mechanisms that drive this process are unknown. Flt3, like M-CSFR and c-Kit, belongs to the class III subfamily of receptor tyrosine kinases and plays a role in the regulation of haematopoietic cell survival, proliferation and differentiation [344-346]. The receptor has an extracellular domain consisting of five immunoglobulin-like motifs, a single-pass transmembrane domain, a juxtamembrane domain, and two intracellular kinase domains. When inactive, it is present on the cell membrane as a monomeric unphosphorylated protein. Binding of Flt3L promotes dimerisation of the receptor and, subsequently, autophosphorylation of tyrosine residues in the juxtamembrane domain [347, 348]. This results in the recruitment and activation of a number of adapter proteins, such as SHC, GRB2 and CBL [349-351]. Stimulation of Flt3 leads to activation of phosphoinositide 3 kinase (PI3K) and Ras pathways [352, 353]. Downstream PI3K signalling is mediated *via* Akt and mammalian target of rapamycin (mTOR), while Ras stimulates the activation of mitogen-activated protein kinase (MAPK) and ERKs. Both pathways mediate protein translation *via* the activation of the

ribosomal protein S6, which is part of the 40S ribosomal subunit [353]. S6 is phosphorylated by ribosomal protein S6 kinases which are activated by mTOR, and to a lesser extent, MAPK [353, 354]. Transcription is also initiated by both the PI3K and Ras pathways and is promoted by the activation of STAT proteins, cyclic adenosine monophosphate response element-binding protein and Elk1 [353].

Given their clinical relevance, many studies have investigated how Flt3 containing internal tandem duplications (Flt3-ITD), which are commonly found in acute myeloid leukaemias, control transcriptional regulation [353, 355-357]. On the other hand, transcriptional targets of canonical Flt3 signalling have not been as well characterised. Furthermore, studies carried out with transfected cell lines indicate that the transcriptional targets of canonical Flt3 and Flt3-ITD signalling do not entirely overlap [358]. In one particular study, Mizuki *et al.* analysed the gene expression of 32Dcl3 cells (a myeloid cell line) transfected with WT Flt3 or Flt3-ITD following Flt3L stimulation [358]. The authors found that Flt3-ITD signalling suppressed expression of *SPI1* and *CEBPA*, while WT Flt3 signalling stimulated expression of these genes. Similarly, sorted Lin⁻ IL-7R α ⁻ Thy1.1⁻ c-Kit⁺ Flt3⁻ mouse BM cells which include MEPs, upregulate *SPI1* and *CEBPA*, and their dendritic cell potential greatly increases, when transfected with human Flt3 [276]. *SPI1* and *CEBPA* encode TFs that are associated with lineage priming and differentiation of HSPCs [125, 359-361]. If these genes are targets of canonical Flt3 signalling, they may mediate the instructional effects of Flt3L.

4.1.3 Aims of chapter

The Rolink group has proposed from studies of Flt3-Tg mice that Flt3L acts on LSK CD150⁻ CD48⁺ cells to drive production of GM-lymphoid cells at the expense of erythrocytes and platelets. However, as can be seen in **Chapter 3**, Flt3 protein is present within compartments upstream of the LSK CD150⁻ CD48⁺ population. The majority of LSK CD150⁻ CD48⁻ MPPs express high levels of Flt3 (See **Figure 3.27** and [34]), so it is possible that Flt3L acts on this population to regulate the generation of GM-lymphoid cells. Furthermore, Flt3 protein was detected within the LSK CD150⁺ CD48⁻ compartment, so Flt3L might also regulate the differentiation of a small proportion of HSCs within the BM.

In the mouse, Flt3L has been long thought to act on maturing progenitors rather than HSCs. This is in contrast to human haematopoiesis, in which Flt3L has been shown to regulate hHSCs survival [336]. However, the findings from **Chapter 3**, and previous reports from Chu *et al.*, indicate that a small number of cells within the murine HSC compartment express Flt3 [329]. If a small population of murine HSCs express functional Flt3 on their surface, then it is possible that Flt3 plays similar roles in both human and mouse haematopoiesis during the early stages of HSPC development. This is important to consider when interpreting results from studies that have used FLT3-ITD mice as a model of human acute myeloid leukaemia. Furthermore, if Flt3 expression does mark a small subpopulation of HSCs within the LSK CD150⁺ CD48⁻ compartment of the mouse BM, then isolation and characterisation of this population will be crucial in improving our understanding of how Flt3 regulates early haematopoiesis. Thus, the purpose of this chapter was to determine at what stage during haematopoiesis do cells express functional Flt3. To investigate this, the response of the early HSPC compartments to

Flt3L was characterised using a number of *in vitro* techniques.

Firstly, the Flt3 signalling pathway in HSCs and MPPs were analysed following a short period of stimulation with Flt3L. This was carried out using flow cytometry to monitor phosphorylation events within the Flt3 signalling pathway in single cells stimulated with Flt3L. Secondly, the potential role of Flt3 in HSPC transcriptional regulation was investigated by analysing the expression of *SPI1* in single cells cultured with and without Flt3L. Finally, to investigate if Flt3 was involved in HSC differentiation and survival, colony forming assays using methylcellulose medium containing Flt3L were utilised to monitor progenitor output.

4.2 Phospho-protein analysis of downstream signalling proteins within the haematopoietic stem cell compartment following stimulation with Flt3L

One of the most direct methods of investigating the presence of functional receptors on the cell surface is to monitor activation and phosphorylation of downstream signalling proteins following receptor-ligand interactions. Western blotting is a commonly used technique for identifying phosphorylated proteins. However, this technique requires a large number of cells for experiments and measures the average expression of a target within a population. Therefore, signalling events within sub-fractions of a population may not be detected. Analysis of phosphorylated proteins using flow cytometry, or phosphoflow analysis, allows for interrogation of signalling events at the single cell level. Thus, phosphoflow was used to monitor the Flt3 signalling cascade in LSK CD150⁺ CD48⁻ cells after culture with Flt3L.

In order to stain for intracellular phosphorylated targets, cells need to be fixed and permeabilised. Recent studies have used methanol and acetone to permeabilise haematopoietic cells for phosphoflow analysis [362-364]. A study by Krutzik and Nolan in 2003 suggests that permeabilisation with methanol provides better staining of some phosphoflow targets when compared to acetone, such as pSTAT1, pERK and pJNK [363]. However, analysis of HSPC-associated cell surface markers after methanol permeabilisation indicates that methanol destroys particular antigens that are crucial for HSPC analysis, including Sca1 and CD150 [364, 365]. On the other hand, acetone has been reported to only affect CD150 antigen integrity [364]. To examine if either organic solvent would allow for accurate analysis of LSK CD150⁺ CD48⁻ and LSK CD150⁻ CD48⁻ cells, the integrity of the cell surface markers used to identify HSPCs in this study was determined following treatment with either methanol or acetone.

Whole BM was stained for the lineage markers CD3 ϵ , CD11b, B220, Gr-1, TER-119, and the HSPC markers, CD48, c-Kit, Sca1, CD150, and CD34. Once the cells were stained, they were fixed using 1.6% PFA (prepared in the lab) for 15 minutes at room temperature and, subsequently, permeabilised for 15 minutes at -20°C using either ice-cold methanol or acetone. Samples were analysed using flow cytometry, and the staining profiles of treated samples were compared to untreated samples to determine if methanol or acetone affected the antigen integrity of any of the cell surface markers.

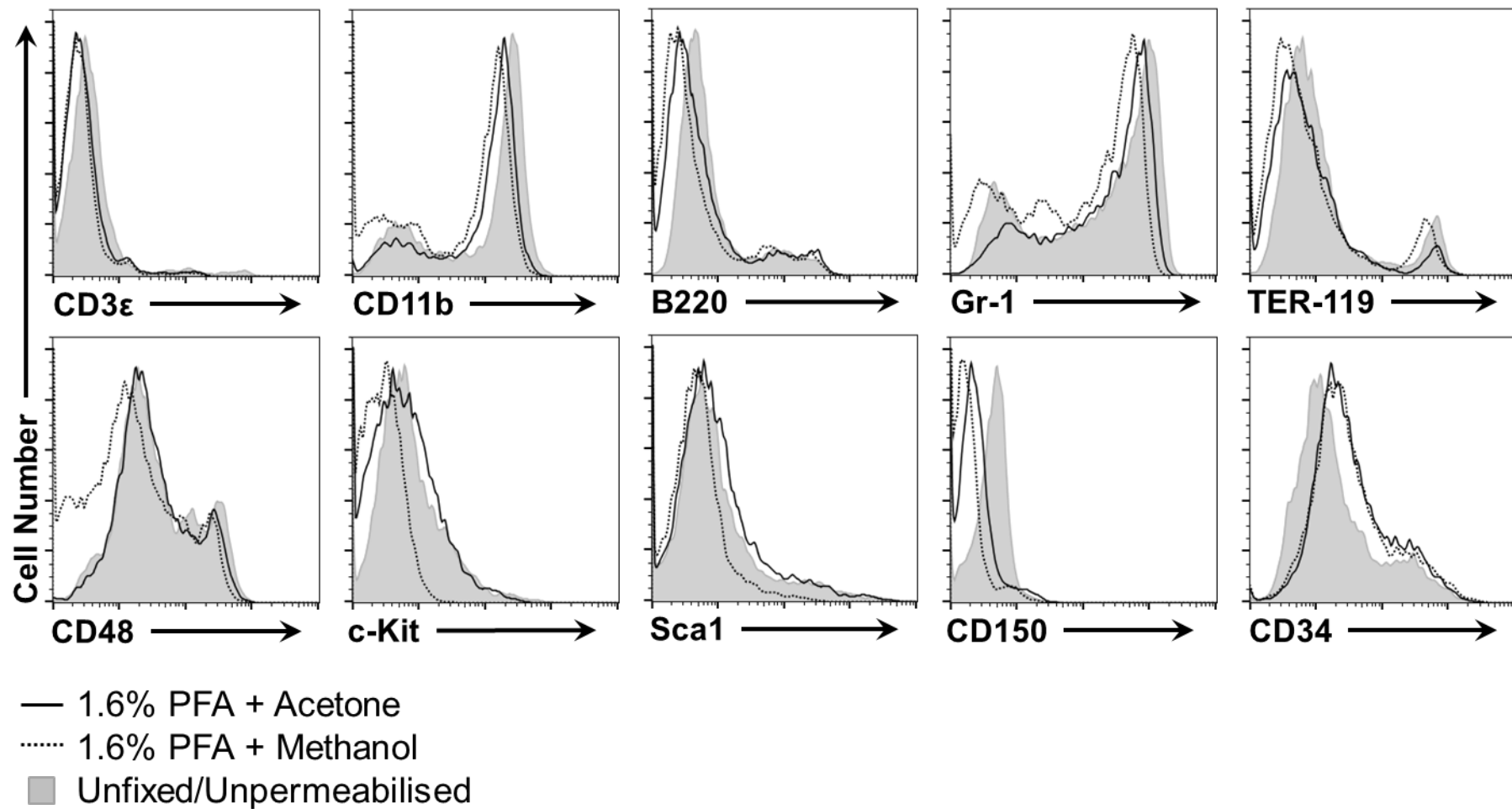


Figure 4.1. Verification of cell surface marker antigenicity following fixation and permeabilisation of cells. Bone marrow cells were stained with antibodies specific for CD3ε, CD11b, B220, Gr-1, TER-119, CD48, c-Kit, Sca1, CD150, and CD34, and then fixed for 15 minutes with 1.6% PFA at room temperature. Cells were then either permeabilised with ice-cold acetone (solid black lines) or ice-cold methanol (dotted black lines) for 15 minutes at -20°C before being analysed. Untreated cells are included for comparison (shaded histograms). PFA, paraformaldehyde.

Compared to untreated samples, methanol treatment resulted in a loss of c-Kit staining and a decrease in the levels of Sca1 and CD150 staining (**Figure 4.1**). However, CD3ε, CD11b, B220, Gr-1, TER-119, CD48, and CD34 staining was unaffected. Acetone treatment preserved staining for all markers except CD150 (**Figure 4.1**). Interestingly, acetone treatment also affected the fluorescence of the anti-CD48 APC-Cy7 antibody. When analysing the fluorescence of the APC-Cy7 antibody, a large signal was observed in the APC channel and this could not be resolved through compensation (**Figure 4.2**). The level of fluorescence detected in the APC channel suggested that the permeabilisation treatment had caused the APC-Cy7 complex to unconjugate, which prevented the use of the anti-CD48 APC-Cy7 antibody together with the anti-CD34 APC antibody when performing phosphoflow. To overcome this, CD48 expression was measured using a FITC conjugated antibody, and this antibody was included with the lineage cocktail on the FITC channel, for all future phosphoflow experiments.

Although the staining of CD150 following acetone treatment was greatly reduced in samples of whole BM (**Figure 4.1**), it was not clear whether the remaining fluorescence was significant enough to distinguish between CD150⁺ HSCs and CD150⁻ MPPs within the LSK CD48⁻ compartment. To investigate this, the phosphoflow protocol was repeated using whole BM cells stained for all HSPC surface antigens. Samples were fixed and permeabilised, and then analysed to determine the level of CD150 staining within the LSK compartment alongside an untreated control that was prepared from the same BM.

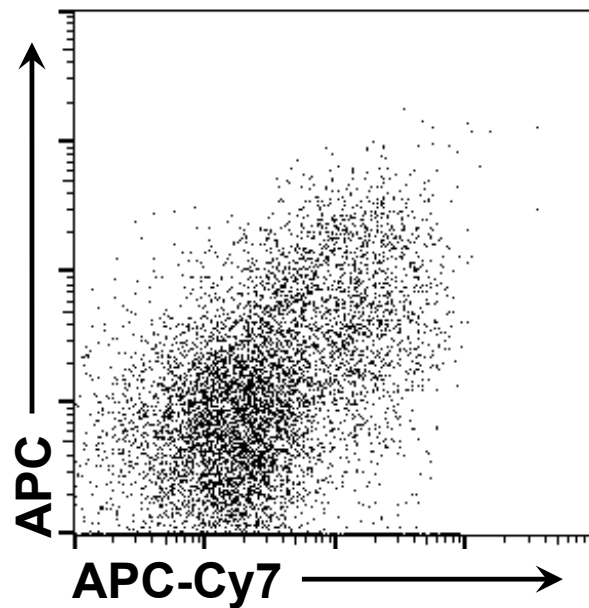


Figure 4.2. Degredation of APC-Cy7 following fixation and permeabilisation of cells. Whole bone marrow cells were stained for CD48 with an APC-Cy7 antibody. The cells were then fixed with 1.6% paraformaldehyde and permeabilised with ice-cold acetone. Analysis of the APC-Cy7⁺ cells revealed that there was an increased amount of signal within the APC channel. Compensation did not resolve the issue, indicating that the APC-Cy7 antibody was not suitable for use when using acetone as a permeabilisation agent. APC, allophycocyanin

As before, when the two samples were compared, the CD150 staining of whole BM was decreased in the fixed and permeabilised sample (**Figure 4.3C**). Despite this, the CD150 staining was bright enough to distinguish LT-HSC, ST-HSC and MPP populations within the LSK compartment in the treated sample (**Figure 4.3B**). Furthermore, all populations gated in the fixed and permeabilised sample represented comparable fractions of BM singlets when compared to the untreated sample. In the untreated sample, 0.0044%, 0.0094% and 0.023% of all BM singlets were LT-HSCs, ST-HSCs and MPPs, respectively. Similarly, in the fixed and permeabilised sample, 0.0051%, 0.0111% and 0.026% of all BM stained positive for the LT-

HSC, ST-HSC and MPP immunophenotypes, respectively. The results indicated that, following fixation and permeabilisation, CD150 antigen integrity is maintained within the LSK compartment. The reason for this is unclear, but may be explained by differences in splice variants or glycosylation patterns of CD150 [366]. Nonetheless, these results confirmed that LT-HSCs, ST-HSCs and MPPs could be successfully distinguished when using the phosphoflow protocol.

Once the fixation and permeabilisation treatments for the protocol were chosen, downstream signalling proteins of the Flt3 receptor were considered as a target for monitoring Flt3 stimulation. Both the Ras and PI3K pathways converge by promoting phosphorylation of the ribosomal protein S6 *via* activation of p90 and p70 S6 kinases, respectively [353]. By monitoring a protein within both main Flt3 signalling pathways, analysis may benefit from an increased number of targets due to signal amplification, and an increased level of fluorescence.

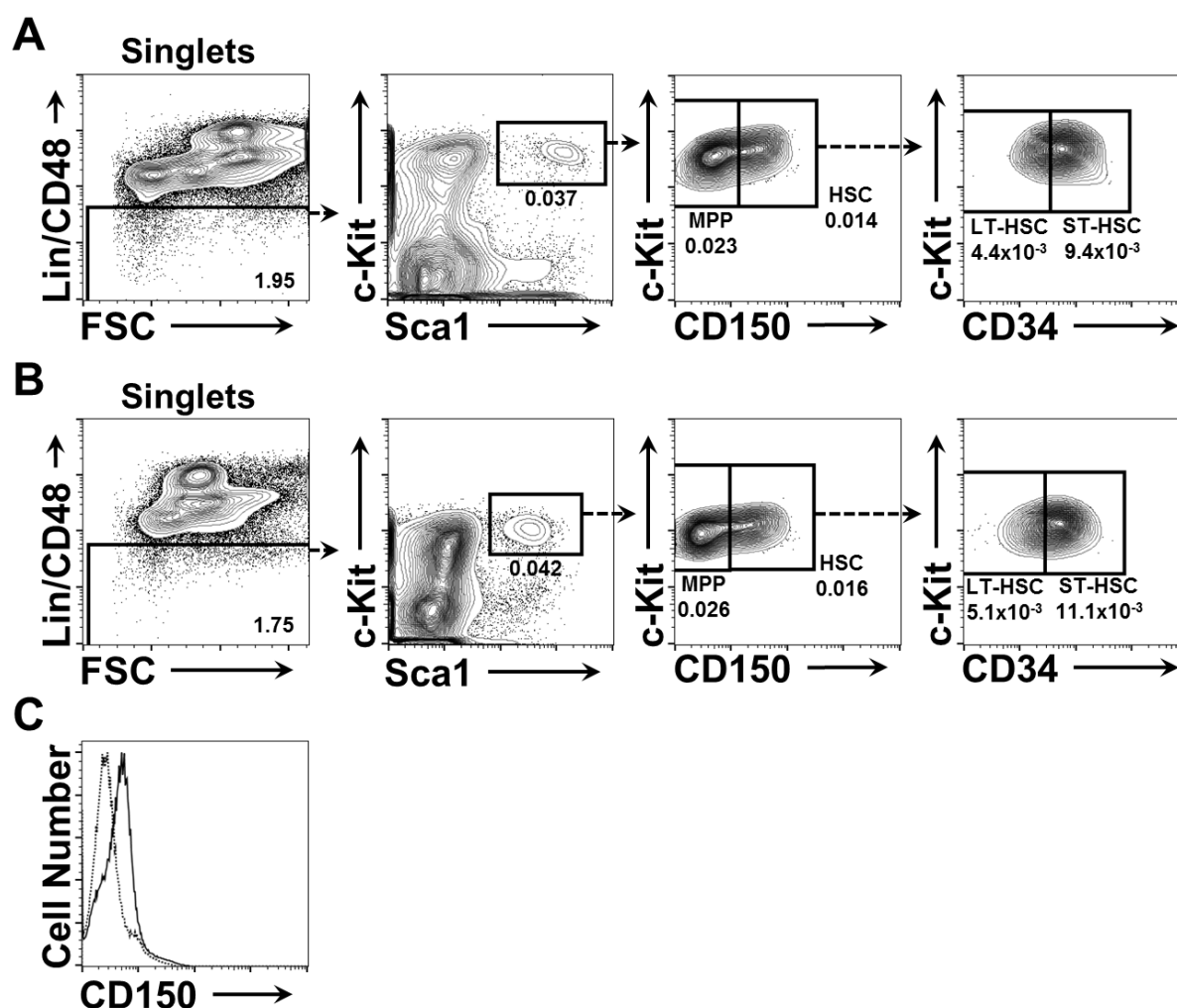


Figure 4.3. Verification of HSPC staining protocol following fixation with PFA and permeabilisation with acetone. Bone marrow cells were stained with an antibody panel for the analysis of LT-HSCs, ST-HSCs and MPPs. Half of the sample was fixed for 15 minutes with 1.6% PFA at room temperature and then permeabilised with ice-cold acetone for 15 minutes at -20°C , while the other half was left untreated. Both the **(A)** untreated and **(B)** fixed/permeabilised cells were then analysed to compare staining of LT-HSCs, ST-HSCs and MPPs. All three populations represented comparable fractions of BM singlets in both samples. Despite the similar levels of CD150 staining within the LSK compartment between **(A, B)** both samples, CD150 staining was decreased when comparing the expression of CD150 by **(C)** whole bone marrow cells in the fixed/permeabilised sample (dotted black line) when compared to the untreated sample (solid black line). LT-HSC, long-term haematopoietic stem cell; ST-HSC, short-term haematopoietic stem cell; MPP, multipotent progenitor; PFA, paraformaldehyde.

Kalaitzidis and Neel measured levels of phospho-proteins in Lin^{-} cells following stimulation with a number of HGFs [364]. Of the HGFs analysed, they observed a large increase in the levels of pS6 following Flt3 stimulation. As such, an antibody specific for the S235/236

phosphorylation sites of S6 was used to determine if the phosphoflow protocol described here was able to accurately detect pS6 expression in whole BM after culture with Flt3L. To ensure that any changes to pS6 levels were due to Flt3 activation, and not events that are related to the isolation and processing of the samples, the cells were starved for 3 hours in serum-free IMDM immediately prior to Flt3L treatment. Cells were then stimulated with 150ng/mL Flt3L before being fixed with 1.6% PFA for 15 minutes at room temperature and permeabilised using ice-cold acetone for 15 minutes at -20°C. Subsequently, the sample was stained for pS6. A second, unstimulated, cell suspension was prepared as a control in the same manner. In agreement with the findings of Kalaitzidis and Neel [364], analysis revealed a clear shift in the levels of pS6 in Flt3L treated whole BM cells when compared to the untreated control (**Figure 4.4**).

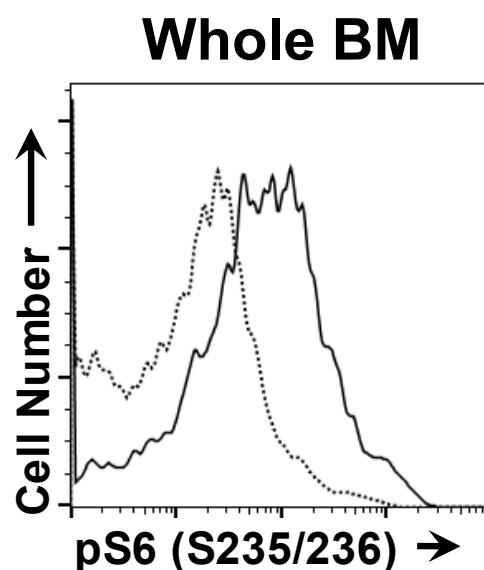


Figure 4.4. Staining of pS6 in BM cells using flow cytometry. Unstained BM cells were starved in serum-free medium for 3 hours and then stimulated with 150ng/mL Flt3L for 7.5 minutes before being fixed and permeabilised using 1.6% paraformaldehyde and ice-cold acetone. Cells were then stained for expression of pS6 (S235/236). Histograms show the level of pS6 expressed by Flt3L stimulated cells (solid black line) compared to unstimulated cells (black dotted line). pS6, phosphorylated ribosomal protein S6; Flt3L, fms-like tyrosine kinase 3 ligand; BM, bone marrow.

Having successfully identified a downstream signalling protein of the Flt3L cascade that could be measured using the phosphoflow protocol, the next step was to upscale the number of cells used in the experiment so that HSCs and MPPs could be analysed. BM cells were isolated and stained using the HSPC antibody staining panel, and the phosphoflow protocol was repeated as before. As a large number of MPPs express Flt3, the level of pS6 was monitored in this cell population as a positive control. Unfortunately, when analysing the samples, there was no clear shift in the levels of pS6 in MPPs treated with Flt3L, indicating that the protocol was unsuccessful (**Figure 4.5**).

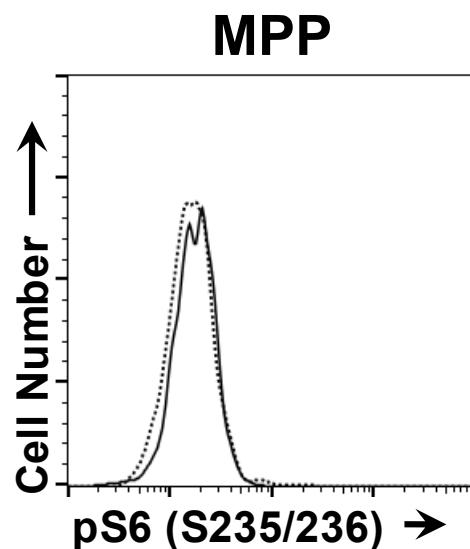


Figure 4.5. Staining of pS6 in MPPs using flow cytometry. As the pS6 staining of whole BM was successful, a second experiment was carried out to determine if a shift in pS6 could be seen in Flt3L simulated MPPs. BM cells were isolated and stained using an antibody panel to identify MPPs. The cells were then starved in serum-free medium for 3 hours. Following the starvation period, the sample was stimulated with 150ng/mL Flt3L for 7.5 minutes before being fixed and permeabilised using 1.6% paraformaldehyde and ice-cold acetone. Histograms show the level of pS6 expressed by Flt3L stimulated MPPs (solid black line) compared to unstimulated MPPs (black dotted line). There was no significant difference between the levels of pS6 expressed by Flt3L stimulated MPPs and untreated controls, indicating that the phosphoflow protocol was working intermittently and, thus, not reliable. pS6, phosphorylated ribosomal protein S6; Flt3L, fms-like tyrosine kinase 3 ligand; MPP, multipotent progenitor; BM, bone marrow.

The protocol was previously successful when using whole BM, and it was unclear why the experiment had failed when analysing MPPs. Regardless, this suggested that the current phosphoflow protocol was not reliable and could not be used to produce consistently reproducible data. As such, the protocol needed to be optimised further. For the initial phosphoflow experiments, cells were fixed using PFA that had been prepared in the laboratory. To determine if the quality of the PFA prepared in the laboratory was an issue, the experiment was repeated using commercial EM-grade PFA. Using the same protocol as before, BM cells were stained using the HSPC antibody staining panel, stimulated with Flt3L, and then fixed with either laboratory prepared PFA or EM-grade PFA to compare the two solutions. Finally, the samples were permeabilised, stained for pS6 and then analysed on a flow cytometer.

As observed in the previous experiment, a clear shift was not seen for Flt3L treated MPPs that had been fixed using laboratory prepared PFA when compared to untreated controls. However, there was a large shift in the level of pS6 in Flt3L stimulated MPPs fixed with commercial EM-grade PFA (**Figure 4.6**). This indicated that the quality of the PFA used to fix the cells during the phosphoflow protocol was important for optimal staining of phosphoproteins, and so commercial EM-grade PFA was used for all future experiments. The experiments also revealed that the LSK CD150⁺ CD48⁺ compartment contains a large number of Flt3L responsive cells.

Once the phosphoflow method had been optimised for the analysis pS6 expression by LSK cells, the method was used to investigate whether incubation of LT-HSCs and ST-HSCs with Flt3L resulted in an increase in the levels of intracellular pS6. To ensure changes in pS6 levels were analysed in a consistent manner, treated and untreated cells from the same mouse were

compared. Samples of BM cells were stained using the HSPC antibody panel, and starved in serum-free IMDM for 3 hours. After the starvation period, each cell suspension was divided into a treated sample (150ng/ml Flt3L for 7.5 minutes), an untreated sample (maintained in starvation medium (-Flt3L) for the period of stimulation) and an isotype control sample. All three samples were subsequently fixed (using EM-grade PFA), permeabilised, and then stained for pS6. The samples were then analysed and the levels of pS6 in gated LT-HSCs, ST-HSCs and MPPs were determined (**Figure 4.7A**).

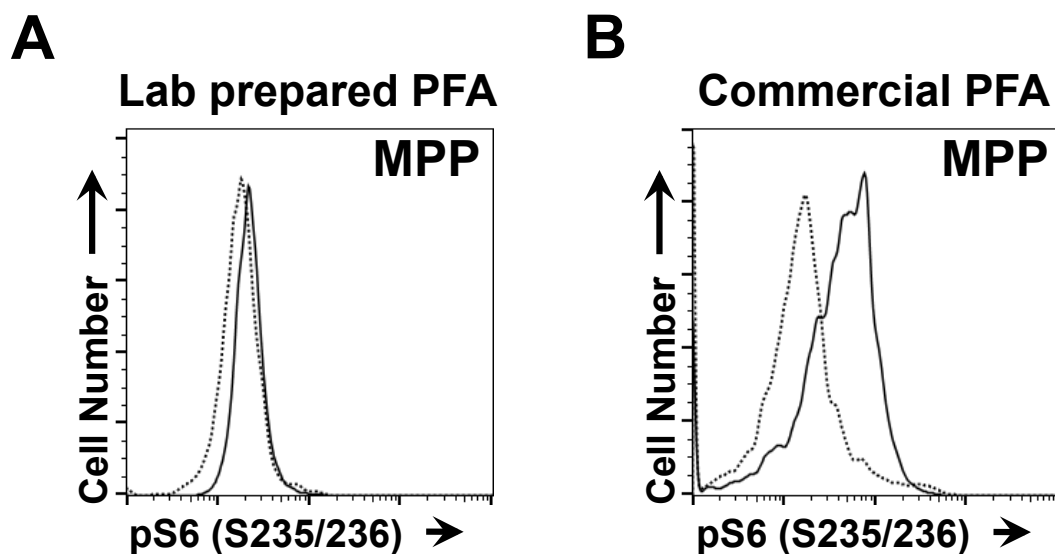


Figure 4.6. Comparison of lab prepared PFA to commercial EM-grade PFA for the use in the phosphoflow pS6 staining protocol for LSK cells. As the pS6 staining method was not reliably reproducible, pS6 levels in MPPs were measured following fixation with; **(A)** laboratory prepared PFA, or **(B)** commercially available EM-grade PFA. Whole bone marrow cells were stained using the HSPC antibody staining panel, starved in serum-free medium for approximately 3 hours and then stimulated with 150ng/mL Flt3L for 7.5 minutes. One of the samples **(A)** was fixed with 1.6% PFA that was prepared in the laboratory, while the other **(B)** was fixed using 1.6% commercial EM-grade PFA. Both samples were permeabilised using ice-cold acetone and were subsequently stained for pS6 before being analysed using flow cytometry. The sample that was fixed with **(B)** EM-grade PFA showed a clear shift in pS6 staining within the MPP compartment when compared to the unstimulated control. However, the sample that was fixed with **(A)** laboratory prepared PFA did not show an increase in pS6 staining when compared to the untreated control. pS6, phosphorylated ribosomal protein S6; Flt3L, fms-like tyrosine kinase 3 ligand; MPP, multipotent progenitor; PFA, paraformaldehyde; EM, electron-microscopy.

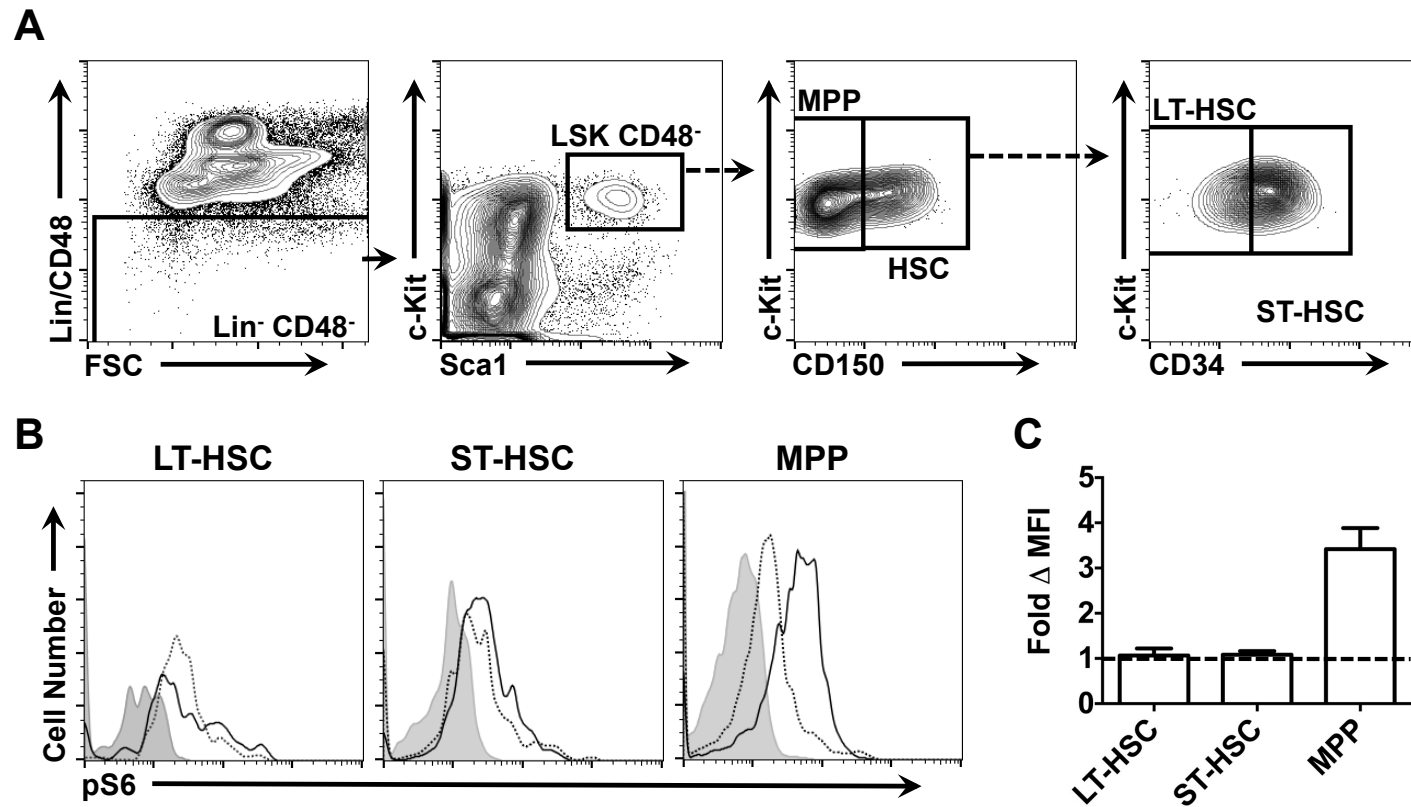


Figure 4.7. Response of HSCs and MPPs to Flt3L. Bone marrow cells were starved in serum-free medium for approximately 3 hours prior to stimulation with 150 ng/ml Flt3L for 7.5 minutes. For analysis, LT-HSCs, ST-HSCs and MPPs were identified using the gating strategy depicted in **(A)**. The histograms presented in **(B)** show representative flow cytometric analysis of pS6 staining in LT-HSCs, ST-HSCs and MPPs for treated (solid black line) and untreated cells (dotted black line). Shaded histograms depict the isotype control staining. **(C)** Shows the fold change in the MFI of pS6 staining in LT-HSCs, ST-HSCs and MPPs treated with 150ng/mL Flt3L for 7.5 minutes compared to untreated cells. Data in **(C)** are the mean and standard error of the values obtained from $n=5$ mice from 5 separate experiments. LT-HSC, long-term haematopoietic stem cell; ST-HSC short-term haematopoietic stem cell; MPP, multipotent progenitor; pS6, phosphorylated ribosomal S6 protein; Flt3L, fms-like tyrosine kinase 3 ligand; MFI, mean fluorescence intensity.

When comparing the pS6 staining to the isotype control staining, it was clear that there was a basal level of S6 phosphorylation in untreated LT-HSCs, ST-HSCs and MPPs (**Figure 4.7B**). Therefore, to accurately measure the Flt3L response, samples were compared by calculating the fold change in pS6 mean fluorescence intensity (Δ MFI) between treated and untreated LT-HSCs, ST-HSCs and MPPs (**Figure 4.7C**). When compared to untreated MPPs, the MFI of pS6 staining in treated MPPs was increased by 3.42 ± 0.46 -fold ($n=5$ mice), once again confirming that a large number of cells within this population respond to Flt3L. On the other hand, MFI of pS6 staining in treated LT-HSCs and ST-HSCs was only increased 1.06 ± 0.16 - ($n=5$ mice) and 1.08 ± 0.08 -fold ($n=5$ mice), respectively, when compared to untreated samples. These findings indicated that MPPs, but not LT-HSCs and ST-HSCs, phosphorylated detectable levels of S6 following stimulation with 150ng/mL of Flt3L. Accordingly, these data do not support the presence of functional Flt3 on the surface of LSK CD150⁺ CD48⁻ cells.

4.3 Expression of *SPI1* within the haematopoietic stem cell compartment following stimulation with Flt3L

Culturing of HSCs in the presence of Flt3L did not result in an increase in the levels of intracellular pS6, indicating that cells within the LSK CD150⁺ CD48⁻ compartment do not express functional Flt3 receptor. However, as only a small percentage of the HSC compartment express detectable levels of Flt3 on their surface [34, 329], and **Figure 3.28**, any response of these cells to Flt3L may have been overshadowed by the large proportion of Flt3⁻ HSCs. Additionally, Flt3⁺ LSK CD150⁺ CD48⁻ cells express very low levels of Flt3, so it is possible that any phosphorylation of S6 following Flt3 stimulation could have been below the limit of

detection of flow cytometry [367]. As an alternative method of investigating the presence of Flt3 in the HSC compartment, single cell gene expression analysis of cells following culture with Flt3L may provide a more accurate measurement of a response to Flt3L. Thus, a single cell qRT-PCR assay for a potential Flt3 target gene was designed and optimised for analysis of LSK CD150⁺ CD48⁻ cells following culture with Flt3L.

Table 12: Details of the *SPI1* qRT-PCR assay

<i>SPI1</i> qRT-PCR assay	
Forward primer	5'-GCCATAGCGATCACTACTGGGATT-3'
Reverse primer	5'-CACACTCTGCAGCTCTGTGA-3'
Hydrolysis probe	5'-CCGCACACCATGTCCACAACAAC-3'
Interrogated exon-exon junction	Exon 2 – exon 3
Intron size	13,728 nt

nt, nucleotides.

As described in **Section 4.1**, studies using cells transfected with Flt3 suggest that *SPI1* and *CEBPA* are both downstream targets of Flt3 signalling [276, 358]. As the Rolink group has proposed that Flt3L instructs lineage fate [288], this process may be mediated by PU.1 and C-EBP α TFs, given their role in HSPC specification/differentiation [125, 359-361]. PU.1, which is encoded by the *SPI1* gene, is a key player in lineage commitment of HSCs and drives a myeloid-bias in M-CSF stimulated HSCs [267]. If LT-HSCs and ST-HSCs express functional Flt3, and Flt3L provides lineage instruction, it is possible that PU.1 mediates this process. Furthermore, PU.1 controls Flt3 expression in DCs, so Flt3 expression may control its own expression through a positive feedback mechanism [368]. As such, to determine if *SPI1* is upregulated in cells

expressing Flt3 and particularly in a subpopulation of LSK CD150⁺ CD48⁻ cells following treatment with Flt3L, a single-cell qRT-PCR assay to detect *SPI1* transcripts was designed.

The *SPI1* assay was designed and optimised in the same manner as described in **Section 3.4**. The details and the alignment of the assay are shown in **Figure 4.9** and **Table 12**. The assay was designed to span the exon junction between exon 2 and exon 3, and no pseudogenes were detected when the sequence was analysed using the BLAST genomic database. The assay was first tested using reactions with and without the RT to determine if the assay was specific for *Spi1* mRNA. Surprisingly, the assay amplified targets in both the +RT and –RT samples, indicating that the assay detected gDNA. This suggested that the mouse genome contains a *SPI1* processed pseudogene that lacks the intron between exon 2 and exon 3, and that the detected pseudogene is not present in the BLAST genomic database (**Figure 4.9A**). However, the detection of gDNA was not considered to be an issue. The *SPI1* qRT-PCR assay was designed to quantify the difference in expression of *SPI1* between cells treated with and without Flt3L, so -RT controls could be used during analysis to help discriminate amplification of gDNA from RNA.

```

GCCATAG CGATCACTAC TGGGATT
1 AAAGCCATAG CGATCACTAC TGGGATTTCT CCGCACACCA TGTCCACAAC AACGAGTTTG
   TTTCGGTATC GCTAGTGATG ACCCTAAAGA GCGGTGTGGT ACAGGTGTTG TTGCTCAAAC
61 AGAACTTCCC TGAGAACCAC TTCACAGAGC TGCAGAGTGT GCAGC
   TCTTGAAGGG ACTCTTGGTG AAGTGTCTCG ACGTCTCACA CGTCG
   AGTGTCTCG ACGTCTCACA C

```

Figure 4.8. Sequence alignment of *SPI1* qRT-PCR assay within the *SPI1* gene. A region within the *SPI1* gene is depicted to show the alignment of the *SPI1* qRT-PCR assay primers and hydrolysis probe. The forward primer, reverse primer and probe sequences are shown highlighted in green, blue, and pink, respectively. The red box highlights the junction between exon 2 and exon 3.

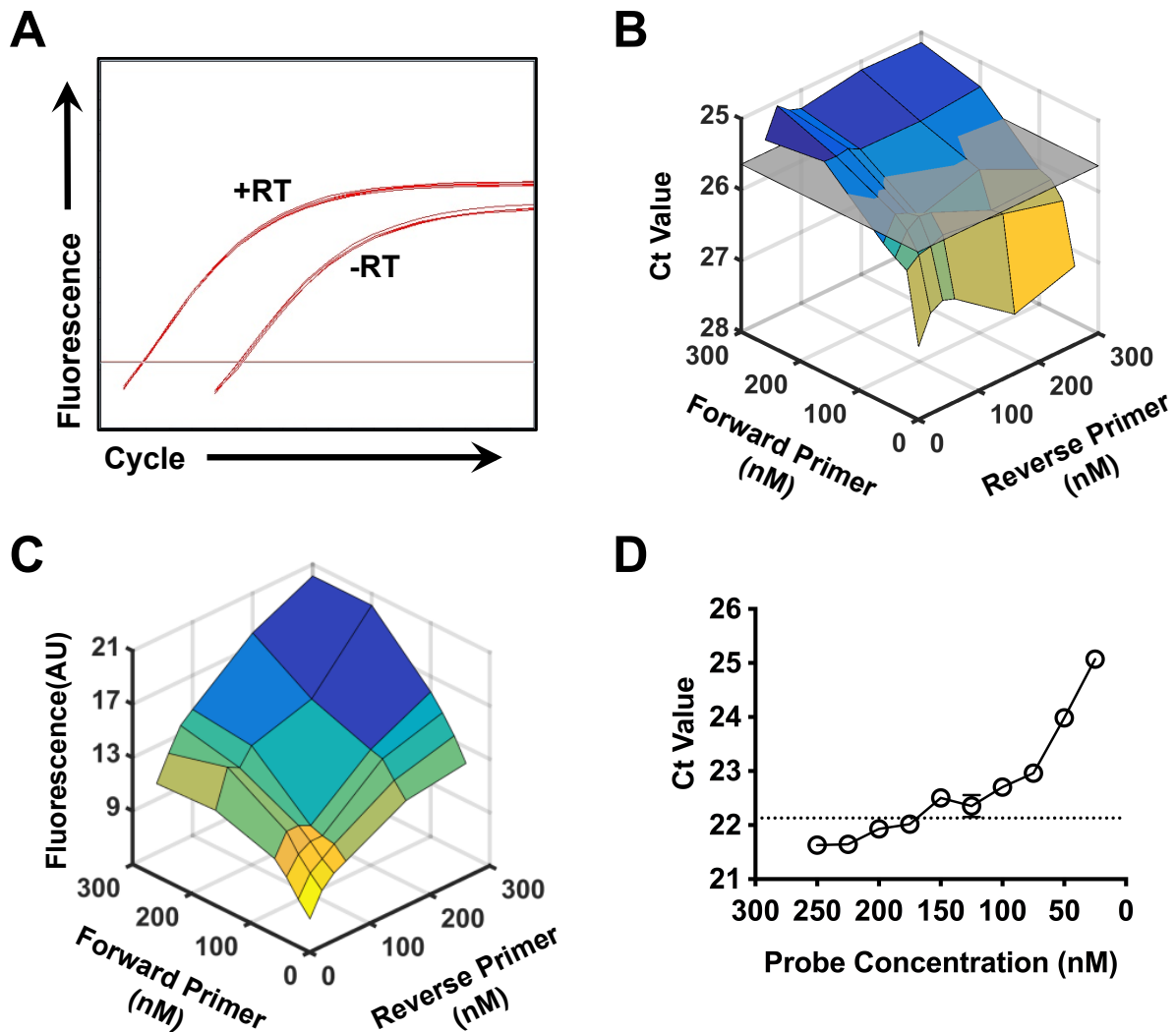


Figure 4.9. Optimisation of the *SPI1* qRT-PCR assay for detection of single cell gene expression. (A) When the *SPI1* assay was tested with (+RT) and without (-RT) reverse transcriptase the assay amplified targets in both samples, indicating that the assay detected gDNA. (B, C) To determine the optimum limiting primer concentrations for the *SPI1* qRT-PCR assay, amplification of target sequences in whole bone marrow lysate was carried out using multiple combinations of different primer concentrations (B) The Ct for all primer combinations was determined, and any sample with a Ct value of >0.5 cycles greater than the Ct value of the reference reaction (300nM forward primer/300nM reverse primer) was considered to have low efficiency (below the transparent grey pane). (C) Of the remaining efficient reactions, the primer combination with the lowest peak fluorescence value was selected as the limiting reaction. (D) Similarly, multiple hydrolysis probe concentrations were tested to determine the optimum probe conditions. Of the reactions with a Ct value that was not >0.5 cycles greater than the Ct value of the reference reaction (250nM hydrolysis probe; below the dotted line), the lowest probe concentration was selected as the optimum. Optimum forward primer, reverse primer and hydrolysis probe concentrations were found to be 300nM, 40nM and 175nM, respectively. gDNA, genomic DNA; RT, reverse transcriptase; Ct, threshold cycle; AU, arbitrary units.

Next, the primer and probe concentrations of the assay were optimised. The optimal limiting primer concentrations for the forward and reverse primers were found to be 300nM and 40nM, respectively (**Figure 4.9B, C**). The optimum probe concentration was found to be 175nM (**Figure 4.9D**). To test the single cell sensitivity of the *SPI1* qRT-PCR assay, single GMPs were used, as these cells are known to express *Spi1* transcripts [369]. The assay successfully detected expression of *SPI1* by single GMPs and, on average, an increase of 1 cycle was observed for each cell number doubling, indicated that the assay was efficiently amplifying target sequences in single cells (**Figure 4.10**).

Mossadegh-Keller *et al.* designed an *in vitro* experiment to analyse gene expression of HSCs after 16 hours of culture with M-CSF, and found *SPI1* to be upregulated in a number of cells [267]. The response of HSCs to Flt3L was examined by adapting the protocol described in the above paper, and the expression of *SPI1* by HSCs following incubation with Flt3L was investigated. As studies to date have only shown that *SPI1* is a direct target of Flt3 signalling in cells that ectopically express Flt3, it was difficult to identify an endogenous haematopoietic cell population that could be used as a positive control. Stimulation of CMPs with Flt3L promotes the development of DCs, and *SPI1* plays an integral role in DC differentiation, suggesting an endogenous relationship between the two [311, 368]. Thus, single CMPs were used as a control to determine if *SPI1* is a direct target of endogenous Flt3 signalling. As a negative control, single MEPs were chosen as these cells do not express the Flt3 receptor and should not respond to Flt3L (**Figure 3.27**).

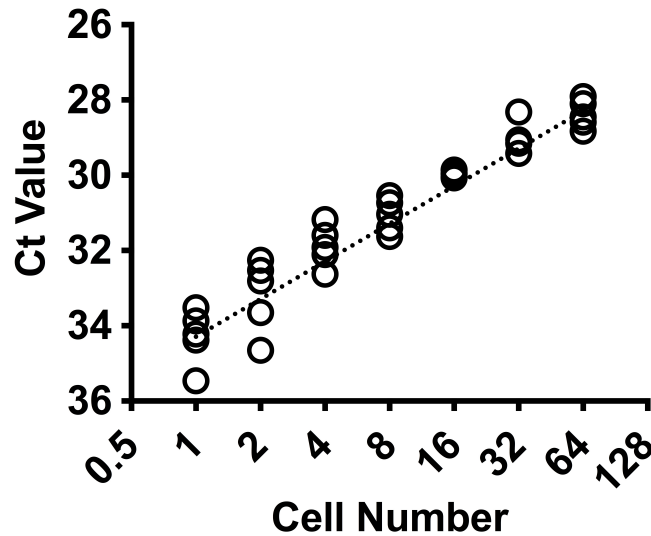


Figure 4.10. Detection of single cell gene expression using the *SPI1* qRT-PCR assay. The optimised primer and probe concentrations for the *SPI1* qRT-PCR assay were used to amplify *SPI1* expression by single GMPs. The assay clearly amplified expression of *SPI1* by single GMPs and there was an average increase of 1 cycle per cell number doubling (dotted line represents an increase of 1 cycle per cell number doubling for comparison). GMP, granulocyte-macrophage progenitor; Ct, threshold cycle.

To determine if Flt3 stimulation results in upregulation of *SPI1* in HSPCs, LT-HSCs, ST-HSCs, CMPs and MEPs were bulk sorted from whole mouse BM into IMDM containing 10% FCS, 1,000 U/mL penicillin and 1,000 µg/mL streptomycin, 50 ng/mL Tpo and 20 ng/mL Scf, with and without Flt3L. As 150ng/mL of Flt3L produced a strong response in MPPs when monitoring pS6 levels; the same concentration of Flt3L was used to investigate if Flt3 signalling upregulates *SPI1* expression. These cells were then cultured in medium supplemented with the above factors ± Flt3L overnight for 18 hours. Following the overnight incubation, single LT-HSCs, ST-HSCs, CMPs and MEPs were sorted from the cultures into wells of a 384-well PCR plate and analysis of *SPI1* expression by single cells was performed. To avoid sorting noise/debris events, the same FSC/SSC gating strategy that was used to sort the bulk populations for the overnight culture was applied when sorting the cells into the PCR plates (Figure 4.11).

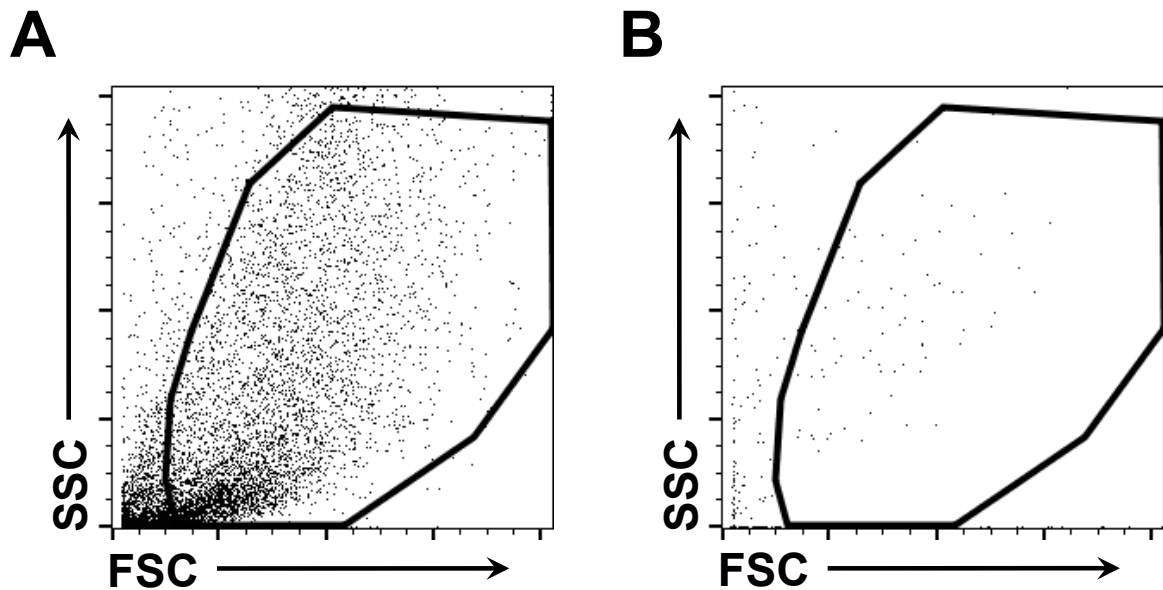


Figure 4.11. Sorting of single cells to determine the effects Flt3L stimulation on *SPI1* expression. Representative plots show the FSC and SSC profile for **(A)** whole bone marrow and **(B)** purified cells following Flt3L stimulation in culture for 18 hours. The FSC/SSC gating strategy used during **(B)** was identical to **(A)**. FSC, forward scatter; SSC, side scatter; Flt3L, fms-like tyrosine kinase 3 ligand.

As the *SPI1* qRT-PCR assay detected gDNA, samples that were negative for *SPI1* amplification were likely due to empty wells. Thus, only samples that were positive for *SPI1* amplification were included during analysis. However, when analysing the expression of *SPI1* in LT-HSCs, ST-HSCs, CMPs and MEPs, it was difficult to discern between positive and negative amplification curves (**Figure 4.12C**). This was likely to be due to amplification of *SPI1* gDNA and the amplification was not of major importance as -RT control samples could be used to distinguish RNA amplification.

Of the cells cultured with 150ng/mL of Flt3L, successful amplification of *SPI1* was detected in 25 LT-HSC, 183 ST-HSC, 31 CMP and 18 MEP samples. Additionally, *SPI1* was detected in 58 LT-HSC, 122 ST-HSC, 80 CMP and 50 MEP samples that were cultured without Flt3L. Analysis revealed that virtually all MEPs, and all of the -RT samples had Ct values of >35, indicating

that a Ct value of 35 cycles or lower was due to amplification of *Spi1* mRNA transcripts (**Figure 4.12A**). The majority of reactions containing *SPI1*⁺ CMPs had Ct values of <35 cycles but there was no difference in levels of mean expression when comparing cells that had been cultured with and without Flt3L [$p=0.7541$]. Furthermore, the expression of *SPI1* by the LT-HSCs and ST-HSCs suggested that a large percentage of cells within these populations were also positive for *Spi1* mRNA transcripts (<35 Ct) (**Figure 4.12A**). However, as seen for the CMPs, there was no change seen in the expression levels of *SPI1* when LT-HSCs [$p=0.2512$] and ST-HSCs [$p=0.6638$] were cultured with Flt3L.

As *SPI1* was detected after 35 cycles in almost all of the MEP and RT samples, any amplification of *SPI1* detected before 35 cycles was likely due to mRNA amplification and not gDNA amplification. To determine if Flt3L stimulation initiated the expression of *Spi1* mRNA in cells, the percentage of LT-HSCs, ST-HSCs and MPPs expressing *SPI1* at levels above the gDNA threshold (<35 cycles) within the -Flt3L and +Flt3L groups were determined. When analysed, there was a slight decrease in the number of Flt3L stimulated LT-HSCs expressing *Spi1* mRNA (<35 cycles) (44%) when compared to the LT-HSCs that were cultured without Flt3L (53%). However, this change was not significant [$p=0.4794$]. Similarly, there was no significant difference between the number of Flt3L treated ST-HSCs that expressed *Spi1* mRNA (<35 cycles, 65%) and when compared to the number of *Spi1*⁺ ST-HSCs that were not treated with Flt3L (68%) [$p=0.6224$]. Furthermore, there was no change in *Spi1* mRNA expression (<35 cycles) when comparing the CMPs that were cultured with (85%) or without (78%) Flt3L [$p=0.6067$].

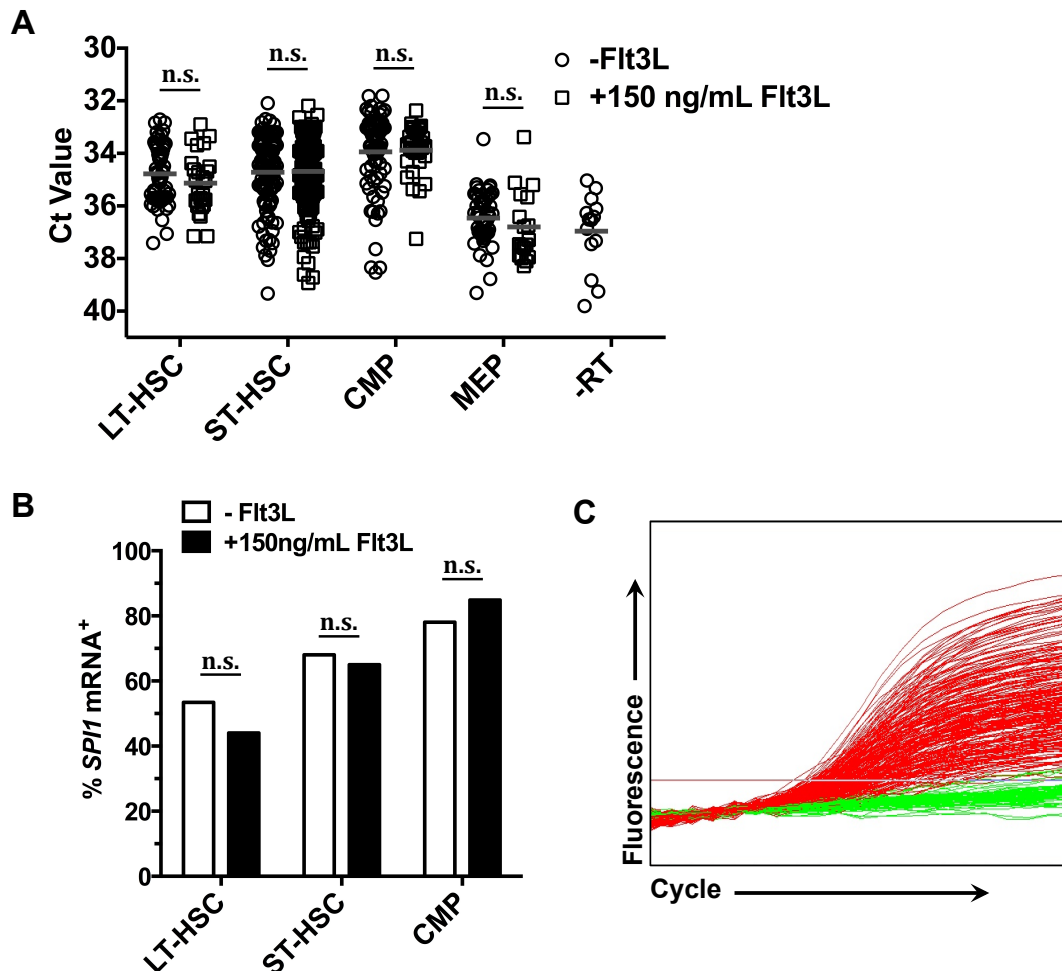


Figure 4.12. Expression of *SPI1* by HSCs after culture with or without Flt3L. (A) Expression of *SPI1* by LT-HSCs, ST-HSCs, CMPs and MEPs after culture in 10% FCS, 1,000 U/mL penicillin, 1,000 µg/mL streptomycin, 50 ng/mL Tpo and 20 ng/mL Scf, with and without 150ng/mL Flt3L for 18 hours, including -RT control reactions. The mean values of expression are depicted by the grey lines. (B) The percentage of LT-HSCs, ST-HSCs and MPPs that expressed *SPI1* mRNA (Expression of *SPI1* at levels above the gDNA threshold [<35 cycles]) were compared between the treated (+Flt3L) and untreated (-Flt3L) groups (C) Amplification of *SPI1* in single HSCs. Red curves represent amplification and green curves represent background fluorescence. Fluorescence is plotted on a log scale. *p* values were obtained by performing (A) two-tailed non-parametric student's t-tests or (B) Fisher's exact tests where; n.s., $p > 0.05$. HSC, haematopoietic stem cell; LT, long-term; ST, short-term; CMP, common myeloid progenitor; MEP, megakaryocyte-erythroid progenitor; -RT, reactions without reverse transcriptase; Flt3L, Fms-like tyrosine kinase 3 ligand; n.s., not significant.

When analysing the response of cells to Flt3L using the phosphoflow technique, cells were starved in serum-free medium prior to stimulation with Flt3L to minimise the activity of biological pathways. As this strategy worked well for the phosphoflow analysis, the *SPI1* expression analysis was repeated to examine whether the inclusion of a starvation period

prior to stimulating the cells with Flt3L would reveal a response. The experiment was repeated by first sorting cells into serum-free IMDM and starving them for 3 hours before supplementing the medium with 10% FCS, 1,000 U/mL penicillin and 1,000 µg/mL streptomycin, 50 ng/mL Tpo and 20 ng/mL Scf, with and without 150ng/mL Flt3L. The cells were cultured overnight for 18 hours as before. To ensure that the cells were accurately analysed the next day, the FSC/SSC gating strategy that was used to initially sort the cells into starvation medium was used again to sort the cells into PCR plates after culture with Flt3L (Figure 4.13).

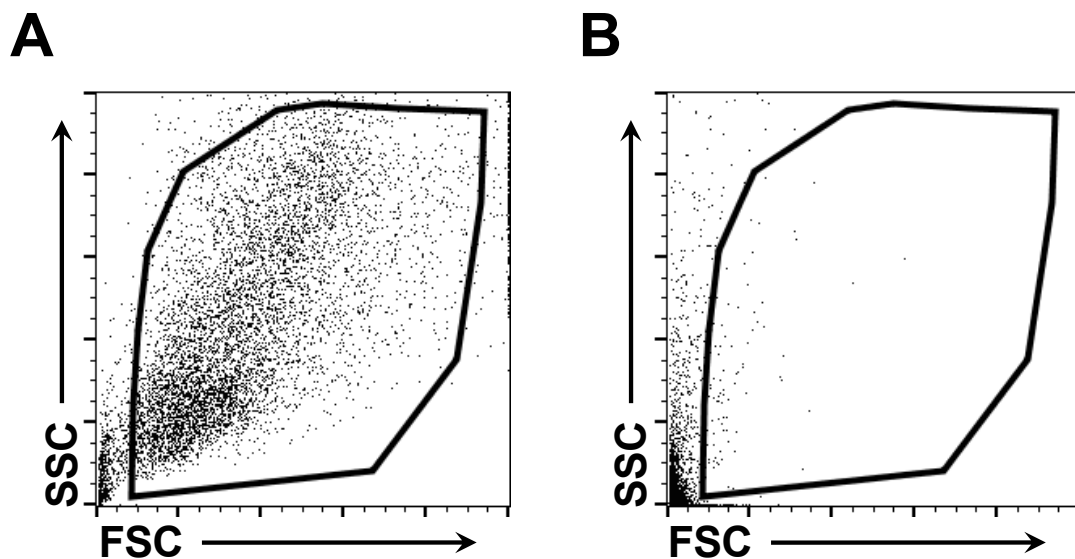


Figure 4.13. Sorting of single cells to determine the effects Flt3L stimulation after a serum-free starvation period on *SPI1* expression. Representative plots show the FSC and SSC profile for (A) whole bone marrow and (B) purified cells that were starved for 3 hours in serum-free medium and then stimulated with Flt3L stimulation in culture for 18 hours. When sorting the cells after the 18 hour incubation period, it was clear that the cells were in the process of dying or had died during the overnight culture, as they had a very low FSC profile. This made it difficult to discriminate between background noise and cells. The FSC/SSC gating strategy used during (B) was identical to (A). FSC, forward scatter; SSC, side scatter; Flt3L, fms-like tyrosine kinase 3 ligand.

Once the cells had been starved for 3 hours, and subsequently stimulated with Flt3L overnight for 18 hours, the cells were sorted by FACS. When comparing the FSC/SSC profile of the cells that were cultured with Flt3L (Figure 4.13B) to the FSC/SSC profiles that were obtained when

sorting the cells from whole BM (**Figure 4.13A**), there was a clear change in the FSC profile of the cells. All of the events appeared to have very low levels of FSC, and there were very few live cells. From the FSC/SSC profile, it was clear that the cells were in the process of dying or had died during the overnight culture. Therefore, cells were not sorted into PCR plates for analysis.

As there was no change detected in the expression of *SPI1* by CMPs when they were cultured with Flt3L in the first experiment (**Figure 4.12**), this set of experiments provides inconclusive data in regard to the expression of Flt3 by HSCs. However, it may provide some insight into the relationship between Flt3 and *SPI1*, as discussed in **Section 4.5.1**.

4.4 Effects of Flt3L on haematopoietic stem cells during colony formation *in vitro*

Analysis of the Flt3 response within the signalling pathway and at the transcriptional level do not support the presence of functional Flt3 receptor within the HSC compartment. However, these experiments measured the response to Flt3L over short periods of exposure. By measuring downstream effects of Flt3 signalling such as differentiation and survival after longer periods of treatment, the analysis may benefit from an amplified response that is easier to detect. There is evidence to suggest that Flt3L stimulates HSPCs to differentiate towards non-MegE fates [288]. In addition, Flt3 signalling promotes cell survival [352]. Thus, culturing HSCs in methylcellulose medium and monitoring the formation of colonies after 11 days of culture with Flt3L may provide insight into whether Flt3 promotes survival and/or differentiation of these cells towards a certain lineage. To investigate this, a colony forming

assay was performed using HSCs (LSK CD150⁺ CD48⁻), with and without Flt3L.

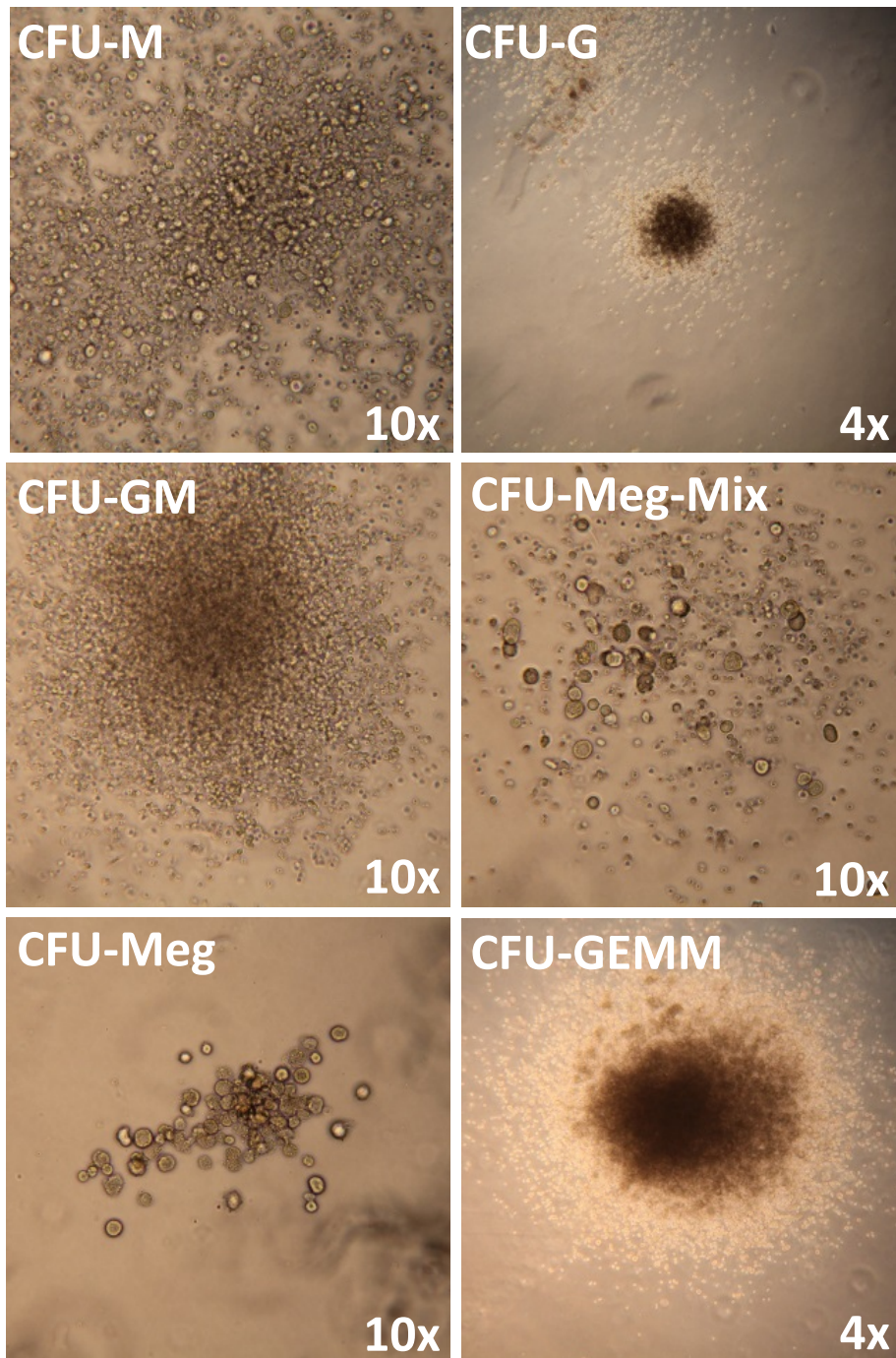


Figure 4.14. Brightfield images of colonies formed after seeding HSCs into methylcellulose medium. HSCs (LSK CD150⁺ CD48⁻) were sorted from murine bone marrow and seeded into M3434 supplemented with 25ng/mL thrombopoietin, 1,000 U/mL penicillin and 1,000 µg/mL streptomycin. M3434 cultures were incubated at 37°C, 5% CO₂ for 11 days and colonies were identified. Representative images of each colony type scored are shown. The magnification used to take the image is shown in the bottom right of each picture. HSC, haematopoietic stem cell; CFU, colony forming unit; M, macrophage; G, granulocyte; GM, granulocyte-macrophage; GEMM, granulocyte-erythroid-macrophage-megakaryocyte; Meg, megakaryocyte.

HSCs were sorted from the BM of 3 mice into IMDM supplemented with 10% FCS, 1,000 U/mL penicillin and 1,000 µg/mL streptomycin. These HSC samples were then mixed into Methocult M3434 (supplemented with 25ng/mL Tpo to allow for measurement of megakaryocyte output) with and without Flt3L. Flt3L was used at a similar concentration (25ng/mL) to the other HGFs in the M3434 medium (50ng/mL SCF, 10ng/mL IL-3, 10ng/mL IL-6, 3 units/mL Epo, 25ng/mL Tpo). The samples were then plated in duplicate and incubated at 37°C 5% CO₂ for 11 days. Colonies were scored on day 11, and CFU-M, CFU-G, CFU-GM, CFU-GEMM, CFU-Meg and CFU-MegMix were observed (**Figure 4.14**). Colony types were confirmed by centrifuging representative colonies onto slides and staining them using a Differential Quik Staining kit (**Figure 4.15**). The criteria used to score the types of colonies and analyse the cytopsin preparations are described in **Section 2.13.3**. Once all of the colonies had been scored and their nature confirmed using the cytopsin preparations, the data obtained for HSCs plated into M3434 with and without Flt3L were compared. There were no differences in the number of total colonies [$p=0.75$] (**Figure 4.16B**), or the number of CFU-M [$p>0.999$], CFU-G [$p=0.75$], CFU-GM [$p>0.999$], CFU-GEMM [$p>0.999$], CFU-Meg [$p>0.999$] or CFU-MegMix [$p>0.999$] (**Figure 4.16A**) ($n=3$ mice) between plates with and without Flt3L. Similarly, there were no differences in colony size between the two cultures. These findings indicated that addition of 25ng/mL of Flt3L to M3434 did not confer a survival advantage or maturation bias when seeding HSCs onto methylcellulose. All of the duplicate plating values are shown in **Table 13**.

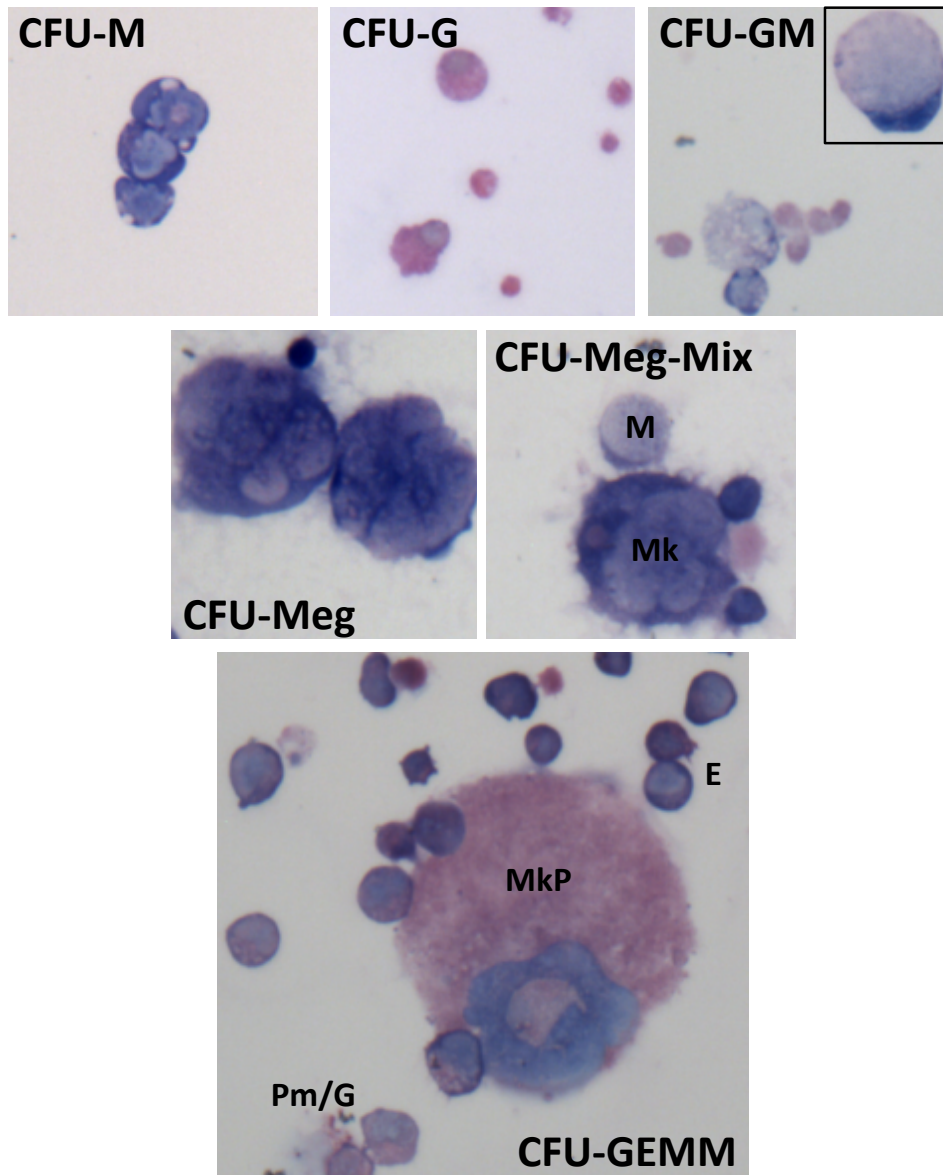


Figure 4.15. Cytospin preparations of colonies formed after seeding HSCs into methylcellulose medium. Representative colonies were picked from methylcellulose cultures that were seeded with HSCs (LSK CD150⁺ CD48⁻). Cultures were incubated at 37°C, 5% CO₂ for 11 days, and then representative colonies of each colony type were centrifuged onto glass slides for staining with a Differential Quik stain kit. Macrophage/monocytes (M) were recognised as cells with abundant dull blue/grey cytoplasms and usually dark blue kidney shaped nuclei [300]. Promyelocytes (Pm) and granulocytes (G) were identified as cells with dark to pale pink cytoplasms [300, 301]. Megakaryocytes (Mk) and promegakaryocytes (MkP) were distinguished by their size. Promegakaryocytes had dark pink granular cytoplasms, while megakaryocytes were highly polyploidy cells with intense blue (basophilic) cytoplasms [300, 302, 303]. Erythroblasts (E) were identified as cells with high a nucleus to cytoplasm ratio, that had intensely basophilic-purple cytoplasms [301, 302]. The insert at the top right of the CFU-GM picture shows a macrophage/monocytes from the same cytospin preparation. All images were taken at the same magnification (x200). HSC, haematopoietic stem cell; CFU, colony forming unit; M, macrophage; G, granulocyte; GM, granulocyte-macrophage; GEMM, granulocyte-erythroid-macrophage-megakaryocyte; Meg, megakaryocyte.

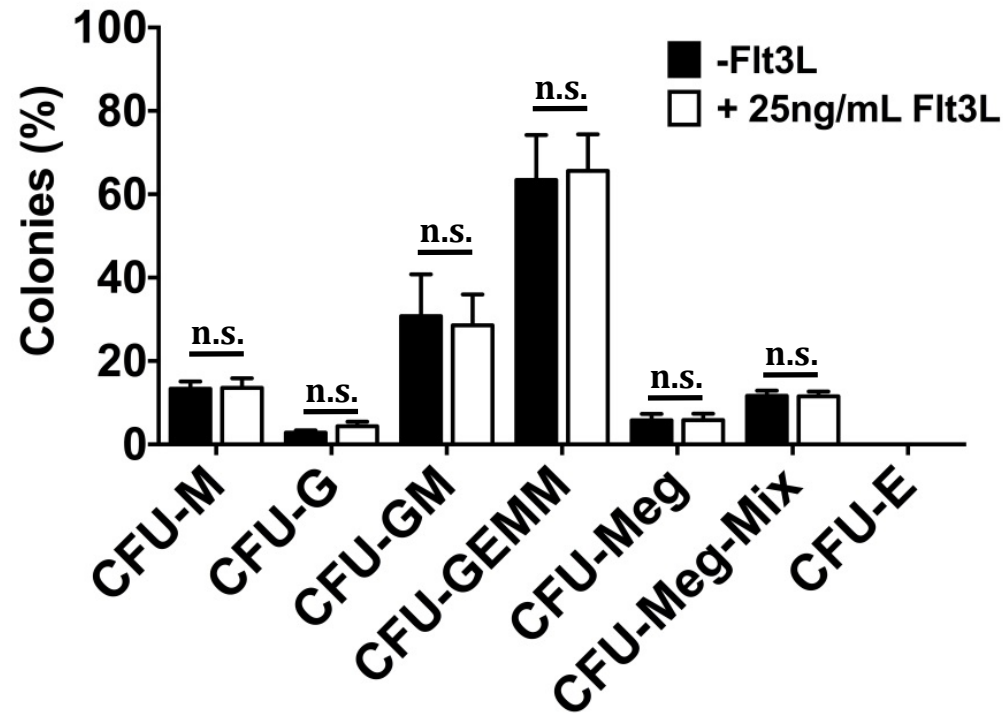
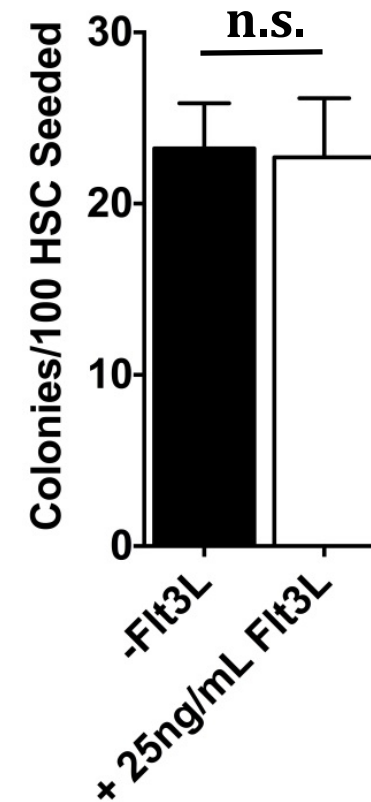
A**B**

Figure 4.16. Effects of Flt3L on colony formation after seeding HSCs into methylcellulose medium. HSCs (LSK CD150⁺ CD48⁻) were sorted from murine bone marrow and seeded into M3434 (supplemented with 10% FCS, 25ng/mL thrombopoietin and 1,000U/mL penicillin/streptomycin) with and without 25ng/ml Flt3L. **(A)** colony type and **(B)** total colony numbers (per 100 HSCs) were counted on day 11, $n = 3$ mice. For confirmation, representative colonies were centrifuged onto microscope slides, air-dried and stained using a Differential Quik Staining kit. p values obtained by two-tailed non-parametric student's t-test where; n.s., $p > 0.05$. HSC, haematopoietic stem cell; Flt3L, fms-like tyrosine kinase 3 ligand; CFU, colony forming unit; M, macrophage; G, granulocyte; GM, granulocyte-macrophage; GEMM, granulocyte-erythroid-macrophage-megakaryocyte; Meg, megakaryocyte; n.s., not significant.

Table 13: Types and number of colonies identified when scoring the growth and development of HSCs in M3434 with and without Flt3L

	-Flt3L						+25ng/mL Flt3L					
	Mouse #1		Mouse #2		Mouse #3		Mouse #1		Mouse #2		Mouse #3	
Number of HSCs seeded/plate	278		335		433		278		335		433	
	Plate 1	Plate 2	Plate 1	Plate 2	Plate 1	Plate 2	Plate 1	Plate 2	Plate 1	Plate 2	Plate 1	Plate 2
CFU-GEMM	40	40	49	60	54	49	18	26	65	47	85	104
CFU-GM	9	13	19	12	72	53	21	18	11	28	26	18
CFU-M	8	4	8	10	19	22	8	8	8	7	23	10
CFU-G	0	2	3	2	2	6	2	4	1	4	6	2
CFU-Meg	5	5	13	6	16	15	8	4	10	9	9	14
CFU-Meg-Mix	5	3	2	2	12	6	5	3	5	1	6	6
Total	67	67	94	92	175	151	62	63	100	96	155	154

M3434 medium allows for the formation of CFU-GEMM, CFU-GM, CFU-M, CFU-G, CFU-Meg, CFU-Meg-Mix. HSCs were sorted from murine bone marrow and seeded onto M3434 and incubated at 37°C 5% CO₂ for 11 days. On day 11, the colony type was determined based on their morphology. For this experiment, M3434 was supplemented with 10% fetal calf serum, 25ng/mL thrombopoietin, 1,000 U/mL penicillin and 1,000 µg/mL streptomycin. For confirmation, representative colonies were centrifuged onto glass slides and stained using a Differential Stain kit. Groupings of 50 or more cells were considered a colony. Flt3L, fms-like tyrosine kinase 3 ligand; CFU, colony forming unit; M, macrophage; G, granulocyte; GM, granulocyte-macrophage; GEMM, granulocyte-erythroid-macrophage-megakaryocyte; Meg, megakaryocyte, CFU-Meg-Mix, sparse colonies that contained megakaryocytes and macrophages/granulocytes.

4.5 Discussion

4.5.1 Multipotent progenitors but not haematopoietic stem cells respond to Flt3L stimulation *in vitro*

The Rolink group has proposed that Flt3L drives LSK CD150⁻ CD48⁺ cells towards GM-lymphoid cell fates [288]. However, the data generated in **Chapter 3** revealed the presence of *FLT3* transcripts and Flt3 protein within the LSK CD150⁺ CD48⁻ HSC and LSK CD150⁻ CD48⁻ MPP compartments, suggesting that Flt3L may also act on these cells. Hence, the focus of this chapter was to investigate the presence of functional Flt3 expression within early HSPC compartments by monitoring for the downstream effects of Flt3 activation. While it is clear that LSK CD150⁺ CD48⁻ MPPs responded to Flt3L, the data presented here does not provide evidence to support the viewpoint that Flt3L can stimulate cells within the LSK CD150⁺ CD48⁻ HSC compartment.

By monitoring the phosphorylation of ribosomal protein S6 (a target of both the PI3k and Ras pathways during Flt3 signalling [353, 354]) using flow cytometry, activation of intracellular signalling in MPPs was clearly identified following *in vitro* stimulation with 150 ng/mL Flt3L. Given that such a high proportion of MPPs are Flt3⁺ (63.65% ± 3), it was not surprising to find that there was a 3.42 ± 0.46-fold (*n*=5 mice) increase in pS6 MFI when comparing Flt3L treated MPPs to untreated MPPs. On the other hand, there was no clear shift in pS6 levels observed in either the LT-HSC or ST-HSC compartments following culture with Flt3L, and the mean expression level of pS6 did not change in either population when compared to untreated controls (1.06 ± 0.16- (*n*=5 mice) and 1.08 ± 0.08-fold (*n*=5 mice), respectively). These findings

show that Flt3L elicits a large response within the MPP (LSK CD150⁺ CD48⁻), but not the HSC, population, supporting a model whereby Flt3L drives lineage decisions in the non-self-renewing multipotent compartment of the BM [288]. On a technical note, the phosphoflow protocol described here allows for the novel analysis of phosphorylation events within HSCs (LSK CD150⁺ CD48⁻) and MPPs (LSK CD150⁻ CD48⁻). Previous studies have reported difficulty in distinguishing between these two groups when performing phosphoflow due to the loss of HSPC surface antigen integrity following permeabilisation [364]. However, while the integrity of the CD150 antigen is compromised when analysing whole BM cells after acetone treatment, CD150 can still be used to successfully distinguish HSCs from MPPs using the phosphoflow protocol described here (**Figure 4.3**).

When monitoring the Flt3 signalling cascade, cells within the HSC compartment did not respond to Flt3L. Therefore, the expression of a potential transcriptional target of the Flt3 signalling pathway was investigated. However, a lack of information regarding canonical Flt3 gene targets made it difficult to select an adequate experimental controls. If Flt3L acts on cells to drive lineage bias [288], it likely controls the regulation of TFs important in GM-lymphoid differentiation, such as *SPI1*, *CEBPA* or *IKZF1* [125, 359, 360, 370]. Indeed, upregulation of *SPI1* occurs in *FLT3* transfected cells following receptor stimulation [276, 358], so the expression of *SPI1* by HSCs, following culture with Flt3L, was measured to determine if these cells expressed functional Flt3. As the results from these studies have not been confirmed by means of endogenous Flt3 signalling, cells that are known to express the Flt3 receptor were cultured with Flt3L alongside HSCs as an endogenous control. A large proportion of CMPs are Flt3⁺ (36.8% ± 1.4), and CMPs are efficient at producing DCs [371]. As *SPI1* is integral for the development of DCs, Flt3⁺ CMPs provided a good control to determine if *SPI1* was upregulated

following activation of Flt3 [311, 368]. Interestingly, no response was seen in either cell type following culture with Flt3L. As such, nothing could be inferred regarding the expression of Flt3 by LSK CD150⁺ CD48⁻ cells.

It is unclear why CMPs did not upregulate *SPI1* following Flt3 stimulation. The lack of Flt3L response may be explained by the death of the cells during the overnight culture. However, this is unlikely, as dead cells can be identified by their FSC/SSC profile (**Figure 4.13**). Furthermore, while the culture conditions used are adequate for HSC culture [267], they may not have been adequate for the culture of CMPs. For example, IL-3 was not included in the medium, and IL-3 is known to promote the survival of myeloid progenitors [372]. Alternatively, the experiment may have failed due to a technical issue, such as the culture conditions. This is also unlikely, considering the same medium and Flt3L stock was used for the phosphoflow experiments, and a response was seen in MPPs (**Figure 4.7**), leaving the final possibilities; either *SPI1* is not a target of endogenous Flt3 signalling in HSPCs or, if *SPI1* is a target of Flt3 signalling, an increase in transcription may not be detected at 18 hours after Flt3L stimulation.

Measurement of *SPI1* expression at other time points may provide a more comprehensive analysis when investigating the transcriptional response of haematopoietic cells to Flt3L. Furthermore, real-time tracking of *PU.1-GFP* HSPCs cultures containing Flt3L would be useful in determining if *SPI1* is a transcriptional target of Flt3 signalling. Alternatively, other potential targets could be used to monitor HSPC response to Flt3L, such as *CEBPA* [276, 358, 373]. Given the limited information currently available in the literature regarding transcriptional regulation of canonical Flt3 signalling, monitoring changes in gene expression using a single gene has its pitfalls. Gene expression analysis of Flt3L stimulated haematopoietic cells at a

single cell level using an Affymetrix gene chip would be useful in identifying a downstream target of Flt3 signalling. The use of such techniques in future experiments would provide greater clarity on the transcriptional regulation of Flt3 signalling in cells that are known to express Flt3 and, thus, could be used to determine if single HSCs respond to Flt3L.

In addition to monitoring the molecular changes of HSCs following culture with Flt3L, the cellular response of HSCs to Flt3L was also investigated. If a fraction of LSK CD150⁺ CD48⁻ cells expressed functional Flt3, stimulation of the receptor may improve their survival [352]. Additionally, if Flt3L is indeed instructive, any Flt3⁺ HSCs would be driven away from megakaryocyte/erythroid fates and towards myelomonocytic/lymphoid fates [288]. Thus, HSCs were seeded into M3434 with and without Flt3L to monitor these responses. When the colony formation of HSCs was analysed, the number of colonies, and the types of colonies observed were similar to the results obtained by Oguro *et al.* when they monitored the colony forming potential of HSC-1 (LSK CD150⁺ CD48⁻ CD229^{-/low}) and HSC-2 (LSK CD150⁺ CD48⁻ CD229⁺) [34]. Comparison of the colony forming potential of HSCs in M3434 with and without 25ng/mL Flt3 revealed no change in the numbers of CFU-M, CFU-G, CFU-GM, CFU-GEMM, CFU-Meg or CFU-MegMix. Additionally, the total number of colonies in both samples was similar. Together, these indicate that the presence of 25ng/mL Flt3L did not alter the contribution of HSCs to particular lineages or confer a survival advantage to HSCs during colony formation.

While the data presented in this chapter do not suggest that Flt3L acts on HSCs, the experiments and analysis carried out may have lacked the sensitivity required to accurately measure the response of such a small number of Flt3⁺ cells within the HSC compartment (4.6% \pm 1 of LT-HSCs [$n=6$], 7.7% \pm 1.1 of ST-HSCs [$n=6$]). By using the fold change in MFI during

analysis of the phosphoflow experiments, an average response within the whole HSC population was calculated. This analysis may have neglected any changes that occurred at the single cell level. Ideally, the response of cells to Flt3L would be presented as a percentage of the total population so that the exact number of cells that upregulated pS6 following stimulation could be obtained. However, as cells express a basal level of pS6 at rest, gating on pS6 expression was not feasible. Additionally, as mentioned previously, the limit of detection for flow cytometry has been estimated to be 2,000 molecules [367], so cells with a limited number of receptors on their surface may not express levels of pS6 above this threshold following Flt3 stimulation and would not be detected. Indeed, it has been estimated early HSPCs may express less than 100 copies of certain HGF receptors on their surface, such as G-CSF and M-CSF [374].

The concentration of Flt3L used for the colony forming assays was lower than the concentration used in the phosphoflow assays, so the results from the colony forming assay do not preclude the possibility that higher amounts of Flt3L are required to elicit a response from LSK CD150⁺ CD48⁻ cells. In fact, in the model proposed by the Rolink group, a high threshold of Flt3L is required to drive multipotent cells towards myelomonocytic, granulocytic and lymphoid fates. Also, Flt3L plays an integral role in DC and lymphoid development [288, 311, 343, 375], but the production of DCs and lymphoid cells from HSCs stimulated with Flt3L was not monitored in the colony forming experiments.

Lastly, if Flt3 is present in the HSC compartment it may only have a minor role, or share function with another receptor on the surface of HSCs, making it difficult to detect. Indeed, Flt3 shares overlapping signalling pathways with c-Kit [234, 376, 377], and there is evidence to suggest that c-Kit and Flt3 may heterodimerise [378]. Early studies investigating the effects

of Flt3L on primitive HSPC colony formation also suggest that Flt3L provides weak proliferative signals in isolation, but primarily acts synergistically with other HGFs, such as the CSFs [196, 379, 380]. Moreover, Flt3 is known to be expressed on fetal HSCs, but Flt3L^{-/-} mice show no deficiency of the LSK CD150⁺ compartment in E14.5 liver, suggesting that Flt3 expression may be redundant in HSCs [340]. A combination of the factors highlighted above may have hindered the detection of any HSC response during the experiments carried in this chapter. Altogether, it is clear from the findings presented here that the LSK CD150⁻ CD48⁻ MPP compartment responds to Flt3L, but the presence of functional Flt3 within the HSC compartment remains uncertain.

4.5.2 A role for Flt3L in the regulation of multipotent progenitors during steady-state haematopoiesis

Tsapogas *et al.* observed the expansion of BM DCs and a rapid decrease in BM MegE progenitors following administration of Flt3L to WT mice, and suggested that Flt3L may drive an upstream progenitor towards a GM-lymphoid fate at the expense of MegE production [288]. As there was a significant expansion of LSK CD150⁻ CD48⁺ cells in Flt3-Tg mice when compared to wild type controls, the Rolink group largely attributed the Flt3L response to this population. However, the LSK CD150⁻ CD48⁺ compartment contains GM-lymphoid primed progenitors that possess limited MegE potential during steady state haematopoiesis [34, 381], indicating that stimulation of this population with Flt3L would not cause a significant decrease in MegE progenitor production. Thus, another multipotent population upstream of LSK CD150⁻ CD48⁺ is likely responsible for driving GM-lymphoid production at the expense of the MegE lineage in this model. Flt3 expression was detected on the surface of LSK

CD150⁺CD48⁻ HSCs and LSK CD150⁺ CD48⁻ MPPs (**Figure 3.27**), which are both upstream of LSK CD150⁻ CD48⁺ progenitors [34], so the response of these populations to Flt3L was investigated. The findings presented in this chapter indicate that any Flt3L-mediated instruction away from the MegE lineage would be predominantly driven from the LSK CD150⁻ CD48⁻ MPP compartment, and not from the HSC compartment.

Recent studies have reported that non-self-renewing multipotent cells, rather than HSCs, are the main drivers of blood production during steady-state haematopoiesis. This highlights the importance of Flt3L as a regulator of GM-lymphoid development at the MPP stage. Busch *et al.* have used a mouse model, whereby tamoxifen administration induces the expression of the yellow fluorescent protein (YFP) in *Tie2*⁺ HSCs (LSK CD150⁺ CD48⁻), to describe the kinetics of HSPC differentiation *in situ* [382]. By monitoring the development of YFP⁺ cells through various haematopoietic progenitor stages, the authors observed that only a small percentage (approximately 30%) of HSCs were active, and, on an average, 1 in 110 HSCs gave rise to a LSK CD150⁻ CD48⁻ cell per day. On the other hand, populations of upstream progenitors were maintained through proliferation and had a much higher rate of differentiation. For example, a single LSK CD150⁻ CD48⁺ cell gave rise to 4 CMPs per day, and the net proliferation rate of this compartment was over 30-fold higher than that of the HSC compartment. Similarly, Sun *et al.* monitored the contribution of individual HSPCs to the haematopoietic system by using a temporarily inducible hyperactive 'Sleeping Beauty' transposase mouse model [383]. Doxycycline induction of the hyperactive Sleeping Beauty transposase results in the mobilisation of a specific transposon within the genome. Due to the variable nature of transposon insertion, individual cells and its progeny could be identified based on unique patterns of genomic transposition. By sequencing the genome of single mature

haematopoietic cells at a number of time points after hyperactive Sleeping Beauty transposase induction, the authors revealed that production of mature cells was mostly driven by large pools of progenitors, and not HSCs.

While these studies implicate an important role for MPPs, and therefore Flt3L, during steady-state haematopoiesis, further investigation is required to determine how Flt3L might regulate MPP development towards non-MegE fates. As discussed in **Section 3.7.3**, previous findings indicate that currently defined HSPC compartments are not homogeneous populations with mixed state progenitors, but contain a number of distinct lineage-biased or lineage-restricted progenitors [24, 304, 332]. LSK CD150⁻ CD48⁻ MPPs robustly reconstitute platelets and erythroid cells *in vivo* [22, 34]. However, this compartment can be divided into Flt3⁻ and Flt3⁺ fractions, and studies have yet to characterise these two populations to determine their lineage potential. For Flt3L responses to cause a significant decrease in MegE progenitor development, then the Flt3⁺ MPP population would need to possess substantial potential for this lineage. While the Flt3^{hi} fraction of the LSK compartment minimally contributes to the megakaryocyte lineage [334], the Kondo group has shown that Flt3^{lo} LSK cells can give rise to CMPs and MEPs indicating significant MegE potential [324]. Hence, Flt3L might act on the Flt3^{lo} fraction of the LSK CD150⁻ CD48⁻ MPP compartment to instruct lineage fate. Further study of the Flt3⁺ and Flt3⁻ LSK CD150⁻ CD48⁻ compartments will be required to confirm this.

Ultimately, this chapter clearly shows Flt3L stimulates a large response in LSK CD150⁻ CD48⁻ MPPs, and not in LSK CD150⁺ CD48⁻ HSCs, suggesting that the Flt3L response seen in Flt3L-Tg mice might be related to the LSK CD150⁻ CD48⁻ compartment. As Flt3 is differentially expressed by cells within this population, further studies will be required to confirm whether Flt3L acts to instruct the development of multipotent cells away from a MegE fate, or if Flt3L

acts on a subpopulation of lineage-restricted/biased progenitors with limited MegE potential. Lastly, while *FLT3* and its encoded protein are present within the HSC compartment [34, 323, 329], **Figure 3.17** and **Figure 3.27**, the role and/or function of Flt3⁺ LSK CD150⁺ CD48⁻ is still not entirely clear. Isolation and characterisation of Flt3⁺ LSK CD150⁺ CD48⁻ cells might provide further insight into the relationship between Flt3 and self-renewal.

CHAPTER 5: CONCLUSIONS

5.1 Final Discussion

Various studies, carried out since the 1980s, have provided contradictory evidence regarding the role of HGFs in the lineage commitment of HSPCs. Some studies support a permissive action of HGFs, whereby these factors provide proliferative and survival cues to permit the stochastic lineage-specification of HSPCs. Other studies support a deterministic model in which HGFs act on HSPCs to influence their commitment towards a particular lineage fate. Early evidence for these two very different models was obtained from the analysis of ectopic expression of growth factor receptors, transgenic ligand/receptor knock-out mouse models and studies that investigated the effects of growth factors on the commitment of paired progenitor daughter cells. Given the conflicting data from such early studies, the effects of growth factors on HSPCs lineage commitment was largely unclear at the time.

The recent use of single cell analysis and real-time bioimaging techniques has provided strong support for a deterministic role of HGFs. In 2009, Rieger *et al.* demonstrated, for the first time using unmanipulated progenitor cells, that G-CSF and M-CSF can instruct bipotent GMPs to become granulocytes and macrophages, respectively [268]. As both cell death and differentiation were monitored at the single cell level, the data firmly argue against the permissive action of G-CSF and M-CSF. M-CSF has also been shown to drive single HSCs towards a GM fate *via* upregulation of PU.1 [267]. Similarly, Pietras *et al.* have reported that IL-1 acts on HSCs to stimulate PU.1 expression and drive their maturation towards the GM lineage [175]. In 2014, Grover and colleagues demonstrated that Epo induces the expression of erythroid-associated genes in single LSK CD150⁺ Flt3⁻ progenitors, and promotes

differentiation towards an erythroid fate [269]. Finally, work by the Rolink group suggests that Flt3L drives multipotent progenitors towards a lympho-GM fate at the expense of MegE development [288]. As a result of these studies, the deterministic model of haematopoiesis has become more popular in recent years.

In a deterministic model of haematopoiesis in which HSPC lineage specification is regulated by cell-extrinsic factors, one would expect receptors for such factors to be co-expressed on the surface of HSPCs. This would allow for the lineage output of HSPCs to be modulated based on the availability of each instructive factor. However, there is evidence to suggest that HGF receptors are expressed by subpopulations of multipotent HSPCs and not to any appreciable extent co-expressed [115, 116, 304]. For example, Miyamoto *et al.* have reported that *CSF3R* and *EPOR* are variably expressed by the LSK CD34⁻ Thy1.1^{lo} HSC compartment, and that *CSF3R* and *EPOR* are rarely co-expressed in these cells [116]. Similarly, Hu *et al.* have demonstrated that the genes encoding the CSF receptors are rarely co-expressed with *EPOR* in FDCP-mix and mouse CD34⁺ Lin⁻ BM cells [115]. Analysis of individual cells following treatment with M-CSF, Epo and IL-1 have also demonstrated that these factors act on some, but not all, cells within early HSPC compartments [175, 268, 269].

While these reports have provided some insight into the selective expression of growth factor receptor genes during haematopoiesis, it is unclear to what extent co-expression of growth factor receptor genes and proteins occurs in currently defined multipotent compartments. Furthermore, single cell analysis has not been used to investigate how expression of these receptors changes as multipotent cells make a transition from a quiescent to a proliferative state and begin to commit towards a particular lineage(s). Hence, the purpose of this study was to generate a comprehensive map of growth factor receptor expression during

haematopoiesis, and determine whether co-expression of HGF receptors regularly occurs in the LT-HSC, ST-HSC and MPP compartments.

Using single-cell analysis techniques, Flt3, EpoR and M-CSFR were shown to be expressed to a varying degree in almost all HSPC compartments (**Figure 3.17** and **Figure 3.27**). The expression patterns of these receptors identified a number of novel and distinct HSPC subpopulations, including subpopulations within the LT-HSC, ST-HSC and MPP compartments. As quiescent LT-HSCs transitioned into a more proliferative MPP phenotype, the expression of Flt3, EpoR and M-CSFR primarily occur at different stages of development, indicating that the ligands for these receptors regulate haematopoiesis at different stages of multipotent cell maturity. Notably, multiplex analysis revealed that co-expression of these receptors is uncommon within the multipotent compartments, though co-expression of M-CSFR and Flt3 increases as HSCs differentiated into MPPs. Finally, as Flt3 was detected within the HSC compartment, it was investigated whether LSK CD150⁺ CD48⁻ cells could respond to Flt3L, or if this ligand predominantly acts on LSK CD150⁻ CD48⁻ MPPs. No signalling, transcriptional or cellular responses were detected when HSCs were cultured with Flt3L. A large response was observed within the LSK CD150⁻ CD48⁻ MPP compartment following stimulation of Flt3, suggesting that Flt3L predominantly acts further upstream than M-CSF and Epo (**Figure 4.7**). However, this study may underestimate the number of Flt3⁺ cells within the HSC compartment. The techniques used in this study may not have been sensitive enough to identify HSCs that express very few Flt3 proteins on their surface (further discussed below).

The data generated in this study indicate that Epo, M-CSF and Flt3L primarily regulate haematopoiesis by acting on distinct subpopulations of early HSPCs that selectively express particular growth factor receptors. Therefore, these findings support a permissive rather than

deterministic role of Epo, M-CSF and Flt3L within the multipotent compartment of the BM. This is surprising considering the findings of Rieger and colleagues [268]. M-CSF and G-CSF were shown to stimulate bipotent GMPs to differentiate towards macrophage and granulocyte fates, respectively. By tracking cell death using real-time imaging, Rieger *et al.* demonstrated that this response was not due to the selective expansion of distinct unilineage subpopulations, indicating that M-CSFR and G-CSFR are co-expressed by committed progenitors [268]. Additionally, Hu *et al.* have shown that the genes encoding M-CSFR, GM-CSFR and G-CSFR are commonly co-expressed by individual mouse Lin⁻ CD34⁺ BM cells [115]. On the other hand, past studies that have investigated multilineage gene expression in early HSPCs have rarely observed the co-expression of *EPOR* and genes encoding GM-associated growth factor receptors (*CSF1R*, *CSF2R* or *CSF3R*) [115, 116]. The extent to which HGF receptors are co-expressed by HSPCs is still a matter of debate. However, evidence suggests that some HSPCs might co-express receptors that are associated with lineages that are closely related, such as the granulocyte and macrophage lineages. The expression of G-CSFR by early HSPCs was not investigated in **Chapter 3**, and therefore, it is uncertain whether M-CSFR and G-CSFR are co-expressed by multipotent cells.

As to co-expression of receptors, the results from this study showed that Flt3 and M-CSFR (**Figure 3.31**) are more commonly co-expressed by early HSPCs than *FLT3* and *EPOR* (**Figure 3.24**). When analysing Flt3 and M-CSFR expression, $1.12\% \pm 0.48$, $2.8\% \pm 0.7$ and $9.9\% \pm 1.9$ of LT-HSCs, ST-HSCs and MPPs were found to co-express both receptors. When the LT-HSC and MPP compartments were analysed for *FLT3* and *EPOR* expression, a total of 284 cells were interrogated and co-expression of *FLT3* and *EPOR* was not detected. Of the 139 ST-HSCs analysed, only 2 cells were found to co-express *FLT3* and *EPOR*. Flt3 and M-CSFR are both

important for the development of myelomonocytic cells, while Flt3 and EpoR signalling regulate distinct lineages [384, 385]. Therefore, in light of the findings of this study, it is possible that if co-expression of HGF receptors does occur, certain combinations are more likely than others.

As discussed in detail in **Section 3.7**, the selective expression of particular HGF receptors may mark distinct lineage-biased or lineage-restricted subpopulations within HSPCs compartments. Functionally distinct subpopulations within currently defined HPC compartments, such as CMP, LMPP and CLP, have been isolated based on the expression of growth factor receptors [77, 304, 311]. This suggests the selective expression of such receptors within more primitive HSPC compartments might identify novel lineage-biased or lineage-restricted cells. Indeed, certain HGFs have been shown to differentially regulate distinct lineage-biased HSC subpopulations and their progeny. Platelet-biased vWF^+ HSCs but not vWF^- HSCs are dependent on Tpo [29]. TGF- β 1 positively regulates MyHSCs but inhibits the proliferation of LyHSCs [25]. The lymphoid progeny of MyHSCs are unresponsive to IL-7 and express lower levels of *IL7R* when compared to LyHSC-derived lymphoid progenitors. Furthermore, evidence suggest that lineage-specification occurs within early HSPC populations. A number of studies have identified lineage-restricted progenitors within the HSC compartment, including long-term repopulating CMRPs, MkRPs and MERPs [23, 24]. Other studies have shown that currently defined HPCs are heterogeneous populations containing a mixture of unilineage and bipotent progenitors, indicating that lineage commitment occurs upstream of the HPC compartments. [24, 304, 332]. For example, Paul *et al.* have demonstrated that the CMP compartment of the mouse BM contains at least 19 transcriptionally distinct progenitor populations, including those restricted to the megakaryocyte, erythrocyte, monocyte,

basophil and DC fates [304]. The findings shown in **Figure 3.17** and **Figure 3.27** further support this viewpoint, as a number of late HPC populations, such as CMP and LMPP, were observed to be heterogeneous as to their expression of at least one HGF receptor.

If selective upregulation of particular receptors indicates an early stage in the maturation of a cell toward a particular lineage, then the findings from this study will be useful for the isolation and characterisation of the lineage-biased and/or lineage committed cells within the early HSPC compartments. For example, $8.2\% \pm 4.6$ of MPPs expressed *EPOR*, while *Flt3* and *M-CSFR* were expressed on the surface of $63.65\% \pm 3$ and $13.4\% \pm 2.5$ of MPPs, respectively. A large proportion of *M-CSFR*⁺ MPPs also expressed *Flt3* ($69.17\% \pm 3.29$ of *M-CSFR*⁺ MPPs were *Flt3*⁺). On the other hand, no *Epor*⁺ cells were found to co-express *FLT3*. This suggests the existence of at least 5 distinct subpopulations within the MPP compartment based on the expression of these three receptors; *Flt3*⁺ *M-CSFR*⁻ MPPs, *Flt3*⁻ *M-CSFR*⁺ MPPs, *Flt3*⁺ *M-CSFR*⁺ MPPs, *EpoR*⁺ MPPs and MPPs that do not express any of these receptors on their surface.

Given that *Flt3* is associated with DC, granulocyte, monocyte and lymphoid development [288], the *Flt3*⁺ *M-CSFR*⁻ MPP fraction may represent a population of GM-lymphoid biased cells. *M-CSFR* is important in the development of GM cells. Thus, *Flt3*⁻ *M-CSFR*⁺ MPPs might be biased towards a GM fate. The *Flt3*⁺ *M-CSFR*⁺ population may display a lineage-potential somewhere between these two, while *EpoR*⁺ MPPs might be biased towards the erythroid lineage. The isolation and characterisation of such MPP subpopulations will be required to confirm whether they display such distinct lineage potentials (**Figure 5.1**).

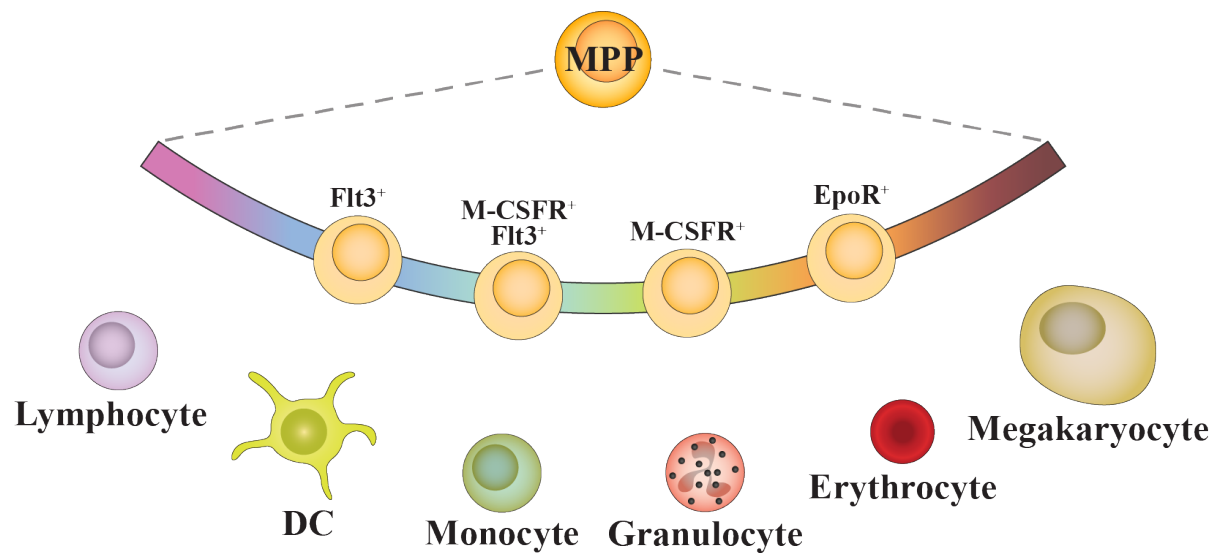


Figure 5.1. Selective expression of haematopoietic growth factors within the MPP compartment. Recent evidence suggests that currently defined HSPC populations contain a number of distinct subpopulations that express different lineage-potentials. During this study, Flt3^+ M-CSFR^- , Flt3^+ M-CSFR^+ , Flt3^+ M-CSFR^+ and EpoR^+ subpopulations were identified within the $\text{LSK CD150}^- \text{CD48}^-$ MPP compartment of the BM, suggesting that these phenotypes mark distinct lineage-restricted and/or lineage-biased subpopulations. The isolation and characterisation of the lineage potentials of these cell fractions will be required to confirm this. MPP, multipotent progenitor; EpoR, erythropoietin receptor; M-CSFR, macrophage-colony stimulating factor; Flt3, fms-like tyrosine kinase 3.

Although the data described in this thesis indicates that Flt3, EpoR and M-CSFR are primarily selectively expressed during the early stages of haematopoiesis, there is still a large amount of data that supports a deterministic model of haematopoiesis. It is possible that some early HSPCs express a very small number of HGF receptor molecules on their surface, resulting in an underestimate of the number of Flt3^+ and M-CSFR^+ cells within the HSC and MPP compartments. McKinstry *et al.* have estimated that less than 100 molecules of HGF receptors, such as G-CSF and M-CSF, are expressed on the surface of early HSPCs [374], which is well below the limit of detection of conventional flow cytometry [367]. Additionally, gene expression does not always correlate to protein expression, so the expression of *EPOR* might not accurately represent the number of early HSPCs that express functional EpoR protein. It

is also possible that co-expression of other HGF receptors is commonplace during haematopoiesis. As highlighted above, there is evidence to suggest that HSPCs co-express certain receptors, such as M-CSFR and G-CSFR. Co-expression of such receptors may help HSPCs to choose between closely related fates.

Even if HGF receptors are selectively expressed by multipotent cells, their activation may still provide instructional cues to cells that might otherwise still have the capacity to generate all cell types in a balanced fashion. This is supported by the findings of Mossadegh-Keller and co-workers [267]. The group cultured LSK CD150⁺ CD34⁻ Flt3⁻ cells in the presence of M-CSF, and reported that M-CSF is capable of upregulating PU.1 in a large number of these cells. Transplantation of M-CSF-stimulated PU.1⁺ HSCs into irradiated hosts revealed that, although these cells were multipotent, their development was skewed towards the GM lineage. However, after 6 weeks, this bias had disappeared and the contribution of these cells to other lineages had become comparable to the lineage-output of unstimulated HSCs. These findings indicate that M-CSF-responsive cells are not permanently biased towards the GM lineage. Rather, M-CSF had temporarily skewed the development of these cells.

There are a number of caveats to the conclusion that HGFs do not play a deterministic role, as a number of additional factors need to be taken into consideration. Studies have shown that a high concentration of a particular HGF is required to elicit the lineage commitment of HSPCs [267, 269, 288]. This suggests that signalling below a certain threshold, due to low growth factor availability or a low level of receptor expression, does not mediate lineage instruction. There is also evidence to suggest that HGFs regulate lineage-specification in a dose-dependent manner. Metcalf has reported that low concentrations of GM-CSF promote the differentiation of GM-CFU daughter cells towards a myeloid fate, while high

concentrations promote a granulocyte fate [257]. Similarly, Kulesa *et al.* have reported that there is a relationship between the levels of Gata-1 expressed by a cell and its lineage potential [386]. For example, the group ectopically expressed GATA-1 in a macrophage cell line and demonstrated that these cells were transformed into three distinct cell types. Low levels of GATA-1 expression were shown to transform these cells into myeloblasts, intermediate levels induced an eosinophilic fate and high expression levels of GATA-1 promoted their transformation into erythroblasts. As Epo has been shown to induce expression of GATA-1 [269], these findings suggest that Epo may regulate lineage commitment in a dose-dependent fashion.

The Sieweke group has proposed that the ability of HGFs to regulate lineage commitment is reliant on the intrinsic state of the target cell [387]. Sarrazin *et al.* have demonstrated that MafB expression regulates HSC sensitivity to M-CSF-mediated lineage instruction [388]. The authors reported that MafB^{-/-} LSK cells proliferate at a much higher rate and produce significantly more GM cells in response to M-CSFR stimulation when compared to WT HSCs. Ectopic expression of MafB in an M-CSFR-transduced T-lymphocyte cell line prevented these cells from proliferating in the presence of M-CSF. However, their response to IL-7 was unaffected. Furthermore, using a *PU.1:GFP* reporter model, it was shown that an increased number of MafB^{-/-} LSK Flt3⁻ cells upregulated PU.1 in the presence of M-CSF when compared to WT cells. Oburoglu *et al.* have also shown that Epo-mediated erythroid specification in CD34⁺CD38⁻ hHSCs is sensitive to the availability of cell metabolites [289]. The group reported that blocking glutaminolysis in Epo-stimulated hHSCs abrogated erythroid output and promoted differentiation towards a GM fate. Conversely, inhibiting glycolysis enhanced Epo-mediated erythropoiesis. These studies highlight the importance of cell-intrinsic mechanisms

in regulating the sensitivity of cells to instructive cues.

The findings of Sarrazin *et al.* [388] and Oburoglu *et al.* [289] may explain the contradictory evidence that has been generated from studies that have reported on the ectopic expression of HGF receptors. For example, ectopic expression of GM-CSFR by pro-T-lymphocytes and CLPs restores GM potential in these cells [275, 389]. However, enforced expression of GM-CSFR in pro-B-lymphocytes or MEPs does not restore GM potential [389]. Future studies of HGFs will need to consider receptor signalling thresholds and the intrinsic state of target cells when investigating their role in lineage commitment. Specifically, characterisation of relevant intrinsic factors will help to determine the mechanisms that regulate the sensitivity of certain cells to HGF signalling.

To further explore how HGFs regulate lineage commitment during haematopoiesis, the factors that control the expression of their receptors will need to be determined. There is evidence to suggest that some HGF receptors are upregulated following the activation of other growth factor receptor signalling cascades. IL-1 has been shown to stimulate the upregulation of the genes encoding GM-CSFR and M-CSFR in HSCs [175]. M-CSF induces expression of PU.1 in HSCs [267], and *FLT3* is a target of PU.1 [368], suggesting that M-CSFR signalling upregulates Flt3 expression. It has also been reported that expression of particular growth factor receptors can be induced during periods of stress, allowing HSPCs to adapt to the requirements of the host. Chen *et al.* have reported that type I interferon, a cytokine produced during infection [390], stimulates the upregulation of Flt3 on the surface CLPs [373]. A number of studies have also demonstrated that EpoR expression is regulated by oxygen tension [391-393]. In mice embryos lacking the hypoxia-sensitive α subunit of hypoxia-inducible factor-1, *EPOR* expression is decreased, and erythropoiesis is significantly impaired

[394].

A further consideration is that the selective expression of HGFs may occur as a result of gene expression noise. While popularity for a stochastic model of haematopoiesis has faded over recent years, gene expression noise is an intrinsic property of many biological systems. Chang *et al.* have demonstrated that transcriptional noise can mediate the transition of HSPC populations through lineage-biased metastable states [118]. These transitions can lead to changes in the expression of cell surface proteins and lineage-associated TFs, such as PU.1 and GATA-1. In turn, PU.1 and GATA-1 have been shown to upregulate the expression of M-CSFR [395] and EpoR [396], respectively, so this suggests that expression of HGF receptors might be affected by stochastic fluctuations in gene transcription. However, the viewpoint that PU.1 and GATA-1 are co-expressed in multipotent HSPCs has been recently challenged [138], so it remains to be seen if the findings of Chang *et al.* are relevant to the lineage commitment processes that occur *in vivo* [118]. Even so, though it is evident that a number of different factors regulate the expression of HGFs, it is unclear how they contribute towards the selective expression of such receptors by distinct HSPCs subpopulations.

Ultimately, while there is strong evidence to suggest that cell-extrinsic factors play a role in regulating lineage commitment during haematopoiesis, the results obtained from this study indicate that aspects of a selective model still hold true. In a selective model whereby HSPCs can differentiate towards certain lineage fates based on selective growth factor expression, it is unlikely that this lineage-specification arises in a stochastic manner. Progressive lineage commitment of HSPCs does not occur randomly. Only particular cell-fate combinations are possible. For example, progenitors with granulocyte and macrophage potential exist, but a bipotent progenitor with megakaryocyte and T-lymphocyte potential has not been described.

There is still more work to be done to truly identify the mechanisms that regulate lineage commitment during haematopoiesis. However, this study has provided an insight into the expression patterns of HGF receptors by HSPCs and has revealed several novel findings. Firstly, the observation that early HSPCs rarely co-express Flt3, M-CSFR and/or EPOR adds further complexity to the debate regarding the role of HGFs in the lineage-specification of HSPCs. It appears that simply defining lineage specification using either a deterministic or selective model of haematopoiesis is impractical; the findings from this study, taken together with previous studies, suggest that HGFs regulate haematopoiesis in both a selective and deterministic manner. Secondly, Flt3, EpoR, M-CSFR are predominantly expressed by distinct subpopulations within the multipotent compartment of the BM, and can be used to identify small subfractions of cells within progenitor populations. As discussed before, it is possible that these receptors can be used to isolate lineage-biased and restricted progenitors within currently defined HSPC compartments. Thirdly, Flt3 is expressed within the HSC compartment of the adult mouse BM. However, it is currently unclear what relevance this has, and the studies carried out here indicate that Flt3L primarily acts on upstream MPPs.

These findings are important, as their translation to human haematopoiesis will be useful for the advancement of clinical therapies. Firstly, understanding how HGFs regulate HSPC differentiation will help to improve a number of haematological therapies. For example, *in vitro* manipulation of HSPCs for the purpose of cell manufacturing, such as erythrocytes and platelets for transfusions, will benefit from a greater understanding of lineage specification during haematopoiesis. Similarly, if HGF receptor expression marks lineage-biased/restricted HSPCs in humans, then these receptors could be used for the isolation of cells that are highly efficient at producing particular cell types. It is also important to consider the effects of HGF

on HSPCs in currently used therapies, such as the use of G-CSF to harvest hHSC for stem cell transplants. If G-CSF induces a granulocyte bias (as M-CSF induces a temporary GM bias [267]) in HSPCs, does this result in an increased production of granulocytes in the recipient during the early stages of recovery? Alternatively, if G-CSF selects for a subpopulation of HSCs, then do recipients receive a long-term granulocyte-biased transplant? As infection is a severe complication of BM transplantation [397], an increased production in granulocytes following the procedure would be favoured as to avoid post-transplantation infections. However, this is an important consideration so that we understand the physiological mechanisms that underlie this therapy. Finally, as mentioned previously, if Flt3 is expressed on the surface of mouse HSCs, then this would make Flt3-ITD mouse models even more relevant to the study of acute myeloid leukaemia than currently thought.

Further work is required to fully elucidate how selective growth factor receptor expression is regulated and, as highlighted above, how the intrinsic state of target cells affects lineage instruction. Specifically, the isolation and characterisation of distinct HSPC subpopulations based on the expression of HGF receptors will be important to investigate the mechanism(s) that underlies fate determination during haematopoiesis. The work carried out here is an important step towards understanding such processes.

5.2 Future Directions

Whilst the findings from this study provide an insight into the selective expression and co-expression of HGF receptors by HSPCs, a lot more work is required to understand the significance of these patterns of HGF receptor expression and how they emerge. To determine the significance of selective HGF receptor expression within HSPC compartments,

Flt3⁺, M-CSFR⁺ and EPOR⁺ cells within each BM compartment should be isolated and characterised. It will be of interest to perform *in vitro* colony forming assays and *in vivo* reconstitution assays to determine the lineage potential and self-renewal capacity of these cells. Additional analysis, such as the use of single cell gene expression assays, will help to identify the functional and transcriptional properties of these cells. These approaches will confirm whether or not selective expression of HGF receptors marks lineage-biased/restricted progenitors, especially within the early HSPC compartments. Specifically, the characterisation of Flt3⁺ cells within the LSK CD150⁺ CD48⁻ compartment is of particular interest, as it is important to determine whether a small population of HSCs express functional Flt3, or if this receptor marks non-self-renewing progenitors within the compartment.

It is also important to determine if the findings reported here accurately reflect the expression patterns of other HGF receptors. Initially, it would be advantageous to analyse the expression of a large number of other HGF receptors, such as G-CSF, GM-CSF, TPO and IL-1R, using a single cell gene chip. The findings from this could then be later confirmed using more sensitive multiplex qRT-PCR analysis and protein expression analysis. Any subpopulations identified from this approach would then be isolated and characterised as described above.

Lastly, most studies of HGF function in HSPC lineage specification have focused on the effects of a single growth factor or a high concentration of growth factor on HSPCs differentiation. However, it is likely that this does not truly represent the physiological environment within the HSPC niches. It will be important for future studies to investigate the effects of stimulating multiple HGF signalling pathways in HSPCs. For example, it would be interesting to assess how early Flt3⁺ M-CSFR⁺ HSPCs respond to stimulation with Flt3L and M-CSF in combination when compared to stimulation with only one of these growth factors, as this would more accurately

represent what occurs in the BM microenvironment.

APPENDIX A: MATERIALS

All materials used during this project are listed in **Table 14**.

Table 14: Materials used during study

Agar Scientific	Square covergals (15x15mm)
BD Biosciences	See Table 15 for antibodies purchased from BD Biosciences.
Biolegend	See Table 15 for antibodies purchased from Biolegend. Recombinant mouse Flt3 ligand (carrier-free)
Biosearch Technologies	All primers and probes (as listed in Table 3) were purchased from Biosearch Technologies
eBiosciences	See Table 15 for antibodies purchased from eBiosciences
Greiner	Sterile 96-well plates, V-bottomed
Innova Biosciences	Lightning-Link Allophycocyanin Kit
Peprtech	Recombinant murine thrombopoietin Recombinant murine stem cell factor
Qiagen	QuantiTect Multiplex RT-PCR Kit
Roche	LightCycler 480 multiwell plate 384, white RealTime ready RNA Virus Master LightCycler Multiplex RNA Virus Master
Sigma Aldrich	Dulbecco's Phosphate-Buffered Saline without Ca^{2+} Mg^{2+} Fetal Calf Serum (Heat inactivated) EDTA Acetone Methanol
StemCell Technologies	MethoCult GF M3434 60mm Gridded Scoring Dish
Sysmex	Partec CellTrics Sterile Filters
Thermo Fisher Scientific	ACK Lysis buffer Iscove's Modified Dulbecco's Medium (With phenol red) Penicillin/Streptomycin Twin frosted microscope slides
VWR International	Cytology funnel 8-tube strips PCR tubes, individually attached domed caps

PCR, polymerase chain reaction; Flt3, fms-like tyrosine kinase.

APPENDIX B: ANTIBODIES

All antibodies used during this project are listed in **Table 15**.

Table 15: Monoclonal antibodies used for flow cytometric analysis

Specificity	Isotype	Clone	Source	Conjugate	Dilution
Lin Cocktail	-	-	eBiosciences	FITC	1/10
CD3	Rat IgG2b, κ	17A2	BioLegend	AF488	1/100
CD11b	Rat IgG2b, κ	M1/70	BioLegend	AF488	1/200
B220/CD45R	Rat IgG2a, κ	RA3-6B2	BioLegend	AF488	1/100
TER-119	Rat IgG2b, κ	TER-119	BioLegend	AF488	1/400
Gr-1	Rat IgG2b, κ	RB6-8C5	BioLegend	AF488	1/200
CD11b	Rat IgG2b, κ	M1/70	BioLegend	AF488	1/200
CD48	Ar Ham IgG1	HM48-1	BioLegend	AF488	1/200
CD71	Rat IgG2a, λ	R17217	eBiosciences	PE	1/200
CD16/32	Rat IgG2a, λ	93	BioLegend	PE	1/200
CD150	Rat IgG2a, λ	TC15-12F12.2	BD Biosciences	PE	1/50
IL-7R α (CD127)	Rat IgG2a, κ	A7R34	eBiosciences	PE	1/50
Flt3 (CD135)	Rat IgG2a, κ	A2F10	eBiosciences	PE	1/100
pS6	Rb IgG	D57.2.2E	Cell Signalling	PE	1/50
Flt3 (CD135)	Rat IgG2a, κ	A2F10.1	BD Biosciences	PE-CF594	1/200
c-Kit (CD117)	Rat IgG2b, κ	2B8	BD Biosciences	PE-CF594	1/400
Sca1 (Ly-6a)	Rat IgG2a, κ	D7	eBiosciences	PE-Cy5	1/100
IL-7R α (CD127)	Rat IgG2a, κ	A7R34	BioLegend	PE-Cy5	1/200
CD150	Rat IgG2a, λ	TC15-12F12.2	BioLegend	PE-Cy5	1/100
Sca1 (Ly-6a)	Rat IgG2a, κ	D7	eBiosciences	PCP-Cy5.5	1/100
CD48	Ar Ham IgG	HM48-1	BD Biosciences	PE-Cy7	1/200
Sca1 (Ly-6a)	Rat IgG2a, κ	D7	eBiosciences	PE-Cy7	1/100
IL-7R α (CD127)	Rat IgG2a, κ	A7R34	eBiosciences	PE-Cy7	1/50
CD115	Rat IgG2a, κ	AFS98	BD Biosciences	BV421	1/200
CD16/32	Rat IgG2a, λ	93	BioLegend	BV421	1/200
CD150	Rat IgG2a, λ	TC15-12F12.2	BioLegend	PB	1/50
IL-3R (CD123)	Rat IgG2a, κ	5B11	eBiosciences	APC	1/50
Sca1 (Ly-6a)	Rat IgG2a, κ	D7	eBiosciences	APC	1/100
CD34	Rat IgG2a, λ	RAM34	eBiosciences	eFluor 660	1/50
CD48	Ar Ham IgG1	HM48-1	BioLegend	APC-Cy7	1/200
CD114	Rat IgG2A	723806	R&D Systems	Purified	-

Lin, lineage; Ar Ham, Armenian hamster; AF488, alexa fluor 488; pS6, phospho-S6 ribosomal protein; PB, pacific blue; IL-7R, interleukin-7 receptor α subunit; IL-3R, interleukin-3 receptor; Flt3, fms-like tyrosine kinase 3; APC, allophycocyanin.

REFERENCES

1. Murphy, K., et al., *Janeway's immunobiology*. 8th ed. 2012, New York: Garland Science. xix, 868 p.
2. Davies, L.C. and P.R. Taylor, *Tissue-resident macrophages: then and now*. Immunology, 2015. **144**(4): p. 541-8.
3. Franco, C.B., et al., *Distinguishing mast cell and granulocyte differentiation at the single-cell level*. Cell Stem Cell, 2010. **6**(4): p. 361-8.
4. Schulze, H. and R.A. Shivdasani, *Mechanisms of thrombopoiesis*. J Thromb Haemost, 2005. **3**(8): p. 1717-24.
5. Tsiftoglou, A.S., I.S. Vizirianakis, and J. Strouboulis, *Erythropoiesis: model systems, molecular regulators, and developmental programs*. IUBMB Life, 2009. **61**(8): p. 800-30.
6. Garraud, O. and F. Cognasse, *Are Platelets Cells? And if Yes, are They Immune Cells?* Front Immunol, 2015. **6**: p. 70.
7. Morera, D. and S.A. MacKenzie, *Is there a direct role for erythrocytes in the immune response?* Vet Res, 2011. **42**: p. 89.
8. Ishikawa, F., et al., *The developmental program of human dendritic cells is operated independently of conventional myeloid and lymphoid pathways*. Blood, 2007. **110**(10): p. 3591-660.
9. Naik, S.H., et al., *Diverse and heritable lineage imprinting of early haematopoietic progenitors*. Nature, 2013. **496**(7444): p. 229-32.
10. Spangrude, G.J., S. Heimfeld, and I.L. Weissman, *Purification and characterization of mouse hematopoietic stem cells*. Science, 1988. **241**(4861): p. 58-62.
11. Okada, S., et al., *In vivo and in vitro stem cell function of c-kit- and Sca-1-positive murine hematopoietic cells*. Blood, 1992. **80**(12): p. 3044-50.
12. Coffman, R.L. and I.L. Weissman, *B220: a B cell-specific member of the T200 glycoprotein family*. Nature, 1981. **289**(5799): p. 681-3.
13. Kanelloupolous, J.M., et al., *Biosynthesis and molecular nature of the T3 antigen of human T lymphocytes*. EMBO J, 1983. **2**(10): p. 1807-14.
14. Metlay, J.P., et al., *The distinct leukocyte integrins of mouse spleen dendritic cells as identified with new hamster monoclonal antibodies*. J Exp Med, 1990. **171**(5): p. 1753-71.
15. Fleming, T.J., M.L. Fleming, and T.R. Malek, *Selective expression of Ly-6G on myeloid lineage cells in mouse bone marrow. RB6-8C5 mAb to granulocyte-differentiation antigen (Gr-1) detects members of the Ly-6 family*. J Immunol, 1993. **151**(5): p. 2399-408.
16. Kina, T., et al., *The monoclonal antibody TER-119 recognizes a molecule associated with glycophorin A and specifically marks the late stages of murine erythroid lineage*. Br J Haematol, 2000. **109**(2): p. 280-7.
17. Miller, C.L., B. Dykstra, and C.J. Eaves, *Characterization of mouse hematopoietic stem and progenitor cells*. Curr Protoc Immunol, 2008. **Chapter 22**: p. Unit 22B.2.
18. Morrison, S.J. and I.L. Weissman, *The long-term repopulating subset of hematopoietic stem cells is deterministic and isolatable by phenotype*. Immunity, 1994. **1**(8): p. 661-73.

19. Adolfsson, J., et al., *Upregulation of Flt3 expression within the bone marrow Lin(-)Sca1(+)-kit(+) stem cell compartment is accompanied by loss of self-renewal capacity*. Immunity, 2001. **15**(4): p. 659-69.
20. Christensen, J.L. and I.L. Weissman, *Flk-2 is a marker in hematopoietic stem cell differentiation: a simple method to isolate long-term stem cells*. Proc Natl Acad Sci U S A, 2001. **98**(25): p. 14541-6.
21. Yang, L., et al., *Identification of Lin(-)Sca1(+)-kit(+)-CD34(+)-Flt3- short-term hematopoietic stem cells capable of rapidly reconstituting and rescuing myeloablated transplant recipients*. Blood, 2005. **105**(7): p. 2717-23.
22. Kiel, M.J., et al., *SLAM family receptors distinguish hematopoietic stem and progenitor cells and reveal endothelial niches for stem cells*. Cell, 2005. **121**(7): p. 1109-21.
23. Yamamoto, R., et al., *Clonal analysis unveils self-renewing lineage-restricted progenitors generated directly from hematopoietic stem cells*. Cell, 2013. **154**(5): p. 1112-26.
24. Notta, F., et al., *Distinct routes of lineage development reshape the human blood hierarchy across ontogeny*. Science, 2016. **351**(6269): p. aab2116.
25. Challen, G.A., et al., *Distinct hematopoietic stem cell subtypes are differentially regulated by TGF-beta1*. Cell Stem Cell, 2010. **6**(3): p. 265-78.
26. Beerman, I., et al., *Functionally distinct hematopoietic stem cells modulate hematopoietic lineage potential during aging by a mechanism of clonal expansion*. Proc Natl Acad Sci U S A, 2010. **107**(12): p. 5465-70.
27. Morita, Y., H. Ema, and H. Nakauchi, *Heterogeneity and hierarchy within the most primitive hematopoietic stem cell compartment*. J Exp Med, 2010. **207**(6): p. 1173-82.
28. Lu, R., et al., *Tracking single hematopoietic stem cells in vivo using high-throughput sequencing in conjunction with viral genetic barcoding*. Nat Biotechnol, 2011. **29**(10): p. 928-33.
29. Sanjuan-Pla, A., et al., *Platelet-biased stem cells reside at the apex of the haematopoietic stem-cell hierarchy*. Nature, 2013. **502**(7470): p. 232-6.
30. Gekas, C. and T. Graf, *CD41 expression marks myeloid-biased adult hematopoietic stem cells and increases with age*. Blood, 2013. **121**(22): p. 4463-72.
31. Shimazu, T., et al., *CD86 is expressed on murine hematopoietic stem cells and denotes lymphopoietic potential*. Blood, 2012. **119**(21): p. 4889-97.
32. Shin, J.Y., et al., *High c-Kit expression identifies hematopoietic stem cells with impaired self-renewal and megakaryocytic bias*. J Exp Med, 2014. **211**(2): p. 217-31.
33. Morrison, S.J., et al., *Identification of a lineage of multipotent hematopoietic progenitors*. Development, 1997. **124**(10): p. 1929-39.
34. Oguro, H., L. Ding, and S.J. Morrison, *SLAM family markers resolve functionally distinct subpopulations of hematopoietic stem cells and multipotent progenitors*. Cell Stem Cell, 2013. **13**(1): p. 102-16.
35. Muller-Sieburg, C.E., C.A. Whitlock, and I.L. Weissman, *Isolation of two early B lymphocyte progenitors from mouse marrow: a committed pre-pre-B cell and a clonogenic Thy-1-lo hematopoietic stem cell*. Cell, 1986. **44**(4): p. 653-62.
36. Uchida, N. and I.L. Weissman, *Searching for hematopoietic stem cells: evidence that Thy-1.1lo Lin- Sca-1+ cells are the only stem cells in C57BL/Ka-Thy-1.1 bone marrow*. J Exp Med, 1992. **175**(1): p. 175-84.

37. Osawa, M., et al., *Long-term lymphohematopoietic reconstitution by a single CD34-low/negative hematopoietic stem cell*. Science, 1996. **273**(5272): p. 242-5.
38. Matsuoka, S., et al., *CD34 expression on long-term repopulating hematopoietic stem cells changes during developmental stages*. Blood, 2001. **97**(2): p. 419-25.
39. Chen, J.Y., et al., *Hoxb5 marks long-term haematopoietic stem cells and reveals a homogenous perivascular niche*. Nature, 2016. **530**(7589): p. 223-7.
40. Sutherland, H.J., et al., *Characterization and partial purification of human marrow cells capable of initiating long-term hematopoiesis in vitro*. Blood, 1989. **74**(5): p. 1563-70.
41. Takenaka, K., et al., *Polymorphism in Sirpa modulates engraftment of human hematopoietic stem cells*. Nat Immunol, 2007. **8**(12): p. 1313-23.
42. van der Loo, J.C., et al., *Nonobese diabetic/severe combined immunodeficiency (NOD/SCID) mouse as a model system to study the engraftment and mobilization of human peripheral blood stem cells*. Blood, 1998. **92**(7): p. 2556-70.
43. Gunji, Y., et al., *Human primitive hematopoietic progenitor cells are more enriched in KITlow cells than in KIThigh cells*. Blood, 1993. **82**(11): p. 3283-9.
44. Kawashima, I., et al., *CD34+ human marrow cells that express low levels of Kit protein are enriched for long-term marrow-engrafting cells*. Blood, 1996. **87**(10): p. 4136-42.
45. Laver, J.H., et al., *Characterization of c-kit expression by primitive hematopoietic progenitors in umbilical cord blood*. Exp Hematol, 1995. **23**(14): p. 1515-9.
46. Sogo, S., et al., *Induction of c-kit molecules on human CD34+/c-kit < low cells: evidence for CD34+/c-kit < low cells as primitive hematopoietic stem cells*. Stem Cells, 1997. **15**(6): p. 420-9.
47. Ishikawa, F., et al., *Human cord blood long-term engrafting cells are CD34+ CD38-*. Leukemia, 2003. **17**(5): p. 960-4.
48. Hao, Q.L., et al., *A functional comparison of CD34 + CD38- cells in cord blood and bone marrow*. Blood, 1995. **86**(10): p. 3745-53.
49. Hogan, C.J., E.J. Shpall, and G. Keller, *Differential long-term and multilineage engraftment potential from subfractions of human CD34+ cord blood cells transplanted into NOD/SCID mice*. Proc Natl Acad Sci U S A, 2002. **99**(1): p. 413-8.
50. Terstappen, L.W., et al., *Sequential generations of hematopoietic colonies derived from single nonlineage-committed CD34+CD38- progenitor cells*. Blood, 1991. **77**(6): p. 1218-27.
51. Lu, L., et al., *Enrichment, characterization, and responsiveness of single primitive CD34 human umbilical cord blood hematopoietic progenitors with high proliferative and replating potential*. Blood, 1993. **81**(1): p. 41-8.
52. Bhatia, M., et al., *A newly discovered class of human hematopoietic cells with SCID-repopulating activity*. Nat Med, 1998. **4**(9): p. 1038-45.
53. Zanjani, E.D., et al., *Human bone marrow CD34- cells engraft in vivo and undergo multilineage expression that includes giving rise to CD34+ cells*. Exp Hematol, 1998. **26**(4): p. 353-60.
54. Kimura, T., et al., *Proliferative and migratory potentials of human cord blood-derived CD34- severe combined immunodeficiency repopulating cells that retain secondary reconstituting capacity*. Int J Hematol, 2004. **79**(4): p. 328-33.
55. Dao, M.A., J. Arevalo, and J.A. Nolta, *Reversibility of CD34 expression on human hematopoietic stem cells that retain the capacity for secondary reconstitution*. Blood, 2003. **101**(1): p. 112-8.

56. Zanjani, E.D., et al., *Reversible expression of CD34 by adult human bone marrow long-term engrafting hematopoietic stem cells*. Exp Hematol, 2003. **31**(5): p. 406-12.
57. Nakamura, Y., et al., *Ex vivo generation of CD34(+) cells from CD34(-) hematopoietic cells*. Blood, 1999. **94**(12): p. 4053-9.
58. Notta, F., et al., *Isolation of single human hematopoietic stem cells capable of long-term multilineage engraftment*. Science, 2011. **333**(6039): p. 218-21.
59. Traycoff, C.M., et al., *Evaluation of the in vitro behavior of phenotypically defined populations of umbilical cord blood hematopoietic progenitor cells*. Exp Hematol, 1994. **22**(2): p. 215-22.
60. Huang, S. and L.W. Terstappen, *Lymphoid and myeloid differentiation of single human CD34+, HLA-DR+, CD38- hematopoietic stem cells*. Blood, 1994. **83**(6): p. 1515-26.
61. Rusten, L.S., et al., *Functional differences between CD38- and DR- subfractions of CD34+ bone marrow cells*. Blood, 1994. **84**(5): p. 1473-81.
62. Craig, W., et al., *Expression of Thy-1 on human hematopoietic progenitor cells*. J Exp Med, 1993. **177**(5): p. 1331-42.
63. Yin, A.H., et al., *AC133, a novel marker for human hematopoietic stem and progenitor cells*. Blood, 1997. **90**(12): p. 5002-12.
64. Baum, C.M., et al., *Isolation of a candidate human hematopoietic stem-cell population*. Proc Natl Acad Sci U S A, 1992. **89**(7): p. 2804-8.
65. Majeti, R., C.Y. Park, and I.L. Weissman, *Identification of a hierarchy of multipotent hematopoietic progenitors in human cord blood*. Cell Stem Cell, 2007. **1**(6): p. 635-45.
66. Kondo, M., I.L. Weissman, and K. Akashi, *Identification of clonogenic common lymphoid progenitors in mouse bone marrow*. Cell, 1997. **91**(5): p. 661-72.
67. Akashi, K., et al., *A clonogenic common myeloid progenitor that gives rise to all myeloid lineages*. Nature, 2000. **404**(6774): p. 193-7.
68. Kawamoto, H., K. Ohmura, and Y. Katsura, *Direct evidence for the commitment of hematopoietic stem cells to T, B and myeloid lineages in murine fetal liver*. Int Immunol, 1997. **9**(7): p. 1011-9.
69. Katsura, Y. and H. Kawamoto, *Stepwise lineage restriction of progenitors in lympho-myelopoiesis*. Int Rev Immunol, 2001. **20**(1): p. 1-20.
70. Kawamoto, H., H. Wada, and Y. Katsura, *A revised scheme for developmental pathways of hematopoietic cells: the myeloid-based model*. Int Immunol, 2010. **22**(2): p. 65-70.
71. Lu, M., et al., *The common myelolymphoid progenitor: a key intermediate stage in hemopoiesis generating T and B cells*. J Immunol, 2002. **169**(7): p. 3519-25.
72. Katsura, Y., *Redefinition of lymphoid progenitors*. Nat Rev Immunol, 2002. **2**(2): p. 127-32.
73. Adolfsson, J., et al., *Identification of Flt3+ lympho-myeloid stem cells lacking erythro-megakaryocytic potential a revised road map for adult blood lineage commitment*. Cell, 2005. **121**(2): p. 295-306.
74. Nozad Charoudeh, H., et al., *Identification of an NK/T cell-restricted progenitor in adult bone marrow contributing to bone marrow- and thymic-dependent NK cells*. Blood, 2010. **116**(2): p. 183-92.
75. Ceredig, R., et al., *Increasing Flt3L availability alters composition of a novel bone marrow lymphoid progenitor compartment*. Blood, 2006. **108**(4): p. 1216-22.

76. Balciunaite, G., et al., *A B220⁺ CD117⁺ CD19⁻ hematopoietic progenitor with potent lymphoid and myeloid developmental potential*. Eur J Immunol, 2005. **35**(7): p. 2019-30.
77. Chi, A.W., et al., *Identification of Flt3⁺CD150⁻ myeloid progenitors in adult mouse bone marrow that harbor T lymphoid developmental potential*. Blood, 2011. **118**(10): p. 2723-32.
78. Ceredig, R., A.G. Rolink, and G. Brown, *Models of haematopoiesis: seeing the wood for the trees*. Nat Rev Immunol, 2009. **9**(4): p. 293-300.
79. Brown, G., et al., *The versatility of haematopoietic stem cells: implications for leukaemia*. Crit Rev Clin Lab Sci, 2010. **47**(4): p. 171-80.
80. Bell, J.J. and A. Bhandoola, *The earliest thymic progenitors for T cells possess myeloid lineage potential*. Nature, 2008. **452**(7188): p. 764-7.
81. Wada, H., et al., *Adult T-cell progenitors retain myeloid potential*. Nature, 2008. **452**(7188): p. 768-72.
82. Lu, M., et al., *The earliest thymic progenitors in adults are restricted to T, NK, and dendritic cell lineage and have a potential to form more diverse TCRbeta chains than fetal progenitors*. J Immunol, 2005. **175**(9): p. 5848-56.
83. Cumano, A., et al., *Bipotential precursors of B cells and macrophages in murine fetal liver*. Nature, 1992. **356**(6370): p. 612-5.
84. Montecino-Rodriguez, E., H. Leathers, and K. Dorshkind, *Bipotential B-macrophage progenitors are present in adult bone marrow*. Nat Immunol, 2001. **2**(1): p. 83-8.
85. Izon, D., et al., *A common pathway for dendritic cell and early B cell development*. J Immunol, 2001. **167**(3): p. 1387-92.
86. Hou, Y.H., et al., *Identification of a human B-cell/myeloid common progenitor by the absence of CXCR4*. Blood, 2005. **105**(9): p. 3488-92.
87. Gauvreau, G.M., A.K. Ellis, and J.A. Denburg, *Haemopoietic processes in allergic disease: eosinophil/basophil development*. Clin Exp Allergy, 2009. **39**(9): p. 1297-306.
88. Fogg, D.K., et al., *A clonogenic bone marrow progenitor specific for macrophages and dendritic cells*. Science, 2006. **311**(5757): p. 83-7.
89. TILL, J.E., E.A. MCCULLOCH, and L. SIMINOVITCH, *A STOCHASTIC MODEL OF STEM CELL PROLIFERATION, BASED ON THE GROWTH OF SPLEEN COLONY-FORMING CELLS*. Proc Natl Acad Sci U S A, 1964. **51**: p. 29-36.
90. BECKER, A.J., E.A. McCULLOCH, and J.E. TILL, *Cytological demonstration of the clonal nature of spleen colonies derived from transplanted mouse marrow cells*. Nature, 1963. **197**: p. 452-4.
91. Waugh, W.A.O.N., *An age-dependent birth and death process*. Biometrika, 1955. **42**(3-4).
92. Korn, A.P., et al., *Investigations of a stochastic model of haemopoiesis*. Exp Hematol, 1973. **1**(6): p. 362-75.
93. Humphries, R.K., A.C. Eaves, and C.J. Eaves, *Self-renewal of hemopoietic stem cells during mixed colony formation in vitro*. Proc Natl Acad Sci U S A, 1981. **78**(6): p. 3629-33.
94. Nakahata, T., A.J. Gross, and M. Ogawa, *A stochastic model of self-renewal and commitment to differentiation of the primitive hemopoietic stem cells in culture*. J Cell Physiol, 1982. **113**(3): p. 455-8.
95. Wu, A.M., *Regulation of self-renewal of human T lymphocyte colony-forming units (TL-CFUs)*. J Cell Physiol, 1983. **117**(1): p. 101-8.

96. Kurnit, D.M., et al., *Stochastic branching model for hemopoietic progenitor cell differentiation*. J Cell Physiol, 1985. **123**(1): p. 55-63.
97. Abkowitz, J.L., S.N. Catlin, and P. Gutter, *Evidence that hematopoiesis may be a stochastic process in vivo*. Nat Med, 1996. **2**(2): p. 190-7.
98. Abkowitz, J.L., et al., *In vivo kinetics of murine hemopoietic stem cells*. Blood, 2000. **96**(10): p. 3399-405.
99. Roeder, I., et al., *Competitive clonal hematopoiesis in mouse chimeras explained by a stochastic model of stem cell organization*. Blood, 2005. **105**(2): p. 609-16.
100. Hyrien, O., et al., *Stochastic modeling of stress erythropoiesis using a two-type age-dependent branching process with immigration*. J Math Biol, 2015. **70**(7): p. 1485-521.
101. Ogawa, M., P.N. Porter, and T. Nakahata, *Renewal and commitment to differentiation of hemopoietic stem cells (an interpretive review)*. Blood, 1983. **61**(5): p. 823-9.
102. Suda, T., J. Suda, and M. Ogawa, *Single-cell origin of mouse hemopoietic colonies expressing multiple lineages in variable combinations*. Proc Natl Acad Sci U S A, 1983. **80**(21): p. 6689-93.
103. Suda, T., J. Suda, and M. Ogawa, *Disparate differentiation in mouse hemopoietic colonies derived from paired progenitors*. Proc Natl Acad Sci U S A, 1984. **81**(8): p. 2520-4.
104. Leary, A.G., et al., *Single cell origin of multilineage colonies in culture. Evidence that differentiation of multipotent progenitors and restriction of proliferative potential of monopotent progenitors are stochastic processes*. J Clin Invest, 1984. **74**(6): p. 2193-7.
105. Leary, A.G., et al., *Disparate differentiation in hemopoietic colonies derived from human paired progenitors*. Blood, 1985. **66**(2): p. 327-32.
106. Spooncer, E., D. Boettiger, and T.M. Dexter, *Continuous in vitro generation of multipotential stem cell clones from src-infected cultures*. Nature, 1984. **310**(5974): p. 228-30.
107. Heberlein, C., et al., *The gene for erythropoietin receptor is expressed in multipotential hematopoietic and embryonal stem cells: evidence for differentiation stage-specific regulation*. Mol Cell Biol, 1992. **12**(4): p. 1815-26.
108. Jiménez, G., et al., *Activation of the beta-globin locus control region precedes commitment to the erythroid lineage*. Proc Natl Acad Sci U S A, 1992. **89**(22): p. 10618-22.
109. Ford, A.M., et al., *Multilineage phenotypes of interleukin-3-dependent progenitor cells*. Blood, 1992. **79**(8): p. 1962-71.
110. Ford, A.M., et al., *Immunoglobulin heavy-chain and CD3 delta-chain gene enhancers are DNase I-hypersensitive in hemopoietic progenitor cells*. Proc Natl Acad Sci U S A, 1992. **89**(8): p. 3424-8.
111. Berthou, C., et al., *Granzyme B and perforin lytic proteins are expressed in CD34+ peripheral blood progenitor cells mobilized by chemotherapy and granulocyte colony-stimulating factor*. Blood, 1995. **86**(9): p. 3500-6.
112. Hampson, I.N., et al., *Expression and downregulation of cytotoxic cell protease 1 or Granzyme 'B' transcripts during myeloid differentiation of interleukin-3-dependent murine stem cell lines*. Blood, 1992. **80**(12): p. 3097-105.

113. Ford, A.M., et al., *Regulation of the myeloperoxidase enhancer binding proteins Pu1, C-EBP alpha, -beta, and -delta during granulocyte-lineage specification*. Proc Natl Acad Sci U S A, 1996. **93**(20): p. 10838-43.
114. Zhu, J., et al., *A myeloid-lineage-specific enhancer upstream of the mouse myeloperoxidase (MPO) gene*. Leukemia, 1994. **8**(5): p. 717-23.
115. Hu, M., et al., *Multilineage gene expression precedes commitment in the hemopoietic system*. Genes Dev, 1997. **11**(6): p. 774-85.
116. Miyamoto, T., et al., *Myeloid or lymphoid promiscuity as a critical step in hematopoietic lineage commitment*. Dev Cell, 2002. **3**(1): p. 137-47.
117. Raj, A. and A. van Oudenaarden, *Nature, nurture, or chance: stochastic gene expression and its consequences*. Cell, 2008. **135**(2): p. 216-26.
118. Chang, H.H., et al., *Transcriptome-wide noise controls lineage choice in mammalian progenitor cells*. Nature, 2008. **453**(7194): p. 544-7.
119. Volfson, D., et al., *Origins of extrinsic variability in eukaryotic gene expression*. Nature, 2006. **439**(7078): p. 861-4.
120. Becskei, A., B.B. Kaufmann, and A. van Oudenaarden, *Contributions of low molecule number and chromosomal positioning to stochastic gene expression*. Nat Genet, 2005. **37**(9): p. 937-44.
121. Elowitz, M.B., et al., *Stochastic gene expression in a single cell*. Science, 2002. **297**(5584): p. 1183-6.
122. Raser, J.M. and E.K. O'Shea, *Control of stochasticity in eukaryotic gene expression*. Science, 2004. **304**(5678): p. 1811-4.
123. Rekhtman, N., et al., *Direct interaction of hematopoietic transcription factors PU.1 and GATA-1: functional antagonism in erythroid cells*. Genes Dev, 1999. **13**(11): p. 1398-411.
124. Chou, S.T., et al., *Graded repression of PU.1/Sfpi1 gene transcription by GATA factors regulates hematopoietic cell fate*. Blood, 2009. **114**(5): p. 983-94.
125. Zhang, P., et al., *PU.1 inhibits GATA-1 function and erythroid differentiation by blocking GATA-1 DNA binding*. Blood, 2000. **96**(8): p. 2641-8.
126. Stopka, T., et al., *PU.1 inhibits the erythroid program by binding to GATA-1 on DNA and creating a repressive chromatin structure*. EMBO J, 2005. **24**(21): p. 3712-23.
127. Nerlov, C., et al., *GATA-1 interacts with the myeloid PU.1 transcription factor and represses PU.1-dependent transcription*. Blood, 2000. **95**(8): p. 2543-51.
128. Burda, P., et al., *GATA-1 Inhibits PU.1 Gene via DNA and Histone H3K9 Methylation of Its Distal Enhancer in Erythroleukemia*. PLoS One, 2016. **11**(3): p. e0152234.
129. Okuno, Y., et al., *Potential autoregulation of transcription factor PU.1 by an upstream regulatory element*. Mol Cell Biol, 2005. **25**(7): p. 2832-45.
130. Nishikawa, K., et al., *Self-association of Gata1 enhances transcriptional activity in vivo in zebra fish embryos*. Mol Cell Biol, 2003. **23**(22): p. 8295-305.
131. Nozawa, D., et al., *GATA2-dependent and region-specific regulation of Gata2 transcription in the mouse midbrain*. Genes Cells, 2009. **14**(5): p. 569-82.
132. Timchenko, N., et al., *Autoregulation of the human C/EBP alpha gene by stimulation of upstream stimulatory factor binding*. Mol Cell Biol, 1995. **15**(3): p. 1192-202.
133. Bakri, Y., et al., *Balance of MafB and PU.1 specifies alternative macrophage or dendritic cell fate*. Blood, 2005. **105**(7): p. 2707-16.

134. Dahl, R., et al., *Regulation of macrophage and neutrophil cell fates by the PU.1:C/EBPalpha ratio and granulocyte colony-stimulating factor*. Nat Immunol, 2003. **4**(10): p. 1029-36.
135. Reddy, V.A., et al., *Granulocyte inducer C/EBPalpha inactivates the myeloid master regulator PU.1: possible role in lineage commitment decisions*. Blood, 2002. **100**(2): p. 483-90.
136. Walsh, J.C., et al., *Cooperative and antagonistic interplay between PU.1 and GATA-2 in the specification of myeloid cell fates*. Immunity, 2002. **17**(5): p. 665-76.
137. Iwasaki, H., et al., *The order of expression of transcription factors directs hierarchical specification of hematopoietic lineages*. Genes Dev, 2006. **20**(21): p. 3010-21.
138. Hoppe, P.S., et al., *Early myeloid lineage choice is not initiated by random PU.1 to GATA1 protein ratios*. Nature, 2016. **535**(7611): p. 299-302.
139. Anderson, D.M., et al., *Molecular cloning of mast cell growth factor, a hematopoietin that is active in both membrane bound and soluble forms*. Cell, 1990. **63**(1): p. 235-43.
140. Stein, J., G.V. Borzillo, and C.W. Rettenmier, *Direct stimulation of cells expressing receptors for macrophage colony-stimulating factor (CSF-1) by a plasma membrane-bound precursor of human CSF-1*. Blood, 1990. **76**(7): p. 1308-14.
141. Cluitmans, F.H., et al., *The role of cytokines and hematopoietic growth factors in the autocrine/paracrine regulation of inducible hematopoiesis*. Ann Hematol, 1997. **75**(1-2): p. 27-31.
142. Carnot, P. and C. Deflandr, *Sur l'activite hemopoietique des differents organeau au cours de la regeneration du sang*. Comptes Rendus de l'Académie des Sciences, 1906. **143**: p. 432-435.
143. Miyake, T., C.K. Kung, and E. Goldwasser, *Purification of human erythropoietin*. J Biol Chem, 1977. **252**(15): p. 5558-64.
144. Lee-Huang, S., *Cloning and expression of human erythropoietin cDNA in Escherichia coli*. Proc Natl Acad Sci U S A, 1984. **81**(9): p. 2708-12.
145. Lin, F.K., et al., *Cloning and expression of the human erythropoietin gene*. Proc Natl Acad Sci U S A, 1985. **82**(22): p. 7580-4.
146. Shoemaker, C.B. and L.D. Mitsock, *Murine erythropoietin gene: cloning, expression, and human gene homology*. Mol Cell Biol, 1986. **6**(3): p. 849-58.
147. Noguchi, C.T., et al., *Cloning of the human erythropoietin receptor gene*. Blood, 1991. **78**(10): p. 2548-56.
148. Maouche, L., et al., *Cloning of the gene encoding the human erythropoietin receptor*. Blood, 1991. **78**(10): p. 2557-63.
149. Eckardt, K.U., *Erythropoietin production in liver and kidneys*. Curr Opin Nephrol Hypertens, 1996. **5**(1): p. 28-34.
150. McLeod, D.L., M.M. Shreeve, and A.A. Axelrad, *Improved plasma culture system for production of erythrocytic colonies in vitro: quantitative assay method for CFU-E*. Blood, 1974. **44**(4): p. 517-34.
151. Koury, M.J. and M.C. Bondurant, *Erythropoietin retards DNA breakdown and prevents programmed death in erythroid progenitor cells*. Science, 1990. **248**(4953): p. 378-81.
152. Eschbach, J.W., et al., *Recombinant human erythropoietin in anemic patients with end-stage renal disease. Results of a phase III multicenter clinical trial*. Ann Intern Med, 1989. **111**(12): p. 992-1000.

153. Pluznik, D.H. and L. Sachs, *The cloning of normal "mast" cells in tissue culture*. J Cell Physiol, 1965. **66**(3): p. 319-24.
154. Bradley, T.R. and D. Metcalf, *The growth of mouse bone marrow cells in vitro*. Aust J Exp Biol Med Sci, 1966. **44**(3): p. 287-99.
155. Stanley, E.R., et al., *Colony stimulating factor and the regulation of granulopoiesis and macrophage production*. Fed Proc, 1975. **34**(13): p. 2272-8.
156. Stanley, E.R. and P.M. Heard, *Factors regulating macrophage production and growth. Purification and some properties of the colony stimulating factor from medium conditioned by mouse L cells*. J Biol Chem, 1977. **252**(12): p. 4305-12.
157. Burgess, A.W., J. Camakaris, and D. Metcalf, *Purification and properties of colony-stimulating factor from mouse lung-conditioned medium*. J Biol Chem, 1977. **252**(6): p. 1998-2003.
158. Gough, N.M., et al., *Molecular cloning of cDNA encoding a murine haematopoietic growth regulator, granulocyte-macrophage colony stimulating factor*. Nature, 1984. **309**(5971): p. 763-7.
159. Ihle, J.N., et al., *Procedures for the purification of interleukin 3 to homogeneity*. J Immunol, 1982. **129**(6): p. 2431-6.
160. Ihle, J.N., et al., *Phenotypic characteristics of cell lines requiring interleukin 3 for growth*. J Immunol, 1982. **129**(4): p. 1377-83.
161. Ihle, J.N., et al., *Biologic properties of homogeneous interleukin 3. I. Demonstration of WEHI-3 growth factor activity, mast cell growth factor activity, p cell-stimulating factor activity, colony-stimulating factor activity, and histamine-producing cell-stimulating factor activity*. J Immunol, 1983. **131**(1): p. 282-7.
162. Prystowsky, M.B., et al., *Multiple hemopoietic lineages are found after stimulation of mouse bone marrow precursor cells with interleukin 3*. Am J Pathol, 1984. **117**(2): p. 171-9.
163. Nicola, N.A., et al., *Purification of a factor inducing differentiation in murine myelomonocytic leukemia cells. Identification as granulocyte colony-stimulating factor*. J Biol Chem, 1983. **258**(14): p. 9017-23.
164. Metcalf, D. and N.A. Nicola, *Proliferative effects of purified granulocyte colony-stimulating factor (G-CSF) on normal mouse hemopoietic cells*. J Cell Physiol, 1983. **116**(2): p. 198-206.
165. Hosing, C., *Hematopoietic stem cell mobilization with G-CSF*. Methods Mol Biol, 2012. **904**: p. 37-47.
166. Metcalf, D., et al., *Production of hematopoietic regulatory factors in cultures of adult and fetal mouse organs: measurement by specific bioassays*. Leukemia, 1995. **9**(9): p. 1556-64.
167. Wilkins, B.S. and D.B. Jones, *Sites of M-CSF messenger RNA production in bone marrow trephine biopsy specimens and long term cultures demonstrated by nonisotopic in situ hybridisation*. Clin Mol Pathol, 1995. **48**(1): p. M35-9.
168. Sherr, C.J., M.F. Roussel, and C.W. Rettenmier, *Colony-stimulating factor-1 receptor (c-fms)*. J Cell Biochem, 1988. **38**(3): p. 179-87.
169. Kastelein, R.A. and A.B. Shanafelt, *GM-CSF receptor: interactions and activation*. Oncogene, 1993. **8**(2): p. 231-6.
170. Korpelainen, E.I., et al., *IL-3 receptor expression, regulation and function in cells of the vasculature*. Immunol Cell Biol, 1996. **74**(1): p. 1-7.

171. de Koning, J.P. and I.P. Touw, *Advances in understanding the biology and function of the G-CSF receptor*. Curr Opin Hematol, 1996. **3**(3): p. 180-4.
172. Lachman, L.B., S.O. Page, and R.S. Metzgar, *Purification of human interleukin 1*. J Supramol Struct, 1980. **13**(4): p. 457-66.
173. March, C.J., et al., *Cloning, sequence and expression of two distinct human interleukin-1 complementary DNAs*. Nature, 1985. **315**(6021): p. 641-7.
174. Orelia, C., et al., *Interleukin-1 regulates hematopoietic progenitor and stem cells in the midgestation mouse fetal liver*. Haematologica, 2009. **94**(4): p. 462-9.
175. Pietras, E.M., et al., *Chronic interleukin-1 exposure drives haematopoietic stem cells towards precocious myeloid differentiation at the expense of self-renewal*. Nat Cell Biol, 2016. **18**(6): p. 607-18.
176. Pinteaux, E., et al., *Expression of interleukin-1 receptors and their role in interleukin-1 actions in murine microglial cells*. J Neurochem, 2002. **83**(4): p. 754-63.
177. Gardella, S., et al., *Secretion of bioactive interleukin-1beta by dendritic cells is modulated by interaction with antigen specific T cells*. Blood, 2000. **95**(12): p. 3809-15.
178. Marsh, C.B., et al., *Lymphocytes produce IL-1beta in response to Fc gamma receptor cross-linking: effects on parenchymal cell IL-8 release*. J Immunol, 1998. **160**(8): p. 3942-8.
179. Hastie, A.T., et al., *IL-1 beta release from cultured bronchial epithelial cells and bronchoalveolar lavage cells from allergic and normal humans following segmental challenge with ragweed*. Cytokine, 1996. **8**(9): p. 730-8.
180. Daig, R., et al., *Human intestinal epithelial cells secrete interleukin-1 receptor antagonist and interleukin-8 but not interleukin-1 or interleukin-6*. Gut, 2000. **46**(3): p. 350-8.
181. Mauviel, A., et al., *Induction of interleukin-1 beta production in human dermal fibroblasts by interleukin-1 alpha and tumor necrosis factor-alpha. Involvement of protein kinase-dependent and adenylate cyclase-dependent regulatory pathways*. J Cell Biochem, 1991. **47**(2): p. 174-83.
182. Colotta, F., et al., *The type II 'decoy' receptor: a novel regulatory pathway for interleukin 1*. Immunol Today, 1994. **15**(12): p. 562-6.
183. Sims, J.E., J.G. Giri, and S.K. Dower, *The two interleukin-1 receptors play different roles in IL-1 actions*. Clin Immunol Immunopathol, 1994. **72**(1): p. 9-14.
184. Namen, A.E., et al., *Stimulation of B-cell progenitors by cloned murine interleukin-7*. Nature, 1988. **333**(6173): p. 571-3.
185. Watson, J.D., et al., *Effect of IL-7 on the growth of fetal thymocytes in culture*. J Immunol, 1989. **143**(4): p. 1215-22.
186. Wiles, M.V., P. Ruiz, and B.A. Imhof, *Interleukin-7 expression during mouse thymus development*. Eur J Immunol, 1992. **22**(4): p. 1037-42.
187. Kröncke, R., et al., *Human follicular dendritic cells and vascular cells produce interleukin-7: a potential role for interleukin-7 in the germinal center reaction*. Eur J Immunol, 1996. **26**(10): p. 2541-4.
188. Hara, T., et al., *Identification of IL-7-producing cells in primary and secondary lymphoid organs using IL-7-GFP knock-in mice*. J Immunol, 2012. **189**(4): p. 1577-84.
189. Watanabe, M., et al., *Interleukin 7 is produced by human intestinal epithelial cells and regulates the proliferation of intestinal mucosal lymphocytes*. J Clin Invest, 1995. **95**(6): p. 2945-53.

190. Heufler, C., et al., *Interleukin 7 is produced by murine and human keratinocytes*. J Exp Med, 1993. **178**(3): p. 1109-14.
191. Park, L.S., et al., *Murine interleukin 7 (IL-7) receptor. Characterization on an IL-7-dependent cell line*. J Exp Med, 1990. **171**(4): p. 1073-89.
192. Zsebo, K.M., et al., *Identification, purification, and biological characterization of hematopoietic stem cell factor from buffalo rat liver--conditioned medium*. Cell, 1990. **63**(1): p. 195-201.
193. Williams, D.E., et al., *Identification of a ligand for the c-kit proto-oncogene*. Cell, 1990. **63**(1): p. 167-74.
194. Ikuta, K. and I.L. Weissman, *Evidence that hematopoietic stem cells express mouse c-kit but do not depend on steel factor for their generation*. Proc Natl Acad Sci U S A, 1992. **89**(4): p. 1502-6.
195. Matthews, W., et al., *A receptor tyrosine kinase specific to hematopoietic stem and progenitor cell-enriched populations*. Cell, 1991. **65**(7): p. 1143-52.
196. Lyman, S.D., et al., *Molecular cloning of a ligand for the flt3/flk-2 tyrosine kinase receptor: a proliferative factor for primitive hematopoietic cells*. Cell, 1993. **75**(6): p. 1157-67.
197. Kim, S.W., et al., *Flt3 ligand induces monocyte proliferation and enhances the function of monocyte-derived dendritic cells in vitro*. J Cell Physiol, 2015. **230**(8): p. 1740-9.
198. Wendling, F., et al., *Myeloid progenitor cells transformed by the myeloproliferative leukemia virus proliferate and differentiate in vitro without the addition of growth factors*. Leukemia, 1989. **3**(7): p. 475-80.
199. Wendling, F., et al., *Factor-independent erythropoietic progenitor cells in leukemia induced by the myeloproliferative leukemia virus*. Blood, 1989. **73**(5): p. 1161-7.
200. Souyri, M., et al., *A putative truncated cytokine receptor gene transduced by the myeloproliferative leukemia virus immortalizes hematopoietic progenitors*. Cell, 1990. **63**(6): p. 1137-47.
201. Vigon, I., et al., *Molecular cloning and characterization of MPL, the human homolog of the v-mpl oncogene: identification of a member of the hematopoietic growth factor receptor superfamily*. Proc Natl Acad Sci U S A, 1992. **89**(12): p. 5640-4.
202. Debili, N., et al., *The Mpl receptor is expressed in the megakaryocytic lineage from late progenitors to platelets*. Blood, 1995. **85**(2): p. 391-401.
203. Kuter, D.J., D.L. Beeler, and R.D. Rosenberg, *The purification of megapoietin: a physiological regulator of megakaryocyte growth and platelet production*. Proc Natl Acad Sci U S A, 1994. **91**(23): p. 11104-8.
204. Lok, S., et al., *Cloning and expression of murine thrombopoietin cDNA and stimulation of platelet production in vivo*. Nature, 1994. **369**(6481): p. 565-8.
205. de Sauvage, F.J., et al., *Stimulation of megakaryocytopoiesis and thrombopoiesis by the c-Mpl ligand*. Nature, 1994. **369**(6481): p. 533-8.
206. Kaushansky, K., et al., *Thrombopoietin, the Mpl ligand, is essential for full megakaryocyte development*. Proc Natl Acad Sci U S A, 1995. **92**(8): p. 3234-8.
207. Yoshihara, H., et al., *Thrombopoietin/MPL signaling regulates hematopoietic stem cell quiescence and interaction with the osteoblastic niche*. Cell Stem Cell, 2007. **1**(6): p. 685-97.

208. Zhou, J., et al., *Thrombopoietin protects the brain and improves sensorimotor functions: reduction of stroke-induced MMP-9 upregulation and blood-brain barrier injury*. J Cereb Blood Flow Metab, 2011. **31**(3): p. 924-33.
209. Baker, J.E., et al., *Human thrombopoietin reduces myocardial infarct size, apoptosis, and stunning following ischaemia/reperfusion in rats*. Cardiovasc Res, 2008. **77**(1): p. 44-53.
210. Sungaran, R., B. Markovic, and B.H. Chong, *Localization and regulation of thrombopoietin mRNA expression in human kidney, liver, bone marrow, and spleen using in situ hybridization*. Blood, 1997. **89**(1): p. 101-7.
211. Zhang, J., et al., *Inflammation stimulates thrombopoietin (Tpo) expression in rat brain-derived microvascular endothelial cells, but suppresses Tpo in astrocytes and microglia*. J Interferon Cytokine Res, 2010. **30**(7): p. 465-9.
212. Pluznik, D.H., R.E. Cunningham, and P.D. Noguchi, *Colony-stimulating factor (CSF) controls proliferation of CSF-dependent cells by acting during the G1 phase of the cell cycle*. Proc Natl Acad Sci U S A, 1984. **81**(23): p. 7451-5.
213. London, L. and J.P. McKearn, *Activation and growth of colony-stimulating factor-dependent cell lines is cell cycle stage dependent*. J Exp Med, 1987. **166**(5): p. 1419-35.
214. Spivak, J.L., et al., *Erythropoietin is both a mitogen and a survival factor*. Blood, 1991. **77**(6): p. 1228-33.
215. Valledor, A.F., et al., *Macrophage colony-stimulating factor induces the expression of mitogen-activated protein kinase phosphatase-1 through a protein kinase C-dependent pathway*. J Immunol, 1999. **163**(5): p. 2452-62.
216. von Freeden-Jeffry, U., et al., *The earliest T lineage-committed cells depend on IL-7 for Bcl-2 expression and normal cell cycle progression*. Immunity, 1997. **7**(1): p. 147-54.
217. Traycoff, C.M., et al., *Rapid exit from G0/G1 phases of cell cycle in response to stem cell factor confers on umbilical cord blood CD34+ cells an enhanced ex vivo expansion potential*. Exp Hematol, 1994. **22**(13): p. 1264-72.
218. Kamijo, T., et al., *Synergism between stem cell factor and granulocyte-macrophage colony-stimulating factor on cell proliferation by induction of cyclins*. Cytokine, 2002. **19**(6): p. 267-75.
219. Kobayashi, H., *Effect of c-kit ligand (stem cell factor) in combination with interleukin-5, granulocyte-macrophage colony-stimulating factor, and interleukin-3, on eosinophil lineage*. Int J Hematol, 1993. **58**(1-2): p. 21-6.
220. Williams, G.T., et al., *Haemopoietic colony stimulating factors promote cell survival by suppressing apoptosis*. Nature, 1990. **343**(6253): p. 76-9.
221. Rodriguez-Tarduchy, G., M. Collins, and A. López-Rivas, *Regulation of apoptosis in interleukin-3-dependent hemopoietic cells by interleukin-3 and calcium ionophores*. EMBO J, 1990. **9**(9): p. 2997-3002.
222. Ritchie, A., S. Vadhan-Raj, and H.E. Broxmeyer, *Thrombopoietin suppresses apoptosis and behaves as a survival factor for the human growth factor-dependent cell line, M07e*. Stem Cells, 1996. **14**(3): p. 330-6.
223. Hassan, H.T. and A. Zander, *Stem cell factor as a survival and growth factor in human normal and malignant hematopoiesis*. Acta Haematol, 1996. **95**(3-4): p. 257-62.
224. Kelley, T.W., et al., *Macrophage colony-stimulating factor promotes cell survival through Akt/protein kinase B*. J Biol Chem, 1999. **274**(37): p. 26393-8.

225. Ward, A.C., et al., *Multiple signals mediate proliferation, differentiation, and survival from the granulocyte colony-stimulating factor receptor in myeloid 32D cells*. J Biol Chem, 1999. **274**(21): p. 14956-62.
226. Santini, V., et al., *The carboxy-terminal region of the granulocyte colony-stimulating factor receptor transduces a phagocytic signal*. Blood, 2003. **101**(11): p. 4615-22.
227. Smith, A., et al., *A role for JNK/SAPK in proliferation, but not apoptosis, of IL-3-dependent cells*. Curr Biol, 1997. **7**(11): p. 893-6.
228. Metcalf, D. and G.R. Johnson, *Interactions between purified GM-CSF, purified erythropoietin and spleen conditioned medium on hemopoietic colony formation in vitro*. J Cell Physiol, 1979. **99**(2): p. 159-74.
229. Udupa, K.B. and K.R. Reissmann, *In vivo erythropoietin requirements of regenerating erythroid progenitors (BFU-e, CFU-e) in bone marrow of mice*. Blood, 1979. **53**(6): p. 1164-71.
230. Sonoda, Y., et al., *Analysis in serum-free culture of the targets of recombinant human hemopoietic growth factors: interleukin 3 and granulocyte/macrophage-colony-stimulating factor are specific for early developmental stages*. Proc Natl Acad Sci U S A, 1988. **85**(12): p. 4360-4.
231. Metcalf, D., G.R. Johnson, and A.W. Burgess, *Direct stimulation by purified GM-CSF of the proliferation of multipotential and erythroid precursor cells*. Blood, 1980. **55**(1): p. 138-47.
232. Sieff, C.A., et al., *Human recombinant granulocyte-macrophage colony-stimulating factor: a multilineage hematopoietin*. Science, 1985. **230**(4730): p. 1171-3.
233. Ogawa, M., *Hemopoietic stem cells: stochastic differentiation and humoral control of proliferation*. Environ Health Perspect, 1989. **80**: p. 199-207.
234. Ogawa, M., *Differentiation and proliferation of hematopoietic stem cells*. Blood, 1993. **81**(11): p. 2844-53.
235. Suda, T., et al., *Permissive role of interleukin 3 (IL-3) in proliferation and differentiation of multipotential hemopoietic progenitors in culture*. J Cell Physiol, 1985. **124**(2): p. 182-90.
236. Fairbairn, L.J., et al., *Suppression of apoptosis allows differentiation and development of a multipotent hemopoietic cell line in the absence of added growth factors*. Cell, 1993. **74**(5): p. 823-32.
237. Dranoff, G., et al., *Involvement of granulocyte-macrophage colony-stimulating factor in pulmonary homeostasis*. Science, 1994. **264**(5159): p. 713-6.
238. Stanley, E., et al., *Granulocyte/macrophage colony-stimulating factor-deficient mice show no major perturbation of hematopoiesis but develop a characteristic pulmonary pathology*. Proc Natl Acad Sci U S A, 1994. **91**(12): p. 5592-6.
239. Wu, H., et al., *Generation of committed erythroid BFU-E and CFU-E progenitors does not require erythropoietin or the erythropoietin receptor*. Cell, 1995. **83**(1): p. 59-67.
240. Lin, C.S., et al., *Differential effects of an erythropoietin receptor gene disruption on primitive and definitive erythropoiesis*. Genes Dev, 1996. **10**(2): p. 154-64.
241. Peschon, J.J., et al., *Early lymphocyte expansion is severely impaired in interleukin 7 receptor-deficient mice*. J Exp Med, 1994. **180**(5): p. 1955-60.
242. Akashi, K., et al., *Bcl-2 rescues T lymphopoiesis in interleukin-7 receptor-deficient mice*. Cell, 1997. **89**(7): p. 1033-41.
243. Marks, S.C. and P.W. Lane, *Osteopetrosis, a new recessive skeletal mutation on chromosome 12 of the mouse*. J Hered, 1976. **67**(1): p. 11-18.

244. Wiktor-Jedrzejczak, W.W., et al., *Hematological characterization of congenital osteopetrosis in op/op mouse. Possible mechanism for abnormal macrophage differentiation.* J Exp Med, 1982. **156**(5): p. 1516-27.
245. Wiktor-Jedrzejczak, W., et al., *Total absence of colony-stimulating factor 1 in the macrophage-deficient osteopetrotic (op/op) mouse.* Proc Natl Acad Sci U S A, 1990. **87**(12): p. 4828-32.
246. Lagasse, E. and I.L. Weissman, *Enforced expression of Bcl-2 in monocytes rescues macrophages and partially reverses osteopetrosis in op/op mice.* Cell, 1997. **89**(7): p. 1021-31.
247. Pharr, P.N., et al., *Expression of an activated erythropoietin or a colony-stimulating factor 1 receptor by pluripotent progenitors enhances colony formation but does not induce differentiation.* Proc Natl Acad Sci U S A, 1994. **91**(16): p. 7482-6.
248. McArthur, G.A., L.R. Rohrschneider, and G.R. Johnson, *Induced expression of c-fms in normal hematopoietic cells shows evidence for both conservation and lineage restriction of signal transduction in response to macrophage colony-stimulating factor.* Blood, 1994. **83**(4): p. 972-81.
249. Stoffel, R., et al., *Permissive role of thrombopoietin and granulocyte colony-stimulating factor receptors in hematopoietic cell fate decisions in vivo.* Proc Natl Acad Sci U S A, 1999. **96**(2): p. 698-702.
250. Semerad, C.L., et al., *A role for G-CSF receptor signaling in the regulation of hematopoietic cell function but not lineage commitment or differentiation.* Immunity, 1999. **11**(2): p. 153-61.
251. Mayani, H., W. Dragowska, and P.M. Lansdorp, *Lineage commitment in human hemopoiesis involves asymmetric cell division of multipotent progenitors and does not appear to be influenced by cytokines.* J Cell Physiol, 1993. **157**(3): p. 579-86.
252. Mayani, H., W. Dragowska, and P.M. Lansdorp, *Cytokine-induced selective expansion and maturation of erythroid versus myeloid progenitors from purified cord blood precursor cells.* Blood, 1993. **81**(12): p. 3252-8.
253. Ward, D., et al., *Mathematical modeling reveals differential effects of erythropoietin on proliferation and lineage commitment of human hematopoietic progenitors in early erythroid culture.* Haematologica, 2016. **101**(3): p. 286-96.
254. Wolf, N.S. and J.J. Trentin, *Hemopoietic colony studies. V. Effect of hemopoietic organ stroma on differentiation of pluripotent stem cells.* J Exp Med, 1968. **127**(1): p. 205-14.
255. Trentin, J.J., *Determination of bone marrow stem cell differentiation by stromal hemopoietic inductive microenvironments (HIM).* Am J Pathol, 1971. **65**(3): p. 621-8.
256. Curry, J.L. and J.J. Trentin, *Hemopoietic spleen colony studies. I. Growth and differentiation.* Dev Biol, 1967. **15**(5): p. 395-413.
257. Metcalf, D., *Clonal analysis of proliferation and differentiation of paired daughter cells: action of granulocyte-macrophage colony-stimulating factor on granulocyte-macrophage precursors.* Proc Natl Acad Sci U S A, 1980. **77**(9): p. 5327-30.
258. Metcalf, D. and A.W. Burgess, *Clonal analysis of progenitor cell commitment of granulocyte or macrophage production.* J Cell Physiol, 1982. **111**(3): p. 275-83.
259. Burgess, A.W. and D. Metcalf, *Characterization of a serum factor stimulating the differentiation of myelomonocytic leukemic cells.* Int J Cancer, 1980. **26**(5): p. 647-54.
260. Li, J., et al., *Regulation of the differentiation of WEHI-3B D+ leukemia cells by granulocyte colony-stimulating factor receptor.* J Cell Biol, 1993. **120**(6): p. 1481-9.

261. Souza, L.M., et al., *Recombinant human granulocyte colony-stimulating factor: effects on normal and leukemic myeloid cells*. Science, 1986. **232**(4746): p. 61-5.
262. Bedi, A., et al., *Growth factor-mediated terminal differentiation of chronic myeloid leukemia*. Cancer Res, 1994. **54**(21): p. 5535-8.
263. Dong, F., et al., *Distinct cytoplasmic regions of the human granulocyte colony-stimulating factor receptor involved in induction of proliferation and maturation*. Mol Cell Biol, 1993. **13**(12): p. 7774-81.
264. Fukunaga, R., E. Ishizaka-Ikeda, and S. Nagata, *Growth and differentiation signals mediated by different regions in the cytoplasmic domain of granulocyte colony-stimulating factor receptor*. Cell, 1993. **74**(6): p. 1079-87.
265. Hu, N., Y. Qiu, and F. Dong, *Role of Erk1/2 signaling in the regulation of neutrophil versus monocyte development in response to G-CSF and M-CSF*. J Biol Chem, 2015. **290**(40): p. 24561-73.
266. Dong, F., et al., *Mutations in the gene for the granulocyte colony-stimulating-factor receptor in patients with acute myeloid leukemia preceded by severe congenital neutropenia*. N Engl J Med, 1995. **333**(8): p. 487-93.
267. Mossadegh-Keller, N., et al., *M-CSF instructs myeloid lineage fate in single haematopoietic stem cells*. Nature, 2013. **497**(7448): p. 239-43.
268. Rieger, M.A., et al., *Hematopoietic cytokines can instruct lineage choice*. Science, 2009. **325**(5937): p. 217-8.
269. Grover, A., et al., *Erythropoietin guides multipotent hematopoietic progenitor cells toward an erythroid fate*. J Exp Med, 2014. **211**(2): p. 181-8.
270. Rohrschneider, L.R., et al., *Growth and differentiation signals regulated by the M-CSF receptor*. Mol Reprod Dev, 1997. **46**(1): p. 96-103.
271. Smith, A., D. Metcalf, and N.A. Nicola, *Cytoplasmic domains of the common beta-chain of the GM-CSF/IL-3/IL-5 receptors that are required for inducing differentiation or clonal suppression in myeloid leukaemic cell lines*. EMBO J, 1997. **16**(3): p. 451-64.
272. Matsuguchi, T., et al., *The cytoplasmic domain of granulocyte-macrophage colony-stimulating factor (GM-CSF) receptor alpha subunit is essential for both GM-CSF-mediated growth and differentiation*. J Biol Chem, 1997. **272**(28): p. 17450-9.
273. Alexander, W.S., et al., *Tyrosine-599 of the c-Mpl receptor is required for Shc phosphorylation and the induction of cellular differentiation*. EMBO J, 1996. **15**(23): p. 6531-40.
274. Borzillo, G.V., R.A. Ashmun, and C.J. Sherr, *Macrophage lineage switching of murine early pre-B lymphoid cells expressing transduced fms genes*. Mol Cell Biol, 1990. **10**(6): p. 2703-14.
275. Kondo, M., et al., *Cell-fate conversion of lymphoid-committed progenitors by instructive actions of cytokines*. Nature, 2000. **407**(6802): p. 383-6.
276. Onai, N., et al., *Activation of the Flt3 signal transduction cascade rescues and enhances type I interferon-producing and dendritic cell development*. J Exp Med, 2006. **203**(1): p. 227-38.
277. Carroll, M., B. Mathey-Prevot, and A. D'Andrea, *Differentiation domains of the erythropoietin receptor*. Proc Soc Exp Biol Med, 1994. **206**(3): p. 289-94.
278. Zandstra, P.W., et al., *Cytokine manipulation of primitive human hematopoietic cell self-renewal*. Proc Natl Acad Sci U S A, 1997. **94**(9): p. 4698-703.

279. Audet, J., et al., *Distinct role of gp130 activation in promoting self-renewal divisions by mitogenically stimulated murine hematopoietic stem cells*. Proc Natl Acad Sci U S A, 2001. **98**(4): p. 1757-62.
280. Carras, S., et al., *Instructive role of M-CSF on commitment of bipotent myeloid cells involves ERK-dependent positive and negative signaling*. J Leukoc Biol, 2016. **99**(2): p. 311-9.
281. Grasset, M.F., et al., *Macrophage differentiation of myeloid progenitor cells in response to M-CSF is regulated by the dual-specificity phosphatase DUSP5*. J Leukoc Biol, 2010. **87**(1): p. 127-35.
282. Hamdorf, M., et al., *PKC δ -induced PU.1 phosphorylation promotes hematopoietic stem cell differentiation to dendritic cells*. Stem Cells, 2011. **29**(2): p. 297-306.
283. Starck, J., et al., *Inducible Fli-1 gene deletion in adult mice modifies several myeloid lineage commitment decisions and accelerates proliferation arrest and terminal erythrocytic differentiation*. Blood, 2010. **116**(23): p. 4795-805.
284. Tsapogas, P., et al., *IL-7 mediates Ebf-1-dependent lineage restriction in early lymphoid progenitors*. Blood, 2011. **118**(5): p. 1283-90.
285. Inlay, M.A., et al., *Ly6d marks the earliest stage of B-cell specification and identifies the branchpoint between B-cell and T-cell development*. Genes Dev, 2009. **23**(20): p. 2376-81.
286. Thal, M.A., et al., *Ebf1-mediated down-regulation of Id2 and Id3 is essential for specification of the B cell lineage*. Proc Natl Acad Sci U S A, 2009. **106**(2): p. 552-7.
287. Roessler, S., et al., *Distinct promoters mediate the regulation of Ebf1 gene expression by interleukin-7 and Pax5*. Mol Cell Biol, 2007. **27**(2): p. 579-94.
288. Tsapogas, P., et al., *In vivo evidence for an instructive role of fms-like tyrosine kinase-3 (FLT3) ligand in hematopoietic development*. Haematologica, 2014. **99**(4): p. 638-46.
289. Oburoglu, L., et al., *Glucose and glutamine metabolism regulate human hematopoietic stem cell lineage specification*. Cell Stem Cell, 2014. **15**(2): p. 169-84.
290. Xia, P., et al., *Insulin-InsR signaling drives multipotent progenitor differentiation toward lymphoid lineages*. J Exp Med, 2015. **212**(13): p. 2305-21.
291. Müller-Sieburg, C.E., et al., *Deterministic regulation of hematopoietic stem cell self-renewal and differentiation*. Blood, 2002. **100**(4): p. 1302-9.
292. Muller-Sieburg, C.E., et al., *Myeloid-biased hematopoietic stem cells have extensive self-renewal capacity but generate diminished lymphoid progeny with impaired IL-7 responsiveness*. Blood, 2004. **103**(11): p. 4111-8.
293. Cho, R.H., H.B. Sieburg, and C.E. Muller-Sieburg, *A new mechanism for the aging of hematopoietic stem cells: aging changes the clonal composition of the stem cell compartment but not individual stem cells*. Blood, 2008. **111**(12): p. 5553-61.
294. Guo, G., et al., *Mapping cellular hierarchy by single-cell analysis of the cell surface repertoire*. Cell Stem Cell, 2013. **13**(4): p. 492-505.
295. Mountford, J., E. Olivier, and M. Turner, *Prospects for the manufacture of red cells for transfusion*. Br J Haematol, 2010. **149**(1): p. 22-34.
296. Bagger, F.O., et al., *HemaExplorer: a database of mRNA expression profiles in normal and malignant haematopoiesis*. Nucleic Acids Res, 2013. **41**(Database issue): p. D1034-9.

297. Bagger, F.O., et al., *BloodSpot: a database of gene expression profiles and transcriptional programs for healthy and malignant haematopoiesis*. Nucleic Acids Res, 2016. **44**(D1): p. D917-24.
298. Mount, D.W., *Using the Basic Local Alignment Search Tool (BLAST)*. CSH Protoc, 2007. **2007**: p. pdb.top17.
299. Rieger, M.A., B.M. Smejkal, and T. Schroeder, *Improved prospective identification of megakaryocyte-erythrocyte progenitor cells*. Br J Haematol, 2009. **144**(3): p. 448-51.
300. Treuting, P. and S. Dintzis, *Comparative anatomy and histology : a mouse and human atlas*. 1st ed. 2012, London ; Waltham, MA: Academic Press. xii, 461 p.
301. Gartner, L.P. and J.L. Hiatt, *Color atlas of histology*. 5th ed. 2009, Philadelphia: Wolters Kluwer Health/Lippincott William & Wilkins. xv, 459 p.
302. Ross, M.H. and W. Pawlina, *Histology : a text and atlas : with correlated cell and molecular biology*. 6th ed. 2011, Philadelphia: Wolters Kluwer/Lippincott Williams & Wilkins Health. xviii, 974 p.
303. Mescher, A.L. and L.C.U. Junqueira, *Junqueira's basic histology : text and atlas*. 13th ed. 2013, New York: McGraw-Hill Medical. xi, 544 p.
304. Paul, F., et al., *Transcriptional Heterogeneity and Lineage Commitment in Myeloid Progenitors*. Cell, 2015. **163**(7): p. 1663-77.
305. Tsang, J.C., et al., *Single-cell transcriptomic reconstruction reveals cell cycle and multi-lineage differentiation defects in Bcl11a-deficient hematopoietic stem cells*. Genome Biol, 2015. **16**: p. 178.
306. Wilson, N.K., et al., *Combined Single-Cell Functional and Gene Expression Analysis Resolves Heterogeneity within Stem Cell Populations*. Cell Stem Cell, 2015. **16**(6): p. 712-24.
307. Moignard, V., et al., *Characterization of transcriptional networks in blood stem and progenitor cells using high-throughput single-cell gene expression analysis*. Nat Cell Biol, 2013. **15**(4): p. 363-72.
308. Petriv, O.I., et al., *Comprehensive microRNA expression profiling of the hematopoietic hierarchy*. Proc Natl Acad Sci U S A, 2010. **107**(35): p. 15443-8.
309. Benz, C., et al., *Hematopoietic stem cell subtypes expand differentially during development and display distinct lymphopoietic programs*. Cell Stem Cell, 2012. **10**(3): p. 273-83.
310. Yoshida, K. and K. Matsuzaki, *Differential Regulation of TGF- β /Smad Signaling in Hepatic Stellate Cells between Acute and Chronic Liver Injuries*. Front Physiol, 2012. **3**: p. 53.
311. Karsunky, H., et al., *Flt3 ligand regulates dendritic cell development from Flt3+ lymphoid and myeloid-committed progenitors to Flt3+ dendritic cells in vivo*. J Exp Med, 2003. **198**(2): p. 305-13.
312. Volpe, G., et al., *Regulation of the Flt3 Gene in Haematopoietic Stem and Early Progenitor Cells*. PLoS One, 2015. **10**(9): p. e0138257.
313. Terszowski, G., et al., *Prospective isolation and global gene expression analysis of the erythrocyte colony-forming unit (CFU-E)*. Blood, 2005. **105**(5): p. 1937-45.
314. Tersikh, A.V., et al., *Gene expression analysis of purified hematopoietic stem cells and committed progenitors*. Blood, 2003. **102**(1): p. 94-101.
315. Kulkarni, B., et al., *Validation of endogenous control genes for gene expression studies on human ocular surface epithelium*. PLoS One, 2011. **6**(8): p. e22301.

316. Kheirelseid, E.A., et al., *Identification of endogenous control genes for normalisation of real-time quantitative PCR data in colorectal cancer*. BMC Mol Biol, 2010. **11**: p. 12.
317. Pérez, S., et al., *Identifying the most suitable endogenous control for determining gene expression in hearts from organ donors*. BMC Mol Biol, 2007. **8**: p. 114.
318. Donovan, J.A. and G.A. Koretzky, *CD45 and the immune response*. J Am Soc Nephrol, 1993. **4**(4): p. 976-85.
319. Rose, S., A. Misharin, and H. Perlman, *A novel Ly6C/Ly6G-based strategy to analyze the mouse splenic myeloid compartment*. Cytometry A, 2012. **81**(4): p. 343-50.
320. Karlsson, G., et al., *The tetraspanin CD9 affords high-purity capture of all murine hematopoietic stem cells*. Cell Rep, 2013. **4**(4): p. 642-8.
321. Sitnicka, E., et al., *Key role of flt3 ligand in regulation of the common lymphoid progenitor but not in maintenance of the hematopoietic stem cell pool*. Immunity, 2002. **17**(4): p. 463-72.
322. Böiers, C., et al., *Expression and role of FLT3 in regulation of the earliest stage of normal granulocyte-monocyte progenitor development*. Blood, 2010. **115**(24): p. 5061-8.
323. Buza-Vidas, N., et al., *FLT3 expression initiates in fully multipotent mouse hematopoietic progenitor cells*. Blood, 2011. **118**(6): p. 1544-8.
324. Lai, A.Y. and M. Kondo, *Asymmetrical lymphoid and myeloid lineage commitment in multipotent hematopoietic progenitors*. J Exp Med, 2006. **203**(8): p. 1867-73.
325. Arinobu, Y., et al., *Reciprocal activation of GATA-1 and PU.1 marks initial specification of hematopoietic stem cells into myeloerythroid and myelolymphoid lineages*. Cell Stem Cell, 2007. **1**(4): p. 416-27.
326. Vogel, C. and E.M. Marcotte, *Insights into the regulation of protein abundance from proteomic and transcriptomic analyses*. Nat Rev Genet, 2012. **13**(4): p. 227-32.
327. Schwanhäusser, B., et al., *Global quantification of mammalian gene expression control*. Nature, 2011. **473**(7347): p. 337-42.
328. Semerad, C.L., et al., *G-CSF is an essential regulator of neutrophil trafficking from the bone marrow to the blood*. Immunity, 2002. **17**(4): p. 413-23.
329. Chu, S.H., et al., *FLT3-ITD knockin impairs hematopoietic stem cell quiescence/homeostasis, leading to myeloproliferative neoplasm*. Cell Stem Cell, 2012. **11**(3): p. 346-58.
330. Månsson, R., et al., *Molecular evidence for hierarchical transcriptional lineage priming in fetal and adult stem cells and multipotent progenitors*. Immunity, 2007. **26**(4): p. 407-19.
331. Weksberg, D.C., et al., *CD150- side population cells represent a functionally distinct population of long-term hematopoietic stem cells*. Blood, 2008. **111**(4): p. 2444-51.
332. Perié, L., et al., *The Branching Point in Erythro-Myeloid Differentiation*. Cell, 2015. **163**(7): p. 1655-62.
333. Akashi, K., et al., *Transcriptional accessibility for genes of multiple tissues and hematopoietic lineages is hierarchically controlled during early hematopoiesis*. Blood, 2003. **101**(2): p. 383-9.
334. Luc, S., et al., *Down-regulation of Mpl marks the transition to lymphoid-primed multipotent progenitors with gradual loss of granulocyte-monocyte potential*. Blood, 2008. **111**(7): p. 3424-34.

335. Xiao, M., et al., *Expression of Flt3 and c-kit during growth and maturation of human CD34+CD38- cells*. Exp Hematol, 1999. **27**(5): p. 916-27.
336. Kikushige, Y., et al., *Human Flt3 is expressed at the hematopoietic stem cell and the granulocyte/macrophage progenitor stages to maintain cell survival*. J Immunol, 2008. **180**(11): p. 7358-67.
337. Zeigler, F.C., et al., *Cellular and molecular characterization of the role of the flk-2/flt-3 receptor tyrosine kinase in hematopoietic stem cells*. Blood, 1994. **84**(8): p. 2422-30.
338. Mackarechtschian, K., et al., *Targeted disruption of the flk2/flt3 gene leads to deficiencies in primitive hematopoietic progenitors*. Immunity, 1995. **3**(1): p. 147-61.
339. McKenna, H.J., et al., *Mice lacking flt3 ligand have deficient hematopoiesis affecting hematopoietic progenitor cells, dendritic cells, and natural killer cells*. Blood, 2000. **95**(11): p. 3489-97.
340. Buza-Vidas, N., et al., *FLT3 receptor and ligand are dispensable for maintenance and posttransplantation expansion of mouse hematopoietic stem cells*. Blood, 2009. **113**(15): p. 3453-60.
341. Forsberg, E.C., et al., *New evidence supporting megakaryocyte-erythrocyte potential of flk2/flt3+ multipotent hematopoietic progenitors*. Cell, 2006. **126**(2): p. 415-26.
342. Boyer, S.W., et al., *All hematopoietic cells develop from hematopoietic stem cells through Flk2/Flt3-positive progenitor cells*. Cell Stem Cell, 2011. **9**(1): p. 64-73.
343. Beaudin, A.E., S.W. Boyer, and E.C. Forsberg, *Flk2/Flt3 promotes both myeloid and lymphoid development by expanding non-self-renewing multipotent hematopoietic progenitor cells*. Exp Hematol, 2014. **42**(3): p. 218-229.e4.
344. Lisovsky, M., et al., *Flt3 ligand stimulates proliferation and inhibits apoptosis of acute myeloid leukemia cells: regulation of Bcl-2 and Bax*. Blood, 1996. **88**(10): p. 3987-97.
345. Dolence, J.J., et al., *Threshold levels of Flt3-ligand are required for the generation and survival of lymphoid progenitors and B-cell precursors*. Eur J Immunol, 2011. **41**(2): p. 324-34.
346. Drexler, H.G., C. Meyer, and H. Quentmeier, *Effects of FLT3 ligand on proliferation and survival of myeloid leukemia cells*. Leuk Lymphoma, 1999. **33**(1-2): p. 83-91.
347. Meshinchi, S. and F.R. Appelbaum, *Structural and functional alterations of FLT3 in acute myeloid leukemia*. Clin Cancer Res, 2009. **15**(13): p. 4263-9.
348. Griffith, J., et al., *The structural basis for autoinhibition of FLT3 by the juxtamembrane domain*. Mol Cell, 2004. **13**(2): p. 169-78.
349. Zhang, S., C. Mantel, and H.E. Broxmeyer, *Flt3 signaling involves tyrosyl-phosphorylation of SHP-2 and SHIP and their association with Grb2 and Shc in Baf3/Flt3 cells*. J Leukoc Biol, 1999. **65**(3): p. 372-80.
350. Marchetto, S., et al., *SHC and SHIP phosphorylation and interaction in response to activation of the FLT3 receptor*. Leukemia, 1999. **13**(9): p. 1374-82.
351. Lavagna-Sévenier, C., et al., *FLT3 signaling in hematopoietic cells involves CBL, SHC and an unknown P115 as prominent tyrosine-phosphorylated substrates*. Leukemia, 1998. **12**(3): p. 301-10.
352. Gilliland, D.G. and J.D. Griffin, *The roles of FLT3 in hematopoiesis and leukemia*. Blood, 2002. **100**(5): p. 1532-42.
353. Stirewalt, D.L. and J.P. Radich, *The role of FLT3 in haematopoietic malignancies*. Nat Rev Cancer, 2003. **3**(9): p. 650-65.

354. Ruvinsky, I. and O. Meyuhas, *Ribosomal protein S6 phosphorylation: from protein synthesis to cell size*. Trends Biochem Sci, 2006. **31**(6): p. 342-8.
355. Neben, K., et al., *Distinct gene expression patterns associated with FLT3- and NRAS-activating mutations in acute myeloid leukemia with normal karyotype*. Oncogene, 2005. **24**(9): p. 1580-8.
356. Schwäble, J., et al., *RGS2 is an important target gene of Flt3-ITD mutations in AML and functions in myeloid differentiation and leukemic transformation*. Blood, 2005. **105**(5): p. 2107-14.
357. Chen, P., et al., *FLT3/ITD mutation signaling includes suppression of SHP-1*. J Biol Chem, 2005. **280**(7): p. 5361-9.
358. Mizuki, M., et al., *Suppression of myeloid transcription factors and induction of STAT response genes by AML-specific Flt3 mutations*. Blood, 2003. **101**(8): p. 3164-73.
359. Wölfler, A., et al., *Lineage-instructive function of C/EBPα in multipotent hematopoietic cells and early thymic progenitors*. Blood, 2010. **116**(20): p. 4116-25.
360. Hasemann, M.S., et al., *C/EBPα is required for long-term self-renewal and lineage priming of hematopoietic stem cells and for the maintenance of epigenetic configurations in multipotent progenitors*. PLoS Genet, 2014. **10**(1): p. e1004079.
361. Fisher, R.C. and E.W. Scott, *Role of PU.1 in hematopoiesis*. Stem Cells, 1998. **16**(1): p. 25-37.
362. Schulz, K.R., et al., *Single-cell phospho-protein analysis by flow cytometry*. Curr Protoc Immunol, 2012. **Chapter 8**: p. Unit 8.17.1-20.
363. Krutzik, P.O. and G.P. Nolan, *Intracellular phospho-protein staining techniques for flow cytometry: monitoring single cell signaling events*. Cytometry A, 2003. **55**(2): p. 61-70.
364. Kalaitzidis, D. and B.G. Neel, *Flow-cytometric phosphoprotein analysis reveals agonist and temporal differences in responses of murine hematopoietic stem/progenitor cells*. PLoS One, 2008. **3**(11): p. e3776.
365. Du, J., et al., *Signaling profiling at the single-cell level identifies a distinct signaling signature in murine hematopoietic stem cells*. Stem Cells, 2012. **30**(7): p. 1447-54.
366. Welstead, G.G., et al., *Mechanism of CD150 (SLAMF7) down regulation from the host cell surface by measles virus hemagglutinin protein*. J Virol, 2004. **78**(18): p. 9666-74.
367. Zola, H., *High-sensitivity immunofluorescence/flow cytometry: detection of cytokine receptors and other low-abundance membrane molecules*. Curr Protoc Cytom, 2004. **Chapter 6**: p. Unit 6.3.
368. Carotta, S., et al., *The transcription factor PU.1 controls dendritic cell development and Flt3 cytokine receptor expression in a dose-dependent manner*. Immunity, 2010. **32**(5): p. 628-41.
369. Nutt, S.L., et al., *Dynamic regulation of PU.1 expression in multipotent hematopoietic progenitors*. J Exp Med, 2005. **201**(2): p. 221-31.
370. Wu, L., et al., *Cell-autonomous defects in dendritic cell populations of Ikaros mutant mice point to a developmental relationship with the lymphoid lineage*. Immunity, 1997. **7**(4): p. 483-92.
371. Manz, M.G., et al., *Dendritic cell potentials of early lymphoid and myeloid progenitors*. Blood, 2001. **97**(11): p. 3333-41.
372. Burgess, W., et al., *Insulin-like growth factor-I and the cytokines IL-3 and IL-4 promote survival of progenitor myeloid cells by different mechanisms*. J Neuroimmunol, 2003. **135**(1-2): p. 82-90.

373. Chen, Y.L., et al., *A type I IFN-Flt3 ligand axis augments plasmacytoid dendritic cell development from common lymphoid progenitors*. J Exp Med, 2013. **210**(12): p. 2515-22.
374. McKinstry, W.J., et al., *Cytokine receptor expression on hematopoietic stem and progenitor cells*. Blood, 1997. **89**(1): p. 65-71.
375. Waskow, C., et al., *The receptor tyrosine kinase Flt3 is required for dendritic cell development in peripheral lymphoid tissues*. Nat Immunol, 2008. **9**(6): p. 676-83.
376. Lyman, S.D. and S.E. Jacobsen, *c-kit ligand and Flt3 ligand: stem/progenitor cell factors with overlapping yet distinct activities*. Blood, 1998. **91**(4): p. 1101-34.
377. Metcalf, D., *Hematopoietic regulators: redundancy or subtlety?* Blood, 1993. **82**(12): p. 3515-23.
378. Otto, K.G., et al., *Cell proliferation through forced engagement of c-Kit and Flt-3*. Blood, 2001. **97**(11): p. 3662-4.
379. Jacobsen, S.E., et al., *The FLT3 ligand potently and directly stimulates the growth and expansion of primitive murine bone marrow progenitor cells in vitro: synergistic interactions with interleukin (IL) 11, IL-12, and other hematopoietic growth factors*. J Exp Med, 1995. **181**(4): p. 1357-63.
380. Hannum, C., et al., *Ligand for FLT3/FLK2 receptor tyrosine kinase regulates growth of haematopoietic stem cells and is encoded by variant RNAs*. Nature, 1994. **368**(6472): p. 643-8.
381. Pietras, E.M., et al., *Functionally Distinct Subsets of Lineage-Biased Multipotent Progenitors Control Blood Production in Normal and Regenerative Conditions*. Cell Stem Cell, 2015. **17**(1): p. 35-46.
382. Busch, K., et al., *Fundamental properties of unperturbed haematopoiesis from stem cells in vivo*. Nature, 2015. **518**(7540): p. 542-6.
383. Sun, J., et al., *Clonal dynamics of native haematopoiesis*. Nature, 2014. **514**(7522): p. 322-7.
384. Geissmann, F., et al., *Development of monocytes, macrophages, and dendritic cells*. Science, 2010. **327**(5966): p. 656-61.
385. Fried, W., *Erythropoietin and erythropoiesis*. Exp Hematol, 2009. **37**(9): p. 1007-15.
386. Kulesa, H., J. Frampton, and T. Graf, *GATA-1 reprograms avian myelomonocytic cell lines into eosinophils, thromboblats, and erythroblasts*. Genes Dev, 1995. **9**(10): p. 1250-62.
387. Sarrazin, S. and M. Sieweke, *Integration of cytokine and transcription factor signals in hematopoietic stem cell commitment*. Semin Immunol, 2011. **23**(5): p. 326-34.
388. Sarrazin, S., et al., *MafB restricts M-CSF-dependent myeloid commitment divisions of hematopoietic stem cells*. Cell, 2009. **138**(2): p. 300-13.
389. Iwasaki-Arai, J., et al., *Enforced granulocyte/macrophage colony-stimulating factor signals do not support lymphopoiesis, but instruct lymphoid to myelomonocytic lineage conversion*. J Exp Med, 2003. **197**(10): p. 1311-22.
390. Perry, A.K., et al., *The host type I interferon response to viral and bacterial infections*. Cell Res, 2005. **15**(6): p. 407-22.
391. Beleslin-Cokic, B.B., et al., *Erythropoietin and hypoxia stimulate erythropoietin receptor and nitric oxide production by endothelial cells*. Blood, 2004. **104**(7): p. 2073-80.
392. Heir, P., et al., *Oxygen-Dependent Regulation of Erythropoietin Receptor Turnover And Signaling*. J Biol Chem, 2016.

- 393. Cokic, B.B., et al., *Nitric oxide and hypoxia stimulate erythropoietin receptor via MAPK kinase in endothelial cells*. Microvasc Res, 2014. **92**: p. 34-40.
- 394. Yoon, D., et al., *Hypoxia-inducible factor-1 deficiency results in dysregulated erythropoiesis signaling and iron homeostasis in mouse development*. J Biol Chem, 2006. **281**(35): p. 25703-11.
- 395. Zhang, D.E., et al., *The macrophage transcription factor PU.1 directs tissue-specific expression of the macrophage colony-stimulating factor receptor*. Mol Cell Biol, 1994. **14**(1): p. 373-81.
- 396. Layon, M.E., et al., *Expression of GATA-1 in a non-hematopoietic cell line induces beta-globin locus control region chromatin structure remodeling and an erythroid pattern of gene expression*. J Mol Biol, 2007. **366**(3): p. 737-44.
- 397. Przybylski, M., et al., *Infections due to alphaherpesviruses in early post-transplant period after allogeneic haematopoietic stem cell transplantation: Results of a 5-year survey*. J Clin Virol, 2016. **87**: p. 67-72.